

APPENDIX J
CONCEPTUAL STRUCTURE OF TSPA-LA

J1 INTRODUCTION

Performance assessment (PA) for a complex system requires detailed calculations that bring together a probabilistic description of the events that could affect the system, models for physical processes associated with the system, and an assessment of the level confidence that can be ascribed to individual assumptions that underlie the PA. Owing to its inherent complexity, a PA needs a clear conceptual structure that provides both an overview of what the PA is intended to calculate and guidance on the computational structure required to implement the PA. Without an overarching structure, it is difficult to communicate exactly what a PA is intended to calculate and also to design and carry out a conceptually consistent set of calculations. The purpose of this appendix is to describe the conceptual structure on which the TSPA-LA is based.

J2 REQUIREMENTS UNDERLYING CONCEPTUAL STRUCTURE OF TSPA-LA

The conceptual structure of any PA should derive from the intended use of that PA and the information that the PA is intended to summarize. The TSPA-LA is intended to summarize information about the Yucca Mountain facility for use in a regulatory decision. Thus, the conceptual structure of the TSPA-LA derives from the regulatory requirements that are placed on the Yucca Mountain facility. As initially promulgated, these regulatory requirements have three primary sources: (i) 40 CFR Part 197, *Public Health and Environmental Radiation Protection Standards for Yucca Mountain, NV; Final Rule*, which has been promulgated by the U.S. Environmental Protection Agency (EPA) (66 FR 32074 [DIRS 155216]), (ii) 10 CFR Parts 2, 19, 20, 21, etc., *Disposal of High-Level Radioactive Wastes in a Proposed Geologic Repository at Yucca Mountain, Nevada; Final Rule*, which has been promulgated by the U.S. Nuclear Regulatory Commission (NRC) (66 FR 55732 [DIRS 156671]), and (iii) *Yucca Mountain Review Plan; Final Report*, which has been published by the NRC (NRC 2003 [DIRS 163274], Section 2.2) to guide assessing compliance with 10 CFR Parts 2, 19, 20, 21, etc.

The initial promulgations indicated above specified conditions that the Yucca Mountain facility was required to satisfy for the first 10,000 yr after its closure. In a subsequent suit [DIRS 176542], it was ruled that the EPA did not follow guidance in a National Academy of Science (NAS) study (National Research Council 1995 [DIRS 100018]) as mandated by Congress in the Energy Policy Act of 1992 [DIRS 100017]. In particular, it was ruled that the EPA had failed to follow the guidance in the NAS study that the regulatory period for the Yucca Mountain facility should extend over the period of geologic stability at the facility site, which was suggested to be 10^6 yr. As a result, the initial regulation for the Yucca Mountain facility was remanded to the EPA for revision.

In response to this remand, the EPA promulgated 40 CFR Part 197, *Public Health and Environmental Radiation Protection Standards for Yucca Mountain, Nevada; Proposed Rule* (70 FR 49014 [DIRS 177357]), which contained revised standards for the Yucca Mountain facility. In turn and in consistency with the EPA's revised standard, the NRC promulgated 10 CFR Part 63, *Implementation of a Dose Standard After 10,000 Years* (70 FR 53313 [DIRS 178394]). The EPA's and NRC's regulations proposed in response to the remand left the requirements for the first 10,000 yr after repository closure unchanged. However, new conditions were specified for the time interval [10^4 , 10^6 yr].

Because the regulations for the first 10,000 yr after repository closure are unchanged, the regulations and supporting rationale for this time period are initially discussed for the EPA (Section J2.1) and the NRC (Section J2.2). This discussion includes quotes from the original regulations and supporting material that provides insights on the type of analysis desired and the implementation of such an analysis. Then, the regulations for the time interval [10⁴, 10⁶ yr] proposed by the EPA (Section J2.3) and the NRC (Section J2.4) are discussed. Finally, the Yucca Mountain review plan as originally published is discussed (Section J2.5). At present, there has been no change to the review plan in response to the proposed regulations.

J2.1 EPA Requirements: 40 CFR Part 197 Before Remand

As mandated in the Energy Policy Act of 1992 [DIRS 100017], the EPA promulgated public health and safety standards for radioactive material stored or deposited in the potential repository at Yucca Mountain, NV in 40 CFR Part 197 (66 FR 32074 [DIRS 155216]). In turn, the NRC is required to incorporate these standards into its licensing standards, and the U.S. Department of Energy (DOE) must demonstrate compliance with these standards. Selected requirements and explanatory material from 40 CFR Part 197 (66 FR 32074 [DIRS 155216]) that influence the conceptual structure of the TSPA-LA for postclosure conditions follow. Specifically, the primary focus is on Subpart B of 40 CFR Part 197 (66 FR 32074 [DIRS 155216]), which relates to postclosure requirements.

The core requirement in 40 CFR 197 (66 FR 32074 [DIRS 155216]) that ultimately gives rise to the conceptual structure of the TSPA-LA is an individual-protection standard. Specifically, the following standard was mandated (66 FR 32074 [DIRS 155216], p. 32134):

§ 197.20 What standard must DOE meet?

The DOE must demonstrate, using performance assessment, that there is a reasonable expectation that, for 10,000 years following disposal, the reasonably maximally exposed individual receives no more than an annual committed effective dose equivalent of 150 microsieverts (15 millirems) from releases from the undisturbed Yucca Mountain disposal system. The DOE's analysis must include all potential pathways of radionuclide transport and exposure. (EPA1)

A reading of the preceding requirement immediately gives rise to three questions: (i) "What is a PA?", (ii) "What is reasonable expectation?", and (iii) "What is the reasonably maximally exposed individual (RMEI)?"

In answer to the first question, the EPA defined a PA in 40 CFR Part 197 (66 FR 32074 [DIRS 155216], p. 32133):

Performance assessment means an analysis that:

- (1) Identifies the features, events, processes, (except human intrusion), and sequences of events and processes (except human intrusion) that might affect the Yucca Mountain disposal system and their probabilities of occurring during 10,000 years after disposal;

- (2) Examines the effects of those features, events, processes, and sequences of events and processes upon the performance of the Yucca Mountain disposal system; and
- (3) Estimates the annual committed effective dose equivalent incurred by the reasonably maximally exposed individual, including the associated uncertainties, as a result of releases caused by all significant features, events, processes, and sequences of events and processes, weighted by their probability of occurrence. (EPA2)

In answer to the second question, the EPA defined reasonable expectation in 40 CFR Part 197 (66 FR 32074 [DIRS 155216], p. 32133):

§ 197.14 What is a reasonable expectation?

Reasonable expectation means that NRC is satisfied that compliance will be achieved based upon the full record before it. Characteristics of reasonable expectation include that it:

- (a) Requires less than absolute proof because absolute proof is impossible to attain for disposal due to the uncertainty of projecting long-term performance;
- (b) Accounts for the inherently greater uncertainties in making long-term projections of the performance of the Yucca Mountain disposal system;
- (c) Does not exclude important parameters from assessments and analyses simply because they are difficult to precisely quantify to a high degree of confidence; and
- (d) Focuses performance assessments and analyses upon the full range of defensible and reasonable parameter distributions rather than only upon extreme physical situations and parameter values. (EPA3)

Finally, in answer to the third question, the EPA defined the reasonably maximally exposed individual (RMEI) in 40 CFR Part 197 (66 FR 32074 [DIRS 155216], p. 32134):

§ 197.21 Who is the reasonably maximally exposed individual?

The reasonably maximally exposed individual is a hypothetical person who meets the following criteria:

- (a) Lives in the accessible environment above the highest concentration of radionuclides in the plume of contamination;
- (b) Has a diet and living style representative of the people who now reside in the Town of Amargosa Valley, Nevada. The DOE must use projections based upon surveys of the people residing in the Town of Amargosa Valley,

Nevada, to determine their current diets and living styles and use the mean values of these factors in the assessments conducted for §§ 197.20 and 197.25; and

- (c) Drinks 2 liters of water per day from wells drilled into the ground water at the location specified in paragraph (a) of this section. (EPA4)

With respect to the preceding statements, the definitions of PA and reasonable expectation are particularly important with respect to the conceptual structure of the TSPA-LA because they relate to requirements that affect the overall organization of the analysis. In contrast, the definition of the RMEI is less important to the conceptual structure of the analysis because it simply relates to a particular result that must be calculated.

A PA is often described as an analysis intended to answer three questions about a system and one additional question about the analysis itself (Kaplan and Garrick 1981 [DIRS 100557]). The first three questions are:

- (i) What could happen? (Q1)
- (ii) How likely is it to happen? (Q2)

and

- (iii) What are the consequences if it does happen? (Q3)

The fourth question is:

- (iv) What is the uncertainty (or equivalently, how much confidence do you have) in the answers to the first three questions? (Q4)

The posing of the first three questions in the definition of a PA in (EPA2) is clearly evident. Specifically, “Identifies features, events and processes” corresponds to answering Q1 and “Identifies... their probabilities of occurring” corresponds to answering Q2. Similarly, “Examines the effects of those features, events and processes” and “Estimates the annual committed effective dose equivalent” correspond to answering Q3. The presence of Q4 is not as immediately obvious but is imbedded in the definition of PA in (EPA2) in the statement “including the associated uncertainties” and in the definition of reasonable expectation in (EPA3) in the statements “Accounts for the inherently greater uncertainties in making long-term projections” and “Focuses performance assessments upon the full range of defensible and reasonable parameter values”. The four questions in (Q1) – (Q4) are introduced here because they will later be used as an intuitive lead into the conceptual structure of the TSPA-LA.

The EPA provided the following guidance on the implementation of the postclosure requirements in 40 CFR 197.13 (66 FR 32074 [DIRS 155216], p. 32133):

§ 197.13 How is subpart B implemented?

The NRC implements this subpart B. The DOE must demonstrate to NRC that there is a reasonable expectation of compliance with this subpart before NRC may issue a license. In the case of the specific numerical requirements in § 197.20 of this subpart, and if performance assessment is used to demonstrate compliance with the specific numerical requirements in §§ 197.25 and 197.30 of this subpart, NRC will determine compliance based upon the mean of the distribution of projected doses of DOE's performance assessments which project the performance of the Yucca Mountain disposal system for 10,000 years after disposal. (EPA5)

Of particular importance is the statement that "In the case of the specific numerical requirements in § 197.20..., NRC will determine compliance based upon the mean of projected doses." This is a very important requirement with respect to the conceptual and computational structure of the TSPA-LA, and a requirement that is not easy to interpret. In particular, a mean is a quantity that is defined by an integral, and it is not immediately obvious exactly what this integral is supposed to be over.

Identifying what is intended by the "mean" indicated in (EPA5) is complicated by the required consideration of two types of uncertainty in the EPA mandated PA for the Yucca Mountain facility. First, there is the uncertainty that arises from the different types of disruptions that could occur at the Yucca Mountain facility in the future. This uncertainty appears in the EPA's definition of PA in (EPA2) in the statements "Identifies features, events and processes ... and their probabilities of occurring during 10,000 years after disposal" and "Estimates the annual effective dose equivalent ... as a result of releases caused by all significant features, events and processes, and sequences of events and processes, weighted by their probability of occurrence." The latter statement appears to imply a mean, i.e., an integral, over what could happen in the future. This is the uncertainty associated with questions (Q1) and (Q2). Second, there is the uncertainty that arises from a lack of knowledge about properties of the Yucca Mountain site. This uncertainty appears in the EPA's definition of PA in (EPA2) in the statement "including the associated uncertainties" and in the definition of reasonable expectation in (EPA3) in the statements "due to the uncertainty of projecting long-term performance" and "the full range of defensible and reasonable parameter distributions." Given that these uncertainties are to be characterized probabilistically as implied by the last quote, then there would also be a mean over these uncertainties. These are the uncertainties associated with question (Q4).

Possibilities include a mean over what could happen in the future, a mean over uncertainty with respect to parameter values and other modeling assumptions, and a mean over both types of uncertainty. When read in full, the following final part of the definition of PA in (EPA2) suggests, but does not explicitly state, the last of the three indicated possibilities: "Estimates the annual committed effective dose equivalent incurred by the reasonably maximally exposed individual, *including the associated uncertainties*, as a result of releases caused by all significant features, events, processes and sequences of events and processes, *weighted by their probability of occurrence*," with the italics added for emphasis. As a further consideration, doses to the RMEI vary as a function of time, and this variation must be incorporated in some manner in the determination of mean doses.

The EPA does not provide a definitive statement in 40 CFR Part 197 (66 FR 32074 [DIRS 155216]) of what is intended by a mean dose. However, a number of additional

statements are included in 40 CFR Part 197 (66 FR 32074 [DIRS 155216]) that indicate the EPA's emphasis on consideration of a mean dose in assessing compliance:

In line with our use of the term "reasonable expectation," the fundamental compliance measure consistent with a literal mathematical interpretation of this term would be the mean value of the distribution of calculated doses (66 FR 32074 [DIRS 155216], p. 32125). (EPA6)

By specifying the mean as the performance measure and probability limits for the processes and events to be considered (§ 197.36), and in concert with the intent of our "reasonable expectation" approach in general, we have implied that probabilistic approaches for the disposal system performance assessments are expected (66 FR 32074 [DIRS 155216], p. 32125). (EPA7)

The mean or median are reasonably conservative measures because they are influenced by high exposure estimates found when analyzing the full range of site conditions and relevant processes, without being geared to exclusively reflect high-end results, as would be the case if we selected as the measure a high-end percentile of the calculated dose distribution (such as the 95th or 99th percentile). Our final rule for Yucca Mountain specifies only that the mean be used, as we believe that it is appropriately conservative in this situation (66 FR 32074 [DIRS 155216], p. 32126). (EPA8)

Thus, although some ambiguity exists with respect to exactly how a mean dose is to be defined and calculated, there is no ambiguity in the EPA's intent that compliance with its dose standard for the RMEI is to be determined with a mean dose. As an aside, it is perhaps worth noting that the statement with respect to the median in (EPA8) is not correct; in particular, the median unlike the mean is not particularly influenced by the high values associated with a skewed distribution.

The discussion of the requirements promulgated by the EPA in 40 CFR Part 197 (66 FR 32074 [DIRS 155216]) ends with several additional quotes that provide insights into the nature of the desired properties of a PA used to assess compliance with the EPA's Yucca Mountain standard:

It is NRC's responsibility to determine how DOE must demonstrate compliance with our standards; however, we envision the use of a probabilistic assessment for the compliance demonstration. (66 FR 32074 [DIRS 155216], p. 32086) (EPA9)

DOE and NRC may not assume that future geologic, hydrologic, and climatic conditions will be the same as they are at present. We require that these conditions be varied within reasonably ascertainable bounds over the required compliance period (66 FR 32074 [DIRS 155216], p. 32096). (EPA10)

If choices are made that make the simulations very unrealistic, the confidence that can be placed on modeling results is very limited. Inappropriate simplifications can mask the effects of processes that will in reality determine disposal system performance, if the uncertainties involved with these simplifications are not recognized. Overly conservative assumptions made in developing performance scenarios can bias the analyses in the direction of unrealistically extreme

situations, which in reality may be highly improbable, and can deflect attention from questions critical to developing an adequate understanding of the expected features, events, and processes (66 FR 32074 [DIRS 155216], p. 32102), (EPA 11)

The reasonable expectation approach is aimed simply at focusing attention on understanding the uncertainties in projecting disposal system performance so that regulatory decision making will be done with a full understanding of the uncertainties involved (66 FR 32074 [DIRS 155216], p. 32102). (EPA12)

The statement in (EPA9) clearly indicates that the EPA expects a probabilistic analysis. The statement in (EPA10) indicates the need to consider events that can happen in the future (e.g., volcanic eruptions, earthquakes, climatic changes). The statement in (EPA11) is important because it clearly indicates that the EPA does not desire a conservative analysis. The statement in (EPA12) indicates the EPA's desire for an appropriate representation of the uncertainties associated with a PA for the Yucca Mountain site. However, the EPA's desire "that regulatory decision making will be done with a full understanding of the uncertainties involved" as stated in (EPA12) is inconsistent with the intent to regulate on mean results as the calculation of means suppresses the implications of uncertainty.

J2.2 NRC Requirements: 10 CFR Parts 2, 19, 20, 21, etc. Before Remand

As mandated in the Energy Policy Act of 1992 [DIRS 100017], the NRC has promulgated licensing standards for the disposal of radioactive waste at the Yucca Mountain facility that are consistent with the EPA public health and safety standards in 40 CFR Part 197 (66 FR 32074 [DIRS 155216]) (see Section J2.1). Selected requirements and explanatory material from 10 CFR Parts 2, 19, 20, 21, etc. (66 FR 55732 [DIRS 156671]) that influence the conceptual structure of the TSPA-LA for postclosure conditions follow. Specifically, the primary focus is on Subpart L of 10 CFR Part 63 (66 FR 55732 [DIRS 156671]), which relates to postclosure requirements.

The core requirement in 10 CFR Part 63 (66 FR 55732 [DIRS 156671]) that ultimately gives rise to the conceptual structure of the TSPA-LA is an individual protection standard. Specifically, the following standard was mandated (66 FR 55732 [DIRS 156671], p. 55814):

§ 63.311 Individual protection standard after permanent closure.

DOE must demonstrate, using performance assessment, that there is a reasonable expectation that, for 10,000 years following disposal, the reasonably maximally exposed individual receives no more than an annual dose of 0.15 mSv (15 mrem) from releases from the undisturbed Yucca Mountain disposal system. DOE's analysis must include all potential pathways of radionuclide transport and exposure. (NRC1)

The preceding mandate is identical to the corresponding mandate from the EPA in (EPA1) provided the terminology in the two mandates has the same meaning. In particular, the phrases performance assessment, reasonable expectation and reasonably maximally exposed individual (RMEI) appear in both mandates.

Specifically, the NRC defined PA in 10 CFR Part 63.2 (66 FR 55732 [DIRS 156671], p. 55794):

Performance assessment means an analysis that:

- (1) Identifies the features, events, processes (except human intrusion), and sequences of events and processes (except human intrusion) that might affect the Yucca Mountain disposal system and their probabilities of occurring during 10,000 years after disposal;
- (2) Examines the effects of those features, events, processes, and sequences of events and processes upon the performance of the Yucca Mountain disposal system; and
- (3) Estimates the dose incurred by the reasonably maximally exposed individual, including the associated uncertainties, as a result of releases caused by all significant features, events, processes, and sequences of events and processes, weighted by their probability of occurrence. (NRC2)

The preceding definition of PA is identical to the definition given by the EPA in (EPA2) except for the use of “dose” rather than “annual committed effective dose”; presumably, the NRC intends the same dose measure as specified by the EPA. Further, the NRC defined reasonable expectation in 10 CFR Part 63.304 (66 FR 55732 [DIRS 156671], p. 55813):

§ 63.304 Reasonable expectation.

Reasonable expectation means that the Commission is satisfied that compliance will be achieved based upon the full record before it. Characteristics of reasonable expectation include that it:

- (1) Requires less than absolute proof because absolute proof is impossible to attain for disposal due to the uncertainty of projecting long-term performance;
- (2) Accounts for the inherently greater uncertainties in making long-term projections of the performance of the Yucca Mountain disposal system;
- (3) Does not exclude important parameters from assessments and analyses simply because they are difficult to precisely quantify to a high degree of confidence; and
- (4) Focuses performance assessments and analyses on the full range of defensible and reasonable parameter distributions rather than only upon extreme physical situations and parameter values. (NRC3)

The preceding is identical to the EPA’s definition of reasonable expectation in (EPA3) except for the replacement of “NRC” by “the Commission.” Finally, the RMEI was defined by the NRC in 10 CFR Part 63.312 (66 FR 55732 [DIRS 156671], p. 55814):

§ 63.312 Required characteristics of the reasonably maximally exposed individual.

The reasonably maximally exposed individual is a hypothetical person who meets the following criteria:

- (a) Lives in the accessible environment above the highest concentration of radionuclides in the plume of contamination;
- (b) Has a diet and living style representative of the people who now reside in the Town of Amargosa Valley, Nevada. DOE must use projections based upon surveys of the people residing in the Town of Amargosa Valley, Nevada, to determine their current diets and living styles and use the mean values of these factors in the assessments conducted for §§ 63.311 and 63.321;
- (c) Uses well water with average concentrations of radionuclides based on an annual water demand of 3000 acre-feet;
- (d) Drinks 2 liters of water per day from wells drilled into the ground water at the location specified in paragraph (a) of this section; and
- (e) Is an adult with metabolic and physiological considerations consistent with present knowledge of adults. (NRC4)

Except for some additional guidance on the determination of exposure, the definition of the RMEI given by the NRC is the same as the definition given by the EPA in (EPA4).

As a result of the effective identical content of the requirements/definitions given by the NRC in (NRC1) – (NRC4) and the EPA in (EPA1) – (EPA4), both organizations are specifying the same analysis. Hence, the four core questions underlying a PA indicated in (Q1) – (Q4) are present in the requirements of both the NRC and the EPA.

Because the NRC has regulatory authority for the Yucca Mountain facility, it is important to examine any additional requirements and/or specifications that it has made with respect to PA in support of a license application for this facility. The following guidance given in 10 CFR 63.303 (66 FR 55732 [DIRS 156671], p. 55813) on the implementation of postclosure requirements provides a high-level summary of what the NRC expects in a PA for the Yucca Mountain facility:

§ 63.303 Implementation of Subpart L.

DOE must demonstrate that there is a reasonable expectation of compliance with this subpart before a license may be issued. In the case of the specific numerical requirements in § 63.311 of this subpart, and if performance assessment is used to demonstrate compliance with the specific numerical requirements in §§ 63.321 and 63.331 of this subpart, compliance is based upon the mean of the distribution of projected doses of DOE's performance assessments which project the

performance of the Yucca Mountain disposal system for 10,000 years after disposal. (NRC5)

Except for minor changes in wording, the preceding implementation guidance is identical with the guidance given by the EPA in (EPA5). Of particular importance is the statement that “compliance is based upon the mean of the distribution of projected doses.” As discussed in conjunction with (EPA5), this requirement has a major effect on the conceptual and computational structure of the TSPA-LA.

Like the EPA in 40 CFR Part 197 (66 FR 32074 [DIRS 155216]), the NRC does not provide a definitive statement of what is intended by a mean dose. However, it seems reasonable to assume that the NRC was guided by the same perspectives with respect to the concept of a mean as expressed by the EPA in (EPA6) – (EPA8). The following statement by the NRC from 10 CFR Parts 2, 19, 20, 21, etc. (66 FR 55732 [DIRS 156671], p. 55752) actually provides a more specific indication of what is intended by a mean than any of the statements from the EPA:

The Commission expects that performance assessments conducted by the applicant in support of any potential license application will use probabilistic methods to simulate a wide range of possible future behaviors of the repository system. Each possible future behavior of the repository system is represented by a curve describing the annual dose to the RMEI as a function of time. Generally, but not necessarily, each of the possible curves is assumed to be equally likely. Because none of these possible futures can be demonstrated to describe the actual future behavior of the repository system, the Commission requires that the applicant calculate the mean of these dose versus time curves, properly weighted by their individual probabilities. (NRC6)

This statement specifically describes the weighting of doses by their likelihood of occurrence (i.e., a calculation involving answers to questions (Q1), (Q2) and (Q3)). However, no mention is made of uncertainty in the sense of question (Q4).

The description of a PA by the NRC in (NRC2) is at a very high level. Owing to the central role played by PA in the licensing of the Yucca Mountain facility, it is important to examine any additional statements made by the NRC with respect to the desired characteristics of a PA carried out for this purpose. Such statements help provide guidance with respect to the conceptual and computational structure of the TSPA-LA. Specifically, the following statement given in 10 CFR 63.102 (66 FR 55732 [DIRS 156671], p. 55805) helps provide insights with respect to what the NRC considers to be an appropriately designed and conducted PA:

- (j) *Performance assessment.* Demonstrating compliance with the postclosure performance objective specified at § 63.113(b) requires a performance assessment to quantitatively estimate radiological exposures to the reasonably maximally exposed individual at any time during the compliance period. The performance assessment is a systematic analysis that identifies the features, events, and processes (i.e., specific conditions or attributes of the geologic setting, degradation, deterioration, or alteration processes of engineered barriers, and interactions between the natural and engineered

barriers) that might affect performance of the geologic repository; examines their effects on performance; and estimates the radiological exposures to the reasonably maximally exposed individual. The features, events, and processes considered in the performance assessment should represent a wide range of both beneficial and potentially adverse effects on performance (e.g., beneficial effects of radionuclide sorption; potentially adverse effects of fracture flow or a criticality event). Those features, events, and processes expected to materially affect compliance with § 63.113(b) or be potentially adverse to performance are included, while events (event classes or scenario classes) that are very unlikely (less than one chance in 10,000 over 10,000 years) can be excluded from the analysis. An event class consists of all possible specific initiating events that are caused by a common natural process (e.g., the event class for seismicity includes the range of credible earthquakes for the Yucca Mountain site). Radiological exposures to the reasonably maximally exposed individual are estimated using the selected features, events, and processes, and incorporating the probability that the estimated exposures will occur. (NRC7)

The first three questions, (Q1) – (Q3), related to PA are clearly imbedded in the preceding description. For example, references to “events” and “event classes” involve the question (Q1): “What can happen?”; the statement “incorporating the probability that the estimated exposures will occur” involves the question (Q2): “How likely is it to happen?”; and statements such as “quantitatively estimate radiological exposures” and “examines their effects on performance” involve answering question (Q3): “What are the consequences if it does happen?”.

The NRC’s description of PA in (NRC7) does not include any statement that can be identified with question (Q4): “What is the uncertainty in the answers to the first three questions?” However, the answering of this question is clearly intended to be part of the NRC’s concept of what a PA should be as indicted in 10 CFR 63.114 (66 FR 55732 [DIRS 156671], p. 55807):

§ 63.114 Requirements for performance assessment.

Any performance assessment used to demonstrate compliance with § 63.113 must:

- (a) Include data related to the geology, hydrology, and geochemistry (including disruptive processes and events) of the Yucca Mountain site, and the surrounding region to the extent necessary, and information on the design of the engineered barrier system used to define parameters and conceptual models used in the assessment.
- (b) Account for uncertainties and variabilities in parameter values and provide for the technical basis for parameter ranges, probability distributions, or bounding values used in the performance assessment.
- (c) Consider alternative conceptual models of features and processes that are consistent with available data and current scientific understanding and

evaluate the effects that alternative conceptual models have on the performance of the geologic repository.

- (d) Consider only events that have at least one chance in 10,000 of occurring over 10,000 years.
- (e) Provide the technical basis for either inclusion or exclusion of specific features, events, and processes in the performance assessment. Specific features, events, and processes must be evaluated in detail if the magnitude and time of the resulting radiological exposures to the reasonably maximally exposed individual, or radionuclide releases to the accessible environment, would be significantly changed by their omission.
- (f) Provide the technical basis for either inclusion or exclusion of degradation, deterioration, or alteration processes of engineered barriers in the performance assessment, including those processes that would adversely affect the performance of natural barriers. Degradation, deterioration, or alteration processes of engineered barriers must be evaluated in detail if the magnitude and time of the resulting radiological exposures to the reasonably maximally exposed individual, or radionuclide releases to the accessible environment, would be significantly changed by their omission.
- (g) Provide the technical basis for models used in the performance assessment such as comparisons made with outputs of detailed process-level models and/or empirical observations (e.g., laboratory testing, field investigations, and natural analogs). (NRC8)

Statement (b) clearly involves asking and answering question (Q4). Further, much of the above statement involves the formulation of models used to answer question (Q3), and statement (d) involves obtaining answers to questions (Q1) and (Q2).

The following two statements from 10 CFR 63.101 (66 FR 55732 [DIRS 156671]) also indicate the importance that the NRC attaches to an adequate treatment of uncertainty:

For such long-term performance, what is required is reasonable expectation, making allowance for the time period, hazards, and uncertainties involved, that the outcome will conform with the objectives for postclosure performance for the geologic repository. Demonstrating compliance will involve the use of complex predictive models that are supported by limited data from field and laboratory tests, site-specific monitoring, and natural analog studies that may be supplemented with prevalent expert judgment. Compliance demonstrations should not exclude important parameters from assessments and analyses simply because they are difficult to precisely quantify to a high degree of confidence. The performance assessments and analyses should focus upon the full range of defensible and reasonable parameter distributions rather than only upon extreme physical situations and parameter values (66 FR 55732 [DIRS 156671], p. 55804).(NRC9)

Once again, although the criteria may be written in unqualified terms, the demonstration of compliance must take uncertainties and gaps in knowledge into account so that the Commission can make the specified finding with respect to paragraph (a)(2) of § 63.31 (66 FR 55732 [DIRS 156671], p. 55804). (NRC10)

Both the preceding statements clearly indicate that a realistic treatment of uncertainty should be a fundamental part of a PA used to support a licensing application for the Yucca Mountain facility.

In addition, a number of statements provided by the NRC as supplementary information with respect to 10 CFR Parts 2, 19, 20, 21, etc. (66 FR 55732 [DIRS 156671]) emphasize the importance that the NRC places on the assessment and representation of uncertainty:

Part 63 requires consideration of uncertainties in DOE's representation of the repository (uncertainty and variability in parameter values must be taken into account—§63.114(b)) and the events that can happen during the compliance period (consideration of potentially disruptive events with a probability of occurrence as low as one chance in 10,000 of occurring over 10,000 years—§ 63.114(d)) to be directly included in the quantitative estimate of performance (66 FR 55732 [DIRS 156671], p. 55747). (NRC11)

DOE is expected to conduct uncertainty analyses (i.e., evaluation of how uncertainty in parameter values affects uncertainty in the estimate of dose), including the consideration of disruptive events and associated probability of occurrence (66 FR 55732 [DIRS 156671], p. 55747). (NRC12)

The approach defined in part 63, which requires DOE to fully address uncertainties in its performance assessment rather than requiring DOE to meet a specific level of uncertainty, is appropriate. The treatment of uncertainty in DOE's performance assessment will be an important part of NRC's review (66 FR 55732 [DIRS 156671], p. 55748). (NRC13)

The statement in (NRC11) is particularly interesting because it involves three distinct concepts related to uncertainty: (i) uncertainty in the epistemic or subjective sense related to knowledge about the appropriateness of assumptions used in an analysis, (ii) spatial variability, and (iii) uncertainty in the aleatory sense related to events that may, or may not, occur in the future. The statement in (NRC12) is informative because it goes beyond asking for an analysis that simply calculates a mean outcome; in particular, it asks for an uncertainty analysis which evaluates "how uncertainty in parameter values affects uncertainty in the estimate of dose," which involves a more complex analysis than simply calculating a mean dose. Finally, the statement in (NRC13) expresses the importance that the NRC places on an adequate treatment of uncertainty.

This section ends by recording several statements by the NRC that relate to the nature of occurrences (i.e., the events of the phrase "features, events and processes") that should, and should not, be included in a PA for the Yucca Mountain facility:

Event sequence means a series of actions and/or occurrences within the natural and engineered components of a geologic repository operations area that could

potentially lead to exposure of individuals to radiation. An event sequence includes one or more initiating events and associated combinations of repository system component failures, including those produced by the action or inaction of operating personnel (66 FR 55732 [DIRS 156671], p. 55793). (NRC14)

Initiating event means a natural or human induced event that causes an event sequence (66 FR 55732 [DIRS 156671], p. 55794). (NRC15)

§ 63.305 Required characteristics of the reference biosphere.

- (a) Features, events, and processes that describe the reference biosphere must be consistent with present knowledge of the conditions in the region surrounding the Yucca Mountain site.
- (b) DOE should not project changes in society, the biosphere (other than climate), human biology, or increases or decreases of human knowledge or technology. In all analyses done to demonstrate compliance with this part, DOE must assume that all of those factors remain constant as they are at the time of submission of the license application.
- (c) DOE must vary factors related to the geology, hydrology, and climate based upon cautious, but reasonable assumptions consistent with present knowledge of factors that could affect the Yucca Mountain disposal system over the next 10,000 years.
- (d) Biosphere pathways must be consistent with arid or semi-arid conditions (66 FR 55732 [DIRS 156671], p. 55813). (NRC16)

DOE's performance assessments should not include consideration of very unlikely features, events, or processes, i.e., those that are estimated to have less than one chance in 10,000 of occurring within 10,000 years of disposal. (10 CFR 63.342 (66 FR 55732 [DIRS 156671], p. 55815); see also revision dated Oct. 8, 2002) (NRC17)

These statements are included because they relate to what is to be included in the conceptual and computational structure of the TSPA-LA.

Finally, it is important to realize that the NRC does not view a PA in support of a licensing application for the Yucca Mountain facility as a risk assessment in the traditional sense of the phrase. In particular, the dose to the RMEI is used as a means to convert potential radionuclide releases into intuitively interpretable quantities (i.e., doses). However, owing to the prescribed and stylized manner in which doses to the RMEI are defined and calculated, they do not realistically represent actual doses to individuals in the future and thus should not be viewed as the consequence component of a risk calculation. This point is emphasized by the NRC in the following statement:

However, it should be kept in mind that the performance assessment evaluates "potential" doses, not "actual" doses. For example, part 63 requires the

performance assessment to assume for the next 10,000 years that the reasonably maximally exposed individual (RMEI) is a member of a community that: (1) Exists where it will intercept potential releases from the repository and (2) uses ground water but never tests the quality of this water nor treats the ground water to remove any contaminants. This specification is considered appropriately conservative for evaluating performance but most likely is not an “accurate” prediction of what will happen during the next 10,000 years (see discussion under RMEI Characteristics and Reference Biosphere for more information on the RMEI). Although the Commission does not require an “accurate” prediction of the future, uncertainty in performance estimates cannot be so large that the Commission cannot find a reasonable expectation that the postclosure performance objectives will be met (see discussion under Reasonable Expectation) (66 FR 55732 [DIRS 156671], p. 55748). (NRC18)

Thus, although a PA in support of a licensing application will have the same conceptual and computational structure as a risk assessment, the actual dose results cannot be given a risk-based interpretation.

J2.3 EPA Requirements: 40 CFR Part 197 after Remand

The revised standards for the Yucca Mountain facility proposed by the EPA after the remand leave the dose requirements for the first 10⁴ year after repository closure unchanged (i.e., the requirement that the maximum dose to the RMEI is to be less than 15 mrem/yr). However, subsequent to the initial 10⁴ year period, a new bounding dose requirement is imposed. This requirement specifies a bound of 350 mrem/yr on the dose to the RMEI after the initial 10⁴ year period, with this bound required to hold over the period of geologic stability. Specifically, the requirement in (EPA1) is replaced by the following requirement (70 FR 49014 [DIRS 177357], p. 49063):

§ 197.20 What standard must DOE meet?

- (a) The DOE must demonstrate, using performance assessment, that there is a reasonable expectation that the reasonably maximally exposed individual receives no more than the following annual committed effective dose equivalent from releases from the undisturbed Yucca Mountain disposal system:
 - (1) 150 microsieverts (15 millirems) for 10,000 years following disposal; and
 - (2) 3.5 millisieverts (350 millirems) after 10,000 years, but within the period of geologic stability.
- (b) The DOE’s performance assessment must include all potential pathways of radionuclide transport and exposure. (EPA13)

Except for the addition of the 350 mrem/yr dose requirement after 10⁴ yr, the above requirement is the same as specified in (EPA1). As noted in conjunction with (EPA1), a careful reading of the

preceding requirement gives rise to three questions: (i) “What is a PA?”, (ii) “What is reasonable expectation?”, and (iii) “What is the RMEI?”. The answers to these questions provided in the proposed revision to 40 CFR Part 197 (70 FR 49014 [DIRS 177357]) are effectively the same as given in the statements (EPA2), (EPA3) and (EPA4) taken from the original promulgation of 40 CFR Part 197 (66 FR 32074 [DIRS 155216]).

In turn, the EPA’s original guidance on the implementation of the 10^4 yr dose standards stated in (EPA5) is revised in the proposed standard to include the time period after 10^4 yr. Specifically, the requirement in (EPA5) is replaced by the following requirement (70 FR 49014 [DIRS 177357], p. 49063):

§ 197.13 How is subpart B implemented?

- (a) The NRC will determine compliance based upon the arithmetic mean of the projected doses from DOE’s performance assessments for the period within 10,000 years after disposal:
 - (1) For § 197.20 of this subpart; and
 - (2) For §§ 197.25 and 197.30 of this subpart, if performance assessment is used to demonstrate compliance with either or both of these sections.
- (b) NRC will determine compliance based upon the median of the projected doses from DOE’s performance assessments for the period after 10,000 years of disposal and through the period of geologic stability:
 - (1) For § 197.20 of this subpart; and
 - (2) For § 197.25, if a performance assessment is used to demonstrate compliance. (EPA14)

The part of the preceding statement relating to dose in the initial 10^4 yr time period is effectively the same as the statement in (EPA5) from the original promulgation of 40 CFR Part 197 (66 FR 32074 [DIRS 155216]). However, the second part relating to dose after 10^4 yr is different. Specifically, a bound of 350 mrem/yr on the median dose to the RMEI is imposed.

The interpretation of what is intended by the specification of a mean dose is extensively discussed in Sections J2.1 and J2.2. The actual calculation of mean dose in the TSPA-LA is discussed in detail in Section J4, where the descriptor expected dose rather than mean dose is used for consistency with standard terminology used in probability and statistical theory. As discussed in Section J4, there are actually two expectations that underlie the “mean” dose specified by the EPA: an expectation over random events that could occur in the future (i.e., over aleatory uncertainty) and an expectation over the appropriate values to use for quantities that are assumed to have fixed but poorly known values in the computational implementation of the TSPA-LA (i.e., over epistemic uncertainty). Expected dose over aleatory uncertainty at a specific point in time corresponds to the concept of individual risk that the NAS committee (National Research Council 1995 [DIRS 100018]) recommended as the basis of regulations for the Yucca Mountain facility; specifically, only a scalar multiplier is needed to convert from expected dose

over aleatory uncertainty to individual risk. In turn, the distribution of expected dose over aleatory uncertainty at a specific point in time that results from epistemic uncertainty provides the representation of uncertainty in TSPA-LA results repeatedly requested by the NAS committee, the EPA and the NRC. To have a unique regulatory quantity, the distribution of expected dose over aleatory uncertainty at a specific point in time can itself be reduced to an expected value (i.e., an expected value over both aleatory and epistemic uncertainty). Then, the specified bound of 15 mrem/yr can be applied to the expected doses over aleatory and epistemic uncertainty for the time interval $[0, 10^4 \text{ yr}]$. The calculations indicated in this paragraph are extensively discussed and illustrated later in this appendix.

For the post 10^4 yr time period, the EPA specifies that the median dose to the RMEI is to be bounded by 350 mrem/yr. This specification immediately raises the question of how to define median dose to the RMEI. The view taken in the development of the TSPA-LA is that median dose should be defined in a manner consistent with both the NAS committee's recommendations and the calculation of mean dose for the initial 10^4 yr period. Consistent with this view, the median dose at a specific point in time is defined in the TSPA-LA as the median of the expected doses over aleatory uncertainty at that time. Thus, median doses are based on the same conceptual epistemic uncertainty distributions for expected dose over aleatory uncertainty that are used to determine mean doses for the time interval $[0, 10^4 \text{ yr}]$. The only difference is that for the $[0, 10^4 \text{ yr}]$ time interval, the distributions of expected dose over aleatory uncertainty are summarized with their means and for the post 10^4 yr time period, the distributions of expected dose over aleatory uncertainty are summarized with their medians. With this approach, the definition of median dose is consistent with the NAS committee's recommendation that the Yucca Mountain facility should be regulated on the basis of risk to an individual and is also consistent with the determination of mean dose as the determination of mean and median doses use conceptually identical distributions. The calculations indicated in this paragraph are extensively discussed and illustrated later in this appendix.

The preceding definitions indicated for mean and median dose involve summarizing distributions for expected dose over aleatory uncertainty at specific points in time. The following statement appears in the introductory discussion associated with the proposed revisions to 40 CFR Part 197 and could be interpreted as implying different definitions for mean and median dose than those just indicated (70 FR 49014 [DIRS 177357], p. 49042): "A distribution of projected peak doses will result from these analyses, each representing a possible "future" and a dose associated with the specific parameter values chosen for each calculation." This statement appears to imply that a peak dose should be determined for each possible future. Then, means and medians could be extracted from the resulting distributions of peak dose (i.e., one peak dose distribution for the $[0, 10^4 \text{ yr}]$ time interval and one peak dose distribution for the post 10^4 yr time interval). With this approach, the indicated peak doses could possibly occur at a different time for each future. The TSPA-LA does not use distributions of peak dose defined in this manner for two reasons. First, use of this approach loses the concept of individual risk that is prominent in the recommendations of the NAS committee. Specifically, the combining of likelihood and consequence that is essential to the concept of individual health risk is lost. Second, the effects of half of all possible futures are eliminated from consideration. As a notional example, if 51 percent of all possible futures result in no dose and 49 percent all possible futures result in a peak dose greater than 1000 mrem/yr, then the median dose would be 0 mrem/yr. As long as

51 percent of the possible futures result in no dose, the peak doses associated with the remaining 49 percent of the futures will have no effect on the median peak dose. Because of the preceding considerations, the TSPA-LA bases its determinations of mean and median doses on distributions of expected doses over aleatory uncertainty at individual points in time rather than on distributions of peak dose over time.

In effect, what the EPA refers to as projected doses in (EPA5) and (EPA14) are assumed to be expected doses over aleatory uncertainty in the TSPA-LA for comparisons with the indicated regulatory requirements. Then, means or medians as appropriate for the time interval under consideration are determined. Because of this, the projected doses under consideration are not actual doses but rather are probabilistically weighted doses. However, because it is important not to lose the actual dose results that are being probabilistically weighted, presentations later in this appendix will show both original unweighted doses and the resultant probabilistically weighted doses.

J2.4 NRC Requirements: 10 CFR Parts 2, 19, 20, 21, etc. after Remand

The NRC has revised its standards for the Yucca Mountain facility for consistency with the revised standards proposed by the EPA. As in the EPA's proposed standards, the dose requirements for the first 10^4 yr after repository closure unchanged (i.e., the requirement that the maximum dose to the RMEI is to be less than 15 mrem/yr). However, subsequent to the initial 10^4 yr period, a new bounding dose requirement is imposed. This requirement specifies a bound of 350 mrem/yr on the dose to the RMEI after the initial 10^4 yr period, with this bound required to hold over the period of geologic stability. Specifically, the requirement in (NRC1) is replaced by the following requirement (70 FR 53313 [DIRS 178394], p. 53319):

§ 63.311 Individual protection standard after permanent closure.

- (a) DOE must demonstrate, using performance assessment, that there is a reasonable expectation that the reasonably maximally exposed individual receives no more than the following annual dose from releases from the undisturbed Yucca Mountain disposal system:
 - (1) 0.15 mSv (15 mrem) for 10,000 years following disposal; and
 - (2) 3.5 mSv (350 mrem) after 10,000 years, but within the period of geologic stability.
- (b) DOE's performance assessment must include all potential environmental pathways of radionuclide transport and exposure. (NRC19)

Except for minor differences in wording, the preceding standard is the same as the proposed standard specified by the EPA in (EPA13). Thus, the NRC has simply repeated back the EPA's individual protection standard.

In turn, the NRC's gives the following guidance on implementing the preceding individual protection standard (70 FR 53313 [DIRS 178394], p. 53319):

§ 63.303 Implementation of Subpart L.

- (a) Compliance is based upon the arithmetic mean of the projected doses from DOE's performance assessments for the period within 10,000 years after disposal for:
 - (1) § 63.311(a)(1); and
 - (2) §§ 63.321(b)(1) and 63.331, if performance assessment is used to demonstrate compliance with either or both of these sections.

- (b) Compliance is based upon the median of the projected doses from DOE's performance assessments for the period after 10,000 years of disposal and through the period of geologic stability for:
 - (1) § 63.311(a)(2); and
 - (2) § 63.321(b)(2), if performance assessment is used to demonstrate compliance. (NRC20)

Except for minor changes in wording, the preceding implementation guidance is identical with the guidance given by the EPA in (EPA14).

The requirements for the time interval $[0, 10^4 \text{ yr}]$ are unchanged. Thus, the discussion in Section J2.2 with respect to this time interval remains unchanged. The NRC is rather sparse in its preliminary discussion of its proposed rule change (70 FR 53313 [DIRS 178394]). Thus, it seems reasonable to assume that the core ideas given in the original promulgation of 10 CFR Parts 2, 19, 20, 21, etc. [DIRS 156671] and summarized in Section J2.2 continue to remain valid. The major change to the present NRC's proposed rule is the addition of the bound of 350 mrem/yr on the median dose to the RMEI after the initial 10^4 yr period. In addressing this bound, the TSPA-LA follows the conceptual and computational approach indicated at the end of Section J2.3. A more detailed description of the determination of mean and median doses in the TSPA-LA is given in Section J4.

J2.5 Yucca Mountain Review Plan

In addition to the NRC rule 10 CFR Parts 2, 19, 20, 21, etc. (66 FR 55732 [DIRS156671], 70 FR 53313 [DIRS 178394]), the NRC has published an extensive review plan for the Yucca Mountain facility, the *Yucca Mountain Review Plan, Final Report* (YMRP), to guide its assessment of the DOE's license application (NRC 2003 [DIRS 163274]). Selected portions of the YMRP (NRC 2003 [DIRS 163274]) that specifically relate to the conceptual and computational structure of the TSPA-LA are presented in this section. The YMRP (NRC 2003 [DIRS 163274]) is a large and detailed document. No attempt is made to summarize everything in it that relates to the TSPA-LA. Rather, only selected material that specifically relates to the overall structure of the TSPA-LA is presented.

Early in the YMRP, the NRC specifically acknowledges that the DOE's license application is to be based on a detailed PA (NRC 2003 [DIRS 163274], p. 2.2-1):

Risk-Informed Review Process for Performance Assessment—The performance assessment quantifies repository performance, as a means of demonstrating compliance with the postclosure performance objectives at 10 CFR 63.113 [DIRS 180319]. The U.S. Department of Energy performance assessment is a systematic analysis that answers the triplet risk questions: what can happen; how likely is it to happen; and what are the consequences. (YMRP1)

The “triplet” referred to above is the classic Kaplan-Garrick ordered triple definition of risk (Kaplan and Garrick 1981 [DIRS 100557]) that evolved out of the Reactor Safety Study conducted by the NRC in the mid 1970s (NRC 1975 [DIRS 107799]) and other reactor probabilistic risk assessments carried out in the late 1970s and early 1980s (PLG 1983 [DIRS 148063]; PLG 1983 [DIRS 107813]; PLG 1982 [DIRS 107812]). This risk representation also provided the conceptual and organizational basis for the NRC’s reassessment of the risk from commercial nuclear power reactors carried out in the late 1980s (i.e., NUREG-1150: NRC 1990 [DIRS 107798]; Breeding et al. 1992 [DIRS 107727]) and the DOE’s PA in support of a successful certification application to the EPA for the Waste Isolation Pilot Plant (WIPP) in the mid 1990s (DOE 1996 [DIRS 100975]; Helton and Marietta 2000 [DIRS 171759]). The three indicted questions have already been referred to as questions (Q1), (Q2), and (Q3) in Section J2.1. As a reminder, there is also a fourth question (i.e., Q4): “What is the uncertainty in the answers to the first three questions?”, or equivalently, “How much confidence do you have in the answers to the first three questions?”.

The NRC provides three acceptance criteria, with multiple subparts, to be used in judging the DOE’s success in meeting regulatory standards related to the use of PA to assess compliance with the postclosure individual protection requirement (i.e., NRC1). These criteria follow (NRC 2003 [DIRS 163274], pp. 2.2-133 and 2.2-134):

Acceptance Criterion 1: Scenarios Used in the Calculation of the Annual Dose as a Function of Time Are Adequate.

- (1) The annual dose as a function of time includes all scenario classes that have been determined to be sufficiently probable, or to have a sufficient effect on overall performance that they could not be screened from the total system performance assessment analyses; and (YMRP2)
- (2) The calculation of the annual dose curve appropriately sums the contribution of each of the disruptive event scenario classes. The contribution to the annual dose from each scenario class calculation properly accounts for the effects that the time of occurrence of the disruptive events comprising the scenario class has on the consequences. The annual probability of occurrence of the events used to calculate the contribution to the annual dose is consistent with the results of the scenario analysis. The probabilities of occurrence of all scenario classes, included in calculating the annual dose curve, sum to one. (YMRP3)

Acceptance Criterion 2: An Adequate Demonstration Is Provided That the Annual Dose to the Reasonably Maximally Exposed Individual in Any Year During the Compliance Period Does Not Exceed the Exposure Standard.

- (1) A sufficient number of realizations has been obtained, for each scenario class, using the total system performance assessment code, to ensure that the results of the calculations are statistically stable; (YMRP4)
- (2) The annual dose curve includes confidence intervals (e.g., 95th and 5th percentile) to represent the uncertainty in the dose calculations; (YMRP5)
- (3) Repository performance and the performance of individual components or subsystems are consistent and reasonable; and (YMRP6)
- (4) The total system performance assessment results confirm that the repository performance results in annual dose, to the reasonably maximally exposed individual, in any year, during the compliance period, that does not exceed the postclosure individual protection standard. (YMRP7)

Acceptance Criterion 3: The Total System Performance Assessment Code Provides a Credible Representation of Repository Performance.

- (1) Assumptions made within the total system performance assessment code are consistent among different modules of the code. The use of assumptions and parameter values that differ among modules of the code is adequately documented; (YMRP8)
- (2) The total system performance assessment code is properly verified, such that there is confidence that the code is modeling the physical processes in the repository system in the manner that was intended. The transfer of data between modules of the code is conducted properly; (YMRP9)
- (3) The estimate of the uncertainty in the performance assessment results is consistent with the model and parameter uncertainty; and (YMRP10)
- (4) The total system performance assessment sampling method ensures that sampled parameters have been sampled across their ranges of uncertainty.(YMRP11)

The preceding acceptance criteria are basically describing what should be expected of any modern PA. Examples of such PAs include the NRC's reassessment of the risk from commercial nuclear power plants ([DIRS 107798], [DIRS 107727]) and the DOE's successful Compliance Certification Application for the Waste Isolation Pilot Plant ([DIRS 100975], [DIRS 171759]).

J3 TUTORIAL ON PROBABILITY, UNCERTAINTY AND THE STRUCTURE OF PERFORMANCE ASSESSMENTS

As clearly indicated by the material presented in Section J2, probability and the treatment of uncertainty are fundamental components of a PA in support of a licensing application for the

Yucca Mountain facility. In particular, determination of expected (i.e., mean) and median dose to the RMEI is an inherently probabilistic calculation. For convenience and to standardize the use of certain terminology, a brief tutorial on probability and uncertainty follows.

J3.1 Probability and the Representation of Uncertainty

Three basic components are involved in a formal definition of probability: a set S that contains everything that could occur in the particular universe under consideration; a suitably restricted collection Σ of subsets of S for which probability is defined; and a function p that defines probability for the elements of Σ (Feller 1971 [DIRS 107822], Section IV.3). At an intuitive level, Σ can be thought of as containing all possible subsets of S . However, to obtain a mathematically rigorous development of probability, Σ and p must have the following properties: (i) if $\mathcal{E} \in \Sigma$, then $\mathcal{E}^c \in \Sigma$, where the superscript c is used to denote the complement of \mathcal{E} , (ii) if $\{\mathcal{E}_i\}$ is a countable collection of elements of Σ , then $\cup_i \mathcal{E}_i$ and $\cap \mathcal{E}_i$ are also elements of Σ , (iii) $p(S) = 1$, (iv) if $\mathcal{E} \in \Sigma$, then $0 \leq p(\mathcal{E}) \leq 1$, and (v) if $\{\mathcal{E}_i\}$ is a countable collection of disjoint elements of Σ (i.e., $\mathcal{E}_i \cap \mathcal{E}_j = \emptyset$ for $i \neq j$), then $p(\cup_i \mathcal{E}_i) = \sum_i p(\mathcal{E}_i)$. The triple (S, Σ, p) is called a probability space and is the fundamental mathematical structure that underlies a careful development of probability. In the usual terminology of probability theory, S is called the sample space; elements of S are called elementary events; elements of Σ are called events; and p is called a probability measure. The idea of a probability space is introduced in this presentation primarily as a notational convenience to facilitate in distinguishing between different uses of probability and in describing the calculation of expected values and distributions.

Although the concept of a probability space is important conceptually and convenient notationally, calculations involving a probability space (S, Σ, p) are often described with a density function d , where

$$p(\mathcal{E}) = \int_{\mathcal{E}} d(\mathbf{x}) d\mathcal{E} \quad (\text{Eq. J3.1-1})$$

for $\mathcal{E} \in \Sigma$, $\mathbf{x} \in \mathcal{E}$, and $d\mathcal{E}$ corresponding to an increment of volume from \mathcal{E} . Then, the expected value, variance, cumulative distribution function (CDF), and complementary cumulative distribution function (CCDF) associated with a real-valued function $y = f(\mathbf{x})$ defined on S are given by

$$E(y) = E[f(\mathbf{x})] = \int_S f(\mathbf{x}) d(\mathbf{x}) dS, \quad (\text{Eq. J3.1-2})$$

$$V(y) = V[f(\mathbf{x})] = \int_S [f(\mathbf{x}) - E(y)]^2 d(\mathbf{x}) dS, \quad (\text{Eq. J3.1-3})$$

$$\text{prob}(\tilde{y} \leq y) = \text{prob}[f(\mathbf{x}) \leq y] = \int_S \delta_y[f(\mathbf{x})] d(\mathbf{x}) dS \quad (\text{Eq. J3.1-4})$$

and

$$prob(\tilde{y} > y) = prob[f(\mathbf{x}) > y] = \int_S \bar{\delta}_y[f(\mathbf{x})] d(\mathbf{x}) dS, \quad (\text{Eq. J3.1-5})$$

respectively, where

$$\underline{\delta}_y[f(\mathbf{x})] = \begin{cases} 1 & \text{if } f(\mathbf{x}) \leq y \\ 0 & \text{otherwise} \end{cases} \quad \text{and} \quad \bar{\delta}_y[f(\mathbf{x})] = 1 - \underline{\delta}_y[f(\mathbf{x})] = \begin{cases} 1 & \text{if } f(\mathbf{x}) > y \\ 0 & \text{otherwise} \end{cases} \quad (\text{Eq. J3.1-6})$$

and dS represents an increment of volume from S . Specifically, $prob(\tilde{y} \leq y)$ denotes the probability that $f(\mathbf{x})$ has a value less than or equal to y ; $prob(\tilde{y} > y)$ denotes the probability that $f(\mathbf{x})$ has a value greater than y ; the points $[y, prob(\tilde{y} \leq y)]$ define the CDF for y ; and the points $[y, prob(\tilde{y} > y)]$ define the CCDF for y .

In turn, the q quantile value (e.g., $q = 0.05, 0.5, 0.95$) for $y = f(\mathbf{x})$ is the value y such that

$$q = prob(\tilde{y} \leq y) = \int_S \underline{\delta}_y[f(\mathbf{x})] d(\mathbf{x}) dS. \quad (\text{Eq. J3.1-7})$$

Specifically, the value y for which

$$0.5 = prob(\tilde{y} \leq y) = \int_S \underline{\delta}_y[f(\mathbf{x})] d(\mathbf{x}) dS \quad (\text{Eq. J3.1-8})$$

is the median value for $y = f(\mathbf{x})$. Notationally, the q quantile value for $y = f(\mathbf{x})$ can be represented by $Q_q(y) = Q_q[f(\mathbf{x})]$. The results in Equations J3.1-7 and J3.1-8 determine $Q_q[f(\mathbf{x})]$ on the basis of the CDF for $y = f(\mathbf{x})$. Equivalently, the value y such that

$$1 - q = prob(\tilde{y} > y) = \int_S \bar{\delta}_y[f(\mathbf{x})] d(\mathbf{x}) dS \quad (\text{Eq. J3.1-9})$$

defines $Q_q[f(\mathbf{x})]$ on the basis of the CCDF for $y = f(\mathbf{x})$.

Results of risk analyses are typically represented with CCDFs rather than CDFs. In particular, a CCDF answers the question ‘‘How likely is it to be this bad or worse?’’, which is usually the question asked with respect to individual consequences in a risk assessment. In contrast, CDFs are usually used as the basis for defining quantiles. However, conversion between CCDFs and CDFs is straightforward as the probabilities defining a CDF are simply one minus the corresponding probabilities defining a CCDF (i.e., $prob(\tilde{y} \leq y) = 1 - prob(\tilde{y} > y)$) and vice versa (i.e., $prob(\tilde{y} > y) = 1 - prob(\tilde{y} \leq y)$).

As discussed in Section J4, expected values of the form defined in Equation J3.1-2 and medians of the form defined in Equation J3.1-8 are of central importance in the EPA’s and the NRC’s regulations for the Yucca Mountain facility.

Before continuing, two technical observations are made. First, the preceding development of expected value and related quantities is done at an intuitive level using density functions and the Riemann integral. A more formal development using measure theory and the Lebesgue integral

is also possible but would not be helpful at an intuitive level. Second, the function $\bar{\delta}_y[f(\mathbf{x})]$ defined in Equation J3.1-6 is effectively the same as the Heaviside function and should not be confused with the Dirac delta function.

The representation and incorporation of uncertainty figures prominently in the EPA's and NRC's standards for the Yucca Mountain facility. For example, see references to uncertainty in statements (EPA2), (EPA3), and (EPA5) – (EPA12) by the EPA and in statements (NRC2), (NRC3), and (NRC5) – (NRC13) by the NRC. In addition, statements such as (YMRP1) – (YMRP5), (YMRP10), and (YMRP11) in the NRC's YMRP also relate to the importance attached to the representation of uncertainty.

Examination of the indicated statements shows that three different concepts of uncertainty are involved in PA for the Yucca Mountain facility: (i) uncertainty about what will happen in the future, (ii) uncertainty about parameters, models, and other analysis assumptions, and (iii) variability.

Uncertainty about what will happen in the future can be seen in statements such as (i) “weighted by their probability of occurrence” in (EPA2) and (NRC2), (ii) “Because none of these possible futures can be demonstrated to describe the actual future behavior of the repository system, the Commission requires that the applicant calculate the mean of these dose curves, properly weighted by their individual probabilities” in (NRC6), and (iii) “The probabilities of occurrence of all scenario classes, included in calculating the annual dose curve sum to one” in (YMRP3). Uncertainty of the type indicated in the preceding statements about events whose future occurrence is assumed to be random, at least insofar as our ability to forecast such occurrences is concerned, is called aleatory uncertainty (Helton and Burmaster 1996 [DIRS 107498]; Paté-Cornell 1996 [DIRS 107499]; Helton 1997 [DIRS 107496]). Other descriptors sometimes used in the designation of aleatory uncertainty include stochastic, type A and irreducible. The preceding statements indicate that the EPA and the NRC intend for probability to be used in the mathematical characterization of aleatory uncertainty. Thus, underlying the TSPA-LA, there must be a probability space (\mathcal{A}, A, p_A) for aleatory uncertainty. The general nature of the probability space (\mathcal{A}, A, p_A) will be discussed in more detail in Section J3.3.

Uncertainty about parameters, models and other analysis assumptions can be seen in statements such as (i) “focuses performance assessments and analyses upon the full range of defensible and reasonable parameter distributions” in (EPA3) and (NRC3), (ii) “Account for uncertainties and variabilities in parameter values and provide for the technical basis for parameter ranges, probability distributions, or bounding values used in the performance assessment” in (NRC8), (iii) “performance assessments and analyses should focus on the full range of defensible and reasonable parameter distributions” in (NRC9), and (iv) “The estimate of the uncertainty in the performance assessment results is consistent with the model and parameter uncertainty” in (YMRP10). Uncertainty of the type indicated in the preceding statements derives from a lack of knowledge about a quantity, a model or an assumption assumed to have a fixed value in the context of a specific analysis and is usually referred to as epistemic uncertainty (Helton and Burmaster 1996 [DIRS 107498]; Paté-Cornell 1996 [DIRS 107499]; Helton 1997 [DIRS 107496]). Other descriptors sometimes used in the designation of epistemic uncertainty include subjective, state of knowledge, type B and reducible. The preceding statements indicate

that the EPA and the NRC intend for probability to be used in the mathematical characterization of the epistemic uncertainty. Thus, underlying the TSPA-LA, there must be a probability space $(\mathcal{E}, \mathcal{E}, p_E)$ for epistemic uncertainty. The general nature of the probability space $(\mathcal{E}, \mathcal{E}, p_E)$ will be discussed in more detail in Section J3.5.

Recognition of the potential importance of variability in assessing the compliance of the Yucca Mountain facility with applicable standards is demonstrated by references to “variability” in (NRC8) and (NRC11). In the two indicated quotes, variability appears in conjunction with uncertainty in the statements “Account for uncertainties and variabilities in parameter values” in (NRC8) and “uncertainty and variability in parameter values must be taken into account” in (NRC11). However, uncertainty in the sense of epistemic uncertainty and variability in the sense of a quantity having different values as a function of space and/or time are very different concepts. In particular, (epistemic) uncertainty involves a lack of knowledge about the appropriate value to use for a quantity that is assumed to have a fixed value in the context of a particular analysis. In the TSPA-LA, probability is used to characterize such uncertainty. In contrast, variability in a quantity is characterized in the TSPA-LA as a function of space and/or time (e.g., $f(x, y)$, $f(x, y, z)$, $f(x, y, z, t)$, $f(t)$, ..., where x, y and z correspond to spatial coordinates and t corresponds to time). For some quantities, functions of the form just indicated are used as input to the TSPA-LA (e.g., infiltration is both spatially and temporally variable); for other quantities, spatial and/or temporal variability is reduced to an expected value over space and/or time, and then this expected value is used as input to the TSPA-LA (e.g., quantities involved in ground water flow and transport such as porosities, fracture spacings and distribution coefficients are spatially-averaged quantities).

An important point to recognize is that there is almost always epistemic uncertainty in the characterization of variability. For example, if a function $f(x, y)$ characterizes the two-dimensional variability of some quantity, there are most likely many possible values for this function of varying levels of credibility. Thus, the function $f(x, y)$ characterizes spatial variability, but a lack of knowledge with respect to how to exactly define $f(x, y)$ is epistemic uncertainty. Similarly, there can be, and almost always is, epistemic uncertainty with respect to the values of quantities used in the characterization of aleatory uncertainty. For example, the occurrence of a certain process (e.g., volcanism) might be assumed to follow a Poisson process with a rate constant λ (units: yr^{-1}). The rate constant λ characterizes aleatory uncertainty and gives rise to probabilities of volcanic events occurring over time intervals of different lengths. However, the inability to confidently assign an exact value for λ is epistemic uncertainty.

It is worthwhile to briefly consider the phrases “features, events, and processes, and sequences of events and processes” and “features, events and processes” that appear often in the EPA and NRC standards for the Yucca Mountain facility (e.g., EPA2, NRC2, NRC7, NRC8, and NRC16). As suggested by its name, a feature is a large-scale property of the system under consideration (e.g., a fault, a geologic formation, an aquifer, ...). A feature either exists or it does not exist. There can be epistemic uncertainty about whether or not a feature exists (i.e., maybe it is there or maybe it is not there) and also epistemic uncertainty about the properties of a feature (e.g., permeability, porosity, fracture spacing, thermal conductivity, ...). Often, there is spatial variability in the properties of a feature. There can also be epistemic uncertainty in how to define such variability. However, as previously discussed, variability and epistemic uncertainty

are distinct concepts. An event is something that occurs over a very short period of time (e.g., igneous or seismic occurrences); in essence, an event is a discontinuity in the behavior of the system that occurs at a specific point in time. The occurrence, or nonoccurrence, of events is considered to be aleatory uncertainty and is distinct from epistemic uncertainty. However, there can be epistemic uncertainty in quantities used to characterize aleatory uncertainty (e.g., means, standard deviations, occurrence rates, ...). The reference to “sequence of events” derives from the fact that the occurrence of one or more aleatory events is always considered over some period of time (e.g., 0 to 10,000 yr in parts of the regulations for the Yucca Mountain facility); such sequences of events correspond to elementary events associated with the probability space for aleatory uncertainty. A process is something that takes place continuously over a long period of time (e.g., groundwater flow, heat flow, corrosion, ...). Although a process may be, but is not necessarily, initiated by a specific aleatory event, it is usually represented by a model (e.g., a system of ordinary or partial differential equations) that predicts the time-dependent, and often spatially dependent, behavior of the process. Often, there is substantial epistemic uncertainty associated with the model inputs used in modeling complex processes (e.g., dual porosity fluid flow and solute transport in a fractured geologic medium) and there can also be epistemic uncertainty with respect to the choice of a model itself (i.e., model uncertainty as it is sometimes called).

The dual use of probability to represent both aleatory uncertainty and epistemic uncertainty, as is done in the TSPA-LA, can be traced back to the beginnings of the formal development of probability theory in the late sixteen hundreds (Hacking 1975 [DIRS 107512], Section 2; Shafer 1978 [DIRS 159070]; Bernstein 1996 [DIRS 105742], pp. 47 to 56; Rechar 1999 [DIRS 145383]). The use of probability in PAs for complex systems is a topic of wide interest and many references are available that provide additional information and perspectives on this use (Paté-Cornell 1996 [DIRS 107499]; Helton 1997 [DIRS 107496], Section 4; Parry and Winter 1981 [DIRS 159059]; Paté-Cornell 1986 [DIRS 170519]; Apostolakis 1989 [DIRS 107710]; Apostolakis 1990 [DIRS 107506]; Helton 1994 [DIRS 107739]; Hoffman and Hammonds 1994 [DIRS 107502]; Kaplan 1993 [DIRS 107741]).

J3.2 Conceptual Structure of a Performance Assessment

A PA for a radioactive waste disposal facility or some other large engineered facility is a very complex undertaking requiring large amounts of information and a variety of mathematical models. Full documentation of a PA can require 1000s of pages of text. Yet, at a conceptual level, the computational implementation of a PA can be viewed as involving three basic entities: (i) EN1, a probabilistic characterization of what could occur at the facility under consideration; (ii) EN2, mathematical models for estimating the consequences of what could occur; and (iii) EN3, a probabilistic characterization of the uncertainty in the parameters used in the definitions of EN1 and EN2. The term parameter in the definition of EN3 is used broadly enough to include designators for alternative models or model structures. Despite the complexity of a PA, much of the overarching conceptual and computational structure of a PA can be described in terms of the preceding three entities. In particular, EN1 corresponds to the probabilistic characterization of aleatory uncertainty used in the analysis; EN2 corresponds to the mathematical models for physical processes used in the analysis; and EN3 corresponds to the probabilistic characterization of epistemic uncertainty used in the analysis. The nature of EN1,

EN2 and EN3 is discussed further in Sections J3.3 – J3.5. This discussion is adapted in part from Helton (2003 [DIRS 170558]).

J3.3 EN1: Probabilistic Characterization of Aleatory Uncertainty

The first entity, EN1, is the probability space (\mathcal{A}, A, p_A) associated with aleatory uncertainty. This probability space is intended to provide a mathematical description of those occurrences that could take place at some time in the future with sufficient likelihood and consequence to merit inclusion in the PA. Typically, these occurrences are constrained to take place over some time interval of interest (e.g., 10,000 yr in parts of the regulations that apply to the Yucca Mountain facility). There are two aspects to the specification of such occurrences: (i) definition of occurrence properties (e.g., time, location, magnitude, ...) within the time interval of interest, and (ii) assignment of probabilities to possible occurrences within the time interval of interest.

The development of probabilities requires a careful specification of exactly what probabilities are to be assigned to. As an example, suppose only two occurrences, designated o_1 and o_2 , with the following properties were selected for inclusion in a PA: (i) the occurrences of o_1 and o_2 are independent, (ii) the occurrences of o_1 and o_2 follow Poisson processes with rate constants λ_1 (yr^{-1}) and λ_2 (yr^{-1}), respectively, and (iii) a time interval $[0, T = 1000 \text{ yr}]$ is under consideration. There are many possible patterns of occurrence of o_1 and o_2 over the interval $[0, T]$. Each possible pattern can be represented by a vector

$$\mathbf{a} = [m, n, t_{11}, t_{12}, \dots, t_{1m}, t_{21}, t_{22}, \dots, t_{2n}], \quad (\text{Eq. J3.3-1})$$

where (i)

$$0 \leq t_{11} \leq t_{12} \leq \dots \leq t_{1m} \leq T = 1000 \text{ yr}$$

and

$$0 \leq t_{21} \leq t_{22} \leq \dots \leq t_{2n} \leq T = 1000 \text{ yr}$$

are the times at which o_1 and o_2 , respectively, occur, (ii) $m = 0$ or $n = 0$ indicates that the corresponding occurrence did not take place in the time interval $[0, T]$, and (iii) the symbol \mathbf{a} for the vector in Equation J3.3-1 is used to be suggestive of aleatory.

Each vector \mathbf{a} of the form appearing in Equation J3.3-1 represents a possible pattern of occurrences over the time interval $[0, T]$. The pattern of occurrences characterized by \mathbf{a} is sometimes referred to as a future in radioactive waste disposal because each \mathbf{a} is describing one possible future at the facility under consideration. The set

$$\mathcal{A} = \{ \mathbf{a} : \mathbf{a} = [m, n, t_{11}, t_{12}, \dots, t_{1m}, t_{21}, t_{22}, \dots, t_{2n}] \} \quad (\text{Eq. J3.3-2})$$

corresponds to the universe of all possible futures that could occur over the time interval $[0, T = 1000 \text{ yr}]$ given the assumption that o_1 and o_2 are the only two occurrences to be considered.

The introduction of \mathbf{a} provides an exact mathematical description (i.e., definition) of occurrence properties within the time interval of interest. The vector \mathbf{a} in Equation J3.3-1 is quite simple; in general, more properties than initiation times are required to define individual occurrences in a PA. A more general formulation of the example would be

$$\mathbf{a} = [m, n, \mathbf{o}_{11}, \mathbf{o}_{12}, \dots, \mathbf{o}_{1m}, \mathbf{o}_{21}, \mathbf{o}_{22}, \dots, \mathbf{o}_{2n}], \quad (\text{Eq. J3.3-3})$$

where \mathbf{o}_{1i} , $i = 1, 2, \dots, m$, and \mathbf{o}_{2j} , $j = 1, 2, \dots, n$, are vectors of properties associated with the occurrence of o_1 and o_2 , respectively. Further, PAs can involve more than two occurrences of interest. However, \mathbf{a} as defined in Equation J3.3-1 is sufficient as an example.

Introduction of the vector \mathbf{a} and the set \mathcal{A} is simply a means of providing a mathematical structure to ideas previously introduced by the NRC in the specification of licensing requirements for the Yucca Mountain facility. Such a mathematical structure must be introduced to provide an unambiguous description of the conceptual and computational structure of the TSPA-LA. With respect to the introduction of ideas by the NRC, the vector \mathbf{a} is a means of giving a formal and mathematically unambiguous description to the concept of “possible future behavior” introduced in (NRC6) and the equivalent concept of an “event sequence” introduced in (NRC14). The elements of individual \mathbf{a} ’s derive from the occurrence of “initiating events” introduced in (NRC15). Although the NRC refers to the \mathbf{a} ’s as future behaviors or event sequences, the standard terminology in probability theory is to refer to the \mathbf{a} ’s as elementary events and to refer to the set \mathcal{A} of all possible \mathbf{a} ’s as the sample space. The NRC refers to “events (event classes or scenario classes)” in (NRC7), “events” in (NRC8), and “scenario classes” in (YMRP2); in each case, what is being referred to is a subset of the sample space \mathcal{A} . The standard terminology from probability theory is to refer to such sets as events (technically, events are elements of the set \mathcal{A} but, at an intuitive level, an event can be thought of as any subset of \mathcal{A}). What is often referred to as a scenario class is an event in the sense that it is a subset of \mathcal{A} . Thus, in NRC terminology, the set \mathcal{A} of subsets of \mathcal{A} appearing in the formal development of probability simply contains all possible event classes (or, equivalently, scenario classes) for which probability can be defined.

Statements relating to completeness such as “Those features, events and processes expected to materially affect compliance with § 63.113(b) (66 FR 55732 [DIRS 156671]) or be potentially adverse to performance are included, while events (event classes or scenario classes) that are very unlikely (less than one chance in 10,000 over 10,000 years) can be excluded from the analysis” in (NRC7) involve the question of whether or not the \mathbf{a} ’s, and hence \mathcal{A} , have been appropriately defined. At a technical level, there are two ways in which unlikely occurrences (e.g., meteor impact) can be formally excluded from an analysis. The first approach is to simply not include such occurrences in the definition of \mathbf{a} . With this approach, such occurrences are not in the formal structure of the analysis. The second approach is to include such occurrences in the definition of \mathbf{a} but then to eliminate subsets of \mathcal{A} that involve these occurrences from consideration on the basis of low probability. With this approach, unlikely occurrences are formally included in the structure of the analysis and then eliminated from computational consideration on the basis of low probability. In effect, both approaches are used at different stages of the TSPA-LA analysis, with the second approach constituting part of the screening of

features, events and processes (FEPs) and the first approach underlying the computational implementation of the TSPA-LA.

In this presentation, subsets of \mathcal{A} will be referred to as scenario classes. Thus, with this usage, a scenario class corresponds to what the NRC refers to at various places as events, event classes, or scenario classes (NRC7, NRC8, and YMRP2). The choice of scenario class to designate a subset of \mathcal{A} is based on a desire to emphasize that, in general, a scenario class contains many possible futures (i.e., elementary events). Thus, in documentation for the TSPA-LA, a scenario class corresponds to what is usually referred to as an event in the standard terminology of probability theory.

The assignment of probabilities is now considered. Typically, individual futures of the form illustrated by \mathbf{a} in Equation J3.3-1 have a probability of zero. An important exception to this is the “degenerate vector” corresponding to undisturbed conditions (i.e., the future in which none of the occurrences under consideration take place and thus for which $m = n = 0$), which has a probability close to one in many PAs. Thus, probabilities are used in reference to sets of futures or, equivalently, to subsets \mathcal{U} of the sample space \mathcal{A} defined in Equation J3.3-2. For example, \mathcal{U} might be defined by

$$\mathcal{U} = \{ \mathbf{a} = [1, 2, t_{11}, t_{21}, t_{22}] : 0 \leq t_{11} \leq 500 \text{ yr}, 0 \leq t_{21} \leq t_{22} \leq 1000 \text{ yr} \}. \quad (\text{Eq. J3.3-4})$$

Then, under the previously stated assumptions that (i) o_1 and o_2 are independent and follow Poisson processes with rate constants λ_1 and λ_2 and (ii) a time interval of length 1000 yrs is under consideration, the probability $p_A(\mathcal{U})$ of \mathcal{U} is given by

$$\begin{aligned} p_A(\mathcal{U}) &= \left\{ \left[(500\lambda_1)^1 / 1! \right] \left[\exp(-500\lambda_1) \right] \right\}_1 \left\{ \left[(500\lambda_1)^0 / 0! \right] \left[\exp(-500\lambda_1) \right] \right\}_2 \\ &\quad \left\{ \left[(1000\lambda_2)^2 / 2! \right] \left[\exp(-1000\lambda_2) \right] \right\}_3 \\ &= \left\{ \left[(500\lambda_1)^1 / 1! \right] \left[\exp(-500\lambda_1) \right] \right\} \left\{ \left[(1000\lambda_2)^2 / 2! \right] \left[\exp(-1000\lambda_2) \right] \right\}. \quad (\text{Eq. J3.3-5}) \end{aligned}$$

where $\{\sim\}_1$ is the probability that occurrence o_1 takes place exactly once in the time interval $[0, 500 \text{ yr}]$, $\{\sim\}_2$ is the probability that occurrence o_1 does not take place in the time interval $[500, 1000 \text{ yr}]$, and $\{\sim\}_3$ is the probability that occurrence o_2 takes place exactly twice in the time interval $[0, 1000 \text{ yr}]$. Thus, in this example and more generally in most situations, probability distributions are introduced for the individual elements of \mathbf{a} and then used to define probabilities for sets of \mathbf{a} 's. The closed form calculation of such probabilities can be difficult or impossible; often, Monte Carlo techniques or other numerical procedures must be used to calculate approximate probabilities.

References to probabilities of events, event classes and scenario classes repeatedly appear in the EPA and NRC standards for the Yucca Mountain facility. For example “weighted by their probability of occurrence” appears in (EPA2) and (NRC2); related statements appear in (NRC6), (NRC7), (NRC8), (NRC11), (NRC12), (NRC17), and (YMRP1) – (YMRP3). As another

specific example, the statement “Consider only events that have at least one chance in 10,000 of occurring over 10,000 years” in (NRC8) clearly mandates the determination of probabilities of the form indicated in Equation J3.3-5.

To the extent practicable, descriptions of the various parts of a PA should use widely recognized mathematical constructions. Then, the computational implementation of the PA can be viewed as the calculation of approximations to these constructions. For the use of probability to represent aleatory uncertainty, the fundamental mathematical construction is a probability space $(\mathcal{A}, \mathbf{A}, p_A)$, which involves three components as previously indicated in Section J3.1: (i) the set \mathcal{A} that contains everything that could occur in the particular universe under consideration, (ii) the set \mathbf{A} of subsets of \mathcal{A} for which probability is defined, and (iii) the function p_A that defines the probability of the individual elements of \mathbf{A} . The preceding three components appear in the previous example and, as already indicated, in the EPA and NRC regulatory requirements for the Yucca Mountain facility. In the terminology of probability theory, \mathcal{A} is the sample space; elements \mathbf{a} of \mathcal{A} are elementary events; elements \mathcal{U} of \mathbf{A} are events; and p_A is a probability measure. In terminology often used in PA for radioactive waste disposal, elements \mathbf{a} of \mathcal{A} are futures; elements \mathcal{U} of \mathbf{A} are scenario classes; the probabilities $p_A(\mathcal{U})$ are scenario probabilities; and questions of “completeness” deal with whether or not \mathcal{A} has been defined in a way that incorporates all significant occurrences at the site under consideration. As previously indicated, the descriptor scenario class instead of scenario is used in the documentation for the TSPA-LA to emphasize that sets containing, in general, many futures are under consideration.

In practice, most probability calculations are based on the distributions assigned to the individual elements of \mathbf{a} and do not rely on the formal properties of the probability space $(\mathcal{A}, \mathbf{A}, p_A)$. For example, the probability space associated with the illustration of aleatory uncertainty for the vector \mathbf{a} in Equation J3.3-1 is defined by distributions D_1 and D_2 of occurrence times for occurrences o_1 and o_2 that derive from the Poisson rate constants λ_1 and λ_2 . In actual calculation, it is the mathematical characterization of these distributions that are used rather than the formal properties of the corresponding probability space. However, the introduction of the concept of a probability space provides a way to formally describe what is being done in a PA and also a way to distinguish between different uses of probability within a PA.

The TSPA-LA incorporates three types of disruptions that are treated as aleatory occurrences: early failures of WPs and DSs, igneous events, and seismic events. Descriptions of the formal probabilistic representations used in the TSPA-LA for the occurrence of early failures of WPs and DSs, igneous events, and seismic events are given in later sections.

J3.4 EN2: Mathematical Models for Estimating Consequences of Individual Futures

The entity EN2 corresponds to the mathematical models required to estimate various consequences in a PA for a radioactive waste disposal site or some other facility. Conceptually, EN2 can be viewed as a function \mathbf{f} of the form

$$\mathbf{y} = \mathbf{f}(\mathbf{a}), \quad (\text{Eq. J3.4-1})$$

where \mathbf{a} is a particular future, \mathbf{f} corresponds to the models used to estimate various outcomes associated with \mathbf{a} , and \mathbf{y} is the estimated outcomes. A vector notation is used for \mathbf{f} and \mathbf{y} because typically a large number of outcomes are estimated for each future \mathbf{a} . Often, the elements of \mathbf{y} include functions of space and/or time. For a radioactive waste disposal site, the models denoted by \mathbf{f} are often systems of ordinary or partial differential equations used to represent processes such as material deformation, corrosion, fluid flow, radionuclide transport in flowing groundwater, and radionuclide movement and associated human radiation exposure in the surface environment. This is certainly the case in the TSPA-LA for the Yucca Mountain facility.

The models used in a particular PA will depend on many things, including the site under consideration, the resolution of the data available for characterization of the site, the desired resolution in model predictions, and the time and resources available for the analysis. However, most models actually consist of three parts: (i) a formal mathematical representation (e.g., a system of nonlinear partial differential equations), (ii) a numerical procedure that produces approximations to the formal mathematical representation (e.g., a finite difference procedure), and (iii) a computer program that implements the numerical procedure. A common situation is to use physically detailed and computationally demanding models for initial assessment of system behavior and then to incorporate the results obtained from these models into less detailed and less computationally demanding models for use in a final, integrated PA. This type of incorporation process is used extensively in the TSPA-LA and is often referred to as model abstraction.

Given the almost universal use of numerical approximations and computer programs to implement these approximations, a PA typically involves two extensions of the representation in Equation J3.4-1:

$$\mathbf{y} = \hat{\mathbf{f}}(\mathbf{a}) \quad (\text{Eq. J3.4-2})$$

and

$$\mathbf{y} = \mathbf{F}(\mathbf{a}), \quad (\text{Eq. J3.4-3})$$

where $\hat{\mathbf{f}}$ is used to represent the numerical approximation that replaces \mathbf{f} , and \mathbf{F} is used to represent the computer program that implements this approximation and actually produces \mathbf{y} . For example, if \mathbf{f} is based on a system of ordinary differential equations, $\hat{\mathbf{f}}$ might correspond to an Adams-Moulten method, a variable order, variable stepsize Runge-Kutta method or a Gear's backward differentiation method, and \mathbf{F} would correspond to the program that actually implemented the method.

The model \mathbf{f} indicated in Equation J3.4-1 is almost always the result of the assembly of many individual models. For example, \mathbf{f} might be of the form

$$\begin{aligned} \mathbf{f}(\mathbf{a}) = & \mathbf{f}_1(\mathbf{a}) + \mathbf{f}_2[\mathbf{a}, \mathbf{f}_3(\mathbf{a})] + \mathbf{f}_4\{\mathbf{a}, \mathbf{f}_2[\mathbf{a}, \mathbf{f}_3(\mathbf{a})], \mathbf{f}_3(\mathbf{a})\} + \mathbf{f}_5[\mathbf{a}, \mathbf{f}_3(\mathbf{a})] \\ & + \mathbf{f}_6[\mathbf{a}, \mathbf{f}_3(\mathbf{a})] + \mathbf{f}_7[\mathbf{a}, \mathbf{f}_3(\mathbf{a})] + \mathbf{f}_8\{\mathbf{a}_N, \mathbf{f}_9(\mathbf{a}_N), \mathbf{f}_{10}[\mathbf{a}, \mathbf{f}_3(\mathbf{a})]\}, \end{aligned} \quad (\text{Eq. J3.4-4})$$

where \mathbf{a} ~ particular future under consideration, \mathbf{a}_N ~ future involving no disruptions, and $\mathbf{f}_1, \mathbf{f}_2, \dots, \mathbf{f}_{10}$ ~ individual models from which \mathbf{f} is constructed. The description of the exact form of \mathbf{f} and its many component models in the TSPA-LA is outside the scope of this introductory presentation. However, in concept, the TSPA-LA employs a model structure of the form indicated, and in reality, has a computational structure more complex than that just indicated.

References and allusions to results that must be obtained by the use of models occur throughout the EPA and NRC regulations for the Yucca Mountain facility. The following statement by the NRC in (NRC9) explicitly acknowledges the necessity of using complex numerical procedures: “Demonstrating compliance will involve the use of complex predictive models ...”. Thus, EN2 unavoidably exists as part of the TSPA-LA for the Yucca Mountain facility.

In a PA, EN1 (i.e., the probability space (\mathcal{A}, A, p_A)) provides a probabilistic characterization of what could happen at the facility under consideration, and EN2 (i.e., the function \mathbf{f} indicated in Equation J3.4-1) provides estimates of the consequences associated with individual futures \mathbf{a} . In many PAs, a representation of results is desired that provides a display of both consequence and likelihood. The usual mathematical construction used to display this information is a complementary cumulative distribution function (CCDF), which provides a display of the probability that individual consequence values will be exceeded (Figure J3.4-1).

A CCDF can be formally defined by an integral involving EN1 and EN2. Specifically,

$$prob_A(c > C) = \int_{\mathcal{A}} \bar{\delta}_C [f(\mathbf{a})] d_A(\mathbf{a}) dA, \quad (\text{Eq. J3.4-5})$$

where $prob_A(c > C)$ is the probability that a future \mathbf{a} yielding a consequence value larger than C will occur, $d_A(\mathbf{a})$ is the density function associated with (\mathcal{A}, A, p_A) , dA is an incremental (i.e., differential) volume from \mathcal{A} ,

$$\bar{\delta}_C [f(\mathbf{a})] = \begin{cases} 1 & \text{if } f(\mathbf{a}) > C \\ 0 & \text{if } f(\mathbf{a}) \leq C, \end{cases}$$

a nonbold representation for f is used because a single consequence (i.e., analysis outcome) is considered in the construction of a CCDF (i.e., f is real valued rather than vector valued in this context), and the subscript A indicates that $prob_A(c > C)$ derives from aleatory uncertainty. The effect of the indicator function $\bar{\delta}_C$ is to pick out the subset of \mathcal{A} for which $f(\mathbf{a}) > C$, with the result that the integral yields the desired probability. The preceding is a specific example of the generic CCDF defined in conjunction with Equation J3.1-5.

In practice, the integral in Equation J3.4-5 is too complex to permit a closed-form evaluation. Part of this complexity comes from the properties of (\mathcal{A}, A, p_A) and part of it comes from the complexity of f . This complexity typically precludes the use of standard numerical procedures for evaluating integrals. In practice, either Monte Carlo techniques or importance sampling are often used in the evaluation of the integral in Equation J3.4-5.

With the Monte Carlo approach, the integral in Equation J3.4-5 is approximated by

$$prob_A(c > C) \cong \sum_{i=1}^{nR} \bar{\delta}_C [f(\mathbf{a}_i)] / nR, \quad (\text{Eq. J3.4-6})$$

where \mathbf{a}_i , $i = 1, 2, \dots, nR$, is a random sample from \mathcal{A} generated in consistency with the definition of (\mathcal{A}, A, p_A) (Figure J3.4-2). In practice, generating a random sample from \mathcal{A} in consistency with the definition of (\mathcal{A}, A, p_A) means generating a sample using the distributions assigned to the individual elements of \mathbf{a} .

In most PAs, evaluation of $f(\mathbf{a})$ is too expensive to permit an evaluation for each sample element \mathbf{a}_i in Equation J3.4-6. Rather, $f(\mathbf{a})$ is evaluated for a relatively small number of elements of \mathcal{A} and then these evaluations are used in the construction (i.e., approximation) of $f(\mathbf{a}_i)$ for use in the summation in Equation J3.4-6. Thus, there are actually three numerical approximations involved: (i) the Monte Carlo procedure to approximate the integral in Equation J3.4-5, (ii) an initial approximation of $f(\mathbf{a})$ for selected elements of \mathcal{A} , and (iii) a subsequent approximation of $f(\mathbf{a}_i)$ from these initial approximations for use in the summation in Equation J3.4-6. As indicated earlier, the use of a limited number of complex calculations to cover a number of different situations is used extensively in the TSPA-LA and is referred to as model abstraction.

With importance sampling, \mathcal{A} is divided into disjoint strata \mathcal{A}_i , $i = 1, 2, \dots, nS$, with $\mathcal{A} = \cup_i \mathcal{A}_i$ and a value \mathbf{a}_i , $i = 1, 2, \dots, nS$, is selected from each strata. Then, the integral in Equation J3.4-5 is approximated by

$$prob_A(c > C) = \sum_{i=1}^{nS} \bar{\delta}_C [f(\mathbf{a}_i)] p_A(\mathcal{A}_i), \quad (\text{Eq. J3.4-7})$$

where $p_A(\mathcal{A}_i)$ is the probability of \mathcal{A}_i . The strata \mathcal{A}_i are simply a collection of scenario classes (i.e., subsets of \mathcal{A}) with the properties $\mathcal{A}_i \cap \mathcal{A}_j = \emptyset$ for $i \neq j$ and $\mathcal{A} = \cup_i \mathcal{A}_i$. When the \mathbf{a}_i are randomly selected within the corresponding strata, importance sampling is a variance reduction technique for simple random (i.e., Monte Carlo) sampling. Importance sampling involves the same approximation considerations as the Monte Carlo approach described in conjunction with Equation J3.4-6. The fault tree and event tree techniques (Breeding et. al. 1992 [DIRS 107727]; Vesely et al. 1981 [DIRS 128494]) used extensively in conjunction with PAs for nuclear reactors and other complex engineered systems can be viewed as algorithms for defining an importance sampling procedure over the sample space associated with all possible accidents at these facilities.

Another approach to importance sampling is to reformulate the integral in Equation J3.4-5 as

$$\int_{\mathcal{A}} \bar{\delta}_C [f(\mathbf{a})] d_A(\mathbf{a}) dA = \int_{\mathcal{A}} \left[\frac{\bar{\delta}_C [f(\mathbf{a})] d_A(\mathbf{a})}{d_I(\mathbf{a})} \right] d_I(\mathbf{a}) dA, \quad (\text{Eq. J3.4-8})$$

where $d_I(\mathbf{a})$ is the density function for a distribution defined on \mathcal{A} selected to accentuate subregions of \mathcal{A} that are believed to be important in the determination of $prob_{\mathcal{A}}(c > C)$. Then, $prob_{\mathcal{A}}(c > C)$ is approximated by

$$prob_{\mathcal{A}}(c > C) \cong \sum_{i=1}^{nR} \left[\frac{\bar{\delta}_C [f(\mathbf{a}_i)] d_A(\mathbf{a}_i)}{d_I(\mathbf{a}_i)} \right] / nR, \quad (\text{Eq. J3.4-9})$$

where $\mathbf{a}_i, i = 1, 2, \dots, nR$, is a random sample from \mathcal{A} generated in consistency with the density function $d_I(\mathbf{a})$.

The TSPA-LA uses both random sampling and importance sampling in various integrations involving aleatory uncertainty.

Another possible display of the combined effects of EN1 and EN2 is given by the expected value and variance of a consequence of interest. The expected value $E_A(f) = E_A[f(\mathbf{a})]$ and variance $V_A(f) = V_A[f(\mathbf{a})]$ of a particular consequence that derive from aleatory uncertainty are formally defined by

$$E_A(f) = E_A[f(\mathbf{a})] = \int_{\mathcal{A}} f(\mathbf{a}) d_A(\mathbf{a}) dA \quad (\text{Eq. J3.4-10})$$

and

$$V_A(f) = V_A[f(\mathbf{a})] = \int_{\mathcal{A}} [f(\mathbf{a}) - E_A(f)]^2 d_A(\mathbf{a}) dA \quad (\text{Eq. J3.4-11})$$

and are easily estimated with the results used in the CCDF approximations in Equations J3.4-6, J3.4-8 and J3.4-9. However, as a large amount of information is lost in the calculation of $E_A(f)$ and $V_A(f)$, the combined effects of EN1 and EN2 are better displayed as CCDFs. The mean and variance defined in Equations J3.4-10 and J3.4-11 are specific examples of the generic results defined in Equations J3.1-2 and J3.1-3.

The NRC's regulations for the Yucca Mountain facility specifically call for the calculation of expected dose to the RMEI (e.g., EPA2, EPA5 – EPA8, NRC2, and NRC5 – NRC7). In particular, the projected doses referred to in (EPA14), (NRC20) and elsewhere are assumed to correspond to expected doses over aleatory uncertainty. Therefore, the TSPA-LA pays special attention to the calculation of expected dose to the RMEI. This is a calculation of the form indicated in Equation J3.4-10. Dose is actually a function of time. Thus, the expected value calculation for dose to the RMEI is perhaps better expressed as

$$\bar{D}(\tau) = E_A[D(\tau|\mathbf{a})] = \int_{\mathcal{A}} D(\tau|\mathbf{a}) d_A(\mathbf{a}) dA, \quad (\text{Eq. J3.4-12})$$

where

$D(\tau|\mathbf{a})$ = dose (mrem/yr) at time τ to the RMEI conditional on the occurrence of future \mathbf{a} (i.e., $\mathbf{a} \in \mathcal{A}$).

In general, dose to the RMEI at time τ changes from future to future, and the indicated expected value $E_A[D(\tau|\mathbf{a})]$ is the expected dose to the RMEI at time τ with the expectation taken over all possible futures (i.e., elements \mathbf{a} of \mathcal{A}).

Application of the approximation procedures indicated in conjunction with Equations J3.4-6, J3.4-7 and J3.4-9 to the integral defining $E_A[D(\tau|\mathbf{a})]$ in Equation J3.4-12 results in the approximations

$$E_A[D(\tau|\mathbf{a})] \cong \sum_{i=1}^{nR} D(\tau|\mathbf{a}_i)/nR, \quad (\text{Eq. J3.4-13})$$

$$E_A[D(\tau|\mathbf{a})] \cong \sum_{i=1}^{nS} D(\tau|\mathbf{a}_i) p_A(\mathcal{A}_i) \quad (\text{Eq. J3.4-14})$$

and

$$E_A[D(\tau|\mathbf{a})] \cong \sum_{i=1}^{nR} [D(\tau|\mathbf{a}_i) d_A(\mathbf{a}_i)/d_I(\mathbf{a}_i)]/nR. \quad (\text{Eq. J3.4-15})$$

The approximation to $E_A[D(\tau)]$ in Equation J3.4-14 can be viewed as the mathematical implementation of the following NRC statement in (YMRP3): “The calculation of the annual dose curve appropriately sums the contribution of each of the disruptive event scenario classes. . . . The probabilities of occurrence of all scenario classes, included in calculating the annual dose curve, sum to one.” In particular, $E_A[D(\tau|\mathbf{a})]$ is the (expected) annual dose curve; $D(\tau|\mathbf{a}_i)$ is a dose curve conditional on the event (i.e., scenario class in NRC terminology) \mathcal{A}_i ; $p_A(\mathcal{A}_i)$ is the probability of \mathcal{A}_i ; and $\sum_i p_A(\mathcal{A}_i) = 1$ because $\mathcal{A}_i \cap \mathcal{A}_j = \emptyset$ for $i \neq j$ and $\mathcal{A} = \cup_i \mathcal{A}_i$. In general, \mathbf{a}_i is only one of many futures contained in \mathcal{A}_i ; however, as long as \mathbf{a}_i is selected randomly from \mathcal{A}_i , an unbiased estimate for $E_A[D(\tau|\mathbf{a})]$ will be obtained. If one or more futures are randomly selected for each \mathcal{A}_i , then the approximation to $E_A[D(\tau|\mathbf{a})]$ in Equation J3.4-14 has the form

$$E_A[D(\tau|\mathbf{a})] \cong \sum_{i=1}^{nS} \left[\sum_{j=1}^{nS(i)} D(\tau|\mathbf{a}_{ij})/nS(i) \right] p_A(\mathcal{A}_i) \quad (\text{Eq. J3.4-16})$$

where $\mathbf{a}_{ij}, j = 1, 2, \dots, nS(i)$, are randomly selected from \mathcal{A}_i for $i = 1, 2, \dots, nS$.

The expressions in Equations J3.4-13 and J3.4-15 provide equally valid approximation procedures for $E_A[D(\tau|\mathbf{a})]$ but do not match the NRC terminology in (YMRP3) as neither scenario classes nor scenario class probabilities are explicitly involved. In particular, $1/nR$ is not a probability but rather a weight used in the estimation of an expected value (e.g., $E_A[D(\tau|\mathbf{a})]$) in a Monte Carlo calculation. The approximation in Equation J3.4-13 is actually closer in spirit to the NRC statement “Each possible future behavior of the repository is represented by a curve describing the annual dose to the RMEI. Generally, but not necessarily, each of the curves is assumed to be equally likely.” in (NRC6). In the approximation in Equation J3.4-13, each of the dose curves is assigned an equal weight (i.e., $1/nR$) but not an equal probability. With the exception of the dose curve corresponding to the nominal scenario class, each individual dose curve will typically have a probability of zero.

J3.5 EN3: Probabilistic Characterization of Epistemic Uncertainty

The entity EN3 is the formal outcome of the data development component of a PA and provides a probabilistic characterization of the uncertainty in the many parameters required in the definitions of EN1 (e.g., occurrence rates, parameters in distributions, ...) and EN2 (e.g., distribution coefficients, solubilities, ...). The term parameter in the description of EN3 is used in a sense that is sufficiently broad to include designators for alternative models or model structures. Formally, EN3 is defined by a probability space $(\mathcal{E}, \mathbf{E}, p_E)$.

The sample space \mathcal{E} associated with EN3 has the form

$$\mathcal{E} = \{\mathbf{e}: \mathbf{e} \text{ is possibly the correct vector of inputs to use with EN1 and EN2 in the calculation of analysis outcomes}\}. \quad (\text{Eq. J3.5-1})$$

Further, \mathbf{e} has the form

$$\mathbf{e} = [e_1, e_2, \dots, e_{nE}], \quad (\text{Eq. J3.5-2})$$

where each element e_i , $i = 1, 2, \dots, nE$, of \mathbf{e} is a quantity required in the formulation of EN1 or EN2 that is assumed to have a fixed value in the context of the particular PA under consideration but with this value being imprecisely known. The basic idea is that the PA and the associated definitions of EN1 and EN2 have been developed to the point that appropriate analysis outcomes would be obtained if the appropriate value of \mathbf{e} was used as input to the analysis.

As an example, the representation for the CCDF in Equation J3.4-5 would now become

$$prob_A(c > C | \mathbf{e}) = \int_{\mathcal{A}} \bar{\delta}_C [f(\mathbf{a}, \mathbf{e})] d_A(\mathbf{a} | \mathbf{e}) d\mathbf{a}, \quad (\text{Eq. J3.5-3})$$

with the addition of \mathbf{e} to the notation for various quantities in Equation J3.4-5 indicating that the values and/or predictions associated with these quantities are dependent on the value assigned to \mathbf{e} . Thus, different values for \mathbf{e} lead to different values for the CCDF in Equation J3.4-1 and other analysis outcomes of interest (Figure J3.5-1). The sample space \mathcal{E} contains all values for \mathbf{e}

consistent with available information about the facility under consideration and thus leads to all possible values for the CCDF defined in Equation J3.4-5 and other analysis outcomes of interest.

The vector \mathbf{e} typically contains elements that affect the value of the analysis outcome under consideration as indicated notationally by $f(\mathbf{a}, \mathbf{e})$ in Equation J3.5-3 and other elements that affect the distribution of \mathbf{a} as indicated notationally by $d_A(\mathbf{a}|\mathbf{e})$ in Equation J3.5-3. The elements of \mathbf{e} relevant to the evaluation of $f(\mathbf{a}, \mathbf{e})$ and the elements of \mathbf{e} relevant to the evaluation of $d_A(\mathbf{a}|\mathbf{e})$ are usually different. To emphasize this distinction, it is often convenient to represent \mathbf{e} by

$$\mathbf{e} = [\mathbf{e}_A, \mathbf{e}_M], \quad (\text{Eq. J3.5-4})$$

where

$$\mathbf{e}_A = [e_{A1}, e_{A2}, \dots, e_{A,nA}]$$

and

$$\mathbf{e}_M = [e_{M1}, e_{M2}, \dots, e_{M,nM}]$$

are vectors of epistemically uncertain quantities affecting the evaluation of $d_A(\mathbf{a})$ and $f(\mathbf{a})$, respectively. That is, $d_A(\mathbf{a})$ and $f(\mathbf{a})$ notationally have the forms $d_A(\mathbf{a}|\mathbf{e}_A)$ and $f(\mathbf{a}, \mathbf{e}_M)$ to emphasize this dependence. The representation for $prob(c > C|\mathbf{e})$ in Equation J3.5-3 becomes

$$prob_A(c > C|\mathbf{e}) = \int_A \bar{\delta}_C [f(\mathbf{a}, \mathbf{e}_M)] d_A(\mathbf{a}|\mathbf{e}_A) dA \quad (\text{Eq. J3.5-5})$$

with the addition of this more explicit notation.

The probability space (\mathcal{E}, E, p_E) that formally defines EN3 provides a characterization of the uncertainty in the elements of \mathbf{e} . In practice, (\mathcal{E}, E, p_E) is defined by specifying a distribution

$$D_j, j = 1, 2, \dots, nE, \quad (\text{Eq. J3.5-6})$$

for each element e_j of \mathbf{e} . Correlations and various other restrictions involving the possible values of e_j can also be specified. The purpose of the D_j is to provide, on the basis of all available information, a quantitative (i.e., probabilistic) description of where the possible values for the e_j are located. In contrast, \mathcal{E} only provides a complete compilation of the possible values for the \mathbf{e} and thus for the e_j . In some instances, it may be possible to use formal statistical procedures to estimate the D_j . However, typically some type of expert review process is needed to develop the D_j (Bonano and Apostolakis 1991 [DIRS 159041]; Cooke 1991 [DIRS 158968]; Hora and Iman 1989 [DIRS 100902]; Keeney and von Winterfeldt 1991 [DIRS 159053]; Meyer and Booker 1991 [DIRS 110460], pp. 4 to 5; Mosleh et al. 1988 [DIRS 159055]; Thorne 1993 [DIRS 159061]).

The EPA and NRC intend for the distributions in Equation J3.5-6 to provide “reasonable” characterizations of uncertainty in the TSPA-LA rather than overtly conservative representations of uncertainty. Here, conservative is used in the designation of assumptions that are contrary to what is believed to be an appropriate representation of system properties and which produce analysis results that are more pessimistic in a regulatory context than should be the case. The EPA and NRC desire for a reasonable characterization of uncertainty is indicated in a number of statements: (i) “Focuses performance assessments and analyses upon the full range of defensible and reasonable parameter distributions rather than only upon extreme physical situations and parameters values.” in (EPA3) and (NRC3), (ii) “If choices are made that make simulations very unrealistic the confidence that can be placed on modeling results is limited.” and “Overly conservative assumptions made in developing performance scenarios can bias the analyses ... and can deflect attention from questions critical to developing an adequate understanding of the expected features, events, and processes.” in (EPA11), and (iii) “so that regulatory decision making will be done with a full understanding of the uncertainties involved” in (EPA12). As a result, the goal in defining the distributions in Equation J3.5-6 for the TSPA-LA is to mathematically capture an honest assessment of the epistemic uncertainty associated with the individual elements of \mathbf{e} without being either deliberately conservative or deliberately nonconservative in this assessment.

For a specific future \mathbf{a} and a single analysis outcome $f(\mathbf{a}, \mathbf{e}_M)$, the resultant distribution of possible values for $f(\mathbf{a}, \mathbf{e}_M)$ is given by

$$prob_E(c > C | \mathbf{a}) = \int_{\mathcal{E}} \bar{\delta}_C [f(\mathbf{a}, \mathbf{e}_M)] d_E(\mathbf{e}) dE, \quad (\text{Eq. J3.5-7})$$

where $prob_E(c > C | \mathbf{a})$ is the probability that $f(\mathbf{a}, \mathbf{e}_M)$ will have a value larger than C due to the uncertainty in \mathbf{e}_M as characterized by (\mathcal{E}, E, p_E) , the subscript E indicates that $prob_E(c > C | \mathbf{a})$ derives from epistemic uncertainty, and the remaining terms are defined similarly to those in Equations J3.4-5 and J3.5-2 except that (\mathcal{E}, E, p_E) rather than (\mathcal{A}, A, p_A) is now under consideration. In concept, this distribution has the same appearance as in Figure J3.4-1 except that $C = f(\mathbf{a}, \mathbf{e}_M)$ appears on the abscissa and $prob_E(c > C | \mathbf{a})$ appears on the ordinate. As a technical point, an element of \mathbf{e} has no effect on the value of the integral in Equation J3.5-7 if it has no effect on the value of $f(\mathbf{a}, \mathbf{e}_M)$.

In practice, closed form evaluation of $prob_E(c > C | \mathbf{a})$ is not practicable. For example, evaluation of $f(\mathbf{a}, \mathbf{e}_M)$ could require the solution of a complex system of nonlinear partial differential equations. Typically, a sampling-based approach is used to approximate $prob_E(c > C | \mathbf{a})$. For example, a random sample $\mathbf{e}_i = [\mathbf{e}_{Ai}, \mathbf{e}_{Mi}]$, $i = 1, 2, \dots, nR$, generated in consistency with the definition of (\mathcal{E}, E, p_E) (i.e., in consistency with the distributions in Equation J3.5-6 and any associated restrictions) leads to the approximation

$$prob_E(c > C | \mathbf{a}) \cong \sum_{i=1}^{nR} \bar{\delta}_C [f(\mathbf{a}, \mathbf{e}_{Mi})] / nR. \quad (\text{Eq. J3.5-8})$$

The resultant approximation is similar in appearance to that shown in Figure J3.4-2 except that $C = f(\mathbf{a}, \mathbf{e}_{Mi})$ appears on the abscissa and $prob_E(c > C|\mathbf{a})$ appears on the ordinate.

The probability space (\mathcal{E}, E, p_E) leads to distributions of CCDFs resulting from aleatory uncertainty as indicated in Figure J3.5-1. When viewed formally, such distributions are defined by double integrals involving $(\mathcal{A}, A, p_A), f$, and (\mathcal{E}, E, p_E) . The formal notation for such integrals is messy (Helton 1996 [DIRS 107823]) and will not be presented here but will be presented in Section J4.

As previously indicated, integrals involving (\mathcal{A}, A, p_A) and f are often evaluated with numerical procedures based on random sampling or importance sampling. Integrals involving (\mathcal{E}, E, p_E) are often evaluated with procedures based on Latin hypercube sampling (Helton and Davis 2003 [DIRS 163475]; Iman 1992 [DIRS 158984]; McKay et al. 1979 [DIRS 127905]) because of its efficient stratification properties. In particular, Latin hypercube sampling shows less sampling variability than simple random sampling (McKay et al. 1979 [DIRS 127905]; Owen 1992 [DIRS 159057]; Stein 1987 [DIRS 159060]) and has been observed to produce stable results in several large analyses (Iman and Helton 1988 [DIRS 159052]; Iman and Helton 1991 [DIRS 159039]; Helton et al. 1995 [DIRS 159560]).

Latin hypercube sampling operates in the following manner to generate a sample of size $nLHS$ from nE variables. The range of each variable (i.e., the e_j in Equation J3.5-2) is divided into $nLHS$ intervals of equal probability and one value is selected at random from each interval. The $nLHS$ values thus obtained for e_1 are paired at random and without replacement with the $nLHS$ values obtained for e_2 . These $nLHS$ pairs are paired at random and without replacement with the $nLHS$ values of e_3 to form $nLHS$ triples. This process is continued until a set of $nLHS$ nE -tuples is formed. These nE -tuples are of the form

$$\mathbf{e}_i = [e_{i1}, e_{i2}, \dots, e_{i,nE}], \quad i = 1, \dots, nLHS, \quad (\text{Eq. J3.5-9})$$

and constitute the Latin hypercube sample (LHS). The individual e_j must be independent for the preceding construction procedure to work; however, a method for generating LHSs from correlated variables has been developed by Iman and Conover (1982 [DIRS 124158]; Iman and Davenport 1982 [DIRS 159050]). As illustrated in Figure J3.5-2 for an LHS from two variables, Latin hypercube sampling results in a dense stratification across the range of each variable (i.e., there is one value from each equal probability interval).

Once the LHS is generated, PA results are calculated for each sample element. For EN2 and an individual future \mathbf{a} , this creates a mapping

$$[\mathbf{e}_{Mi}, \mathbf{f}(\mathbf{a}, \mathbf{e}_{Mi})], \quad i = 1, 2, \dots, nLHS, \quad (\text{Eq. J3.5-10})$$

from uncertain inputs to results conditional on the occurrence of \mathbf{a} . Typically, a relatively small number of futures is selected for detailed analysis of this type (e.g., 5 – 10). As a reminder, \mathbf{f} is usually quite complex and in practice is composed of many models (e.g., see Equation J3.4-4). Further, all models represented by \mathbf{f} may not be used in the analysis of all futures selected for

consideration. In particular, different models or suites of models might be used to analyze different futures at the facility under consideration or to calculate different outcomes of interest for a given future.

For CCDFs, a mapping of the form

$$[\mathbf{e}_i, \text{prob}_E(c > C | \mathbf{e}_i)], i = 1, 2, \dots, nLHS, \quad (\text{Eq. J3.5-11})$$

is created, where $\text{prob}_E(c > C | \mathbf{e}_i)$ defines the CCDF for some consequence of interest as indicated in Equations J3.4-5 and J3.5-3 (i.e., a CCDF results when C is allowed to run across all possible values of the consequence). In most PAs, CCDFs are generated for a large number of consequences.

The mappings in Equations J3.5-10 and J3.5-11 provide the basis for both uncertainty analysis and sensitivity analysis. Uncertainty analysis designates the determination of the uncertainty in analysis outcomes that results from uncertainty in analysis inputs. Specifically, uncertainty analysis involves the determination of the effects of the uncertainty characterized by EN3 and thus is providing an answer to question Q4 introduced in Section J2.1 relating to how much confidence should be placed in the results of the analysis. Once the calculations that lead to the mappings in Equations J3.5-10 and J3.5-11 are completed, the presentation of uncertainty analysis results simply involves the plotting of the predicted results with an equal weight (i.e., the reciprocal of the sample size) given to the individual results when either random or Latin hypercube sampling is used in the generation of the sample in Equation J3.5-9. Sensitivity analysis designates the determination of the effects of individual variables contained in \mathbf{e} on the observed uncertainty in predictions of interest. For sampling-based propagations of uncertainty, sensitivity analysis involves an exploration of mappings of the form appearing in Equations J3.5-10 and J3.5-11 with techniques based on examination of scatterplots, correlation analysis, regression analysis, and the identification of nonrandom patterns (Helton et al. 2006 [DIRS 183873]; Helton and Davis 2002 [DIRS 183872]; Hamby 1994 [DIRS 158798]; Helton 1993 [DIRS 100452]; Kleijnen and Helton 1999 [DIRS 159054]). Extensive analyses of this type are presented in Appendix K.

The importance of uncertainty and sensitivity analyses of the type just indicated is emphasized in many statements made by the EPA and the NRC in their regulations for the Yucca Mountain facility. Examples of such statements include: (i) “Focuses performance assessments and analyses upon the full range of defensible and reasonable parameter distributions” in (EPA3) and (NRC3), (ii) “Account for uncertainties and variabilities in parameter values” in (NRC8), (iii) “the demonstration of compliance must take uncertainties and gaps in knowledge into account” in (NRC10), (iv) “DOE is expected to conduct uncertainty analyses (i.e., evaluation of how uncertainty in parameter values affects the uncertainty in the estimate of dose)” in (NRC12), (v) “The treatment of uncertainty in DOE’s performance assessment will be an important part of NRC’s review” in (NRC13), and (vi) “The total system performance assessment sampling method ensures that sampled parameters have been sampled across their ranges of uncertainty.” in (YMRP11).

The expected dose $\bar{D}(\tau)$ indicated in Equation J3.4-12 depends on the particular vector \mathbf{e} of epistemically uncertain inputs used in its determination. Thus, $\bar{D}(\tau)$ is actually of the form $\bar{D}(\tau|\mathbf{e})$. Specifically,

$$\bar{D}(\tau|\mathbf{e}) = E_A \left[D(\tau|\mathbf{a}, \mathbf{e}_M) \right] = \int_{\mathcal{A}} D(\tau|\mathbf{a}, \mathbf{e}_M) d_A(\mathbf{a}|\mathbf{e}_A) dA \quad (\text{Eq. J3.5-12})$$

when the dependence on elements of $\mathbf{e} = [\mathbf{e}_A, \mathbf{e}_M]$ is added to the representation for $\bar{D}(\tau)$ in Equation J3.4-12. In turn, $\bar{D}(\tau|\mathbf{e})$ has a distribution that derives from the probability space $(\mathcal{E}, \mathcal{E}, p_E)$ (i.e., from the distributions indicated in Equations J3.5-6 assigned to the elements of \mathbf{e} and collectively represented by the density function $d_E(\mathbf{e})$) with an expected value $\bar{\bar{D}}(\tau)$ defined by

$$\bar{\bar{D}}(\tau) = \int_{\mathcal{E}} \bar{D}(\tau|\mathbf{e}) d_E(\mathbf{e}) dE \quad (\text{Eq. J3.5-13})$$

and a q quantile value $Q_q[\bar{D}(\tau|\mathbf{e})]$ defined by the value D such that

$$q = \int_{\mathcal{E}} \delta_D \left[\bar{D}(\tau|\mathbf{e}) \right] d_E(\mathbf{e}) dE. \quad (\text{Eq. J3.5-14})$$

The expected value $\bar{\bar{D}}(\tau)$ and the quantile $Q_q[\bar{D}(\tau|\mathbf{e})]$ are examples of the generic values defined in Equations J3.1-2 and J3.1-7. As discussed in Section J4, $\bar{\bar{D}}(\tau)$ and $Q_{0.5}[\bar{D}(\tau|\mathbf{e})]$ are assumed in the TSPA-LA to correspond to the mean dose and median dose, respectively, specified in (EPA14) and (NRC20).

J3.6 Properties of Poisson Processes

At least two types of disruptions must be considered in PAs for the proposed Yucca Mountain repository: igneous events and seismic events. Both of these disruptions are assumed to have a pattern of occurrence that can be represented as a Poisson process (Ross 1993 [DIRS 172064], Chapter 5). Because the properties of Poisson processes will play an important role in determining expected dose to the RMEI in PAs for the Yucca Mountain repository, it is useful to briefly review these properties at the beginning of this presentation. Then, these properties can be referred to as needed in the subsequent derivation and calculation of expected dose to the RMEI.

The descriptor Poisson process is used to designate a set of potentially realizable sequences of occurrences (e.g., sequences of seismic events occurring at different times in the future) with certain special probabilistic characteristics. For the purposes of this presentation, a Poisson process can be described in terms of a function $N(r, s)$ defined for $0 \leq r < s < \infty$, where

$$N(r, s) = \text{number of occurrences in the time interval } [r, s]. \quad (\text{Eq. J3.6-1})$$

Specifically, the potential sequences of occurrences that give rise to different possible values for $N(r, s)$ are said to follow a (stationary or homogeneous) Poisson process provided

$$prob[N(r, r + \Delta t) = 1] = \lambda \Delta t + o(\Delta t), \quad (\text{Eq. J3.6-2})$$

$$prob[N(r, r + \Delta t) \geq 2] = o(\Delta t) \quad (\text{Eq. J3.6-3})$$

and

$$prob[N(r, s) = k \text{ and } N(u, v) = l | [r, s] \cap [u, v] = \emptyset] = prob[N(r, s) = k] prob[N(u, v) = l], \quad (\text{Eq. J3.6-4})$$

where (i) *prob* denotes probability and the associated vertical line indicates conditionality, (ii) λ is independent of r , and (iii) the $o(\Delta t)$ notation is an abbreviation for

$$\lim_{\Delta t \rightarrow 0^+} prob[N(r, r + \Delta t) = 1] / \Delta t = \lambda \quad (\text{Eq. J3.6-5})$$

and

$$\lim_{\Delta t \rightarrow 0^+} prob[N(r, r + \Delta t) \geq 2] / \Delta t = 0 \quad (\text{Eq. J3.6-6})$$

in Equations J3.6-2 and J3.6-3, respectively.

The conditions in Equations J3.6-2 and J3.6-3 require that, in a small interval of length Δt , the probability of one event occurring is approximately $\lambda \Delta t$ and the probability of two or more events occurring is approximately zero. The condition in Equation J3.6-4 requires independence for the numbers of events occurring in two disjoint intervals. The quantity λ is the defining rate for the process and has units of inverse time (e.g., yr^{-1}).

The following important properties hold for the Poisson process defined by the conditions in Equations J3.6-2 – J3.6-4:

$$prob[N(r, s) = 0] = \exp[-\lambda(s - r)], \quad (\text{Eq. J3.6-7})$$

$$prob[N(r, s) = 1] = \lambda(s - r) \exp[-\lambda(s - r)], \quad (\text{Eq. J3.6-8})$$

$$prob[N(r, s) \geq 1] = 1 - prob[N(r, s) = 0] = 1 - \exp[-\lambda(s - r)] \quad (\text{Eq. J3.6-9})$$

and, in general,

$$prob[N(r, s) = k] = \left\{ \frac{[\lambda(s - r)]^k}{k!} \right\} \exp[-\lambda(s - r)] \quad (\text{Eq. J3.6-10})$$

for $k = 0, 1, 2, \dots$. Further,

$$E[N(r, s)] = \lambda(s - r), \quad (\text{Eq. J3.6-11})$$

where E denotes expected value. When $\lambda(s - r)$ is small (i.e., much less than one), then $\lambda(s - r)$ approximates $\text{prob}[N(r, s) = 1]$; however, $\lambda(s - r)$ ceases to be a valid approximation to $\text{prob}[N(r, s) = 1]$ as it increases in size.

An important property of stationary Poisson processes is that, if the process occurs exactly one time in the interval $[r, s]$ (i.e., if $N(r, s) = 1$), then the occurrence time has a uniform distribution on $[r, s]$. Specifically,

$$d[t|N(r, s) = 1] = 1/(s - r) \quad (\text{Eq. J3.6-12})$$

is the density function defined on $[r, s]$ for time of occurrence.

A new Poisson process with rate

$$\lambda = \lambda_1 + \lambda_2 + \dots + \lambda_n \quad (\text{Eq. J3.6-13})$$

can be created by combining n Poisson processes with rates $\lambda_1, \lambda_2, \dots, \lambda_n$ provided the occurrences across the rates are independent (i.e., the occurrence of an event associated with process i has no effect on the potential occurrence of an event associated with process j and vice versa). Then, λ is the occurrence rate for the process that results when no distinction is made between occurrences associated with the processes characterized by $\lambda_1, \lambda_2, \dots, \lambda_n$.

The Poisson process defined by the conditions in Equations J3.6-2 – J3.6-4 is referred to as a stationary or homogeneous Poisson to emphasize that the value for λ is constant. A generalization is to replace the condition in Equation J3.6-2 with

$$\text{prob}[N(r, r + \Delta t) = 1] = \lambda(r) \Delta t + o(\Delta t). \quad (\text{Eq. J3.6-14})$$

With this formulation, $\lambda(r)$ is now a function of time, and the resultant Poisson process is referred to as a nonstationary or nonhomogeneous Poisson process to emphasize that λ is no longer constant with time. For example, it has been proposed that the occurrence of igneous events in the vicinity of the Yucca Mountain repository can be characterized by a nonstationary Poisson process (Connor and Hill 1995 [DIRS 102646]).

When nonstationary Poisson processes are under consideration, the relationships in Equations J3.6-7 – J3.6-13 have similar but slightly more complicated forms. Specifically,

$$\text{prob}[N(r, s) = 0] = \exp\left[-\int_r^s \lambda(t) dt\right], \quad (\text{Eq. J3.6-15})$$

$$prob[N(r, s) = 1] = \left[\int_r^s \lambda(t) dt \right] \exp \left[- \int_r^s \lambda(t) dt \right], \quad (\text{Eq. J3.6-16})$$

$$prob[N(r, s) \geq 1] = 1 - \exp \left[- \int_r^s \lambda(t) dt \right], \quad (\text{Eq. J3.6-17})$$

$$prob[N(r, s) = k] = \left\{ \left[\int_r^s \lambda(t) dt \right]^k / k! \right\} \exp \left[- \int_r^s \lambda(t) dt \right], \quad (\text{Eq. J3.6-18})$$

$$E[N(r, s)] = \int_r^s \lambda(t) dt \quad (\text{Eq. J3.6-19})$$

and

$$\lambda(t) = \lambda_1(t) + \lambda_2(t) + \dots + \lambda_n(t). \quad (\text{Eq. J3.6-20})$$

Further, if a nonstationary Poisson process with rate $\lambda(t)$ occurs exactly one time in the interval $[r, s]$, then

$$d[t | N(r, s) = 1] = \lambda(t) / \int_r^s \lambda(\tau) d\tau \quad (\text{Eq. J3.6-21})$$

is the density function defined on $[r, s]$ for time of occurrence. The results in Equations J3.6-14 – J3.6-21 reduce to those in Equations J3.6-7 – J3.6-13 when the time-dependent λ 's are replaced by constant values.

A Poisson process involves events occurring over intervals of time. A related process involves occurrences (e.g., failures) associated with individual members of a finite population. If the population has n members and each member of the population has the same probability p of experiencing the occurrence under consideration, then probability $prob(m)$ that exactly m members of the population will experience the occurrence is

$$prob(m) = \binom{n}{m} p^m (1-p)^{n-m}. \quad (\text{Eq. J3.6-22})$$

The preceding defines the density function for the binomial distribution (Ross 1993 [DIRS 172064], p. 27). In turn,

$$prob(i \leq m) = \sum_{i=0}^m \binom{n}{i} p^i (1-p)^{n-i} \quad (\text{Eq. J3.6-23})$$

is the probability of m or fewer occurrences, and

$$\begin{aligned} \text{prob}(m < i) &= \sum_{i=m+1}^n \binom{n}{i} p^i (1-p)^{n-i} \\ &= 1 - \sum_{i=0}^m \binom{n}{i} p^i (1-p)^{n-i} \end{aligned} \quad (\text{Eq. J3.6-24})$$

is the probability of more than m occurrences. An important special case of Equation J3.6-24 is

$$\begin{aligned} \text{prob}(0 < i) &= 1 - \binom{n}{0} p^0 (1-p)^{n-0} \\ &= 1 - (1-p)^n, \end{aligned} \quad (\text{Eq. J3.6-25})$$

which is the probability of one or more failures. In the TSPA-LA, early WP failures and early DS failures are assumed to follow binomial distributions with occurrence probabilities of the form defined in Equations J3.6-22 – J3.6-25.

For $p \leq 0.1$, the Poisson probability model provides a good approximation to the binomial probability model. Specifically,

$$\text{prob}(m) \cong \left[(np)^m / m! \right] \exp(-np), \quad (\text{Eq. J3.6-26})$$

$$\text{prob}(i \leq m) \cong \sum_{i=1}^m \left[(np)^i / i! \right] \exp(-np), \quad (\text{Eq. J3.6-27})$$

$$\begin{aligned} \text{prob}(m \leq i) &\cong \sum_{i=m+1}^n \left[(np)^i / i! \right] \exp(-np) \\ &= 1 - \sum_{i=m+1}^m \left[(np)^i / i! \right] \exp(-np) \end{aligned} \quad (\text{Eq. J3.6-28})$$

and

$$\text{prob}(0 < i) \cong 1 - \exp(-np). \quad (\text{Eq. J3.6-29})$$

The preceding approximations are valid independent of the size of n and also hold for $p \geq 0.9$ (Hahn and Shapiro 1967 [DIRS 146529]).

J4 CONCEPTUAL STRUCTURE OF TSPA-LA

J4.1 Three Basic Entities

The following is written to provide a high-level overview of the calculations that will be performed in the TSPA-LA to determine expected dose and other quantities of interest. As discussed in Section J3, the determination of expected dose is based on operations involving three basic mathematical entities: (i) a probabilistic characterization of aleatory uncertainty, (ii) a model that predicts dose to the RMEI conditional on a specific realization of aleatory uncertainty, and (iii) a probabilistic characterization of the epistemic uncertainty present in quantities used in the characterization of aleatory uncertainty and the determination of dose.

In the preceding, aleatory uncertainty is used in the designation of, in so far as our ability to predict the future is concerned, randomness in the possible future conditions that could affect the Yucca Mountain repository. In concept, each possible future at the Yucca Mountain repository can be represented by a vector

$$\mathbf{a} = [a_1, a_2, \dots, a_{n_A}], \quad (\text{Eq. J4.1-1})$$

where each a_i is a specific property of the future \mathbf{a} (e.g., time of a seismic event, size of a seismic event, ...). In turn, a subset S of the set \mathcal{A} of all possible values for \mathbf{a} constitutes what is referred to as a scenario class in the TSPA-LA. As part of the TSPA-LA development, a probabilistic structure is imposed on the set \mathcal{A} . Formally, this corresponds to defining a probability space $(\mathcal{A}, \mathbf{A}, p_A)$ for aleatory uncertainty. Then, \mathbf{A} is the set of all possible scenario classes, and p_A is the function that defines scenario class probability (i.e., scenario class S is an element of \mathbf{A} and $p_A(S)$ is the probability of scenario class S). Formally, the probability space $(\mathcal{A}, \mathbf{A}, p_A)$ provides a characterization of aleatory uncertainty and constitutes the first of the three basic mathematical entities that underlie the determination of expected dose.

Although useful conceptually and notationally, the probability space $(\mathcal{A}, \mathbf{A}, p_A)$ is never explicitly defined in the TSPA-LA. Rather, the characterization of aleatory uncertainty enters the analysis through the definition of probability distributions for the individual elements of \mathbf{a} . Conceptually, the distributions for the elements of \mathbf{a} lead to a distribution for \mathbf{a} and an associated density function $d_A(\mathbf{a})$.

The second of the three basic mathematical entities that underlie the determination of expected dose is a model that predicts dose to the RMEI. Formally, this model can be represented by the function

$$D(\tau|\mathbf{a}) = \text{dose to RMEI (mrem/yr) at time } \tau \text{ (yr) conditional on the occurrence of the future represented by } \mathbf{a}. \quad (\text{Eq. J4.1-2})$$

Technically, $D(\tau|\mathbf{a})$ is the committed 50 yr dose to the RMEI that results from radiation exposure incurred in a single year. In the computational implementation of the TSPA-LA, $D(\tau|\mathbf{a})$ corresponds to the calculation performed with the GoldSim program for the particular analysis

configuration defined for the future \mathbf{a} . In practice, many results are calculated for \mathbf{a} in addition to dose to the RMEI. Thus, $D(\tau|\mathbf{a})$ is actually a vector $\mathbf{D}(\tau|\mathbf{a})$ containing at least several thousand elements. For notational convenience, $D(\tau|\mathbf{a})$ is treated as a scalar and referred to as dose to the RMEI; however, other TSPA-LA results can be handled in exactly the same manner as described for dose.

The third of the three basic mathematical entities that underlie the determination of expected dose is a probabilistic characterization of epistemic uncertainty. Here, epistemic uncertainty refers to a lack of knowledge with respect to the appropriate value to use for a quantity that is assumed to have constant or fixed value in the context of a specific analysis — the TSPA-LA in this discussion. Specifically, epistemic uncertainty relates to a vector of the form

$$\begin{aligned} \mathbf{e} &= [\mathbf{e}_A, \mathbf{e}_M] \\ &= [e_{A1}, e_{A2}, \dots, \dots, e_{A,nAE}, e_{M1}, e_{M2}, \dots, e_{M,nME}] \\ &= [e_1, e_2, \dots, e_{nE}], nE = nAE + nME, \end{aligned} \tag{Eq. J4.1-3}$$

where

$$\mathbf{e}_A = [e_{A1}, e_{A2}, \dots, e_{A,nAE}]$$

is a vector of epistemically uncertain quantities used in the characterization of aleatory uncertainty (e.g., a rate term that defines a Poisson process) and

$$\mathbf{e}_M = [e_{M1}, e_{M2}, \dots, e_{M,nME}]$$

is a vector of epistemically uncertain quantities used in the determination of dose (e.g., a distribution coefficient).

Epistemic uncertainty results in a set \mathcal{E} of possible values for \mathbf{e} . In turn, probability is used to characterize the level of likelihood or credence that can be assigned to various subsets of \mathcal{E} . In concept, this leads to a probability space $(\mathcal{E}, \mathcal{E}, p_E)$ for epistemic uncertainty. Like the probability space $(\mathcal{A}, \mathcal{A}, p_A)$ for aleatory uncertainty, the probability space $(\mathcal{E}, \mathcal{E}, p_E)$ for epistemic uncertainty is useful conceptually and notationally but is never explicitly defined in the TSPA-LA. Rather, the characterization of epistemic uncertainty enters the analysis through the definition of probability distributions for the individual elements of \mathbf{e} . These distributions serve as mathematical summaries of all available information with respect to where the appropriate values for individual elements of \mathbf{e} are located for use in the TSPA-LA. Conceptually, the distributions for the elements of \mathbf{e} lead to a distribution for \mathbf{e} and an associated density function $d_E(\mathbf{e})$.

J4.2 Expected Dose and Related Definitions of Projected Dose, Mean Dose and Median Dose

Now that the characterization of epistemic uncertainty has been introduced, the notations used to represent aleatory uncertainty and dose need to be expanded. Because the representation of aleatory uncertainty depends on elements of the vector \mathbf{e}_A , each possible value for \mathbf{e}_A could lead to a different probability space (\mathcal{A}, A, p_A) for aleatory uncertainty. For notational convenience, this dependence will be indicated by representing the density function associated with aleatory uncertainty by $d_A(\mathbf{a}|\mathbf{e}_A)$. Similarly, the determination of dose depends on elements of the vector \mathbf{e}_M , with each possible value for \mathbf{e}_M potentially leading to different dose results. For notational convenience, this dependence will be indicated by representing the dose function by $D(\tau|\mathbf{a}, \mathbf{e}_M)$.

The probability space (\mathcal{A}, A, p_A) for aleatory uncertainty characterized by the density function $d_A(\mathbf{a}|\mathbf{e}_A)$, the dose function $D(\tau|\mathbf{a}, \mathbf{e}_M)$, and the probability space (\mathcal{E}, E, p_E) for epistemic uncertainty characterized by the density function $d_E(\mathbf{e})$ constitute the three basic parts of the TSPA-LA that come together in the determination of expected dose to the RMEI and the uncertainty in expected dose to the RMEI. Specifically, the complementary cumulative distribution function (CCDF) for dose at time τ and the expected value for dose at time τ conditional on a specific element $\mathbf{e} = [\mathbf{e}_A, \mathbf{e}_M]$ of \mathcal{E} are given by

$$p_A \left[D < D(\tau|\mathbf{a}, \mathbf{e}_M) \middle| \mathbf{e}_A \right] = \int_{\mathcal{A}} \bar{\delta}_D \left[D(\tau|\mathbf{a}, \mathbf{e}_M) \right] d_A(\mathbf{a}|\mathbf{e}_A) dA \quad (\text{Eq. J4.2-1})$$

and

$$\bar{D}(\tau|\mathbf{e}) = E_A \left[D(\tau|\mathbf{a}, \mathbf{e}_M) \middle| \mathbf{e}_A \right] = \int_{\mathcal{A}} D(\tau|\mathbf{a}, \mathbf{e}_M) d_A(\mathbf{a}|\mathbf{e}_A) dA, \quad (\text{Eq. J4.2-2})$$

respectively, where

$$\bar{\delta}_D \left[D(\tau|\mathbf{a}, \mathbf{e}_M) \right] = \begin{cases} 1 & \text{if } D < D(\tau|\mathbf{a}, \mathbf{e}_M) \\ 0 & \text{otherwise} \end{cases} \quad (\text{Eq. J4.2-3})$$

and $E_A[D(\tau|\mathbf{a}, \mathbf{e}_M)|\mathbf{e}_A]$ denotes expectation over aleatory uncertainty.

In turn, the uncertainty associated with the estimation of $\bar{D}(\tau|\mathbf{e})$ can be determined from the properties of the probability space (\mathcal{E}, E, p_E) for epistemic uncertainty. In particular, the CCDF for $\bar{D}(\tau|\mathbf{e})$ and the expected value for $\bar{D}(\tau|\mathbf{e})$ that derive from epistemic uncertainty are given by

$$p_E \left[D < \bar{D}(\tau|\mathbf{e}) \right] = \int_{\mathcal{E}} \bar{\delta}_D \left[\bar{D}(\tau|\mathbf{e}) \right] d_E(\mathbf{e}) dE \quad (\text{Eq. J4.2-4})$$

and

$$\bar{D}(\tau) = E_E \left[\bar{D}(\tau|\mathbf{e}) \right] = \int_{\mathcal{E}} \bar{D}(\tau|\mathbf{e}) d_E(\mathbf{e}) dE, \quad (\text{Eq. J4.2-5})$$

respectively, where $\bar{\delta}_D[\bar{D}(\tau|\mathbf{e})]$ is defined as indicated in Equation J4.2-3 and $E_E[\bar{D}(\tau|\mathbf{e})]$ denotes expectation over epistemic uncertainty.

Complementary cumulative distribution functions of the form defined in Equations J4.2-1 and J4.2-4 constitute the standard format used to present the results of a performance assessment because they provide the answer to the following basic question that underlies all performance assessments: “How likely is it to be this bad or worse?”

In addition to CCDFs, cumulative distribution functions (CDFs) are also used in the presentation of results obtained in a performance assessment. Specifically, the CDF for dose at time τ conditional on a specific element $\mathbf{e} = [\mathbf{e}_A, \mathbf{e}_M]$ of \mathcal{E} is given by

$$p_A \left[D(\tau|\mathbf{a}, \mathbf{e}_M) \leq D|\mathbf{e}_A \right] = \int_{\mathcal{A}} \underline{\delta}_D \left[D(\tau|\mathbf{a}, \mathbf{e}_M) \right] d_A(\mathbf{a}|\mathbf{e}_A) dA, \quad (\text{Eq. J4.2-6})$$

where

$$\begin{aligned} \underline{\delta}_D \left[D(\tau|\mathbf{a}, \mathbf{e}_M) \right] &= \begin{cases} 1 & \text{if } D(\tau|\mathbf{a}, \mathbf{e}_M) \leq D \\ 0 & \text{otherwise} \end{cases} \\ &= 1 - \bar{\delta}_D \left[D(\tau|\mathbf{a}, \mathbf{e}_M) \right]. \end{aligned} \quad (\text{Eq. J4.2-7})$$

The value of D for which

$$q = p_A \left[D(\tau|\mathbf{a}, \mathbf{e}_M) \leq D|\mathbf{e}_A \right] = \int_{\mathcal{A}} \underline{\delta}_D \left[D(\tau|\mathbf{a}, \mathbf{e}_M) \right] d_A(\mathbf{a}|\mathbf{e}_A) dA \quad (\text{Eq. J4.2-8})$$

defines the q quantile (e.g., $q = 0.05, 0.5$ or 0.95) for the distribution of dose at time τ conditional on the vector $\mathbf{e} = [\mathbf{e}_A, \mathbf{e}_M]$ of epistemically uncertain analysis inputs. For notational purposes, the value of D corresponding to the q quantile of $D(\tau|\mathbf{a}, \mathbf{e}_M)$ defined in Equation J4.2-8 will be represented by $Q_{Aq}[D(\tau|\mathbf{a}, \mathbf{e}_M)|\mathbf{e}_A]$ with the subscript A indicating that the quantile derives from aleatory uncertainty (i.e., from the possible values of \mathbf{a} conditional on the vector $\mathbf{e} = [\mathbf{e}_A, \mathbf{e}_M]$ of epistemically uncertain analysis inputs).

Similarly, the CDF for expected dose at time τ is given by

$$\begin{aligned} p_E \left[\bar{D}(\tau|\mathbf{e}) \leq D \right] &= \int_{\mathcal{E}} \underline{\delta}_D \left[\bar{D}(\tau|\mathbf{e}) \right] d_E(\mathbf{e}) dE \\ &= \int_{\mathcal{E}} \underline{\delta}_D \left[\int_{\mathcal{A}} D(\tau|\mathbf{a}, \mathbf{e}_M) d_A(\mathbf{a}|\mathbf{e}_A) dA \right] d_E(\mathbf{e}) dE \end{aligned} \quad (\text{Eq. J4.2-9})$$

with $\underline{\delta}_D$ defined in the manner indicated in Equation J4.2-7, and the value of D for which

$$q = p_E \left[\bar{D}(\tau|\mathbf{e}) \leq D \right] = \int_E \underline{\delta}_D \left[\bar{D}(\tau|\mathbf{e}) \right] d_E(\mathbf{e}) dE \quad (\text{Eq. J4.2-10})$$

defines the q quantile for the distribution of expected dose over epistemically uncertain analysis inputs. For notational purposes, the value of D corresponding to the q quantile of $\bar{D}(\tau|\mathbf{e})$ defined in Equation J4.2-9 will be represented by $Q_q[\bar{D}(\tau|\mathbf{e})]$.

For assessing compliance with the standards in (EPA14) and (NRC20), projected dose is assumed to correspond to the expected doses $\bar{D}(\tau|\mathbf{e})$ defined in Equation J4.2-2, mean dose is assumed to correspond to the expected dose $\bar{\bar{D}}(\tau)$ defined in Equation J4.2-5, and median dose is assumed to correspond to the $q = 0.5$ quantile $D = Q_{0.5}[\bar{D}(\tau|\mathbf{e})]$ defined in Equation J4.2-10. To facilitate distinguishing between the two expected doses, $\bar{D}(\tau|\mathbf{e})$ will be referred to as expected dose, and $\bar{\bar{D}}(\tau)$ will be referred to as expected (mean) dose.

In contrast, if the actual dose $D(\tau|\mathbf{a}, \mathbf{e}_M)$ for each future \mathbf{a} was assumed to correspond to projected dose, then $\bar{D}(\tau|\mathbf{e})$ would correspond to the mean dose specified in (EPA14) and (NRC20) and the CDF defined by Equation J4.2-9 would characterize the uncertainty in mean dose (i.e., in $\bar{D}(\tau|\mathbf{e})$). With $D(\tau|\mathbf{a}, \mathbf{e}_M)$ interpreted as projected dose, the median dose specified in (EPA14) and (EPA20) would then be $Q_{A,0.5}[D(\tau|\mathbf{a}, \mathbf{e}_M)|\mathbf{e}_A]$ as defined in Equation J4.2-6 for $q = 0.5$. In turn, the uncertainty in median dose would be characterized by the CDF defined by

$$p_E \left\{ Q_{A,0.5} \left[D(\tau|\mathbf{a}, \mathbf{e}_M) | \mathbf{e}_A \right] \leq Q \right\} = \int_E \underline{\delta}_Q \left\{ Q_{A,0.5} \left[D(\tau|\mathbf{a}, \mathbf{e}_M) | \mathbf{e}_A \right] \right\} d_E(\mathbf{e}) dE \quad (\text{Eq. J4.2-11})$$

with $\underline{\delta}_Q\{\sim\}$ defined similarly to $\underline{\delta}_D\{\sim\}$ in Equation J4.2-7. Both interpretations of projected dose use the same information; the only difference is how this information is summarized.

J4.3 Probabilities

As a reminder, probabilities are defined for subsets of a sample space. In Equations J4.2-1 and J4.2-6, the sample space is the set \mathcal{A} of possible futures, and the indicated probabilities $p_A[D < D(\tau|\mathbf{a}, \mathbf{e}_M)|\mathbf{e}_A]$ and $p_A[D(\tau|\mathbf{a}, \mathbf{e}_M) \leq D|\mathbf{e}_A]$ are probabilities for the sets

$$\bar{\mathcal{A}}_D(\tau, \mathbf{e}_M) = \left\{ \mathbf{a} : \mathbf{a} \in \mathcal{A} \text{ and } D < D(\tau|\mathbf{a}, \mathbf{e}_M) \right\} \quad (\text{Eq. J4.3-1})$$

and

$$\underline{\mathcal{A}}_D(\tau, \mathbf{e}_M) = \left\{ \mathbf{a} : \mathbf{a} \in \mathcal{A} \text{ and } D(\tau|\mathbf{a}, \mathbf{e}_M) \leq D \right\}, \quad (\text{Eq. J4.3-2})$$

respectively. The sets $\bar{\mathcal{A}}_D(\tau|\mathbf{e}_M)$ and $\underline{\mathcal{A}}_D(\tau|\mathbf{e}_M)$, and hence the probabilities

$$p_A \left[D < D(\tau|\mathbf{a}, \mathbf{e}_M) | \mathbf{e}_A \right] = p_A \left[\bar{\mathcal{A}}_D(\tau, \mathbf{e}_M) | \mathbf{e}_A \right] \quad (\text{Eq. J4.3-3})$$

and

$$p_A \left[D(\tau | \mathbf{a}, \mathbf{e}_M) \leq D | \mathbf{e}_A \right] = p_A \left[\underline{\mathcal{A}}_D(\tau, \mathbf{e}_M) | \mathbf{e}_A \right], \quad (\text{Eq. J4.3-4})$$

depend on both the time τ at which dose is calculated and the elements of \mathbf{e}_M used in the calculation of dose. As indicated by the conditionality on \mathbf{e}_A , the preceding probabilities also depend on epistemically uncertain quantities that are elements of \mathbf{e}_A . Similarly, the defining relationships for quantiles in Equation J4.2-8 involves probabilities for sets of the form $\underline{\mathcal{A}}_D(\tau | \mathbf{e}_M)$.

In Equations J4.2-4 and J4.2-9, the sample space is the set \mathcal{E} of epistemically uncertain analysis inputs, and the indicated probabilities $p_E[D < \bar{D}(\tau | \mathbf{e})]$ and $p_E[\bar{D}(\tau | \mathbf{e}) \leq D]$ are probabilities for the sets

$$\bar{\mathcal{E}}_D(\tau) = \{ \mathbf{e} : \mathbf{e} \in \mathcal{E} \text{ and } D < \bar{D}(\tau | \mathbf{e}) \} \quad (\text{Eq. J4.3-5})$$

and

$$\underline{\mathcal{E}}_D(\tau) = \{ \mathbf{e} : \mathbf{e} \in \mathcal{E} \text{ and } \bar{D}(\tau | \mathbf{e}) \leq D \}, \quad (\text{Eq. J4.3-6})$$

respectively. As indicated, the sets $\bar{\mathcal{E}}_D(\tau)$ and $\underline{\mathcal{E}}_D(\tau)$, and hence the probabilities

$$p_E \left[D < \bar{D}(\tau | \mathbf{e}) \right] = p_E \left[\bar{\mathcal{E}}_D(\tau) \right] \quad (\text{Eq. J4.3-7})$$

and

$$p_E \left[\bar{D}(\tau | \mathbf{e}) \leq D \right] = p_E \left[\underline{\mathcal{E}}_D(\tau) \right], \quad (\text{Eq. J4.3-8})$$

depend on the time τ at which expected dose is calculated. Similarly, the defining relationship for quantiles in Equation J4.2-10 involves probabilities for sets of the form $\underline{\mathcal{E}}_D(\tau)$.

The discussion associated with Equations J4.3-1 – J4.3-8 may seem pedantic. However, probabilities are defined for sets. In turn, there are two important implications to the dependence of probabilities on sets. First, a probability cannot be meaningfully defined unless the set for which it is being defined is clearly described. Second, even if a probability is appropriately defined for a given set, this probability cannot be meaningfully understood unless the underlying set is also known. All of the results discussed in this presentation are based on the assignment of probabilities to scenario classes, which in turn are subsets of the sample space \mathcal{A} for aleatory uncertainty. As a result, the connection between sets and probabilities is fundamental to the conceptual structure and computational implementation of the TSPA-LA.

In practice, the quantities $p_A[D < D(\tau|\mathbf{a}, \mathbf{e}_M)|\mathbf{e}_A]$, $\bar{D}(\tau|\mathbf{e})$ and $p_A[D(\tau|\mathbf{a}, \mathbf{e}_M) \leq D|\mathbf{e}_A]$ defined in Equations J4.2-1, J4.2-2 and J4.2-6 are often estimated with sampling-based procedures. Specifically, a random sample

$$\mathbf{a}_j, j = 1, 2, \dots, nR, \quad (\text{Eq. J4.3-9})$$

is generated from \mathcal{A} in consistency with the density function $d_A(\mathbf{a}|\mathbf{e}_A)$ (i.e., in consistency with the definition of the probability space (\mathcal{A}, A, p_A) for aleatory uncertainty corresponding to \mathbf{e}_A). Then, approximations to $p_A[D < D(\tau|\mathbf{a}, \mathbf{e}_M)|\mathbf{e}_A]$, $\bar{D}(\tau|\mathbf{e})$ and $p_A[D(\tau|\mathbf{a}, \mathbf{e}_M) \leq D|\mathbf{e}_A]$ are given by

$$p_A \left[D < D(\tau|\mathbf{a}, \mathbf{e}_M) \middle| \mathbf{e}_A \right] \cong \sum_{j=1}^{nR} \bar{\delta}_D \left[D(\tau|\mathbf{a}_j, \mathbf{e}_M) \right] / nR, \quad (\text{Eq. J4.3-10})$$

$$\bar{D}(\tau|\mathbf{e}) \cong \sum_{j=1}^{nR} D(\tau|\mathbf{a}_j, \mathbf{e}_M) / nR \quad (\text{Eq. J4.3-11})$$

and

$$p_A \left[D(\tau|\mathbf{a}, \mathbf{e}_M) \leq D \middle| \mathbf{e}_A \right] \cong \sum_{j=1}^{nR} \underline{\delta}_D \left[D(\tau|\mathbf{a}_j, \mathbf{e}_M) \right] / nR, \quad (\text{Eq. J4.3-12})$$

respectively. In some cases, the use of importance sampling rather than simple random sampling can reduce the sample size required to produce adequate approximations. Further, as indicated in Equation J4.2-8, the approximation in Equation J4.3-12 can be used in the determination of quantile values for $D(\tau|\mathbf{a}, \mathbf{e}_M)$ that derive from the probability distribution over \mathcal{A} defined by $d_A(\mathbf{a}|\mathbf{e}_A)$.

Similarly, the quantities $p_E[D < \bar{D}(\tau|\mathbf{e})]$, $\bar{\bar{D}}(\tau)$ and $p_E[\bar{D}(\tau|\mathbf{e}) \leq D]$ defined in Equations J4.2-4, J4.2-5 and J4.2-9 are usually estimated with sampling-based procedure. As discussed in Section J4.9, the TSPA-LA uses Latin hypercube sampling in the estimation of $p_E[D < \bar{D}(\tau|\mathbf{e})]$, $\bar{\bar{D}}(\tau)$ and $p_E[\bar{D}(\tau|\mathbf{e}) \leq D]$.

J4.4 Scenario Classes and the Characterization of Aleatory Uncertainty

The following conditions/occurrences related to aleatory uncertainty are considered in the TSPA-LA: nominal (i.e., undisturbed) conditions, early waste package (WP) failure, early drip shield (DS) failure, igneous intrusive events, igneous eruptive events, seismic ground motion events, and seismic fault displacement events. Consistent with this, each aleatory future \mathbf{a} over a time interval $[a, b]$ (e.g., $[0, 2 \times 10^4 \text{ yr}]$ or $[0, 10^6 \text{ yr}]$) can be represented by

$$\mathbf{a} = [nEW, nED, nII, nIE, nSG, nSF, \mathbf{a}_{EW}, \mathbf{a}_{ED}, \mathbf{a}_{II}, \mathbf{a}_{IE}, \mathbf{a}_{SG}, \mathbf{a}_{SF}] \quad (\text{Eq. J4.4-1})$$

where, for the time interval $[a, b]$,

nEW = number of early WP failures,

nED = number of early DS failures,

nII = number of igneous intrusive events.

nIE = number of igneous eruptive events,

nSG = number of seismic ground motion events,

nSF = number of seismic fault displacement events,

\mathbf{a}_{EW} = vector defining the nEW early WP failures,

\mathbf{a}_{ED} = vector defining the nED early DS failures,

\mathbf{a}_{II} = vector defining the nII igneous intrusive events,

\mathbf{a}_{IE} = vector defining the nIE igneous eruptive events,

\mathbf{a}_{SG} = vector defining the nSG seismic ground motion events,

\mathbf{a}_{SF} = vector defining the nSF fault displacement events.

Then,

$$\mathcal{A} = \left\{ \mathbf{a} : \mathbf{a} = [nEW, nED, nII, nIE, nSG, nSF, \mathbf{a}_{EW}, \mathbf{a}_{ED}, \mathbf{a}_{II}, \mathbf{a}_{IE}, \mathbf{a}_{SG}, \mathbf{a}_{SF}] \right\} \quad (\text{Eq. J4.4-2})$$

is the set of all futures to be considered in the TSPA-LA (i.e., the sample space for aleatory uncertainty). If needed, the expanded notation $\mathcal{A}(a, b)$ can be used to indicate the time interval over which the individual futures are defined (e.g., $\mathcal{A}(0, 20000)$ and $\mathcal{A}(0, 10^6)$ for $[a, b] = [0, 20,000 \text{ yr}]$ and $[a, b] = [0, 10^6 \text{ yr}]$, respectively); however, this will not be done when the time interval is clear given the context under consideration.

In turn, the vectors \mathbf{a}_{EW} , \mathbf{a}_{ED} , \mathbf{a}_{II} , \mathbf{a}_{IE} , \mathbf{a}_{SG} and \mathbf{a}_{SF} are of the form

$$\mathbf{a}_{EW} = [\mathbf{a}_{EW,1}, \mathbf{a}_{EW,2}, \dots, \mathbf{a}_{EW,nEW}], \quad (\text{Eq. J4.4-3})$$

$$\mathbf{a}_{ED} = [\mathbf{a}_{ED,1}, \mathbf{a}_{ED,2}, \dots, \mathbf{a}_{ED,nED}], \quad (\text{Eq. J4.4-4})$$

$$\mathbf{a}_{II} = [\mathbf{a}_{II,1}, \mathbf{a}_{II,2}, \dots, \mathbf{a}_{II,nII}], \quad (\text{Eq. J4.4-5})$$

$$\mathbf{a}_{IE} = [\mathbf{a}_{IE,1}, \mathbf{a}_{IE,2}, \dots, \mathbf{a}_{IE,nIE}], \quad (\text{Eq. J4.4-6})$$

$$\mathbf{a}_{SG} = [\mathbf{a}_{SG,1}, \mathbf{a}_{SG,2}, \dots, \mathbf{a}_{SG,nSG}] \quad (\text{Eq. J4.4-7})$$

and

$$\mathbf{a}_{SF} = [\mathbf{a}_{SF,1}, \mathbf{a}_{SF,2}, \dots, \mathbf{a}_{SF,nSF}], \quad (\text{Eq. J4.4-8})$$

where

$\mathbf{a}_{EW,j}$ = vector defining early WP failure j for $j = 1, 2, \dots, nEW$,

$\mathbf{a}_{ED,j}$ = vector defining early DS failure j for $j = 1, 2, \dots, nED$,

$\mathbf{a}_{II,j}$ = vector defining igneous intrusive event j for $j = 1, 2, \dots, nII$,

$\mathbf{a}_{IE,j}$ = vector defining igneous eruptive event j for $j = 1, 2, \dots, nIE$,

$\mathbf{a}_{SG,j}$ = vector defining seismic ground motion event j for $j = 1, 2, \dots, nSG$,

$\mathbf{a}_{SF,j}$ = vector defining seismic fault displacement event j for $j = 1, 2, \dots, nSF$.

The vectors $\mathbf{a}_{EW,j}$, $\mathbf{a}_{ED,j}$, $\mathbf{a}_{II,j}$, $\mathbf{a}_{IE,j}$, $\mathbf{a}_{SG,j}$ and $\mathbf{a}_{SF,j}$ will be defined in later sections.

Given an adequate probabilistic characterization of the elements of $\mathbf{a}_{EW,j}$, $\mathbf{a}_{ED,j}$, $\mathbf{a}_{II,j}$, $\mathbf{a}_{IE,j}$, $\mathbf{a}_{SG,j}$ and $\mathbf{a}_{SF,j}$, it is, at least in concept, possible to calculate the probability $p_A(\mathcal{U})$ of any subset \mathcal{U} of \mathcal{A} (modulo certain theoretical restrictions on the nature of \mathcal{U}). More generally, the probability of a subset \mathcal{U} of \mathcal{A} is dependent on values for epistemically uncertain analysis inputs and thus has the conditional representation $p_A(\mathcal{U}|\mathbf{e}_A)$ or possibly $p_A(\mathcal{U}|\mathbf{e})$, where $\mathbf{e} = [\mathbf{e}_A, \mathbf{e}_M]$ is the vector of epistemically uncertain analysis inputs defined in Equation J4.1-3.

A scenario class is a subset of the set \mathcal{A} (i.e., an event in the standard terminology of probability theory). The following basic scenario classes are used in the organization of the TSPA-LA: nominal, early failure, igneous, and seismic. In turn, these scenario classes correspond to the following subsets of \mathcal{A} :

$$\mathcal{A}_N = \{\mathbf{a} : \mathbf{a} \in \mathcal{A} \text{ and } nEW = nED = nII = nIE = nSG = nSF = 0\} \quad (\text{Eq. J4.4-9})$$

for the nominal scenario class (i.e., the set containing the single future \mathbf{a}_N that involves no disruption of any kind);

$$\mathcal{A}_E = \{\mathbf{a} : \mathbf{a} \in \mathcal{A} \text{ and } nEW \geq 1 \text{ or } nED \geq 1\} \quad (\text{Eq. J4.4-10})$$

for the early failure scenario class (i.e., the set containing all elements of \mathcal{A} that involve at least one early WP failure or a least one early DS failure);

$$\mathcal{A}_I = \{\mathbf{a} : \mathbf{a} \in \mathcal{A} \text{ and } nII \geq 1\} \quad (\text{Eq. J4.4-11})$$

for the igneous scenario class (i.e., the set containing all elements of \mathcal{A} that involve at least one igneous intrusive event, which includes all elements of \mathcal{A} with $nIE \geq 1$ as igneous eruptions only, but not necessarily, occur in conjunction with igneous intrusions); and

$$\mathcal{A}_S = \{\mathbf{a} : \mathbf{a} \in \mathcal{A} \text{ and } nSG \geq 1 \text{ or } nSF \geq 1\} \quad (\text{Eq. J4.4-12})$$

for the seismic scenario class (i.e., the set containing all elements of \mathcal{A} that involve at least one seismic ground motion event or at least one seismic fault displacement event).

In turn, the early failure scenario class \mathcal{A}_E is underlain by an early WP failure scenario class \mathcal{A}_{EW} and an early DS failure scenario class \mathcal{A}_{ED} ; the igneous scenario class \mathcal{A}_I is underlain by an igneous intrusive scenario class \mathcal{A}_{II} and an igneous eruptive scenario class \mathcal{A}_{IE} ; and the seismic scenario class \mathcal{A}_S is underlain by a seismic ground motion scenario class \mathcal{A}_{SG} and a seismic fault displacement scenario class \mathcal{A}_{SF} . Specifically, these scenario classes correspond to the following subsets of \mathcal{A} :

$$\mathcal{A}_{EW} = \{\mathbf{a} : \mathbf{a} \in \mathcal{A} \text{ and } nEW \geq 1\} \quad (\text{Eq. J4.4-13})$$

for the early WP failure scenario class;

$$\mathcal{A}_{ED} = \{\mathbf{a} : \mathbf{a} \in \mathcal{A} \text{ and } nED \geq 1\} \quad (\text{Eq. J4.4-14})$$

for the early DS failure scenario class;

$$\mathcal{A}_{II} = \mathcal{A}_I = \{\mathbf{a} : \mathbf{a} \in \mathcal{A} \text{ and } nII \geq 1\} \quad (\text{Eq. J4.4-15})$$

for the igneous intrusive scenario class;

$$\mathcal{A}_{IE} = \{\mathbf{a} : \mathbf{a} \in \mathcal{A} \text{ and } nIE \geq 1\} \quad (\text{Eq. J4.4-16})$$

for the igneous eruptive scenario class;

$$\mathcal{A}_{SG} = \{\mathbf{a} : \mathbf{a} \in \mathcal{A} \text{ and } nSG \geq 1\} \quad (\text{Eq. J4.4-17})$$

for the seismic ground motion scenario class; and

$$\mathcal{A}_{SF} = \{\mathbf{a} : \mathbf{a} \in \mathcal{A} \text{ and } nSF \geq 1\} \quad (\text{Eq. J4.4-18})$$

for the fault displacement scenario class. The scenario classes \mathcal{A}_{EW} , \mathcal{A}_{ED} , \mathcal{A}_{II} , \mathcal{A}_{IE} , \mathcal{A}_{SG} and \mathcal{A}_{SF} defined in Equations J4.4-13 – J4.4-18 and their associated analyses are often referred to as modeling cases in the TSPA-LA.

For the time interval $[a, b]$ underlying the definition of \mathcal{A} ,

$$p_A(\mathcal{A}_N) = \text{probability of no disruptions of any kind,} \quad (\text{Eq. J4.4-19})$$

$$p_A(\mathcal{A}_E) = \text{probability of one or more early failures,} \quad (\text{Eq. J4.4-20})$$

$$p_A(\mathcal{A}_{EW}) = \text{probability of one or more early WP failures,} \quad (\text{Eq. J4.4-21})$$

$$p_A(\mathcal{A}_{ED}) = \text{probability of one or more early DS failures,} \quad (\text{Eq. J4.4-22})$$

$$p_A(\mathcal{A}_{II}) = p_A(\mathcal{A}_I) = \text{probability of one or more igneous intrusive events,} \quad (\text{Eq. J4.4-23})$$

$$p_A(\mathcal{A}_{IE}) = \text{probability of one or more igneous eruptive events,} \quad (\text{Eq. J4.4-24})$$

$$p_A(\mathcal{A}_S) = \text{probability of one or more seismic events,} \quad (\text{Eq. J4.4-25})$$

$$p_A(\mathcal{A}_{SG}) = \text{probability of one or more seismic ground motions} \\ \text{events,} \quad (\text{Eq. J4.4-26})$$

and

$$p_A(\mathcal{A}_{SF}) = \text{probability of one or more fault displacement events,} \quad (\text{Eq. J4.4-27})$$

More generally, the indicated scenario probabilities are conditional on values of epistemically uncertain analysis inputs and thus have conditional representations $p_A(\mathcal{A}_C|\mathbf{e}_A)$ or possibly $p_A(\mathcal{A}_C|\mathbf{e})$ for $C = N, E, EW, ED, I, II, S, SG$ and SF , where $\mathbf{e} = [\mathbf{e}_A, \mathbf{e}_M]$ is the vector of epistemically uncertain analysis inputs defined in Equation J4.1-3. When scenario class probabilities are requested, it is usually some subset of the preceding probabilities that is desired. The determination of these probabilities is discussed in later sections.

J4.5 Scenario Classes and the Determination of Expected Dose

The scenario classes \mathcal{A}_N , \mathcal{A}_{EW} , \mathcal{A}_{ED} , \mathcal{A}_{II} , \mathcal{A}_{IE} , \mathcal{A}_{SG} and \mathcal{A}_{SF} play a fundamental role in the computational determination of expected dose to the RMEI in the TSPA-LA. Specifically, with the assumption that there are no synergisms between disruptions that have significant effects on the expected dose $\bar{D}(\tau|\mathbf{e})$ defined in Equation J4.2-2, $\bar{D}(\tau|\mathbf{e})$ can be approximated by

$$\begin{aligned} \bar{D}(\tau|\mathbf{e}) \cong & D_N(\tau|\mathbf{a}_N, \mathbf{e}_M) + \bar{D}_{EW}(\tau|\mathbf{e}) + \bar{D}_{ED}(\tau|\mathbf{e}) + \bar{D}_{II}(\tau|\mathbf{e}) \\ & + \bar{D}_{IE}(\tau|\mathbf{e}) + \bar{D}_{SG}(\tau|\mathbf{e}) + \bar{D}_{SF}(\tau|\mathbf{e}), \end{aligned} \quad (\text{Eq. J4.5-1})$$

where, conditional on the element $\mathbf{e} = [\mathbf{e}_A, \mathbf{e}_M]$ of \mathcal{E} ,

$$\begin{aligned} D_N(\tau|\mathbf{a}, \mathbf{e}_M) &= \text{dose to RMEI (mrem/yr) at time } \tau \text{ resulting from nominal conditions for} \\ & \text{future } \mathbf{a} \in \mathcal{A} \\ &= D_N(\tau|\mathbf{a}_N, \mathbf{e}_M), \end{aligned} \quad (\text{Eq. J4.5-2})$$

$$\begin{aligned} D_{EW}(\tau|\mathbf{a}, \mathbf{e}_M) &= \text{dose to RMEI (mrem/yr) at time } \tau \text{ resulting from early WP failure for} \\ & \text{future } \mathbf{a} \in \mathcal{A} \\ &= D_{EW}(\tau|\mathbf{a}_{EW}, \mathbf{e}_M), \end{aligned} \quad (\text{Eq. J4.5-3})$$

$$\begin{aligned} D_{ED}(\tau|\mathbf{a}, \mathbf{e}_M) &= \text{dose to RMEI (mrem/yr) at time } \tau \text{ resulting from early DS failure for} \\ & \text{future } \mathbf{a} \in \mathcal{A} \\ &= D_{ED}(\tau|\mathbf{a}_{ED}, \mathbf{e}_M), \end{aligned} \quad (\text{Eq. J4.5-4})$$

$$\begin{aligned} D_{II}(\tau|\mathbf{a}, \mathbf{e}_M) &= \text{dose to RMEI (mrem/yr) at time } \tau \text{ resulting from igneous intrusive events} \\ & \text{for future } \mathbf{a} \in \mathcal{A} \\ &= D_{II}(\tau|\mathbf{a}_{II}, \mathbf{e}_M), \end{aligned} \quad (\text{Eq. J4.5-5})$$

$$\begin{aligned} D_{IE}(\tau|\mathbf{a}, \mathbf{e}_M) &= \text{dose to RMEI (mrem/yr) at time } \tau \text{ resulting from igneous eruptive events} \\ & \text{for future } \mathbf{a} \in \mathcal{A} \\ &= D_{IE}(\tau|\mathbf{a}_{IE}, \mathbf{e}_M), \end{aligned} \quad (\text{Eq. J4.5-6})$$

$$\begin{aligned} D_{SG}(\tau|\mathbf{a}, \mathbf{e}_M) &= \text{dose to RMEI (mrem/yr) at time } \tau \text{ resulting from seismic ground motion} \\ & \text{events for future } \mathbf{a} \in \mathcal{A} \\ &= D_{SG}(\tau|\mathbf{a}_{SG}, \mathbf{e}_M), \end{aligned} \quad (\text{Eq. J4.5-7})$$

$$\begin{aligned} D_{SF}(\tau|\mathbf{a}, \mathbf{e}_M) &= \text{dose to RMEI (mrem/yr) at time } \tau \text{ resulting from seismic fault} \\ & \text{displacement events for future } \mathbf{a} \in \mathcal{A} \\ &= D_{SF}(\tau|\mathbf{a}_{SF}, \mathbf{e}_M), \end{aligned} \quad (\text{Eq. J4.5-8})$$

and in turn

$$\begin{aligned}
 \bar{D}_{EW}(\tau|\mathbf{e}) &= \text{expected dose to RMEI (mrem/yr) at time } \tau \text{ resulting from early WP failure} \\
 &= E_A \left[D_{EW}(\tau|\mathbf{a}, \mathbf{e}_M) \middle| \mathbf{e}_A \right] \\
 &= \int_{\mathcal{A}} D_{EW}(\tau|\mathbf{a}, \mathbf{e}_M) d_A(\mathbf{a}|\mathbf{e}_A) dA \\
 &= \int_{\mathcal{A}_{EW}} D_{EW}(\tau|\mathbf{a}_{EW}, \mathbf{e}_M) d_A(\mathbf{a}|\mathbf{e}_A) dA, \text{ reminder } \mathbf{a} = [\dots \mathbf{a}_{EW} \dots], (\text{Eq. J4.5-9})
 \end{aligned}$$

$$\begin{aligned}
 \bar{D}_{ED}(\tau|\mathbf{e}) &= \text{expected dose to RMEI (mrem/yr) at time } \tau \text{ resulting from early DS failure} \\
 &= E_A \left[D_{ED}(\tau|\mathbf{a}, \mathbf{e}_M) \middle| \mathbf{e}_A \right] \\
 &= \int_{\mathcal{A}} D_{ED}(\tau|\mathbf{a}, \mathbf{e}_M) d_A(\mathbf{a}|\mathbf{e}_A) dA \\
 &= \int_{\mathcal{A}_{ED}} D_{ED}(\tau|\mathbf{a}_{ED}, \mathbf{e}_M) d_A(\mathbf{a}|\mathbf{e}_A) dA, \text{ reminder } \mathbf{a} = [\dots \mathbf{a}_{ED} \dots], (\text{Eq. J4.5-10})
 \end{aligned}$$

$$\begin{aligned}
 \bar{D}_{II}(\tau|\mathbf{e}) &= \text{expected dose to RMEI (mrem/yr) at time } \tau \text{ resulting from igneous intrusive} \\
 &\quad \text{events} \\
 &= E_A \left[D_{II}(\tau|\mathbf{a}, \mathbf{e}_M) \middle| \mathbf{e}_A \right] \\
 &= \int_{\mathcal{A}} D_{II}(\tau|\mathbf{a}, \mathbf{e}_M) d_A(\mathbf{a}|\mathbf{e}_A) dA \\
 &= \int_{\mathcal{A}_{II}} D_{II}(\tau|\mathbf{a}_{II}, \mathbf{e}_M) d_A(\mathbf{a}|\mathbf{e}_A) dA, \text{ reminder } \mathbf{a} = [\dots \mathbf{a}_{II} \dots], (\text{Eq. J4.5-11})
 \end{aligned}$$

$$\begin{aligned}
 \bar{D}_{IE}(\tau|\mathbf{e}) &= \text{expected dose to RMEI (mrem/yr) at time } \tau \text{ resulting from igneous eruptive} \\
 &\quad \text{events} \\
 &= E_A \left[D_{IE}(\tau|\mathbf{a}, \mathbf{e}_M) \middle| \mathbf{e}_A \right] \\
 &= \int_{\mathcal{A}} D_{IE}(\tau|\mathbf{a}, \mathbf{e}_M) d_A(\mathbf{a}|\mathbf{e}_A) dA \\
 &= \int_{\mathcal{A}_{IE}} D_{IE}(\tau|\mathbf{a}_{IE}, \mathbf{e}_M) d_A(\mathbf{a}|\mathbf{e}_A) dA, \text{ reminder } \mathbf{a} = [\dots \mathbf{a}_{IE} \dots], (\text{Eq. J4.5-12})
 \end{aligned}$$

$$\begin{aligned}
 \bar{D}_{SG}(\tau|\mathbf{e}) &= \text{expected dose to RMEI (mrem/yr) at time } \tau \text{ resulting from seismic ground} \\
 &\quad \text{motion events} \\
 &= E_A \left[D_{SG}(\tau|\mathbf{a}, \mathbf{e}_M) \middle| \mathbf{e}_A \right] \\
 &= \int_{\mathcal{A}} D_{SG}(\tau|\mathbf{a}, \mathbf{e}_M) d_A(\mathbf{a}|\mathbf{e}_A) dA
 \end{aligned}$$

$$= \int_{\mathcal{A}_{SG}} D_{SG}(\tau | \mathbf{a}_{SG}, \mathbf{e}_M) d_A(\mathbf{a} | \mathbf{e}_A) dA, \text{ reminder: } \mathbf{a} = [\dots \mathbf{a}_{SG} \dots], \text{ (Eq. J4.5-13)}$$

$\bar{D}_{SF}(\tau | \mathbf{e})$ = expected dose to RMEI (mrem/yr) at time τ resulting from seismic fault displacement events

$$\begin{aligned} &= E_A \left[D_{SF}(\tau | \mathbf{a}, \mathbf{e}_M) | \mathbf{e}_A \right] \\ &= \int_{\mathcal{A}} D_{SF}(\tau | \mathbf{a}, \mathbf{e}_M) d_A(\mathbf{a} | \mathbf{e}_A) dA \\ &= \int_{\mathcal{A}_{SF}} D_{SF}(\tau | \mathbf{a}_{SF}, \mathbf{e}_M) d_A(\mathbf{a} | \mathbf{e}_A) dA, \text{ reminder } \mathbf{a} = [\dots \mathbf{a}_{SF} \dots]. \text{ (Eq. J4.5-14)} \end{aligned}$$

In the preceding, $D_{EW}(\tau | \mathbf{a}, \mathbf{e}_M)$ is equivalent to $D_{EW}(\tau | \mathbf{a}_{EW}, \mathbf{e}_M)$ because only dose from early WP failure is under consideration; for the same reason, the integrals over \mathcal{A} and \mathcal{A}_{EW} in Equation J4.4-20 are equivalent. Specifically, possible synergisms between occurrences associated with different scenario classes are not being considered. Analogous equivalencies hold $D_{ED}(\tau | \mathbf{a}, \mathbf{e}_M)$, $D_{II}(\tau | \mathbf{a}, \mathbf{e}_M)$, $D_{IE}(\tau | \mathbf{a}, \mathbf{e}_M)$, $D_{SG}(\tau | \mathbf{a}, \mathbf{e}_M)$, $D_{SF}(\tau | \mathbf{a}, \mathbf{e}_M)$ and associated integrals.

A more compact representation for Equation J4.5-1 is

$$\bar{D}(\tau | \mathbf{e}) \cong D_N(\tau | \mathbf{a}_N, \mathbf{e}_M) + \sum_{C \in \mathcal{MC}} \bar{D}_C(\tau | \mathbf{e}), \quad \text{(Eq. J4.5-15)}$$

where

$$\mathcal{MC} = \{EW, ED, II, IE, SG, SF\}$$

and the symbol \mathcal{MC} is selected in consistency with the designated modeling case.

The justification of the decomposition of expected dose in Equations J4.5-1 and J4.5-15 ultimately depends on both the properties of the individual dose functions $D_N(\tau | \mathbf{a}_N, \mathbf{e}_M)$ and $D_C(\tau | \mathbf{a}, \mathbf{e}_M)$, $C \in \mathcal{MC}$, and the properties of the corresponding scenario classes \mathcal{A}_N and \mathcal{A}_C . This justification is discussed in Section J10 after results for $p_A(\mathcal{A}_N)$, $p_A(\mathcal{A}_C)$, $D_N(\tau | \mathbf{a}_N, \mathbf{e}_M)$, $D_C(\tau | \mathbf{a}, \mathbf{e}_M)$, and $\bar{D}_C(\tau | \mathbf{e})$ are available.

The quantities $p_A[D < D_C(\tau | \mathbf{a}, \mathbf{e}_M) | \mathbf{e}_A]$, $\bar{D}_C(\tau | \mathbf{e})$ and $p_A[D_C(\tau | \mathbf{a}, \mathbf{e}_M) \leq D | \mathbf{e}_A]$ for $D_C(\tau | \mathbf{a}, \mathbf{e}_M)$, $C \in \mathcal{MC}$, can be approximated with sampling-based procedures in the same manner as indicated in Equations J4.3-10 – J4.3-12 for $D(\tau | \mathbf{e})$. Specifically,

$$\begin{aligned}
 p_A \left[D < D_C(\tau|\mathbf{a}, \mathbf{e}_M) \middle| \mathbf{e}_A \right] &= \int_{\mathcal{A}} \bar{\delta}_D \left[D_C(\tau|\mathbf{a}, \mathbf{e}_M) \right] d_A(\mathbf{a}|\mathbf{e}_A) dA \\
 &\cong \sum_{j=1}^{nR} \bar{\delta}_D \left[D_C(\tau|\mathbf{a}_j, \mathbf{e}_M) \right] / nR, \quad (\text{Eq. J4.5-16})
 \end{aligned}$$

$$\begin{aligned}
 \bar{D}_C(\tau|\mathbf{e}) &= \int_{\mathcal{A}} D_C(\tau|\mathbf{a}, \mathbf{e}_M) d_A(\mathbf{a}|\mathbf{e}_A) dA \\
 &\cong \sum_{j=1}^{nR} D_C(\tau|\mathbf{a}_j, \mathbf{e}_M) / nR \quad (\text{Eq. J4.5-17})
 \end{aligned}$$

and

$$\begin{aligned}
 p_A \left[D_C(\tau|\mathbf{a}, \mathbf{e}_M) \leq D \right] &= \int_{\mathcal{A}} \underline{\delta}_D \left[D_C(\tau|\mathbf{a}, \mathbf{e}_M) \right] d_A(\mathbf{a}|\mathbf{e}_A) dA \\
 &\cong \sum_{j=1}^{nR} \underline{\delta}_D \left[D_C(\tau|\mathbf{a}_j, \mathbf{e}_M) \right] / nR \quad (\text{Eq. J4.5-18})
 \end{aligned}$$

for a random sample $\mathbf{a}_j, j = 1, 2, \dots, nR$, from \mathcal{A} of the form indicated in Equation J4.3-9. Further, as indicated in Equation J4.2-8, the approximation in Equation J4.5-18 can be used in the determination of quantile values for $D_C(\tau|\mathbf{a}, \mathbf{e}_M)$ that derive from the probability distribution over \mathcal{A} defined by $d_A(\mathbf{a}|\mathbf{e}_A)$.

When a specific scenario class is under consideration, and no synergisms are assumed to exist between the effects associated with individual scenario classes, it is only necessary to sample the components of \mathbf{a} that are involved in the evaluation of dose $D_C(\tau|\mathbf{a}, \mathbf{e}_M)$ for this scenario class (i.e., scenario class C) as the remaining components of \mathbf{a} have no effect on $D_C(\tau|\mathbf{a}, \mathbf{e}_M)$. In this case, the representations for the approximations in Equations J4.5-16 – J4.5-18 become

$$p_A \left[D < D_C(\tau|\mathbf{a}, \mathbf{e}_M) \middle| \mathbf{e}_A \right] \cong p_A(\mathcal{A}_C|\mathbf{e}_A) \sum_{j=1}^{nR} \bar{\delta}_D \left[D_S(\tau|\mathbf{a}_{Cj}, \mathbf{e}_M) \right] / nR, \quad (\text{Eq. J4.5-19})$$

$$\bar{D}_C(\tau|\mathbf{e}) \cong p_A(\mathcal{A}_C|\mathbf{e}_A) \sum_{j=1}^{nR} D_S(\tau|\mathbf{a}_{Cj}, \mathbf{e}_M) / nR \quad (\text{Eq. J4.5-20})$$

and

$$p_A \left[D_C(\tau|\mathbf{a}, \mathbf{e}_M) \leq D \right] \cong p_A(\mathcal{A}_C|\mathbf{e}_A) \sum_{j=1}^{nR} \underline{\delta}_D \left[D_C(\tau|\mathbf{a}_{Cj}, \mathbf{e}_M) \right] / nR, \quad (\text{Eq. J4.5-21})$$

where $\mathbf{a}_{Cj}, j = 1, 2, \dots, nR$, is a random sample from \mathcal{A}_C generated in consistency with the part of $d_A(\mathbf{a}|\mathbf{e}_A)$ that applies to the components of \mathbf{a} that enter into the definition of \mathcal{A}_C .

Inclusion of the factor $p_A(\mathcal{A}_C|\mathbf{e}_A)$ in Equations J4.5-19 – J4.5-21 is predicated on the assumption that sampling is being carried out conditional on the occurrence of scenario class \mathcal{A}_C . In contrast, the factor $p_A(\mathcal{A}_C|\mathbf{e}_A)$ is not included in Equations J4.5-16 – J4.5-18 because sampling is being carried out over the entire sample space \mathcal{A} . When $p_A(\mathcal{A}_C|\mathbf{e}_A)$ is small, restriction of sampling to the set \mathcal{A}_C is numerically efficient because it avoids the generation of large numbers of futures \mathbf{a} for which $D_C(\tau|\mathbf{a}, \mathbf{e}_M) = 0$.

Although sampling-based procedures provide one method for estimating $p_A[D < D_C(\tau|\mathbf{a}, \mathbf{e}_M)|\mathbf{e}_A]$, $\bar{D}_C(\tau|\mathbf{e})$ and $p_A[D_C(\tau|\mathbf{a}, \mathbf{e}_M) \leq D|\mathbf{e}_A]$, other methods also exist. This is especially true with respect to the estimation of $\bar{D}_C(\tau|\mathbf{e})$. Typically, these methods are designed to achieve computational efficiencies on the basis of specific properties of $D_C(\tau|\mathbf{a}, \mathbf{e}_M)$ and $d_A(\mathbf{a}|\mathbf{e}_A)$. For the TSPA-LA, alternatives to the use of naïve sampling-based procedures are employed to determine $\bar{D}_{EW}(\tau|\mathbf{e})$, $\bar{D}_{ED}(\tau|\mathbf{e})$, $\bar{D}_{II}(\tau|\mathbf{e})$, $\bar{D}_{IE}(\tau|\mathbf{e})$ and $\bar{D}_{SF}(\tau|\mathbf{e})$ for the $[0, 2 \times 10^4 \text{ yr}]$ and $[0, 10^6 \text{ yr}]$ time intervals and to determine $\bar{D}_{SG}(\tau|\mathbf{e})$ for the $[0, 2 \times 10^4 \text{ yr}]$ time interval. However, owing to the complexity of the calculation, $\bar{D}_{SG}(\tau|\mathbf{e})$ could only be determined with a sampling-based calculation for $[0, 10^6 \text{ yr}]$ time interval.

J4.6 Analysis Decomposition

As previously stated, the approximation in Equations J4.5-1 and J4.5-15 is based on the assumption that there are no synergisms between disruptions that have significant effects on the expected dose $\bar{D}(\tau|\mathbf{e})$ defined in Equation J4.2-2. One way to arrive at this approximation is to start with the assumption that there are no significant synergisms between disruptions that affect the dose $D(\tau|\mathbf{a}, \mathbf{e}_M)$ for individual futures, which is equivalent to the assumption that

$$D(\tau|\mathbf{a}, \mathbf{e}_M) \cong D_N(\tau|\mathbf{a}_N, \mathbf{e}_M) + \sum_{C \in \mathcal{MC}} D_C(\tau|\mathbf{a}, \mathbf{e}_M), \quad (\text{Eq. J4.6-1})$$

where \mathcal{MC} is defined in conjunction with Equation J4.5-15. In turn,

$$\begin{aligned}
 \bar{D}(\tau|\mathbf{e}) &\equiv \int_{\mathcal{A}} \left\{ D_N(\tau|\mathbf{a}_N, \mathbf{e}_M) + \sum_{C \in \mathcal{MC}} D_C(\tau|\mathbf{a}, \mathbf{e}_M) \right\} d_A(\mathbf{a}|\mathbf{e}_A) dA \\
 &= D_N(\tau|\mathbf{a}_N, \mathbf{e}_M) + \sum_{C \in \mathcal{MC}} \int_{\mathcal{A}} D_C(\tau|\mathbf{a}, \mathbf{e}_M) d_A(\mathbf{a}|\mathbf{e}_A) dA \\
 &= D_N(\tau|\mathbf{a}_N, \mathbf{e}_M) + \sum_{C \in \mathcal{MC}} \int_{\mathcal{A}_C} D_C(\tau|\mathbf{a}, \mathbf{e}_M) d_A(\mathbf{a}|\mathbf{e}_A) dA \\
 &= D_N(\tau|\mathbf{a}_N, \mathbf{e}_M) + \sum_{C \in \mathcal{MC}} \bar{D}_C(\tau|\mathbf{e}), \tag{Eq. J4.6-2}
 \end{aligned}$$

which is the result in Equations J4.5-1 and J4.5-15. As previously noted, the appropriateness of this approximation to $\bar{D}(\tau|\mathbf{e})$ depends on both the level of synergisms between disruptions and the probabilities associated with the scenario classes \mathcal{A}_{EW} , \mathcal{A}_{ED} , \mathcal{A}_{II} , \mathcal{A}_{IE} , \mathcal{A}_{SG} and \mathcal{A}_{SF} .

In turn, the expected dose $\bar{\bar{D}}(\tau)$ over both epistemic and aleatory uncertainty defined in Equation J4.2-5 can be approximated by

$$\begin{aligned}
 \bar{\bar{D}}(\tau) &\equiv \int_{\mathcal{E}} \left\{ D_N(\tau|\mathbf{a}_N, \mathbf{e}_M) + \sum_{C \in \mathcal{MC}} \bar{D}_C(\tau|\mathbf{e}) \right\} d_E(\mathbf{e}) dE \\
 &= \int_{\mathcal{E}} D_N(\tau|\mathbf{a}_N, \mathbf{e}_M) d_E(\mathbf{e}) dE + \sum_{C \in \mathcal{MC}} \int_{\mathcal{E}} \bar{D}_C(\tau|\mathbf{e}) d_E(\mathbf{e}) dE \\
 &= \bar{\bar{D}}_N(\tau) + \sum_{C \in \mathcal{MC}} \bar{\bar{D}}_C(\tau), \tag{Eq. J4.6-3}
 \end{aligned}$$

where

$$\begin{aligned}
 \bar{\bar{D}}_N(\tau) &= E_E \left[D_N(\tau|\mathbf{a}_N, \mathbf{e}_M) \right] \\
 &= \int_{\mathcal{E}} D_N(\tau|\mathbf{a}_N, \mathbf{e}_M) d_E(\mathbf{e}) dE \tag{Eq. J4.6-4}
 \end{aligned}$$

and

$$\begin{aligned}
 \bar{\bar{D}}_C(\tau) &= E_E \left[\bar{D}_C(\tau|\mathbf{e}) \right] \\
 &= \int_{\mathcal{E}} \bar{D}_C(\tau|\mathbf{e}) d_E(\mathbf{e}) dE \tag{Eq. J4.6-5}
 \end{aligned}$$

for $C \in \mathcal{MC}$.

If desired, the equality

$$\bar{D}(\tau|\mathbf{e}) = D_N(\tau|\mathbf{a}_N, \mathbf{e}_M) + \sum_{C \in \mathcal{MC}} \int_{\mathcal{A}_C} D_C(\tau|\mathbf{a}, \mathbf{e}_M) d_A(\mathbf{a}|\mathbf{e}_A) dA \quad (\text{Eq. J4.6-6})$$

appearing in Equation J4.6-2 can be reformulated as

$$\begin{aligned} \bar{D}(\tau|\mathbf{e}) &= D_N(\tau|\mathbf{a}_N, \mathbf{e}_M) + \sum_{C \in \mathcal{MC}} p_A(\mathcal{A}_C|\mathbf{e}_A) \int_{\mathcal{A}_C} D_C(\tau|\mathbf{a}, \mathbf{e}_M) \left[d_A(\mathbf{a}|\mathbf{e}_A) / p_A(\mathcal{A}_C|\mathbf{e}_A) \right] dA \\ &= D_N(\tau|\mathbf{a}_N, \mathbf{e}_M) + \sum_{C \in \mathcal{MC}} p_A(\mathcal{A}_C|\mathbf{e}_A) E_A \left[D_C(\tau|\mathbf{a}, \mathbf{e}_M) | \mathcal{A}_C, \mathbf{e}_A \right], \end{aligned} \quad (\text{Eq. J4.6-7})$$

where

$$E_A \left[D_C(\tau|\mathbf{a}, \mathbf{e}_M) | \mathcal{A}_C, \mathbf{e}_A \right] = \int_{\mathcal{A}_C} D_C(\tau|\mathbf{a}, \mathbf{e}_M) \left[d_A(\mathbf{a}|\mathbf{e}_A) / p_A(\mathcal{A}_C|\mathbf{e}_A) \right] dA$$

is the expected value for $D_C(\tau|\mathbf{a}, \mathbf{e}_M)$ given the occurrence of scenario class \mathcal{A}_C and conditional on $\mathbf{e} = [\mathbf{e}_A, \mathbf{e}_M]$. This is the formulation that underlies the approximation to $\bar{D}_C(\tau|\mathbf{e})$ in Equation J4.5-20.

J4.7 Disjoint and Nondisjoint Scenario Classes

Neither the scenario classes $\mathcal{A}_E, \mathcal{A}_I$ and \mathcal{A}_S nor the scenario classes $\mathcal{A}_{EW}, \mathcal{A}_{ED}, \mathcal{A}_{II}, \mathcal{A}_{IE}, \mathcal{A}_{SG}$ and \mathcal{A}_{SF} are disjoint. However, it is straightforward to define disjoint scenario classes on the basis of the same disruptive occurrences that define the preceding scenario classes.

Disjoint scenario classes related to $\mathcal{A}_E, \mathcal{A}_I$ and \mathcal{A}_S can be defined by sets of the form

$$\begin{aligned} \mathcal{A}(r, s, t) = \{ \mathbf{a}: \mathbf{a} \in \mathcal{A} \text{ with } nEW + nED = 0 \text{ if } r = 0, nEW + nED \geq 1 \text{ if } r = 1, \\ nII = 0 \text{ if } s = 0, nII \geq 1 \text{ if } s = 1, nSG + nSF = 0 \text{ if } t = 0, nSG + \\ nSF \geq 1 \text{ if } t = 1 \} \end{aligned} \quad (\text{Eq. J4.7-1})$$

for $r = 0, 1, s = 0, 1, t = 0, 1$. The preceding defines $2^3 = 8$ disjoint scenario classes on the basis of early failures, igneous events and seismic events. Further, the probabilities $p_A[\mathcal{A}(r, s, t)]$ of these scenario classes sum to one.

In like manner, disjoint scenario classes related to $\mathcal{A}_{EW}, \mathcal{A}_{ED}, \mathcal{A}_{II}, \mathcal{A}_{IE}, \mathcal{A}_{SG}$ and \mathcal{A}_{SF} can be defined by sets of the form

$$\begin{aligned} \mathcal{A}(r, s, t, u, v, w) = \{ \mathbf{a}: \mathbf{a} \in \mathcal{A} \text{ with } nEW = 0 \text{ if } r = 0, nEW \geq 1 \text{ if } r = 1, \dots, \\ nSF = 0 \text{ if } w = 0, nSF \geq 1 \text{ if } w = 1 \} \end{aligned} \quad (\text{Eq. J4.7-2})$$

for $r = 0, 1, w = 0, 1$, and similarly for s, t, u and v . The preceding defines $2^6 = 64$ disjoint scenario classes, although all sets of the form $\mathcal{A}(r, s, 0, 1, v, w)$ correspond to the null set because the occurrence of an igneous intrusive event (i.e., $t = 1$) is a necessary, but not sufficient,

condition for the occurrence of an igneous eruptive event (i.e., $u = 1$). As a result, there are only 48 nondegenerate scenario classes of the form $\mathcal{A}(r, s, t, u, v, w)$. Further, the probabilities $p_A[\mathcal{A}(r, s, t, u, v, w)]$ of the 64 scenario classes sum to one.

For perspective, the calculation of expected dose $\bar{D}(\tau|\mathbf{e})$ is illustrated with the disjoint scenario classes $\mathcal{A}(r, s, t)$ defined in Equation J4.7-1. Specifically,

$$\begin{aligned}
 \bar{D}(\tau|\mathbf{e}) &= \int_{\mathcal{A}} D(\tau|\mathbf{a}, \mathbf{e}_M) d_A(\mathbf{a}|\mathbf{e}_A) dA \\
 &= \sum_{\mathbf{r} \in \mathcal{R}} \int_{\mathcal{A}(\mathbf{r})} D_{\mathbf{r}}(\tau|\mathbf{a}, \mathbf{e}_M) d_A(\mathbf{a}|\mathbf{e}_A) dA \\
 &= \sum_{\mathbf{r} \in \mathcal{R}} \int_{\mathcal{A}(\mathbf{r})} [D_N(\tau|\mathbf{a}, \mathbf{e}_M) + \tilde{D}_{\mathbf{r}}(\tau|\mathbf{a}, \mathbf{e}_M)] d_A(\mathbf{a}|\mathbf{e}_A) dA \\
 &= D_N(\tau|\mathbf{a}_N, \mathbf{e}_M) + \sum_{\mathbf{r} \in \tilde{\mathcal{R}}} \int_{\mathcal{A}(\mathbf{r})} \tilde{D}_{\mathbf{r}}(\tau|\mathbf{a}, \mathbf{e}_M) d_A(\mathbf{a}|\mathbf{e}_A) dA \\
 &= D_N(\tau|\mathbf{a}_N, \mathbf{e}_M) + \sum_{C \in \mathcal{MC}} \int_{\mathcal{A}_C} D_C(\tau|\mathbf{a}, \mathbf{e}_M) d_A(\mathbf{a}|\mathbf{e}_A) dA, \tag{Eq. J4.7-3}
 \end{aligned}$$

where

$$\begin{aligned}
 \mathcal{R} &= \{0,1\} \times \{0,1\} \times \{0,1\} \\
 &= \{[0,0,0], [0,0,1], [0,1,0], [0,1,1], [1,0,0], [1,0,1], [1,1,0], [1,1,1]\}, \\
 \tilde{\mathcal{R}} &= \{[0,0,1], [0,1,0], [0,1,1], [1,0,0], [1,0,1], [1,1,0], [1,1,1]\},
 \end{aligned}$$

$$\begin{aligned}
 \tilde{D}_{\mathbf{r}}(\tau|\mathbf{a}, \mathbf{e}_M) &= 0 && \text{if } \mathbf{r} = [0,0,0] \\
 &= D_{SG}(\tau|\mathbf{a}, \mathbf{e}_M) + D_{SF}(\tau|\mathbf{a}, \mathbf{e}_M) && \text{if } \mathbf{r} = [0,0,1] \\
 &= D_{II}(\tau|\mathbf{a}, \mathbf{e}_M) + D_{IE}(\tau|\mathbf{a}, \mathbf{e}_M) && \text{if } \mathbf{r} = [0,1,0] \\
 &= D_{II}(\tau|\mathbf{a}, \mathbf{e}_M) + D_{IE}(\tau|\mathbf{a}, \mathbf{e}_M) + D_{SG}(\tau|\mathbf{a}, \mathbf{e}_M) + D_{SF}(\tau|\mathbf{a}, \mathbf{e}_M) && \text{if } \mathbf{r} = [0,1,1] \\
 &= D_{EW}(\tau|\mathbf{a}, \mathbf{e}_M) + D_{ED}(\tau|\mathbf{a}, \mathbf{e}_M) && \text{if } \mathbf{r} = [1,0,0] \\
 &= D_{EW}(\tau|\mathbf{a}, \mathbf{e}_M) + D_{ED}(\tau|\mathbf{a}, \mathbf{e}_M) + D_{SG}(\tau|\mathbf{a}, \mathbf{e}_M) + D_{SF}(\tau|\mathbf{a}, \mathbf{e}_M) && \text{if } \mathbf{r} = [1,0,1] \\
 &= D_{EW}(\tau|\mathbf{a}, \mathbf{e}_M) + D_{ED}(\tau|\mathbf{a}, \mathbf{e}_M) + D_{II}(\tau|\mathbf{a}, \mathbf{e}_M) + D_{IE}(\tau|\mathbf{a}, \mathbf{e}_M) && \text{if } \mathbf{r} = [1,1,0] \\
 &= D_{EW}(\tau|\mathbf{a}, \mathbf{e}_M) + D_{ED}(\tau|\mathbf{a}, \mathbf{e}_M) + D_{II}(\tau|\mathbf{a}, \mathbf{e}_M) && \\
 &\quad + D_{IE}(\tau|\mathbf{a}, \mathbf{e}_M) + D_{SG}(\tau|\mathbf{a}, \mathbf{e}_M) + D_{SF}(\tau|\mathbf{a}, \mathbf{e}_M) && \text{if } \mathbf{r} = [1,1,1]
 \end{aligned}$$

and

$$D_{\mathbf{r}}(\tau|\mathbf{a}, \mathbf{e}_M) = D_N(\tau|\mathbf{a}_N, \mathbf{e}_M) + \tilde{D}_{\mathbf{r}}(\tau|\mathbf{a}, \mathbf{e}_M)$$

for $\mathbf{r} \in \mathcal{R}$

With respect to the preceding representation of $\bar{D}(\tau|\mathbf{e})$, (i) the first equality corresponds to the definition of $\bar{D}(\tau|\mathbf{e})$ in Equation J4.2-2, (ii) the second equality decomposes the defining integral for $\bar{D}(\tau|\mathbf{e})$ into integrals over the eight disjoint scenario classes $\mathcal{A}(r, s, t) = \mathcal{A}(\mathbf{r})$ indexed by elements of the set \mathcal{R} , (iii) the third equality involves a division of the dose function $D_{\mathbf{r}}(\tau|\mathbf{a}, \mathbf{e}_M)$ for scenario class $\mathcal{A}(\mathbf{r})$ into a constituent part $D_N(\tau|\mathbf{a}_N, \mathbf{e}_M)$ arising from WP failures resulting from nominal processes and a constituent part $\tilde{D}_{\mathbf{r}}(\tau|\mathbf{a}, \mathbf{e}_M)$ arising from WP failures resulting from the disruptions associated with scenario class $\mathcal{A}(\mathbf{r})$, (iv) the fourth equality divides the preceding integrals into an integral of $D_N(\tau|\mathbf{a}_N, \mathbf{e}_M)$ over $\mathcal{A} = \cup \mathcal{A}(\mathbf{r})$, which is equal to $D_N(\tau|\mathbf{a}_N, \mathbf{e}_M)$, and integrals of $\tilde{D}_{\mathbf{r}}(\tau|\mathbf{a}, \mathbf{e}_M)$ over $\mathcal{A}(\mathbf{r})$ for $\mathbf{r} \in \tilde{\mathcal{R}}$, and (v) the fifth and final equality involves a regrouping of the constituent dose functions in the definitions of $\tilde{D}_{\mathbf{r}}(\tau|\mathbf{a}, \mathbf{e}_M)$ into integrals over nondisjoint scenario classes indexed by elements of the set \mathcal{MC} defined in conjunction with Equation J4.5-15 on which these constituent dose functions are potentially nonzero. The overall computational structure used in the TSPA-LA to determine expected dose to the RMEI is based on the final representation for $\bar{D}(\tau|\mathbf{e})$ in Equation J4.7-3.

If desired, the generation of disjoint scenario classes illustrated in Equation J4.7-1 and J4.7-2 can be carried farther by changing the definition of $\mathcal{A}(r, s, t, u, v, w)$ in Equation J4.7-2 to

$$\mathcal{A}(r, s, t, u, v, w) = \{\mathbf{a}: \mathbf{a} \in \mathcal{A} \text{ with } nEW = r, nED = s, nII = t, nIE = u, nSG = v, nSF = w\} \quad (\text{Eq. J4.7-4})$$

for $r = 0, 1, 2, \dots, s = 0, 1, 2, \dots$, and similarly for t, u, v and w . Further, this is only a small start on the possibilities for defining disjoint scenario classes as many additional event properties (e.g., time of occurrence, size, ...) could also be used in the definition of disjoint scenario classes. Actually, this is what is being done in concept when expected doses $\bar{D}(\tau|\mathbf{e})$ and $\bar{D}_C(\tau|\mathbf{e})$, $C \in \mathcal{MC}$, are defined by integrals as indicated in Equations J4.2-2 and J4.5-9 – J4.5-14.

For example, the integral defining $\bar{D}(\tau|\mathbf{e})$ in Equation J4.2-2 is the limit of approximating sums of the form

$$\bar{D}(\tau|\mathbf{e}) \cong \sum_{j=1}^{nS} D(\tau|\mathbf{a}_j, \mathbf{e}_M) p_A(\mathcal{A}_j|\mathbf{e}_A) \quad (\text{Eq. J4.7-5})$$

where (i) $\mathcal{A}_j, j = 1, 2, \dots, nS$, is a sequence of disjoint subsets of \mathcal{A} with $\cup_j \mathcal{A}_j = \mathcal{A}$, (ii) \mathbf{a}_j is a representative element of \mathcal{A}_j , and (iii)

$$p_A(\mathcal{A}_j | \mathbf{e}_A) = \int_{\mathcal{A}_j} d_A(\mathbf{a} | \mathbf{e}_A) dA.$$

In this approximation to $\bar{D}(\tau | \mathbf{e})$, the \mathcal{A}_j are disjoint scenario classes, $p_A(\mathcal{A}_j | \mathbf{e}_A)$ is the probability for scenario class \mathcal{A}_j , and $\sum_j p_A(\mathcal{A}_j | \mathbf{e}_A) = 1$. In turn, $\bar{D}(\tau | \mathbf{e})$ results in the limit as increasingly refined scenario classes are used in the summation in Equation J4.7-5 (i.e., as $p_A(\mathcal{A}_j | \mathbf{e}_A) \rightarrow 0$). In practice, the scenario classes \mathcal{A}_j in Equation J4.7-5 may or may not be computationally present in a specific implementation of a numerical approximation to the integral defining $\bar{D}(\tau | \mathbf{e})$ (e.g., if a Monte Carlo procedure is being used). However, they are conceptually present in the definition of $\bar{D}(\tau | \mathbf{e})$. The same conceptual ideas underlie the definition of $\bar{D}_C(\tau | \mathbf{e})$ for $C \in \mathcal{MC}$. The use of integrals in the definition and computational evaluation of $\bar{D}(\tau | \mathbf{e})$ and $\bar{D}_C(\tau | \mathbf{e})$ avoids the messy notational and computational problems that arise when $\bar{D}(\tau | \mathbf{e})$ and $\bar{D}_C(\tau | \mathbf{e})$ are defined and evaluated on the basis of a large number of disjoint scenario classes.

J4.8 Scenario Classes and the Yucca Mountain Review Plan

The NRC's Yucca Mountain Review Plan (YMRP) requests that TSPA-LA results be developed and presented in the context of the Kaplan and Garrick ordered triple representation for risk. With this representation, risk is characterized by a sequence

$$(S_j, pS_j, cS_j), j = 1, 2, \dots, nS, \quad (\text{Eq. J4.8-1})$$

of triples, where (i) S_j is a set of similar occurrences (i.e., futures), (ii) the sets S_j are disjoint and $\cup_j S_j$ contains all possible occurrences for the system under study, (iii) pS_j is the probability of S_j , and (iv) cS_j is the consequence (or, more generally, a vector \mathbf{cS}_j of consequences) of interest. In the terminology of the TSPA-LA, S_j corresponds to a scenario class; $S = \cup_j S_j$ is the sample space for aleatory uncertainty; pS_j is the probability for scenario class S_j ; and cS_j is the consequence associated with scenario class S_j . In turn, the expected consequence \overline{cS} is approximated by

$$\overline{cS} \cong \sum_{j=1}^{nS} pS_j cS_j. \quad (\text{Eq. J4.8-2})$$

In concept, the preceding approximation improves as $nS \rightarrow \infty$ and the $pS_j \rightarrow 0$ and in the limit becomes

$$\overline{cS} = \int_S cS(\mathbf{a}) d_S(\mathbf{a}) dS, \quad (\text{Eq. J4.8-3})$$

where $cS(\mathbf{a})$ denotes the consequence of interest as a function of individual elements (i.e., occurrences or futures) \mathbf{a} contained in S and $d_S(\mathbf{a})$ denotes the density function associated with the indicated probabilities pS_j .

The ordered triple representation for risk in Equation J4.8-1 is precisely the risk representation that underlies the approximation to $\bar{D}(\tau|\mathbf{e})$ in Equation J4.7-5. Specifically, the corresponding ordered triple representation is

$$\left[\mathcal{A}_j, p_A(\mathcal{A}_j|\mathbf{e}_A), D(\tau|\mathbf{a}_j, \mathbf{e}_M) \right], j=1, 2, \dots, nS, \quad (\text{Eq. J4.8-4})$$

where $\mathcal{A}_j \sim S_j$, $p_A(\mathcal{A}_j|\mathbf{e}_A) \sim pS_j$ and $D(\tau|\mathbf{a}_j, \mathbf{e}_M) \sim cS_j$. In turn, the approximation to $\bar{D}(\tau|\mathbf{e})$ in Equation J4.7-5 corresponds to the approximation to \bar{cS} in Equation J4.8-2. Similarly, the integral in Equation J4.2-2 that formally defines $\bar{D}(\tau|\mathbf{e})$ corresponds to the integral in Equation J4.8-3 that formally defines \bar{cS} .

J4.9 Characterization of Epistemic Uncertainty

As indicated in Equations J4.2-4, J4.2-5 and J4.2-9, $p_E[D < \bar{D}(\tau|\mathbf{e})]$, $\bar{\bar{D}}(\tau)$ and $p_E[\bar{D}(\tau|\mathbf{e}) \leq D]$ can be formally defined by integrals over \mathcal{E} . In practice, closed form evaluation of these integrals is not feasible; instead, these integrals must be approximated with a sampling-based procedure. In the TSPA-LA, this sampling-based integration is performed with Latin hypercube sampling. Specifically, an LHS

$$\mathbf{e}_i = [\mathbf{e}_{Ai}, \mathbf{e}_{Mi}], i=1, 2, \dots, nLHS, \quad (\text{Eq. J4.9-1})$$

is generated in consistency with the definition of the probability space $(\mathcal{E}, \mathbf{E}, p_E)$ (i.e., in consistency with the distributions defined for the individual elements of \mathbf{e}). Then, $p_E[D < \bar{D}(\tau|\mathbf{e})]$, $\bar{\bar{D}}(\tau)$ and $p_E[\bar{D}(\tau|\mathbf{e}) \leq D]$ are approximated by

$$p_E[D < \bar{D}(\tau|\mathbf{e})] \cong \sum_{i=1}^{nLHS} \bar{\delta}_D[\bar{D}(\tau|\mathbf{e}_i)]/nLHS, \quad (\text{Eq. J4.9-2})$$

$$\bar{\bar{D}}(\tau) \cong \sum_{i=1}^{nLHS} \bar{D}(\tau|\mathbf{e}_i)/nLHS \quad (\text{Eq. J4.9-3})$$

and

$$p_E[\bar{D}(\tau|\mathbf{e}) \leq D] \cong \sum_{i=1}^{nLHS} \underline{\delta}_D[\bar{D}(\tau|\mathbf{e}_i)]/nLHS, \quad (\text{Eq. J4.9-4})$$

respectively. Further, this sample can be used in a numerical determination of the quantiles $Q_q[\bar{D}(\tau|\mathbf{e})]$ for $\bar{D}(\tau|\mathbf{e})$ defined in Equation J4.2-10.

Similarly, corresponding approximations for $D_N(\tau|\mathbf{a}_N, \mathbf{e}_M)$ are given by

$$\begin{aligned}
 p_E \left[D < D_N(\tau | \mathbf{a}_N, \mathbf{e}_M) \right] &= \int_{\mathcal{E}} \bar{\delta}_D \left[D_N(\tau | \mathbf{a}_N, \mathbf{e}_M) \right] d_E(\mathbf{e}) dE \\
 &\cong \sum_{i=1}^{nLHS} \bar{\delta}_D \left[D_N(\tau | \mathbf{a}_N, \mathbf{e}_{Mi}) \right] / nLHS, \quad (\text{Eq. J4.9-5})
 \end{aligned}$$

$$\begin{aligned}
 \bar{\bar{D}}_N(\tau) &= \int_{\mathcal{E}} D_N(\tau | \mathbf{a}_N, \mathbf{e}_M) d_E(\mathbf{e}) dE \\
 &\cong \sum_{i=1}^{nLHS} D_N(\tau | \mathbf{a}_N, \mathbf{e}_{Mi}) / nLHS \quad (\text{Eq. J4.9-6})
 \end{aligned}$$

and

$$\begin{aligned}
 p_E \left[D_N(\tau | \mathbf{a}_N, \mathbf{e}_M) \leq D \right] &= \int_{\mathcal{E}} \underline{\delta}_D \left[D_N(\tau | \mathbf{a}_N, \mathbf{e}_M) \right] d_E(\mathbf{e}) dE \\
 &\cong \sum_{i=1}^{nLHS} \underline{\delta}_D \left[D_N(\tau | \mathbf{a}_N, \mathbf{e}_{Mi}) \right] / nLHS, \quad (\text{Eq. J4.9-7})
 \end{aligned}$$

and corresponding approximations for $\bar{D}_C(\tau | \mathbf{e})$ are given by

$$\begin{aligned}
 p_E \left[D < \bar{D}_C(\tau | \mathbf{e}) \right] &= \int_{\mathcal{E}} \bar{\delta}_D \left[\bar{D}_C(\tau | \mathbf{e}) \right] d_E(\mathbf{e}) dE \\
 &\cong \sum_{i=1}^{nLHS} \bar{\delta}_D \left[\bar{D}_C(\tau | \mathbf{e}_i) \right] / nLHS, \quad (\text{Eq. J4.9-8})
 \end{aligned}$$

$$\begin{aligned}
 \bar{\bar{D}}_C(\tau) &= \int_{\mathcal{E}} \bar{D}_C(\tau | \mathbf{e}) d_E(\mathbf{e}) dE \\
 &\cong \sum_{i=1}^{nLHS} \bar{D}_C(\tau | \mathbf{e}_i) / nLHS \quad (\text{Eq. J4.9-9})
 \end{aligned}$$

and

$$\begin{aligned}
 p_E \left[\bar{D}_C(\tau | \mathbf{e}) \leq D \right] &= \int_{\mathcal{E}} \underline{\delta}_D \left[\bar{D}_C(\tau | \mathbf{e}) \right] d_E(\mathbf{e}) dE \\
 &\cong \sum_{i=1}^{nLHS} \underline{\delta}_D \left[\bar{D}_C(\tau | \mathbf{e}_i) \right] / nLHS \quad (\text{Eq. J4.9-10})
 \end{aligned}$$

for $C = EW, ED, II, IE, SG, SF$. Further, the sample can be used in a numerical determination of quantiles for $D_N(\tau | \mathbf{a}_N, \mathbf{e}_M)$ and $\bar{D}_C(\tau | \mathbf{e})$ in the same manner as indicated in Equation J4.2-10 for $\bar{D}(\tau)$.

J4.10 Adequacy of Latin Hypercube Sample Size

The adequacy of an LHS of size $nLHS$ can be assessed with a replicated sampling procedure proposed by R.L. Iman (Iman 1982 [DIRS 146012]). Specifically, the goal of the procedure is to determine how much variability exists in estimated analysis outcomes when different LHSs of size $nLHS$ are used. The procedure is based on independently generating LHSs of size $nLHS$ with different random seeds nRL times. At an intuitive level, the adequacy of the sample size can be assessed by simply comparing the results obtained with the individual samples.

At a more formal level, the t -distribution can be used to place confidence intervals around summary results (e.g., expected values over epistemic uncertainty) obtained from individual samples. Specifically, assume that the LHS has been replicated nRL times to produce $r = 1, 2, \dots, nRL$ independently generated LHSs

$$\mathbf{e}_{ri} = [\mathbf{e}_{Ari}, \mathbf{e}_{Mri}], i = 1, 2, \dots, nLHS, \quad (\text{Eq. J4.10-1})$$

of size $nLHS$ and that C_r is an analysis result of interest obtained for replicated sample r . For example, C might be the expected dose $\bar{D}(\tau)$ at time τ that is estimated with use of Latin hypercube sampling and $C_r = \bar{D}_r(\tau)$ would be the estimate for $\bar{D}(\tau)$ obtained with replicated sample r . Then,

$$\bar{C} = \sum_{r=1}^{nRL} C_r / nRL \quad (\text{Eq. J4.10-2})$$

and

$$SE(\bar{C}) = \left\{ \sum_{r=1}^{nRL} [C_r - \bar{C}]^2 / nRL(nRL - 1) \right\}^{1/2} \quad (\text{Eq. J4.10-3})$$

provide an additional estimate of C and an estimate of the standard error associated with this additional estimate.

The t -distribution with $nRL - 1$ degrees of freedom can now be used to place confidence intervals around the estimate for C in Equation J4.10-2. Specifically, the $1 - \alpha$ confidence interval for C is given by

$$\bar{C} \pm t_{1-\alpha/2} SE(\bar{C}), \quad (\text{Eq. J4.10-4})$$

where $t_{1-\alpha/2}$ is the $1 - \alpha/2$ quantile of the t -distribution with $nRL - 1$ degrees of freedom. For example, $t_{1-\alpha/2} = 4.303$ for $\alpha = 0.05$ and $nRL = 3$.

J5 NOMINAL SCENARIO CLASS: \mathcal{A}_N

For the nominal scenario class \mathcal{A}_N , no disruptions of any kind (i.e., early WP failures, early DS failures, igneous intrusive events, igneous eruptive events, seismic ground motion events, seismic fault displacement events) are assumed to take place. Thus, as discussed in Section J4.4, the vector

$$\mathbf{a}_N = [0, 0, 0, 0, 0, 0] \quad (\text{Eq. J5-1})$$

can be used to represent the realization of aleatory uncertainty associated with nominal conditions, where the 0's indicate the complete absence of any disruptions of the repository (see Equation J4.4-1) with $nEW = nED = nII = nIE = nSG = nSF = 0$). As a result, the set \mathcal{A}_N corresponding to the nominal scenario class contains the single element \mathbf{a}_N (see Equation J4.4-9). In turn, $D_N(\tau|\mathbf{a}_N, \mathbf{e}_M)$ is used to represent dose to the RMEI at time τ for the nominal scenario class conditional on the element $\mathbf{e} = [\mathbf{e}_A, \mathbf{e}_M]$ of \mathcal{E} as indicated in Equation J4.5-2. No component of \mathbf{e}_A is involved in the analysis of results for nominal conditions.

Only epistemic uncertainty is involved in the estimation of $D_N(\tau|\mathbf{a}_N, \mathbf{e}_M)$. As a result and given an LHS

$$\mathbf{e}_i = [\mathbf{e}_{Ai}, \mathbf{e}_{Mi}], i = 1, 2, \dots, nLHS, \quad (\text{Eq. J5-2})$$

from \mathcal{E} of the form indicated in Equation J4.9-1, the expected value, CDF and CCDF for $D_N(\tau|\mathbf{a}_N, \mathbf{e}_M)$ that derive from epistemic uncertainty conditional on the occurrence of the nominal scenario class can be estimated as indicated in Equations J4.9-5 – J4.9-7 by

$$\begin{aligned} \bar{D}_N(\tau|\mathbf{a}_N) &= E_E [D_N(\tau|\mathbf{a}_N, \mathbf{e}_M)] \\ &= \int_{\mathcal{E}} D_N(\tau|\mathbf{a}_N, \mathbf{e}_M) d_E(\mathbf{e}) dE \\ &\equiv \sum_{i=1}^{nLHS} D_N(\tau|\mathbf{a}_N, \mathbf{e}_{Mi}) / nLHS, \end{aligned} \quad (\text{Eq. J5-3})$$

$$\begin{aligned} p_E [D_N(\tau|\mathbf{a}_N, \mathbf{e}_M) \leq D] &= \int_{\mathcal{E}} \delta_D [D_N(\tau|\mathbf{a}_N, \mathbf{e}_M)] d_E(\mathbf{e}) dE \\ &\equiv \sum_{i=1}^{nLHS} \delta_D [D_N(\tau|\mathbf{a}_N, \mathbf{e}_{Mi})] / nLHS \end{aligned} \quad (\text{Eq. J5-4})$$

and

$$\begin{aligned}
 p_E \left[D < D_N(\tau | \mathbf{a}_N, \mathbf{e}_M) \right] &= \int_{\mathcal{E}} \underline{\delta}_D \left[D_N(\tau | \mathbf{a}_N, \mathbf{e}_M) \right] d_E(\mathbf{e}) dE \\
 &\equiv \sum_{i=1}^{nLHS} \bar{\delta}_D \left[D_N(\tau | \mathbf{a}_N, \mathbf{e}_{Mi}) \right] / nLHS, \quad (\text{Eq. J5-5})
 \end{aligned}$$

respectively, with $\underline{\delta}_D[\sim]$ and $\bar{\delta}_D[\sim]$ defined as indicated in Equations J4.2-7 and J4.2-3. Quantiles (e.g., $q = 0.05, 0.5, 0.95$) characterizing epistemic uncertainty in the dose $D_N(\tau | \mathbf{a}_N, \mathbf{e}_M)$ associated with the nominal scenario class can be obtained from the probabilities defined and then approximated in Equation J5-4. Specifically, the q quantile value $Q_q[D_N(\tau | \mathbf{a}_N, \mathbf{e}_M)]$ for the distribution of $D_N(\tau | \mathbf{a}_N, \mathbf{e}_M)$ at time τ over the possible values for $\mathbf{e} = [\mathbf{e}_A, \mathbf{e}_M]$ is formally defined to be the value of D such that

$$q = \int_{\mathcal{E}} \underline{\delta}_D \left[D_N(\tau | \mathbf{a}_N, \mathbf{e}_M) \right] d_E(\mathbf{e}) dE \quad (\text{Eq. J5-6})$$

and in computational practice is the value of D in the summation in Equation J5-4 for which $p_E[D_N(\tau | \mathbf{a}_N, \mathbf{e}_M) \leq D]$ most closely equals q . Equivalently, $Q_q[D_N(\tau | \mathbf{a}_N, \mathbf{e}_M)]$ is the value of D such that

$$1 - q = \int_{\mathcal{E}} \bar{\delta}_D \left[D_N(\tau | \mathbf{a}_N, \mathbf{e}_M) \right] d_E(\mathbf{e}) dE \quad (\text{Eq. J5-7})$$

and correspondingly is the value of D in the summation in Equation J5-5 for which $p_E[D \leq D_N(\tau | \mathbf{a}_N, \mathbf{e}_M)]$ most closely equals $1 - q$.

To support the calculations indicated in conjunction with Equations J5-2 – J5-7, the GoldSim component of the TSPA-LA model calculates and saves

$$D_N(\tau | \mathbf{a}_N, \mathbf{e}_{Mi}) \quad (\text{Eq. J5-8})$$

for $0 \leq \tau \leq 10^6$ yr and all values of \mathbf{e}_{Mi} . In addition, a large number of intermediate results are also saved.

A summary of the resultant dose calculations is given in Figure J5-1. Specifically, Figure J5-1a shows all 300 dose curves (i.e., $D_N(\tau | \mathbf{a}_N, \mathbf{e}_{Mi})$ for $0 \leq \tau \leq 10^6$ yr and $i = 1, 2, \dots, nLHS = 300$); Figure J5-1b shows the first 50 dose curves (i.e., $D_N(\tau | \mathbf{a}_N, \mathbf{e}_{Mi})$ for $0 \leq \tau \leq 10^6$ yr and $i = 1, 2, \dots, 50$); Figure J5-1c shows the expected (mean) value for dose at 6.0×10^5 yr, the CCDF for dose at 6.0×10^5 yr, and selected quantiles for dose at 6.0×10^5 yr (i.e., $\bar{D}_N(\tau | \mathbf{a}_N)$, $p_E[D < D_N(6.0 \times 10^5 \text{ yr} | \mathbf{a}_N, \mathbf{e}_M)]$ and $Q_q[D_N(6.0 \times 10^5 \text{ yr} | \mathbf{a}_N, \mathbf{e}_M)]$, $q = 0.05, 0.5, 0.95$, estimated from $D_N(6.0 \times 10^5 \text{ yr} | \mathbf{a}_N, \mathbf{e}_{Mi})$, $i = 1, 2, \dots, nLHS = 300$); and Figure J5-1d shows expected (mean) dose and quantile curves as a function of time (i.e., $\bar{D}_N(\tau)$ and $Q_q[D_N(\tau | \mathbf{a}_N, \mathbf{e}_M)]$, $q = 0.05, 0.5, 0.95$, estimated from $D_N(\tau | \mathbf{a}_N, \mathbf{e}_{Mi})$, $i = 1, 2, \dots, nLHS = 300$, for $0 \leq \tau \leq 10^6$ yr).

The results in Figure J5-1 are conditional on the occurrence of the nominal scenario class \mathcal{A}_N and thus do not incorporate the probability $p_A(\mathcal{A}_N|\mathbf{e}_A)$ of \mathcal{A}_N . Because the probability of the seismic ground motion scenario class \mathcal{A}_{SG} is effectively one for the time interval $[0, 10^6 \text{ yr}]$, the corresponding probability for \mathcal{A}_N is effectively zero (see Section J8.8). However, because nominal processes affect the evolution of the repository and its performance in the seismic scenario class, nominal processes and associated doses are included in the calculation of dose from seismic ground motion events for the time interval $[0, 10^6 \text{ yr}]$ (see Section J8.4).

Figure J5-1 is in a standard format that is used to summarize the dose results for each scenario class. This format permits (i) display of results for all LHS elements for completeness and results for 50 LHS elements for enhanced resolution of individual dose curves, (ii) selection of a scale on the ordinate that enhances the resolution of individual dose curves, (iii) illustration of the determination of quantiles from a CCDF, and (iv) display of expected (mean) and quantile curves.

In turn, a standardized and more compact display is used to summarize dose results for presentation outside this appendix (Figure J5-2). This display shows all dose curves, the expected (mean) dose curve, and quantile curves in the same plot frame. Further, the same range of values is used on the ordinate for all summary figures of this type. This standardization facilitates the comparison of results across scenario classes but reduces the resolution in the results for individual scenario classes. In contrast, the format used in Figure J5-1 provides better resolution for individual scenario classes but is less convenient for the comparison of results across scenario classes.

Dose $D_N(\tau|\mathbf{a}_N, \mathbf{e}_M)$ to the RMEI is just one of a large number of results that are produced and presented in the TSPA-LA. For example, $D_N(\tau|\mathbf{a}_N, \mathbf{e}_M)$ is defined by the sum

$$D_N(\tau|\mathbf{a}_N, \mathbf{e}_M) = \sum_{r=1}^{nRS} D_{Nr}(\tau|\mathbf{a}_N, \mathbf{e}_M), \quad (\text{J5-9})$$

where

nRS = number of radioactive species potentially causing dose to the RMEI,

$D_{Nr}(\tau|\mathbf{a}_N, \mathbf{e}_M)$ = dose to RMEI (mrem/yr) at time τ for radioactive species r resulting from nominal conditions.

In turn, quantities such as $\bar{\bar{D}}_{Nr}(\tau|\mathbf{a}_N)$, $p_E[D_{Nr}(\tau|\mathbf{a}_N, \mathbf{e}_M) \leq D]$, $p_E[D < D_{Nr}(\tau|\mathbf{a}_N, \mathbf{e}_M)]$ and $Q_q[D_{Nr}(\tau|\mathbf{a}_N, \mathbf{e}_M)]$ can be determined for each radioactive species in exactly the same manner as $\bar{\bar{D}}_N(\tau|\mathbf{a}_N)$, $p_E[D_N(\tau|\mathbf{a}_N, \mathbf{e}_M) \leq D]$, $p_E[D < D_N(\tau|\mathbf{a}_N, \mathbf{e}_M)]$ and $Q_q[D_N(\tau|\mathbf{a}_N, \mathbf{e}_M)]$ are determined in Equations J5-3 – J5-7.

As an example, a summary of the resultant dose calculations for ^{129}I is given in Figure J5-3, which has exactly the same organization as Figure J5-1. Overall, ^{129}I is the largest contributor to the expected (mean) dose $\bar{\bar{D}}_N(\tau|\mathbf{a}_N)$.

Results of the form shown in Figure J5-3 can be obtained for each radioactive species under consideration. This results in too many figures for a complete presentation. A compact summary of this large amount of information is provided by presenting the expected (mean) doses $\bar{\bar{D}}_{Nr}(\tau|\mathbf{a}_N)$ for all radioactive species in a single plot (Figure J5-4). The curve labeled “Total” in Figure J5-4 corresponds to the expected (mean) dose $\bar{\bar{D}}_N(\tau|\mathbf{a}_N)$ previously presented in Figures J5-1 and J5-2. The remaining curves correspond to expected (mean) doses $\bar{\bar{D}}_{Nr}(\tau|\mathbf{a}_N)$ for individual radioactive species.

As discussed in Section J4.10, the numerical stability of results obtained with Latin hypercube sampling can be assessed with replicated sampling. Specifically, the analysis for nominal conditions was performed with the $nRL = 3$ replicated LHSs indicated in Equation J4.10-1. In turn, this analysis shows that the numerical error in using Latin hypercube sampling to estimate $\bar{\bar{D}}_N(\tau|\mathbf{a}_N)$ is small relative to the epistemic uncertainty associated with the possible values for $D_N(\tau|\mathbf{a}_N, \mathbf{e}_M)$ (Figure J5-5).

Further descriptions of the nominal scenario class \mathcal{A}_N and sources of additional information are available in Section 6.3.

J6 EARLY FAILURE SCENARIO CLASSES: \mathcal{A}_E , \mathcal{A}_{EW} AND \mathcal{A}_{ED}

J6.1 Relationships Involving \mathcal{A}_E , \mathcal{A}_{EW} and \mathcal{A}_{ED}

The early WP failure scenario class and the early DS failure scenario class are defined by the sets

$$\mathcal{A}_{EW} = \{\mathbf{a} : \mathbf{a} \in \mathcal{A} \text{ and } nEW \geq 1\} \quad (\text{Eq. J6.1-1})$$

and

$$\mathcal{A}_{ED} = \{\mathbf{a} : \mathbf{a} \in \mathcal{A} \text{ and } nED \geq 1\} \quad (\text{Eq. J6.1-2})$$

as indicated in Equations J4.4-13 and J4.4-14. Further, the combined early failure scenario class \mathcal{A}_E is defined by

$$\mathcal{A}_E = \mathcal{A}_{EW} \cup \mathcal{A}_{ED} = \{\mathbf{a} : \mathbf{a} \in \mathcal{A} \text{ and } nEW + nED \geq 1\}. \quad (\text{Eq. J6.1-3})$$

Then, $p_A(\mathcal{A}_{EW})$ is the probability of one or more early WP failures; $p_A(\mathcal{A}_{ED})$ is the probability of one or more early DS failures; and $p_A(\mathcal{A}_E)$ is the probability of one or more early failures.

The subsets \mathcal{A}_{EW} and \mathcal{A}_{ED} of \mathcal{A} are not disjoint. For the early WP failure scenario class and the early DS failure scenario class to be disjoint from both each other and also from the scenario classes \mathcal{A}_{II} , \mathcal{A}_{IE} , \mathcal{A}_{SG} and \mathcal{A}_{SF} defined in Equations J4.4-15 – J4.4-18 requires their definitions to be based on the sets

$$\tilde{\mathcal{A}}_{EW} = \{\mathbf{a} : \mathbf{a} \in \mathcal{A}, n_{EW} \geq 1 \text{ and } n_{ED} = n_{II} = n_{IE} = n_{SG} = n_{SF} = 0\} \quad (\text{Eq. J6.1-4})$$

and

$$\tilde{\mathcal{A}}_{ED} = \{\mathbf{a} : \mathbf{a} \in \mathcal{A}, n_{ED} \geq 1 \text{ and } n_{EW} = n_{II} = n_{IE} = n_{SG} = n_{SF} = 0\}, \quad (\text{Eq. J6.1-5})$$

respectively. In turn,

$$p_A(\tilde{\mathcal{A}}_{EW}) = p_A(\mathcal{A}_{EW}) p_A(\{\mathbf{a} : \mathbf{a} \in \mathcal{A} \text{ and } n_{ED} = n_{II} = n_{IE} = n_{SG} = n_{SF} = 0\}) \quad (\text{Eq. J6.1-6})$$

and

$$p_A(\tilde{\mathcal{A}}_{ED}) = p_A(\mathcal{A}_{ED}) p_A(\{\mathbf{a} : \mathbf{a} \in \mathcal{A} \text{ and } n_{EW} = n_{II} = n_{IE} = n_{SG} = n_{SF} = 0\}) \quad (\text{Eq. J6.1-7})$$

under the assumption that the occurrences of early WP failure and early DS failure are independent of both each other and also the other types of disruption under consideration. Specifically, $p_A(\tilde{\mathcal{A}}_{EW})$ is the probability that one or more early WP failures occur and also that no other disruptive events take place, and $p_A(\tilde{\mathcal{A}}_{ED})$ is the probability that one or more early DS failures occur and also that no other disruptive events take place.

When the second term in the products in Equations J6.1-6 and J6.1-7 is small, then $p_A(\tilde{\mathcal{A}}_{EW})$ and $p_A(\tilde{\mathcal{A}}_{ED})$ will be much smaller than $p_A(\mathcal{A}_{EW})$ and $p_A(\mathcal{A}_{ED})$. For this reason, it is the probabilities $p_A(\mathcal{A}_{EW})$ and $p_A(\mathcal{A}_{ED})$ for the scenario classes \mathcal{A}_{EW} and \mathcal{A}_{ED} that are usually of interest rather than the probabilities $p_A(\tilde{\mathcal{A}}_{EW})$ and $p_A(\tilde{\mathcal{A}}_{ED})$ for the more restricted (and disjoint) scenario classes $\tilde{\mathcal{A}}_{EW}$ and $\tilde{\mathcal{A}}_{ED}$. If the question is asked “What is the probability of early WP failure?”, then most likely $p_A(\mathcal{A}_{EW})$ is the desired answer. Similarly, if the question is asked “What is the probability of early DS failure?”, then most likely the desired answer is $p_A(\mathcal{A}_{ED})$. It is very unlikely that the desired answers are $p_A(\tilde{\mathcal{A}}_{EW})$ and $p_A(\tilde{\mathcal{A}}_{ED})$ as these probabilities provide little useful information about the likelihood of early WP and early DS failures.

No synergisms are assumed to exist between the doses that result from early WP failures and early DS failures. Further, as indicated in conjunction with Equation J4.5-1, no synergisms are assumed to exist between doses that result from early failures and doses that result from other disruptions. As a result,

$$D_E(\tau|\mathbf{a}, \mathbf{e}_M) = D_{EW}(\tau|\mathbf{a}, \mathbf{e}_M) + D_{ED}(\tau|\mathbf{a}, \mathbf{e}_M), \quad (\text{Eq. J6.1-8})$$

where

$D_E(\tau|\mathbf{a}, \mathbf{e}_M)$ = dose to RMEI (mrem/yr) at time τ resulting from early failures associated with element \mathbf{a} of \mathcal{A}_E ,

$D_{EW}(\tau|\mathbf{a}, \mathbf{e}_M)$ = dose to RMEI (mrem/yr) at time τ resulting from early WP failures associated with element \mathbf{a} of \mathcal{A}_E ,

$D_{ED}(\tau|\mathbf{a}, \mathbf{e}_M)$ = dose to RMEI (mrem/yr) at time τ resulting from early DS failures associated with element \mathbf{a} of \mathcal{A}_E ,

and all results are conditional on the element $\mathbf{e} = [\mathbf{e}_A, \mathbf{e}_M]$ of \mathcal{E} . If \mathbf{a} involves no early WP failures (i.e., if $n_{EW} = 0$ or, equivalently, if $\mathbf{a} \notin \mathcal{A}_{EW}$), then $D_{EW}(\tau|\mathbf{a}, \mathbf{e}_M) = 0$; similarly, if \mathbf{a} involves no early DS failures (i.e., if $n_{ED} = 0$ or, equivalently, if $\mathbf{a} \notin \mathcal{A}_{ED}$), then $D_{ED}(\tau|\mathbf{a}, \mathbf{e}_M) = 0$.

In turn, the expected dose $\bar{D}_E(\tau|\mathbf{e})$ to the RMEI (mrem/yr) at time τ from early failures is given by

$$\begin{aligned}\bar{D}_E(\tau|\mathbf{e}) &= \int_{\mathcal{A}_E} D_E(\tau|\mathbf{a}, \mathbf{e}_M) d_A(\mathbf{a}|\mathbf{e}_A) dA \\ &= \int_{\mathcal{A}_E} [D_{EW}(\tau|\mathbf{a}, \mathbf{e}_M) + D_{ED}(\tau|\mathbf{a}, \mathbf{e}_M)] d_A(\mathbf{a}|\mathbf{e}_A) dA \\ &= \int_{\mathcal{A}_E} D_{EW}(\tau|\mathbf{a}, \mathbf{e}_M) d_A(\mathbf{a}|\mathbf{e}_A) dA + \int_{\mathcal{A}_E} D_{ED}(\tau|\mathbf{a}, \mathbf{e}_M) d_A(\mathbf{a}|\mathbf{e}_A) dA \\ &= \bar{D}_{EW}(\tau|\mathbf{e}) + \bar{D}_{ED}(\tau|\mathbf{e}),\end{aligned}\tag{Eq. J6.1-9}$$

where (i)

$$\begin{aligned}\bar{D}_{EW}(\tau|\mathbf{e}) &= \int_{\mathcal{A}_E} D_{EW}(\tau|\mathbf{a}, \mathbf{e}_M) d_A(\mathbf{a}|\mathbf{e}_A) dA \\ &= \int_{\mathcal{A}_{EW}} D_{EW}(\tau|\mathbf{a}, \mathbf{e}_M) d_A(\mathbf{a}|\mathbf{e}_A) dA\end{aligned}\tag{Eq. J6.1-10}$$

is the expected dose to the RMEI (mrem/yr) at time τ resulting from early WP failures as previously indicated in Equation J4.5-9, (ii)

$$\begin{aligned}\bar{D}_{ED}(\tau|\mathbf{e}) &= \int_{\mathcal{A}_E} D_{ED}(\tau|\mathbf{a}, \mathbf{e}_M) d_A(\mathbf{a}|\mathbf{e}_A) dA \\ &= \int_{\mathcal{A}_{ED}} D_{ED}(\tau|\mathbf{a}, \mathbf{e}_M) d_A(\mathbf{a}|\mathbf{e}_A) dA\end{aligned}\tag{Eq. J6.1-11}$$

is the expected dose to the RMEI (mrem/yr) at time τ resulting from early DS failures as previously indicated in Equation J4.5-10, and (iii) all results are conditional on the element $\mathbf{e} = [\mathbf{e}_A, \mathbf{e}_M]$ of \mathcal{E} . The conversion from an integral over \mathcal{A}_E to an integral over \mathcal{A}_{EW} in Equation

J6.1-10 is possible because $D_{EW}(\tau|\mathbf{a}, \mathbf{e}_M) = 0$ if $\mathbf{a} \notin \mathcal{A}_{EW}$; similarly, the conversion from an integral over \mathcal{A}_E to an integral over \mathcal{A}_{ED} in Equation J6.1-11 is possible because $D_{ED}(\tau|\mathbf{a}, \mathbf{e}_M) = 0$ if $\mathbf{a} \notin \mathcal{A}_{ED}$.

The general form of the elements \mathbf{a} of \mathcal{A} is shown in Equations J4.4-1 – J4.4-8. However, because no synergisms between disruptions are assumed in the determination of $\bar{D}_{EW}(\tau|\mathbf{e})$ and $\bar{D}_{ED}(\tau|\mathbf{e})$, the representations for the elements of \mathcal{A}_{EW} and \mathcal{A}_{ED} can be simplified to

$$\mathbf{a}_{EW} = [nEW, \mathbf{a}_{EW,1}, \mathbf{a}_{EW,2}, \dots, \mathbf{a}_{EW,nEW}] \quad (\text{Eq. J6.1-12})$$

and

$$\mathbf{a}_{ED} = [nED, \mathbf{a}_{ED,1}, \mathbf{a}_{ED,2}, \dots, \mathbf{a}_{ED,nED}], \quad (\text{Eq. J6.1-13})$$

respectively. With this notation, the elements \mathbf{a}_{EW} of \mathcal{A}_{EW} only contain representations for early WP failures, and the elements \mathbf{a}_{ED} of \mathcal{A}_{ED} only contain representations for early DS failures.

The preceding representations for \mathbf{a}_{EW} and \mathbf{a}_{ED} lead to computationally useful representations for the doses $D_{EW}(\tau|\mathbf{a}, \mathbf{e}_M)$ and $D_{ED}(\tau|\mathbf{a}, \mathbf{e}_M)$. Specifically,

$$\begin{aligned} D_{EW}(\tau|\mathbf{a}, \mathbf{e}_M) &= D_{EW}(\tau|\mathbf{a}_{EW}, \mathbf{e}_M) \\ &= \sum_{j=1}^{nEW} D_{EW}(\tau|[1, \mathbf{a}_{EW,j}], \mathbf{e}_M) \end{aligned} \quad (\text{Eq. J6.1-14})$$

provided (i) \mathbf{a}_{EW} as defined in Equation J6.1-12 characterizes the early WP failures associated with \mathbf{a} , (ii) there are no synergisms between the doses associated with individual early WP failures, and (iii) $D_{EW}(\tau|[1, \mathbf{a}_{EW,j}], \mathbf{e}_M)$ equals the dose to the RMEI (mrem/yr) at time τ from an early failed WP with properties defined by $\mathbf{a}_{EW,j}$. Similarly,

$$\begin{aligned} D_{ED}(\tau|\mathbf{a}, \mathbf{e}_M) &= D_{ED}(\tau|\mathbf{a}_{ED}, \mathbf{e}_M) \\ &= \sum_{j=1}^{nED} D_{ED}(\tau|[1, \mathbf{a}_{ED,j}], \mathbf{e}_M) \end{aligned} \quad (\text{Eq. J6.1-15})$$

provided (i) \mathbf{a}_{ED} as defined in Equation J6.1-13 characterizes the early DS failures associated with \mathbf{a} , (ii) there are no synergisms between doses associated with individual early DS failures, and (iii) $D_{ED}(\tau|[1, \mathbf{a}_{ED,j}], \mathbf{e}_M)$ equals the dose to the RMEI (mrem/yr) at time τ from an early failed DS with properties defined by $\mathbf{a}_{ED,j}$. The preceding representations for $D_{EW}(\tau|\mathbf{a}, \mathbf{e}_M)$ and $D_{ED}(\tau|\mathbf{a}, \mathbf{e}_M)$ play a fundamental role in the numerical calculation of $\bar{D}_{EW}(\tau|\mathbf{e})$ and $\bar{D}_{ED}(\tau|\mathbf{e})$.

The expected (mean) dose $\bar{\bar{D}}_E(\tau)$ for the early failure scenario class \mathcal{A}_E over both aleatory and epistemic uncertainty is given by

$$\begin{aligned}
 \bar{\bar{D}}_E(\tau) &= \int_{\mathcal{E}} \bar{D}_E(\tau|\mathbf{e}) d_E(\mathbf{e}) dE \\
 &= \int_{\mathcal{E}} [\bar{D}_{EW}(\tau|\mathbf{e}) + \bar{D}_{ED}(\tau|\mathbf{e})] d_E(\mathbf{e}) dE \\
 &= \int_{\mathcal{E}} \bar{D}_{EW}(\tau|\mathbf{e}) d_E(\mathbf{e}) dE + \int_{\mathcal{E}} \bar{D}_{ED}(\tau|\mathbf{e}) d_E(\mathbf{e}) dE \\
 &= \bar{\bar{D}}_{EW}(\tau) + \bar{\bar{D}}_{ED}(\tau), \tag{Eq. J6.1-16}
 \end{aligned}$$

where

$$\bar{\bar{D}}_{EW}(\tau) = \int_{\mathcal{E}} \bar{D}_{EW}(\tau|\mathbf{e}) d_E(\mathbf{e}) dE \tag{Eq. J6.1-17}$$

is the expected (mean) dose for the early WP failure scenario class \mathcal{A}_{EW} over both aleatory and epistemic uncertainty as defined in Equation J4.6-5 for $C = EW$ and

$$\bar{\bar{D}}_{ED}(\tau) = \int_{\mathcal{E}} \bar{D}_{ED}(\tau|\mathbf{e}) d_E(\mathbf{e}) dE \tag{Eq. J6.1-18}$$

is the expected (mean) dose for the early DS failure scenario class \mathcal{A}_{ED} over both aleatory and epistemic uncertainty as defined in Equation J4.5-6 for $C = ED$.

The CCDF and CDF for $\bar{D}_E(\tau|\mathbf{e})$ over epistemic uncertainty are defined by

$$\begin{aligned}
 p_E[D < \bar{D}_E(\tau|\mathbf{e})] &= \int_{\mathcal{E}} \bar{\delta}_D[\bar{D}_E(\tau|\mathbf{e})] d_E(\mathbf{e}) dE \\
 &= \int_{\mathcal{E}} \bar{\delta}_D[\bar{D}_{EW}(\tau|\mathbf{e}) + \bar{D}_{ED}(\tau|\mathbf{e})] d_E(\mathbf{e}) dE \tag{Eq. J6.1-19}
 \end{aligned}$$

and

$$\begin{aligned}
 p_E[\bar{D}_E(\tau|\mathbf{e}) \leq D] &= 1 - p_E[D < \bar{D}_E(\tau|\mathbf{e})] \\
 &= \int_{\mathcal{E}} \delta_D[\bar{D}_E(\tau|\mathbf{e})] d_E(\mathbf{e}) dE \\
 &= \int_{\mathcal{E}} \delta_D[\bar{D}_{EW}(\tau|\mathbf{e}) + \bar{D}_{ED}(\tau|\mathbf{e})] d_E(\mathbf{e}) dE, \tag{Eq. J6.1-20}
 \end{aligned}$$

respectively. However, unlike the result for $\bar{\bar{D}}_E(\tau)$ in Equation J6.1-16, the CCDF and CDF for $\bar{D}_E(\tau|\mathbf{e})$ cannot be decomposed into a sum of separate results for the early WP failure scenario class \mathcal{A}_{EW} and the early DS failure scenario class \mathcal{A}_{ED} .

Direct evaluation of the integrals that define $\bar{\bar{D}}_E(\tau)$, $p_E[D < \bar{D}_E(\tau|\mathbf{e})]$ and $p_E[\bar{D}_E(\tau|\mathbf{e}) \leq D]$ is not practical. However, the approximations

$$\bar{\bar{D}}_E(\tau) \cong \sum_{i=1}^{nLHS} \bar{D}_E(\tau|\mathbf{e}_i)/nLHS, \quad (\text{Eq. J6.1-21})$$

$$p_E[D < \bar{D}_E(\tau|\mathbf{e})] \cong \sum_{i=1}^{nLHS} \bar{\delta}_D[\bar{D}_E(\tau|\mathbf{e}_i)]/nLHS \quad (\text{Eq. J6.1-22})$$

and

$$p_E[\bar{D}_E(\tau|\mathbf{e}) \leq D] \cong \sum_{i=1}^{nLHS} \underline{\delta}_D[\bar{D}_E(\tau|\mathbf{e}_i)]/nLHS \quad (\text{Eq. J6.1-23})$$

result with use of the LHS in Equation J4.9-1 as previously indicated in conjunction with Equations J4.9-8 – J4.9-10.

Further descriptions of the early failure scenario classes \mathcal{A}_E , \mathcal{A}_{EW} and \mathcal{A}_{ED} and sources of additional information are available in Section 6.4.

J6.2 Early WP Failure Scenario Class: \mathcal{A}_{EW}

In the TSPA-LA, the individual vectors $\mathbf{a}_{EW,j}$, $j = 1, 2, \dots, nEW$, appearing in the definition of \mathbf{a}_{EW} in Equation J6.1-12 are defined by

$$\mathbf{a}_{EW,j} = [t_j, b_j, d_j] \quad (\text{Eq. J6.2-1})$$

and characterize the properties of failed WP j , where t_j designates WP type (i.e., $t_j = 1 \sim$ CSNF WP, $t_j = 2 \sim$ CDSP WP), b_j designates percolation bin in which the failed WP is located (i.e., $b_j = k \sim$ location of failed WP in percolation bin k for $k = 1, 2, 3, 4, 5$), and d_j designates whether the failed WP experiences nondripping or dripping conditions (i.e., $d_j = 0 \sim$ nondripping conditions and $d_j = 1 \sim$ dripping conditions).

The following quantities are available in the TSPA-LA for the characterization of the probability of early WP failure results of the form defined by $\mathbf{a}_{EW,j}$ in Equation J6.2-1 and hence for use in the determination of $\bar{D}_{EW}(\tau|\mathbf{a}, \mathbf{e})$:

nWP = number of WPs in repository,

nWT = number of WP types (i.e., CSNFs, CDSPs, ...),

fWT_r = fraction of WPs of type r , $r = 1, 2, \dots, nWT$,

pWT_r = probability that a randomly selected WP of type r , $r = 1, 2, \dots, nWT$, will experience an early failure (element of \mathbf{e}_A),

nBN = number of percolation bins used for early failure calculations,

fBN_{rs} = fraction of WPs of type r , $r = 1, 2, \dots, nWT$, in bin s , $s = 1, 2, \dots, nBN$,

$fDRP_{rs}$ = fraction of WPs of type r , $r = 1, 2, \dots, nWT$, in bin s , $s = 1, 2, \dots, nBN$, experiencing dripping conditions (function of \mathbf{e}_M).

The probability pWT_r that a randomly selected WP will experience an early failure constitutes the defining parameter for a binomial probability distribution (see Equations J3.6-22 to J3.6-25) and is treated as being epistemically uncertain in the TSPA, with this uncertainty characterized by a lognormal distribution. In the TSPA-LA, the probability pWT_r is assumed to be the same for CSNF and CDSP WPs (i.e., $pW = pWT_1 = pWT_2$). A different value for this probability (i.e., pW_i) is selected in each LHS element $\mathbf{e}_i = [\mathbf{e}_{Ai}, \mathbf{e}_{Mi}]$ indicated in Equation J4.9-1. In turn, this results in $nLHS = 300$ CCDFs for the possible number of early WP failures (Figure J6.2-1). No upper bound was specified for pW ; as a result, large values are possible if the upper tail of the specified lognormal distribution is sampled. An occurrence of this type can be seen in the outlier CCDF in Figure 6.2-1a.

For a given LHS element $\mathbf{e}_i = [\mathbf{e}_{Ai}, \mathbf{e}_{Mi}]$ of the form indicated in Equation J4.9-1, the expected dose $\bar{D}_{EW}(\tau|\mathbf{e}_i)$ is now given by

$$\begin{aligned} \bar{D}_{EW}(\tau|\mathbf{e}_i) &= \int_{\mathcal{A}_{EW}} D_{EW}(\tau|\mathbf{a}, \mathbf{e}_{Mi}) d_A(\mathbf{a}|\mathbf{e}_{Ai}) dA \\ &= \sum_{r=1}^{nWT} \sum_{s=1}^{nBN} \sum_{t=0}^1 pWT_{ri} fWT_r fBN_{rs} pDRP_{rsti} nWP D_{EW}(\tau|[1, r, s, t], \mathbf{e}_{Mi}) \\ &= \sum_{r=1}^2 \sum_{s=1}^5 \sum_{t=0}^1 pWT_{ri} fWT_r fBN_{rs} pDRP_{rsti} nWP D_{EW}(\tau|[1, r, s, t], \mathbf{e}_{Mi}), \end{aligned} \quad (\text{Eq. J6.2-2})$$

where (i)

$$pDRP_{rsti} = \begin{cases} 1 - fDRP_{rsi} & \text{if } t = 0 \\ fDRP_{rsi} & \text{if } t = 1 \end{cases}$$

and (ii) the final equality results when $nWT = 2$ WP types (i.e., CSNFs and CDSPs) and $nBN = 5$ percolation bins are under consideration, which corresponds to the values for nWT and nBN used in the TSPA-LA. As previously indicated, the probability of early failure is assumed to be the same for the two WP types; thus, $pW_i = pWT_{1i} = pWT_{2i}$.

In turn, the estimates for $\bar{D}_{EW}(\tau|\mathbf{e}_i)$ can be used to estimate $\bar{\bar{D}}_{EW}(\tau)$, $p_E[\bar{D}_{EW}(\tau|\mathbf{e}) \leq D]$ and $p_E[D < \bar{\bar{D}}_{EW}(\tau|\mathbf{e})]$. Specifically,

$$\bar{\bar{D}}_{EW}(\tau) \cong \sum_{i=1}^{nLHS} \bar{D}_{EW}(\tau|\mathbf{e}_i)/nLHS, \quad (\text{Eq. J6.2-3})$$

$$p_E[\bar{D}_{EW}(\tau|\mathbf{e}) \leq D] \cong \sum_{i=1}^{nLHS} \underline{\delta}_D[\bar{D}_{EW}(\tau|\mathbf{e}_i)]/nLHS \quad (\text{Eq. J6.2-4})$$

and

$$p_E[D < \bar{D}_{EW}(\tau|\mathbf{e})] \cong \sum_{i=1}^{nLHS} \bar{\delta}_D[\bar{D}_{EW}(\tau|\mathbf{e}_i)]/nLHS, \quad (\text{Eq. J6.2-5})$$

as indicated in Equations J4.9-8 – J4.9-10, where $\bar{\delta}_D(\sim)$ and $\underline{\delta}_D(\sim)$ are defined in Equations J4.2-3 and J4.2-7, respectively. Further, quantiles $Q_q[\bar{D}_{EW}(\tau|\mathbf{e})]$ for $\bar{D}_{EW}(\tau|\mathbf{e})$ can be obtained by solving either

$$q = \int_{\mathcal{A}_{EW}} \underline{\delta}_D[\bar{D}_{EW}(\tau|\mathbf{e})] d_E(\mathbf{e}) dE \quad (\text{Eq. J6.2-6})$$

or

$$1 - q = \int_{\mathcal{A}_{EW}} \bar{\delta}_D[\bar{D}_{EW}(\tau|\mathbf{e})] d_E(\mathbf{e}) dE \quad (\text{Eq. J6.2-7})$$

for D . In practice, the solution of Equation J6.2-6 or Equation J6.2-7 to determine D , and hence $Q_q[\bar{D}_{EW}(\tau|\mathbf{e})]$, is based on the approximating sums in Equations J6.2-4 and J6.2-5.

The determination of $\bar{D}_{EW}(\tau|\mathbf{e}_i)$ as indicated in Equation J6.2-2 requires the evaluation of

$$D_{EW}(\tau|[1, r, s, t], \mathbf{e}_{Mi}) \quad (\text{Eq. J6.2-8})$$

in GoldSim for selected values of τ , $r = 1, 2, \dots, nWT$, $s = 1, 2, \dots, nBN$, $t = 0, 1$, and \mathbf{e}_{Mi} , $i = 1, 2, \dots, nLHS$. The fractions $fDRP_{rst}$ are also determined in GoldSim and are functions of \mathbf{e}_{Mi} . Further, a large number of intermediate results are also generated and saved.

The results indicated in conjunction with Equation J6.2-8 were calculated twice, once for the time interval $[0, 2.0 \times 10^4 \text{ yr}]$ and once for the time interval $[0, 10^6 \text{ yr}]$. Owing to its shorter length, results for the 20,000 yr time interval were saved with use of shorter timesteps (i.e., more closely spaced values for τ) than used to compute results for the 10^6 yr time interval. Specifically, timesteps of 10, 40 and 80 yr were used for the 20,000 yr time interval, and timesteps of 250, 500, 1000, 2000 and 4000 yr were used for the 10^6 yr time interval.

Results obtained for the 20,000 yr time interval are presented first; corresponding results for the 10^6 yr time interval are presented at the end of this section. As a result of the consideration of

$nWT = 2$ waste types, $nBN = 5$ percolation bins, and $nDRP = 2$ dripping conditions, $(2)(5)(2) = 20$ dose calculations are performed by GoldSim for each LHS element. As an example, the values for $D_{EW}(\tau|[1, r, 3, t], \mathbf{e}_{Mi})$ obtained for $r = 1, 2$, $t = 0, 1$, and $i = 1, 2, \dots, nLHS = 300$ are presented in Figure J6.2-2. Specifically, Figure J6.2-2 shows the epistemic uncertainty in dose to the RMEI that results from the early failure of one WP under four conditions: (i) one early failed CSNF WP in bin 3 under nondripping conditions (Figure J6.2-2a), (ii) one early failed CSNF WP in bin 3 under dripping conditions (Figure J6.2-2b), (iii) one early failed CDSP WP in bin 3 under nondripping conditions (Figure J6.2-2c), and (iv) one early failed CDSP WP in bin 3 under dripping conditions (Figure J6.2-2d).

Only 4 of the 20 dose results calculated by GoldSim for each LHS element are presented in Figure J6.2-2. An alternate presentation format is to use box plots to summarize all 20 dose results in a single figure (Figure J6.2-3). Specifically, Figure J6.2-3 shows the 10 dose results calculated for CSNF WPs at three times (i.e., 10,000, 15,000, 20,000 yr) and the 10 dose results calculated for CDSP WPs at three times (i.e., 2000, 5000, 10,000 yr). Different presentation times are used for CSNF and CDSP WPs because the dose results for CSNF WPs are effectively zero prior to 10,000 yr (Figures J6.2-2a,b and J6.2-3a). Figure J6.2-3 does not present individual dose results at the same level of temporal resolution as Figure J6.2-2. However, Figure J6.2-3 has two important properties. First, it summarizes all 20 dose results in a single figure. Second, the horizontal presentation of the box plots facilitates comparison of dose results obtained under different conditions.

Once the dose results indicated in Equation J6.2-8 and illustrated in Figures J6.2-2 and J6.2-3 are available, $\bar{D}_{EW}(\tau|\mathbf{e}_i)$ can be estimated for each LHS element \mathbf{e}_i as shown in Equation J6.2-2. As an example, the resultant estimate $\bar{D}_{EW}(\tau|\mathbf{e}_1)$ for LHS element \mathbf{e}_1 is shown in Figure J6.2-4.

A summary of the calculations involving $\bar{D}_{EW}(\tau|\mathbf{e})$ for all LHS elements is given in Figure J6.2-5. Specifically, Figure J6.2-5a shows all 300 expected dose curves (i.e., $\bar{D}_{EW}(\tau|\mathbf{e}_i)$ for $0 \leq \tau \leq 20,000$ yr and $i = 1, 2, \dots, nLHS = 300$); Figure J6.2-5b shows the first 50 expected dose curves (i.e., $\bar{D}_{EW}(\tau|\mathbf{e}_i)$ for $0 \leq \tau \leq 20,000$ yr and $i = 1, 2, \dots, 50$); Figure J6.2-5c shows the expected (mean) value, the CCDF and selected quantiles for expected dose at 10,000 yr (i.e., $\bar{D}_{EW}(10^4 \text{ yr})$, $p_E[D < \bar{D}_{EW}(10^4 \text{ yr}|\mathbf{e})]$ and $Q_q[\bar{D}_{EW}(10^4 \text{ yr}|\mathbf{e})]$, $q = 0.05, 0.5, 0.95$, estimated from $\bar{D}_{EW}(10^4 \text{ yr}|\mathbf{e}_i)$, $i = 1, 2, \dots, nLHS = 300$); and Figure J6.2-5d shows expected (mean) dose and quantile curves as functions of time (i.e., $\bar{D}_{EW}(\tau)$ and $Q_q[\bar{D}_{EW}(\tau|\mathbf{e})]$, $q = 0.05, 0.5, 0.95$, estimated from $\bar{D}_{EW}(\tau|\mathbf{e}_i)$, $i = 1, 2, \dots, nLHS = 300$, for $0 \leq \tau \leq 20,000$ yr).

In turn, the results in Figure J6.2-5 can be summarized in the standard format appearing in Figure J6.2-6. As discussed in conjunction with Figures J5-1 and J5-2, the format in Figure J6.2-5 facilitates the presentation of results for individual scenario classes, and the format in Figure J6.2-6 facilitates the comparison of results across scenario classes.

As previously discussed in conjunction with Equation J5-9 and illustrated in Figures J5-3 and J5-4 for nominal conditions, dose and expected dose to the RMEI is just one of a large number of

results that can be produced and presented in the TSPA-LA. Similarly to $D_N(\tau|\mathbf{a}_N, \mathbf{e}_M)$ in Equation J5-9, the dose $D_C(\tau|\mathbf{a}_C, \mathbf{e}_M)$ to the RMEI for an arbitrary scenario class C (e.g., $C \in \{EW, ED, II, IE, SG, SF\}$) is defined by the sum

$$D_C(\tau|\mathbf{a}_C, \mathbf{e}_M) = \sum_{r=1}^{nRS} D_{Cr}(\tau|\mathbf{a}_C, \mathbf{e}_M), \quad (\text{Eq. J6.2-9})$$

where

nRS = number of radioactive species potentially causing dose to the RMEI,

$D_{Cr}(\tau|\mathbf{a}_C, \mathbf{e}_M)$ = dose to RMEI (mrem/yr) at time τ for radioactive species r resulting from conditions associated with scenario class C .

In turn, quantities such as $\bar{D}_{Cr}(\tau|\mathbf{e})$, $p_E[\bar{D}_{Cr}(\tau|\mathbf{e}) \leq D]$, $p_E[D < \bar{D}_{Cr}(\tau|\mathbf{e})]$, $Q_q[\bar{D}_{Cr}(\tau|\mathbf{e})]$ and $\bar{\bar{D}}_{Cr}(\tau)$ can be determined for each radioactive species in exactly the same manner as $\bar{D}_C(\tau|\mathbf{e})$, $p_E[\bar{D}_C(\tau|\mathbf{e}) \leq D]$, $p_E[D < \bar{D}_C(\tau|\mathbf{e})]$, $Q_q[\bar{D}_C(\tau|\mathbf{e})]$ and $\bar{\bar{D}}_C(\tau)$. For this section, $C = EW$, and the determinations for $\bar{D}_{EW,r}(\tau|\mathbf{e})$, $p_E[\bar{D}_{EW,r}(\tau|\mathbf{e}) \leq D]$, $p_E[D < \bar{D}_{EW,r}(\tau|\mathbf{e})]$, $Q_q[\bar{D}_{EW,r}(\tau|\mathbf{e})]$ and $\bar{\bar{D}}_{EW,r}(\tau)$ are made in the same manner as the presented determinations for $\bar{D}_{EW}(\tau|\mathbf{e})$, $p_E[\bar{D}_{EW}(\tau|\mathbf{e}) \leq D]$, $p_E[D < \bar{D}_{EW}(\tau|\mathbf{e})]$, $Q_q[\bar{D}_{EW}(\tau|\mathbf{e})]$ and $\bar{\bar{D}}_{EW}(\tau)$.

As an example, a summary of the resultant dose calculations for ^{99}Tc is given in Figure J6.2-7, which has the same organization as Figure J6.2-5. Overall, ^{99}Tc is the largest contributor to the expected (mean) dose $\bar{\bar{D}}_{EW}(\tau)$ for the 20,000 yr time period.

Results of the form shown in Figure J6.2-7 can be obtained for each radioactive species under consideration. This results in too many figures for a complete presentation. As previously done in Figure J5-4 for nominal conditions, a compact summary of this large amount of information is provided by presenting the expected (mean) doses $\bar{\bar{D}}_{EW,r}(\tau)$ for all radioactive species in a single plot (Figure J6.2-8). The curve labeled "Total" in Figure J6-8 corresponds to the expected (mean) dose $\bar{\bar{D}}_{EW}(\tau)$ previously presented in Figures J6.2-5 and J6.2-6. The remaining curves correspond to expected (mean) doses $\bar{\bar{D}}_{EW,r}(\tau)$ for individual radioactive species.

Once the results in Equation J6.2-8 are available, Monte Carlo procedures can also be used to estimate $\bar{D}_{EW}(\tau|\mathbf{e}_i)$, the CDF for $D_{EW}(\tau|\mathbf{a}, \mathbf{e}_{Mi})$, and the CCDF for $D_{EW}(\tau|\mathbf{a}, \mathbf{e}_{Mi})$. Specifically,

$$\begin{aligned}\bar{D}_{EW}(\tau|\mathbf{e}_i) &\cong p_A(\mathcal{A}_{EW}|\mathbf{e}_{Ai}) \sum_{k=1}^{nR} D_{EW}(\tau|\mathbf{a}_{EW,k}, \mathbf{e}_{Mi})/nR \\ &= p_A(\mathcal{A}_{EW}|\mathbf{e}_{Ai}) \sum_{k=1}^{nR} \left\{ \sum_{j=1}^{nEW_k} D_{EW}(\tau|[1, t_{jk}, b_{jk}, d_{jk}], \mathbf{e}_{Mi}) \right\} / nR, \quad (\text{Eq. J6.2-10})\end{aligned}$$

$$\begin{aligned}p_A[D_{EW}(\tau|\mathbf{a}, \mathbf{e}_{Mi}) \leq D|\mathbf{e}_{Ai}] &\cong p_A(\mathcal{A}_{EW}|\mathbf{e}_{Ai}) \sum_{k=1}^{nR} \underline{\delta}_D[D_{EW}(\tau|\mathbf{a}_{EW,k}, \mathbf{e}_{Mi})]/nR \\ &= p_A(\mathcal{A}_{EW}|\mathbf{e}_{Ai}) \sum_{k=1}^{nR} \underline{\delta}_D \left\{ \sum_{j=1}^{nEW_k} D_{EW}(\tau|[1, t_{jk}, b_{jk}, d_{jk}], \mathbf{e}_{Mi}) \right\} / nR \\ & \quad (\text{Eq. J6.2-11})\end{aligned}$$

and

$$\begin{aligned}p_A[D < D_{EW}(\tau|\mathbf{a}, \mathbf{e}_{Mi})|\mathbf{e}_{Ai}] &\cong p_A(\mathcal{A}_{EW}|\mathbf{e}_{Ai}) \sum_{k=1}^{nR} \bar{\delta}_D[D_{EW}(\tau|\mathbf{a}_{EW,k}, \mathbf{e}_{Mi})]/nR \\ &= p_A(\mathcal{A}_{EW}|\mathbf{e}_{Ai}) \sum_{k=1}^{nR} \bar{\delta}_D \left\{ \sum_{j=1}^{nEW_k} D_{EW}(\tau|[1, t_{jk}, b_{jk}, d_{jk}], \mathbf{e}_{Mi}) \right\} / nR, \\ & \quad (\text{Eq. J6.2-12})\end{aligned}$$

as indicated in Equations J4.5-19 – J4.5-21 with $C = EW$, where (i)

$$\mathbf{a}_{EW,k} = [nEW_k, \mathbf{a}_{EW,1k}, \mathbf{a}_{EW,2k}, \dots, \mathbf{a}_{EW,nEW_k,k}], k = 1, 2, \dots, nR,$$

is a random sample from vectors \mathbf{a}_{EW} of the form defined in Equation J6.1-12 generated in consistency with fWT_r , pWT_r , fBN_{rs} and $fDRP_{rs}$ and the assumption that nEW is greater than zero, (ii)

$$\mathbf{a}_{EW,jk} = [t_{jk}, b_{jk}, d_{jk}]$$

for $j = 1, 2, \dots, nEW_k$, and (iii) the indicator functions $\bar{\delta}_D(\sim)$ and $\underline{\delta}_D(\sim)$ are defined in Equations J4.2-3 and (J4.2-7), respectively.

As an example, Figure J6.2-9a shows the CCDF for the dose $D_{EW}(10^4 \text{ yr}|\mathbf{a}_{EW}, \mathbf{e}_{M1})$ to the RMEI at $\tau = 10^4 \text{ yr}$ obtained with LHS element \mathbf{e}_1 . Specifically, the CCDF in Figure J6.2-9a is a plot of the exceedance probabilities $p_A[D < D_{EW}(10^4 \text{ yr}|\mathbf{a}, \mathbf{e}_{M1})|\mathbf{e}_{A1}]$ defined in Equation J6.2-12 and obtained with a random sample of size $nR = 10^4$ from \mathcal{A}_{EW} . In turn, the sampled results used in the construction of the CCDF in Figure J6.2-9a can be reduced to an estimate for the expected

dose $\bar{D}_{EW}(10^4 \text{ yr}|\mathbf{e}_1)$ as indicated in Equation J6.2-10 and illustrated in Figure J6.2-9b. Specifically, Figure J6.2-9b shows the expected dose curve $\bar{D}_{EW}(\tau|\mathbf{e}_1)$, $0 \leq \tau \leq 20,000 \text{ yr}$, previously presented in Figure J6.2-4 and the value $\bar{D}_{EW}(10^4 \text{ yr}|\mathbf{e}_1)$ calculated with the indicated Monte Carlo procedure. As can be seen, the value for $\bar{D}_{EW}(\tau|\mathbf{e}_1)$ produced by the Monte Carlo procedure is effectively the same as the value for $\bar{D}_{EW}(\tau|\mathbf{e}_1)$ produced by integration procedures. As a result, repeating the Monte Carlo estimation procedure for a sequence of values for τ would result in an estimate for $\bar{D}_{EW}(\tau|\mathbf{e}_1)$ for $0 \leq \tau \leq 20,000 \text{ yr}$ that is effectively the same as the estimate that appears in Figures J6.2-4 and J6.2-9b. The integration-based approach to estimate $\bar{D}_{EW}(\tau|\mathbf{e})$ has the advantage of numerical efficiency but does not provide estimates of CCDFs of the form shown in Figure J6.2-9a. In contrast, the sampling-based approach $\bar{D}_{EW}(\tau|\mathbf{e})$ is less efficient numerically but provides CCDFs that summarize the effects of aleatory uncertainty.

The CCDF in Figure J6.2-9a is for a single LHS element. As shown in Figure J6.2-10a,b, a different CCDF results for $D_{EW}(10^4 \text{ yr}|\mathbf{a}_{EW}, \mathbf{e}_{Mi})$ for each LHS element $\mathbf{e}_i = [\mathbf{e}_{Ai}, \mathbf{e}_{Mi}]$. Collectively, these CCDFs are displaying the epistemic uncertainty associated with the distribution of dose $D_{EW}(10^4 \text{ yr}|\mathbf{a}_{EW}, \mathbf{e}_{Mi})$ to the RMEI at $\tau = 10^4 \text{ yr}$ that results from the different possible values for \mathbf{a}_{EW} . In turn, the epistemic uncertainty associated with these CCDFs can be summarized by an expected (mean) CCDF and quantile curves constructed in a manner analogous to the construction of expected (mean) and quantile curves for expected dose $\bar{D}_{EW}(\tau|\mathbf{e})$ (Figure J6.2-10c). The expected (mean) dose $\bar{\bar{D}}_{EW}(10^4 \text{ yr})$ appearing in Figures J6.2-5, J6.2-6 and J6.2-8 is the result of reducing all the information in Figure J6.2-10a to single number (i.e., $\bar{\bar{D}}_{EW}(10^4 \text{ yr})$).

As discussed in Section J4.10, the numerical stability of results obtained with Latin hypercube sampling can be assessed with replicated sampling. Specifically, the analysis for early WP failure was performed with the $n_{RL} = 3$ replicated LHSs indicated in Equation J4.10-1. In turn, this analysis shows that the numerical error in using Latin hypercube sampling to estimate $\bar{\bar{D}}_{EW}(\tau)$ is small relative to the epistemic uncertainty associated with the possible values for $\bar{\bar{D}}_{EW}(\tau|\mathbf{e})$ (Figure J6.2-11).

The results presented in Figures J6.2-2 to J6.2-11 are for the time period $[0, 2.0 \times 10^4 \text{ yr}]$. Corresponding results for the time period $[0, 10^6 \text{ yr}]$ are presented without discussion in Figures J6.2-12 to J6.2-21.

J6.3 Early DS Failure Scenario Class: \mathcal{A}_{ED}

The analyses for the early DS failure scenario class \mathcal{A}_{ED} are structurally identical to the analyses for the early WP failure scenario class \mathcal{A}_{EW} . The individual elements $\mathbf{a}_{ED,j}, j = 1, 2, \dots, n_{ED}$, appearing in the definition of \mathbf{a}_{ED} in Equation J6.1-13 are defined by

$$\mathbf{a}_{ED,j} = [t_j, b_j, d_j] \quad (\text{Eq. J6.3-1})$$

and characterize the properties of failed DS j , where t_j designates WP type (i.e., $t_j = 1 \sim$ CSNF WP, $t_j = 2 \sim$ CDSP WP) underneath the failed DS, b_j designates the percolation bin in which the failed DS is located (e.g., $b_j = k \sim$ location of failed DS in bin k for $k = 1, 2, 3, 4, 5$), and d_j designates whether the failed DS experiences nondripping or dripping conditions (i.e., $d_j = 0 \sim$ nondripping conditions and $d_j = 1 \sim$ dripping conditions).

The quantities nWP , nWT , fWT_r , nBN , fBN_{rs} and $fDRP_{rst}$ are the same as in Section J6.2 and the additional quantity

pD = probability that a randomly selected DS will experience an early failure (element of \mathbf{e}_A)

characterizes the occurrence of early DS failure and is analogous to pWT_r . Specifically, early DS failure is assumed to be characterized by a binomial probability model defined by pD (see Equations J3.6-22 to J3.6-25). A different value for pD is selected in each LHS element $\mathbf{e}_i = [\mathbf{e}_{Ai}, \mathbf{e}_{Mi}]$ indicated in Equation J4.9-1. In turn, this results in $nLHS = 300$ CCDFs for the possible number of early DS failures (Figure J6.3-1).

For a given LHS element $\mathbf{e}_i = [\mathbf{e}_{Ai}, \mathbf{e}_{Mi}]$ of the form defined in Equation J4.9-1, the expected dose $\bar{D}_{ED}(\tau|\mathbf{e}_i)$ from early DS failure is given by

$$\begin{aligned} \bar{D}_{ED}(\tau|\mathbf{e}_i) &= \int_{\mathcal{A}_{ED}} D_{ED}(\tau|\mathbf{a}, \mathbf{e}_{Mi}) d_A(\mathbf{a}|\mathbf{e}_{Ai}) dA \\ &= \sum_{r=1}^{nWT} \sum_{s=1}^{nBN} \sum_{t=0}^1 pD_i fWT_r fBN_{rs} pDRP_{rsti} nWP D_{ED}(\tau|[1, r, s, t], \mathbf{e}_{Mi}) \\ &= \sum_{r=1}^2 \sum_{s=1}^5 \sum_{t=1}^1 pD_i fWT_r fBN_{rs} pDRP_{rsti} nWP D_{ED}(\tau|[1, r, s, t], \mathbf{e}_{Mi}) \\ &= \sum_{r=1}^2 \sum_{s=1}^5 pD_i fWT_r fBN_{rs} pDRP_{rs1i} nWP D_{ED}(\tau|[1, r, s, 1], \mathbf{e}_{Mi}) \quad (\text{Eq. J6.3-2}) \end{aligned}$$

where (i) $pDRP_{rsti}$ is defined in conjunction with Equation J6.2-2, (ii) the third equality results when $nWT = 2$ WP types (i.e., CSNFs and CDSPs) and $nBN = 5$ percolation bins are under consideration, which corresponds to the values for nWT and nBN in the TSPA-LA, and (iii) the fourth and final equality results because releases are only assumed to take place if the DS fails in the presence of dripping conditions, in which case the associated WP is assumed to fail due to localized corrosion.

The determination of $\bar{D}_{ED}(\tau|\mathbf{e}_i)$ as indicated in Equation J6.3-2 requires the evaluation of

$$D_{ED}(\tau|[1, r, s, t], \mathbf{e}_{Mi}) \quad (\text{Eq. J6.3-3})$$

in GoldSim for selected values of τ , $r = 1, 2, \dots, nWT$, $s = 1, 2, \dots, nBN$, $t = 1$, and \mathbf{e}_{Mi} , $i = 1, 2, \dots, nLHS$. The fractions $fDRP_{rsti}$ are also determined in GoldSim and are functions of \mathbf{e}_{Mi} .

Similarly to the analysis for early WP failure, the results indicated in conjunction with Equation J6.3-3 were calculated twice, once for the time interval $[0, 2.0 \times 10^4 \text{ yr}]$ and once for the time interval $[0, 10^6 \text{ yr}]$. Owing to its shorter length, results for the 20,000 yr time interval were computed with use of shorter timesteps (i.e., more closely spaced values for τ) than used to compute results for the 10^6 yr time interval. Specifically, timesteps of 10, 40 and 80 yr were used for the 20,000 yr time interval, and timesteps of 250, 500, 1000, 2000 and 4000 yr were used for the 10^6 time interval.

Once the results in Equation J6.3-3 are available, $\bar{D}_{ED}(\tau|\mathbf{e}_i)$ can be determined as indicated in Equation J6.3-2. Further, additional results involving early DS failure can be determined in the same manner as corresponding results for early WP failure were determined in Section J6.2. For example $\bar{D}_{ED}(\tau)$, $P_E[\bar{D}_{ED}(\tau|\mathbf{e}_i) \leq D]$, $P_E[D < \bar{D}_{ED}(\tau|\mathbf{e})]$ and $Q_q[\bar{D}_{ED}(\tau|\mathbf{e})]$ can be determined in the same manner as $\bar{D}_{EW}(\tau)$, $P_E[\bar{D}_{EW}(\tau|\mathbf{e}) \leq D]$, $P_E[D < \bar{D}_{EW}(\tau|\mathbf{e})]$ and $Q_q[\bar{D}_{EW}(\tau|\mathbf{e})]$ in Equations J6.2-3 – J6.2-7.

For consistency, similar results are presented for early DS failure and early WP failure. Specifically, early DS failure results for $0 \leq \tau \leq 20,000 \text{ yr}$ are presented in Figures J6.3-2 to J6.3-11 and contain results analogous to the results presented in Figures J6.2-2 to J6.2-11 for early WP failure. Similarly, early DS failure results for $0 \leq \tau \leq 10^6 \text{ yr}$ are presented in Figures J6.3-12 to J6.3-21 and contain results analogous to the results presented in Figures J6.2-12 to J6.2-21 for early WP failure.

J6.4 Early Failure Scenario Class: \mathcal{A}_E

As indicated in Equation J6.1-9, the expected dose $\bar{D}_E(\tau|\mathbf{e})$ to the RMEI at time τ from early failures is given by the sum of the expected doses $\bar{D}_{EW}(\tau|\mathbf{e})$ and $\bar{D}_{ED}(\tau|\mathbf{e})$ from early WP failures and early DS failures. The result of this calculation is presented in Figures J6.4-1 and J6.4-2 for the 20,000 and 10^6 yr time intervals, respectively. The organization of Figures J6.4-1 and J6.4-2 is the same as the organization of Figure J6.2-5.

The expected dose resulting from nominal process failures and early failures of WPs and DSs is given by

$$\bar{D}_{NE}(\tau|\mathbf{e}) = D_N(\tau|\mathbf{a}_N, \mathbf{e}_M) + \bar{D}_{EW}(\tau|\mathbf{e}_M) + \bar{D}_{ED}(\tau|\mathbf{e}_M). \quad (\text{Eq. J6.4-1})$$

The result of this calculation is presented in Figure J6.4-3, which also has the same organization as Figure J6.2-5.

J6.5 Probabilities Associated with Early Failure Scenario Classes

The probabilities $p_A(\mathcal{A}_{EW}|\mathbf{e}_A)$, $p_A(\mathcal{A}_{ED}|\mathbf{e}_A)$ and $p_A(\mathcal{A}_E|\mathbf{e}_A)$ for the scenario classes \mathcal{A}_{EW} , \mathcal{A}_{ED} and \mathcal{A}_E conditional on the element $\mathbf{e} = [\mathbf{e}_A, \mathbf{e}_M]$ of \mathcal{E} are given by

$$p_A(\mathcal{A}_{EW}|\mathbf{e}_A) \cong 1 - \exp[-(nWP)(pW)], \quad (\text{Eq. J6.5-1})$$

$$p_A(\mathcal{A}_{ED}|\mathbf{e}_A) \cong 1 - \exp[-(nDS)(pD)] \quad (\text{Eq. J6.5-2})$$

and

$$\begin{aligned} p_A(\mathcal{A}_E|\mathbf{e}_A) &\cong 1 - \exp[-(nWP)(pW) - (nDS)(pD)] \\ &= 1 - \exp[-nWP(pW + pD)], \end{aligned} \quad (\text{Eq. J6.5-3})$$

where $nWP = 11,629$ is the number of WPs in the repository, $nDS = nWP$ is the number of DSs (i.e., one DS for each WP), pW is the element of \mathbf{e}_A that corresponds to the probability that an individual WP will experience an early failure, pD is the element of \mathbf{e}_A that corresponds to the probability that an individual DS will experience an early failure, and the approximations in Equations J6.5-1, J6.5-2, and J6.5-3 follow from Equation J3.6-29. The values for $p_A(\mathcal{A}_{EW}|\mathbf{e}_{Ai})$, $p_A(\mathcal{A}_{ED}|\mathbf{e}_{Ai})$ and $p_A(\mathcal{A}_E|\mathbf{e}_{Ai})$ obtained for the LHS in Equation J4.9-1 are summarized in Figure J6.5-1.

J7 IGNEOUS SCENARIO CLASSES: \mathcal{A}_I , \mathcal{A}_{II} AND \mathcal{A}_{IE}

J7.1 Relationships Involving \mathcal{A}_I , \mathcal{A}_{II} and \mathcal{A}_{IE}

The igneous intrusive scenario class and the igneous eruptive scenario class are defined by the sets

$$\mathcal{A}_{II} = \{\mathbf{a} : \mathbf{a} \in \mathcal{A} \text{ and } nII \geq 1\} \quad (\text{Eq. J7.1-1})$$

and

$$\mathcal{A}_{IE} = \{\mathbf{a} : \mathbf{a} \in \mathcal{A} \text{ and } nIE \geq 1\} \quad (\text{Eq. J7.1-2})$$

as indicated in Equations J4.4-15 and J4.4-16. Further, the igneous scenario class \mathcal{A}_I is defined by

$$\mathcal{A}_I = \mathcal{A}_{II} \cup \mathcal{A}_{IE} = \{\mathbf{a} : \mathbf{a} \in \mathcal{A} \text{ and } nII \geq 1\} = \mathcal{A}_{II} \quad (\text{Eq. J7.1-3})$$

as indicated in Equation J4.4-11. The equality $\mathcal{A}_I = \mathcal{A}_{II}$ results because the occurrence of an igneous intrusive event is a necessary, but not sufficient, condition for the occurrence of an

igneous eruptive event in the TSPA-LA. In turn, $p_A(\mathcal{A}_I) = p_A(\mathcal{A}_{II})$ is the probability of one or more igneous intrusive events and $p_A(\mathcal{A}_{IE})$ is the probability of one or more igneous eruptive events.

The scenario classes \mathcal{A}_{II} and \mathcal{A}_{IE} are not disjoint. However, if the question is asked “What is the probability of an igneous event?” or “What is the probability of an igneous intrusive event?”, then most likely $p_A(\mathcal{A}_{II}) = p_A(\mathcal{A}_I)$ is the desired answer. Similarly, if the question is asked “What is the probability of an igneous eruptive event?”, then most likely $p_A(\mathcal{A}_{IE})$ is the desired answer. If desired, disjoint scenario classes involving igneous intrusive and igneous eruptive scenario classes and their associated probabilities can be defined in the same manner as indicated in Equations J6.1-4 – J6.1-7 for early WP failure and early DS failure. Although possible, such definitions are not very useful computationally.

No synergisms are assumed to exist between the doses that result from the intrusive damage to WPs and the doses that result from the eruptive releases to the atmosphere. Further, as indicated in conjunction with Equation J4.5-1, no synergisms are assumed to exist between doses that result from igneous events and doses that result from other disruptions. As a result,

$$D_I(\tau|\mathbf{a}, \mathbf{e}_M) = D_{II}(\tau|\mathbf{a}, \mathbf{e}_M) + D_{IE}(\tau|\mathbf{a}, \mathbf{e}_M), \quad (\text{Eq. J7.1-4})$$

where

$D_I(\tau|\mathbf{a}, \mathbf{e}_M)$ = dose to RMEI (mrem/yr) at time τ resulting from igneous events associated with element \mathbf{a} of \mathcal{A} ,

$D_{II}(\tau|\mathbf{a}, \mathbf{e}_M)$ = dose to RMEI (mrem/yr) at time τ resulting from intrusive damage to WPs for igneous events associated with element \mathbf{a} of \mathcal{A} ,

$D_{IE}(\tau|\mathbf{a}, \mathbf{e}_M)$ = dose to RMEI (mrem/yr) at time τ resulting from the eruptive releases to the atmosphere for igneous events associated with element \mathbf{a} of \mathcal{A} ,

and all results are conditional on the element $\mathbf{e} = [\mathbf{e}_A, \mathbf{e}_M]$ of \mathcal{E} . If \mathbf{a} involves no igneous intrusive damage to WPs, then $D_{II}(\tau|\mathbf{a}, \mathbf{e}_M) = 0$; similarly, if \mathbf{a} involves no eruptive releases to the atmosphere, then $D_{IE}(\tau|\mathbf{a}, \mathbf{e}_M) = 0$.

In turn, the expected dose $\bar{D}_I(\tau|\mathbf{e})$ to the RMEI (mrem/yr) at time τ is given by

$$\begin{aligned} \bar{D}_I(\tau|\mathbf{e}) &= \int_{\mathcal{A}_I} D_I(\tau|\mathbf{a}, \mathbf{e}_M) d_A(\mathbf{a}|\mathbf{e}_A) dA \\ &= \int_{\mathcal{A}_I} [D_{II}(\tau|\mathbf{a}, \mathbf{e}_M) + D_{IE}(\tau|\mathbf{a}, \mathbf{e}_M)] d_A(\mathbf{a}|\mathbf{e}_A) dA \\ &= \int_{\mathcal{A}_I} D_{II}(\tau|\mathbf{a}, \mathbf{e}_M) d_A(\mathbf{a}|\mathbf{e}_A) dA + \int_{\mathcal{A}_I} D_{IE}(\tau|\mathbf{a}, \mathbf{e}_M) d_A(\mathbf{a}|\mathbf{e}_A) dA \\ &= \bar{D}_{II}(\tau|\mathbf{e}) + \bar{D}_{IE}(\tau|\mathbf{e}), \end{aligned} \quad (\text{Eq. J7.1-5})$$

where (i)

$$\begin{aligned}\bar{D}_{II}(\tau|\mathbf{e}) &= \int_{\mathcal{A}_I} D_{II}(\tau|\mathbf{a}, \mathbf{e}_M) d_A(\mathbf{a}|\mathbf{e}_A) dA \\ &= \int_{\mathcal{A}_{II}} D_{II}(\tau|\mathbf{a}, \mathbf{e}_M) d_A(\mathbf{a}|\mathbf{e}_A) dA\end{aligned}\quad (\text{Eq. J7.1-6})$$

is the expected dose to the RMEI (mrem/yr) at time τ resulting from igneous intrusive events, (ii)

$$\begin{aligned}\bar{D}_{IE}(\tau|\mathbf{e}) &= \int_{\mathcal{A}_I} D_{IE}(\tau|\mathbf{a}, \mathbf{e}_M) d_A(\mathbf{a}|\mathbf{e}_A) dA \\ &= \int_{\mathcal{A}_{IE}} D_{IE}(\tau|\mathbf{a}, \mathbf{e}_M) d_A(\mathbf{a}|\mathbf{e}_A) dA\end{aligned}\quad (\text{Eq. J7.1-7})$$

is the expected dose to the RMEI (mrem/yr) at time τ resulting from igneous eruptive events, and (iii) all results are conditional on the element $\mathbf{e} = [\mathbf{e}_A, \mathbf{e}_M]$ of \mathcal{E} . The conversion from an integral over \mathcal{A}_I to an integral over \mathcal{A}_{II} in Equation J7.1-6 is only notational as $\mathcal{A}_I = \mathcal{A}_{II}$; the conversion from an integral over \mathcal{A}_I to an integral over \mathcal{A}_{IE} in Equation J7.1-7 is possible because $D_{IE}(\tau|\mathbf{a}, \mathbf{e}_M) = 0$ if $\mathbf{a} \notin \mathcal{A}_{IE}$.

The general form of the elements \mathbf{a} of \mathcal{A} is shown in Equations J4.4-1 – J4.4-8. However, because no synergisms between disruptions are assumed in the determination of $\bar{D}_{II}(\tau|\mathbf{e})$ and $\bar{D}_{IE}(\tau|\mathbf{e})$, the representations for the elements of \mathcal{A}_{II} and \mathcal{A}_{IE} can be simplified to

$$\mathbf{a}_{II} = [n_{II}, \mathbf{a}_{II,1}, \mathbf{a}_{II,2}, \dots, \mathbf{a}_{II,n_{II}}] \quad (\text{Eq. J7.1-8})$$

and

$$\mathbf{a}_{IE} = [n_{IE}, \mathbf{a}_{IE,1}, \mathbf{a}_{IE,2}, \dots, \mathbf{a}_{IE,n_{IE}}], \quad (\text{Eq. J7.1-9})$$

respectively. With this notation, the elements \mathbf{a}_{II} of \mathcal{A}_{II} only contain representations for igneous intrusive events, and the elements \mathbf{a}_{IE} of \mathcal{A}_{IE} only contain representations for igneous eruptive events.

The expected (mean) dose $\bar{\bar{D}}_I(\tau)$ for the igneous scenario class \mathcal{A}_I over both aleatory and epistemic uncertainty is given by

$$\begin{aligned}\bar{\bar{D}}_I(\tau) &= \int_{\mathcal{E}} \bar{D}_I(\tau|\mathbf{e}) d_E(\mathbf{e}) dE \\ &= \int_{\mathcal{E}} [\bar{D}_{II}(\tau|\mathbf{e}) + \bar{D}_{IE}(\tau|\mathbf{e})] d_E(\mathbf{e}) dE \\ &= \int_{\mathcal{E}} \bar{D}_{II}(\tau|\mathbf{e}) d_E(\mathbf{e}) dE + \int_{\mathcal{E}} \bar{D}_{IE}(\tau|\mathbf{e}) d_E(\mathbf{e}) dE \\ &= \bar{\bar{D}}_{II}(\tau) + \bar{\bar{D}}_{IE}(\tau),\end{aligned}\quad (\text{Eq. J7.1-10})$$

where

$$\bar{\bar{D}}_{II}(\tau) = \int_{\mathcal{E}} \bar{D}_{II}(\tau|\mathbf{e}) d_E(\mathbf{e}) dE \quad (\text{Eq. J7.1-11})$$

is the expected (mean) dose for the igneous intrusive scenario class \mathcal{A}_{II} over both aleatory and epistemic uncertainty and

$$\bar{\bar{D}}_{IE}(\tau) = \int_{\mathcal{E}} \bar{D}_{IE}(\tau|\mathbf{e}) d_E(\mathbf{e}) dE \quad (\text{Eq. J7.1-12})$$

is the expected (mean) dose for the igneous eruptive scenario class \mathcal{A}_{IE} over both aleatory and epistemic uncertainty.

The CCDF and CDF for $\bar{D}_I(\tau|\mathbf{e})$ over epistemic uncertainty are defined by

$$\begin{aligned} p_E[D < \bar{D}_I(\tau|\mathbf{e})] &= \int_{\mathcal{E}} \bar{\delta}_D[\bar{D}_I(\tau|\mathbf{e})] d_E(\mathbf{e}) dE \\ &= \int_{\mathcal{E}} \bar{\delta}_D[\bar{D}_{II}(\tau|\mathbf{e}) + \bar{D}_{IE}(\tau|\mathbf{e})] d_E(\mathbf{e}) dE \end{aligned} \quad (\text{Eq. J7.1-13})$$

and

$$\begin{aligned} p_E[\bar{D}_I(\tau|\mathbf{e}) < D] &= 1 - p_E[\bar{D}_I(\tau|\mathbf{e})] \\ &= \int_{\mathcal{E}} \underline{\delta}_D[\bar{D}_I(\tau|\mathbf{e})] d_E(\mathbf{e}) dE \\ &= \int_{\mathcal{E}} \underline{\delta}_D[\bar{D}_{II}(\tau|\mathbf{e}) + \bar{D}_{IE}(\tau|\mathbf{e})] d_E(\mathbf{e}) dE, \end{aligned} \quad (\text{Eq. J7.1-14})$$

respectively. However, unlike the result for $\bar{\bar{D}}_I(\tau)$ in Equation J7.1-10, the CCDF and CDF for $\bar{D}_I(\tau|\mathbf{e})$ cannot be decomposed into a sum of separate results for the igneous intrusive scenario class \mathcal{A}_{II} and the igneous eruptive scenario class \mathcal{A}_{IE} .

Direct evaluation of the integrals that define $\bar{\bar{D}}_I(\tau)$, $p_E[D < \bar{D}_I(\tau|\mathbf{e})]$ and $p_E[\bar{D}_I(\tau|\mathbf{e}) \leq D]$ is not practicable. However, the approximations

$$\bar{\bar{D}}_I(\tau) \cong \sum_{i=1}^{nLHS} \bar{D}_I(\tau|\mathbf{e}_i) / nLHS, \quad (\text{Eq. J7.1-15})$$

$$p_E[D < \bar{D}_I(\tau|\mathbf{e})] \cong \sum_{i=1}^{nLHS} \bar{\delta}_D[\bar{D}_I(\tau|\mathbf{e}_i)] / nLHS \quad (\text{Eq. J7.1-16})$$

and

$$p_E \left[\bar{D}_I(\tau|\mathbf{e}) \leq D \right] \cong \sum_{i=1}^{nLHS} \delta_D \left[\bar{D}_I(\tau|\mathbf{e}_i) \right] / nLHS \quad (\text{Eq. J7.1-17})$$

result with use of the LHS in Equation J4.9-1 as previously indicated in conjunction with Equations J4.9-8 – J4.9-10.

Further descriptions of the igneous scenario classes \mathcal{A}_I , \mathcal{A}_{II} and \mathcal{A}_{IE} and sources of additional information are available in Section 6.5.

J7.2 Igneous Intrusive Scenario Class: \mathcal{A}_{II}

The aleatory futures \mathbf{a} associated with the igneous intrusive scenario class \mathcal{A}_{II} are defined by number of igneous intrusive events, the times of these events, and the number of WPs damaged by each of these events. Specifically, the individual vectors $\mathbf{a}_{II,j}$, $j = 1, 2, \dots, nII$, appearing in the definition of \mathbf{a}_{II} in Equation J7.1-8 are defined by

$$\mathbf{a}_{II,j} = [t_j, nWD_j] \quad (\text{Eq. J7.2-1})$$

and characterize the properties of igneous intrusive event j , where t_j (yr) is the time of the event and nWD_j is the number of WPs damaged by the event.

Two quantities define the probabilities associated with \mathcal{A}_{II} :

λ_I = rate of occurrence (yr^{-1}) of igneous events that intersect the repository (element of \mathbf{e}_A),

$d_{II}(N)$ = density function for number N of WPs damaged by an igneous intrusive event (i.e., $N \sim nWD_j$ in Equation J7.2-1).

Specifically, the occurrence of igneous events that intersect the repository is assumed to follow a Poisson process defined by the rate λ_I . The TSPA-LA assumes that an igneous event that intersects the repository damages all nWP WPs in the repository. For this special situation, $d_{II}(N)$ is defined by

$$d_{II}(N) = \delta(N - nWP), \quad (\text{Eq. J7.2-2})$$

where $\delta(\sim)$ is the Dirac delta function. However, the general representation $d_{II}(N)$ for the density function for the number of damaged WPs will be used in the initial description of expected dose for the igneous intrusive scenario class \mathcal{A}_{II} for notational generality.

Given λ_I , $d_{II}(N)$ and an LHS element $\mathbf{e}_i = [\mathbf{e}_{Ai}, \mathbf{e}_{Mi}]$ of the form defined in Equation J4.9-1, the expected dose $\bar{D}_{II}(\tau|\mathbf{e}_i)$ is given by

$$\begin{aligned}\bar{D}_{II}(\tau|\mathbf{e}_i) &= \int_{\mathcal{A}_{II}} D_{II}(\tau|\mathbf{a}, \mathbf{e}_{Mi}) d_A(\mathbf{a}|\mathbf{e}_{Ai}) dA \\ &= \int_0^\tau \left[\int_{\mathcal{N}_{II}} D_{II}(\tau|[1, t, N], \mathbf{e}_{Mi}) d_{II}(N) dN \right] \lambda_I dt, \quad (\text{Eq. J7.2-3})\end{aligned}$$

where

\mathcal{N}_{II} = set of possible values for number N of damaged WPs consistent with the definition of $d_{II}(N)$,

$D_{II}(\tau|[1, t, N], \mathbf{e}_{Mi})$ = dose to RMEI (mrem/yr) at time τ from a single igneous intrusive event that occurs at time t and damages N WPs.

The second integral in Equation J7.2-3 is predicated on the assumption that there are no synergisms between multiple igneous events associated with a given element \mathbf{a} of \mathcal{A}_{II} , which is equivalent to the assumption that each event affects a different group of WPs. In practice, this is satisfied because the probability of the subset of \mathcal{A}_{II} containing values of \mathbf{a} with two or more igneous events (i.e., $nI \geq 2$) is small. However, because the TSPA-LA assumes that the first igneous event affects all WPs in the repository, Equation J7.2-3 produces a slight overestimate of $\bar{D}_{II}(\tau|\mathbf{e}_i)$.

The second integral in Equation J7.2-3 is based on the approximation

$$\bar{D}_{II}(\tau|\mathbf{e}_i) \cong \sum_{k=1}^n \left[\int_{\mathcal{N}_{II}} D_{II}(\tau|[1, t_k, N], \mathbf{e}_{Mi}) d_{II}(N) dN \right] \lambda_I \Delta t_k, \quad (\text{Eq. J7.2-4})$$

where $0 = t_0 < t_1 < t_2 < \dots < t_n = \tau$. The representation for $\bar{D}_{II}(\tau|\mathbf{e}_i)$ in the second integral in Equation J7.2-3 then results in the limit as $\Delta t_k \rightarrow 0$. Intuitively, $\lambda_I \Delta t_k$ can be thought of as the probability that an igneous event occurs in the time interval $[t_{k-1}, t_k]$. However, $\lambda_I \Delta t_k$ is actually the expected number of igneous events in the time interval $[t_{k-1}, t_k]$. As a result, the second integral representation for $\bar{D}_{II}(\tau|\mathbf{e}_i)$ includes the effects of multiple igneous events. However, as previously indicated, there is an underlying assumption that there are no synergisms between multiple events in a given element \mathbf{a} of \mathcal{A}_{II} .

If it is desired to incorporate the effects of only the first igneous event in the time interval $[0, \tau]$ into $\bar{D}_{II}(\tau|\mathbf{e}_i)$, then the final representation in Equation J7.2-3 becomes

$$\bar{D}_{II}(\tau|\mathbf{e}_i) = \int_0^\tau \left[\int_{\mathcal{N}_{II}} D_{II}(\tau|[1, t, N], \mathbf{e}_{Mi}) d_{II}(N) dN \right] \lambda_I \exp[-\lambda_I t] dt. \quad (\text{Eq. J7.2-5})$$

The preceding representation for $\bar{D}_{II}(\tau|\mathbf{e}_i)$ derives from the approximation

$$\bar{D}_{II}(\tau|\mathbf{e}_i) \cong \sum_{k=1}^n \left\{ \int_{\mathcal{N}_{II}} D_{II}(\tau|[1, t_k, N], \mathbf{e}_{Mi}) d_{II}(N) dN \right\} \times \left\{ \left[\exp(-\lambda_I t_{k-1}) \right]_1 \left[\lambda_I \Delta t_k \exp(-\lambda_I \Delta t_k) \right]_2 \right\}, \quad (\text{Eq. J7.2-6})$$

where

$[\sim]_1$ = probability that no igneous event occurs before time t_{k-1} ,

$[\sim]_2$ = probability that exactly one igneous event occurs in the time interval Δt_k ,

$[\sim]_1[\sim]_2$ = probability that first igneous event occurs in the time interval Δt_k ,

and the t_k are defined the same as in Equation J7.2-4. The representation for $\bar{D}_{II}(\tau|\mathbf{e}_i)$ in Equation J7.2-5 then results in the limit as $\Delta t_k \rightarrow 0$.

When $d_{II}(N)$ has the simple form indicated in Equation J7.2-2 and used in the TSPA-LA, the representations for $\bar{D}_{II}(\tau|\mathbf{e}_i)$ in Equations J7.2-3 and J7.2-5 become

$$\bar{D}_{II}(\tau|\mathbf{e}_i) = \int_0^\tau D_{II}(\tau|[1, t, nWP], \mathbf{e}_{Mi}) \lambda_I dt \quad (\text{Eq. J7.2-7})$$

and

$$\bar{D}_{II}(\tau|\mathbf{e}_i) = \int_0^\tau D_{II}(\tau|[1, t, nWP], \mathbf{e}_{Mi}) \lambda_I \exp(-\lambda_I t) dt, \quad (\text{Eq. J7.2-8})$$

respectively. The representation for $\bar{D}_{II}(\tau|\mathbf{e}_i)$ in Equation J7.2-7 actually overestimates the expected value over aleatory uncertainty for $D_{II}(\tau|[1, t, nWP], \mathbf{e}_{Mi})$ because it incorporates the effects of multiple events that destroy all WPs in the repository. This overcounting of damaged WPs is corrected for in the representation for $\bar{D}_{II}(\tau|\mathbf{e}_i)$ in Equation J7.2-8. However, if the product $\lambda_I \tau$ is small, there is little difference in the values for the integrals in Equations J7.2-7 and J7.2-8. In turn, the corresponding quadrature approximations for $\bar{D}_{II}(\tau|\mathbf{e}_i)$ as defined in Equations J7.2-7 and J7.2-8 are

$$\bar{D}_{II}(\tau|\mathbf{e}_i) \cong \sum_{k=1}^n D_{II}(\tau|[1, \hat{t}_k, nWP], \mathbf{e}_{Mi}) \lambda_I \Delta \hat{t}_k \quad (\text{Eq. J7.2-9})$$

and

$$\bar{D}_{II}(\tau|\mathbf{e}_i) \cong \sum_{k=1}^n D_{II}(\tau|[1, \hat{t}_k, nWP], \mathbf{e}_{Mi}) \lambda_I \exp(-\lambda_I \hat{t}_{k-1}) \Delta \hat{t}_k, \quad (\text{Eq. J7.2-10})$$

respectively, where $0 = \hat{t}_0 < \hat{t}_1 < \dots < \hat{t}_n = \tau$.

In situations where the dose $D_{II}(\tau|[1, t, N], \mathbf{e}_{Mi})$ varies linearly with N , a significant simplification to the representations for $\bar{D}_{II}(\tau|\mathbf{e}_i)$ in Equations J7.2-3 and J7.2-5 is possible. Specifically, the representation for $\bar{D}_{II}(\tau|\mathbf{e}_i)$ in Equation J7.2-3 becomes

$$\begin{aligned}\bar{D}_{II}(\tau|\mathbf{e}_i) &= \int_0^\tau \left[\int_{\mathcal{N}_{II}} D_{II}(\tau|[1, t, N], \mathbf{e}_{Mi}) d_{II}(N) dN \right] \lambda_I dt \\ &= \int_0^\tau \left[\int_{\mathcal{N}_{II}} (N/N_0) D_{II}(\tau|[1, t, N_0], \mathbf{e}_{Mi}) d_{II}(N) dN \right] \lambda_I dt \\ &= (\lambda_I \bar{N}/N_0) \int_0^\tau D_{II}(\tau|[1, t, N_0], \mathbf{e}_{Mi}) dt, \quad (\text{Eq. J7.2-11})\end{aligned}$$

where N_0 is an arbitrary value for N and

$$\bar{N}_{II} = \int_{\mathcal{N}_{II}} N d_{II}(N) dN$$

is the expected value for N . Similarly, the representation for $\bar{D}_{II}(\tau|\mathbf{e}_i)$ in Equation J7.2-5 becomes

$$\bar{D}_{II}(\tau|\mathbf{e}_i) = (\lambda_I \bar{N}_{II}/N_0) \int_0^\tau D_{II}(\tau|[1, t, N_0], \mathbf{e}_{Mi}) \exp(-\lambda_I t) dt. \quad (\text{Eq. J7.2-12})$$

When the assumption of linearity in N can be justified, the representations for $\bar{D}_{II}(\tau|\mathbf{e}_i)$ in Equations J7.2-9 and J7.2-10 provide the basis for computational procedures for the approximation of $\bar{D}_{II}(\tau|\mathbf{e}_i)$ that are more efficient than computational procedures based on the representations in Equations J7.2-3 and J7.2-5.

In turn, the estimates for $\bar{D}_{II}(\tau|\mathbf{e}_i)$ can be used to estimate $\bar{\bar{D}}_{II}(\tau)$, $p_E[\bar{D}_{II}(\tau|\mathbf{e}) \leq D]$ and $p_E[D < \bar{D}_{II}(\tau|\mathbf{e})]$. Specifically,

$$\bar{\bar{D}}_{II}(\tau) \cong \sum_{i=1}^{nLHS} \bar{D}_{II}(\tau|\mathbf{e}_i) / nLHS, \quad (\text{Eq. J7.2-13})$$

$$p_E[\bar{D}_{II}(\tau|\mathbf{e}) \leq D] \cong \sum_{i=1}^{nLHS} \delta_D[\bar{D}_{II}(\tau|\mathbf{e}_i)] / nLHS \quad (\text{Eq. J7.2-14})$$

and

$$p_E [D < \bar{D}_{II}(\tau|\mathbf{e})] \cong \sum_{i=1}^{nLHS} \bar{\delta}_D [\bar{D}_{II}(\tau|\mathbf{e}_i)] / nLHS, \quad (\text{Eq. J7.2-15})$$

as indicated in Equations J4.9-8 – J4.9-10, where $\bar{\delta}_D(\sim)$ and $\underline{\delta}_D(\sim)$ are defined in Equations J4.2-3 and J4.2-7, respectively. Further, quantiles $Q_q[\bar{D}_{II}(\tau|\mathbf{e})]$ for $\bar{D}_{II}(\tau|\mathbf{e})$ can be obtained by solving either

$$q = \int_{\mathcal{A}_{II}} \underline{\delta}_D [\bar{D}_{II}(\tau|\mathbf{e})] d_E(\mathbf{e}) dE \quad (\text{Eq. J7.2-16})$$

or

$$1 - q = \int_{\mathcal{A}_{II}} \bar{\delta}_D [\bar{D}_{II}(\tau|\mathbf{e})] d_E(\mathbf{e}) dE \quad (\text{Eq. J7.2-17})$$

for D . In practice, the solution of Equation J7.2-16 or J7.2-17 to determine D , and hence $Q_q[\bar{D}_{II}(\tau|\mathbf{e})]$, is based on the approximating sums in Equations J7.2-14 and J7.2-15.

The TSPA-LA calculates $\bar{D}_{II}(\tau|\mathbf{e}_i)$ on the basis of the representation in Equation J7.2-7. To support this calculation, $D_{II}(\tau|[1, t, nWP], \mathbf{e}_{Mi})$ is evaluated with GoldSim for a selected sequence of times. Two cases are considered in TSPA-LA: events occurring over the time interval $[0, 2.0 \times 10^4 \text{ yr}]$ and events occurring over the time interval $[0, 1.0 \times 10^6 \text{ yr}]$. For the time interval $[0, 2.0 \times 10^4 \text{ yr}]$, the results

$$D_{II}(\tau|[1, t_k, nWP], \mathbf{e}_{Mi}), k = 1, 2, \dots, 10, i = 1, 2, \dots, nLHS = 300, \quad (\text{Eq. J7.2-18})$$

are calculated for (i) $0 \leq \tau \leq 2.0 \times 10^4 \text{ yr}$ and (ii) $t_k = 10, 100, 600, 1000, 2000, 4000, 6000, 10,000, 14,000$ and $18,000 \text{ yr}$. For the time interval $[0, 10^6 \text{ yr}]$, the results indicated in Equation J7.2-18 are calculated for (i) $0 \leq \tau \leq 1.0 \times 10^6 \text{ yr}$ and (ii) $t_k = 250, 600, 1000, 4000, 10,000, 40,000, 100,000, 200,000, 400,000$ and $800,000 \text{ yr}$. The preceding results are then used in numerical integration procedures to evaluate the integral in Equation J2.7-7 over the time intervals $[0, 2.0 \times 10^4 \text{ yr}]$ and $[0, 1.0 \times 10^6 \text{ yr}]$ (see Equation J7.2-9).

Results for the 20,000 yr time interval are presented first; corresponding results for the 10^6 yr time interval are presented at the end of this section. As indicated in conjunction with Equation J2.2-18, the results for 20,000 yr are based on evaluations of $D_{II}(\tau|[1, t_k, nWP], \mathbf{e}_{Mi})$ for ten values of t_k . For illustration, the values obtained for $D_{II}(\tau|[1, t_k, nWP], \mathbf{e}_{Mi})$ are shown in Figure J7.2-1 for $t_k = 10, 600, 2000, 4000, 6000$ and $10,000 \text{ yr}$ and $i = 1, 2, \dots, nLHS = 300$.

The quadrature approximations for $\bar{D}_{II}(\tau|\mathbf{e}_i)$ indicated in Equations J7.2-9 and J7.2-10 are actually of the form

$$\bar{D}_{II}(\tau|\mathbf{e}_i) \cong \sum_{k=1}^n \hat{D}_{II}(\tau|[1, \hat{t}_k, nWP], \mathbf{e}_{Mi}) \lambda_I \Delta \hat{t}_k \quad (\text{Eq. J7.2-19})$$

and

$$\bar{D}_{II}(\tau|\mathbf{e}_i) \cong \sum_{k=1}^n \hat{D}_{II}(\tau|[1, \hat{t}_k, nWP], \mathbf{e}_{Mi}) \lambda_I \exp(-\lambda_I \hat{t}_{k-1}) \Delta \hat{t}_k \quad (\text{Eq. J7.2-20})$$

in the computational implementation of the TSPA-LA, where $\hat{D}_{II}(\tau|[1, \hat{t}_k, nWP], \mathbf{e}_{Mi})$ is an approximation to $D(\tau|[1, \hat{t}_k, nWP], \mathbf{e}_{Mi})$ obtained from interpolations employing the values for $D(\tau|[1, t_k, nWP], \mathbf{e}_{Mi})$ obtained with GoldSim for the 10 values for t_k indicated in conjunction with Equation J7.2-18 (Figure J7.2-2).

Once the dose results indicated in Equation J7.2-18 are available, $\bar{D}_{II}(\tau|\mathbf{e}_i)$ can be approximated with the quadrature procedures indicated in Equations J7.2-19 and J7.2-20, with $\hat{D}_{II}(\tau|[1, \hat{t}_k, nWP], \mathbf{e}_{Mi})$ determined through interpolation as illustrated in Figure J7.2-2. As an example, the resultant estimate $\bar{D}_{II}(\tau|\mathbf{e}_1)$ for LHS element \mathbf{e}_1 is shown in Figure J7.2-3.

A summary of the calculations involving $\bar{D}_{II}(\tau|\mathbf{e})$ for all LHS elements is given in Figure J7.2-4. Specifically, Figure J7.2-4a shows all 300 expected dose curves (i.e., $\bar{D}_{II}(\tau|\mathbf{e}_i)$ for $0 \leq \tau \leq 20,000$ yr and $i = 1, 2, \dots, nLHS = 300$); Figure J7.2-4b shows the first 50 expected dose curves (i.e., $\bar{D}_{II}(\tau|\mathbf{e}_i)$ for $0 \leq \tau \leq 20,000$ yr and $i = 1, 2, \dots, 50$); Figure J7.2-4c shows the CCDF and selected quantiles for expected dose at 10,000 yr (i.e., $p_E[D < \bar{D}_{II}(10^4 \text{ yr}|\mathbf{e})]$ and $Q_q[\bar{D}_{II}(10^4 \text{ yr}|\mathbf{e})]$, $q = 0.05, 0.5, 0.95$, estimated from $\bar{D}_{II}(10^4 \text{ yr}|\mathbf{e}_i)$, $i = 1, 2, \dots, nLHS = 300$); and Figure J7.2-4d shows expected (mean) dose and quantile curves as a function of time (i.e., $\bar{D}_{II}(\tau)$ and $Q_q[\bar{D}_{II}(\tau|\mathbf{e})]$, $q = 0.05, 0.5, 0.95$, estimated from $\bar{D}_{II}(\tau|\mathbf{e}_i)$, $i = 1, 2, \dots, nLHS = 300$, for $0 \leq \tau \leq 20,000$ yr).

In turn, the results in Figure J7.2-4 can be summarized in the standard format appearing in Figure J7.2-5. As discussed in conjunction with Figures J5-1 and J6-2, the format in Figure J7.2-4 facilitates the presentation of results for individual scenario classes, and the format in Figure J7.2-5 facilitates the comparison of results across scenario classes.

As previously discussed in conjunction with Equations J5-9 and J6.2-9, dose and expected dose to the RMEI are just two of a large number of results that can be produced and presented in the TSPA-LA. As an example, a summary of the resultant dose calculations for ^{99}Tc is given in Figure J7.2-6, which has exactly the same organization as Figure J7.2-4. Overall, ^{99}Tc is one of the largest contributors to the expected (mean) dose $\bar{D}_{II}(\tau)$ for the 20,000 yr time period.

Results of the form shown in Figure J7.2-6 can be obtained for each radioactive species under consideration. This results in too many results for a complete presentation. As previously done in Figure J5-4 and other similar figures, a compact summary of this large amount of information is provided by presenting the expected (mean) dose $\bar{\bar{E}}_{II,r}(\tau)$ for each radioactive species in a single plot (Figure J7.2-7). The curve labeled "Total" in Figure J7.2-7 corresponds to the expected (mean) dose $\bar{\bar{E}}_{II}(\tau)$ previously presented in Figures J7.2-4 and J7.2-5. The remaining curves correspond to expected (mean) dose $\bar{\bar{E}}_{II,r}(\tau)$ for individual radioactive species.

Once the results in Equation J7.2-18 are available, Monte Carlo procedures can also be used to estimate $\bar{D}_{II}(\tau|\mathbf{e}_i)$, the CDF for $D_{II}(\tau|\mathbf{a}, \mathbf{e}_{Mi})$ and the CCDF for $D_{II}(\tau|\mathbf{a}, \mathbf{e}_{Mi})$. For illustration, an arbitrary distribution is assumed for N as is done in Equations J7.2-11 and J7.2-12. Then,

$$\begin{aligned}\bar{D}_{II}(\tau|\mathbf{e}_i) &\cong p_A(\mathcal{A}_{II}|\mathbf{e}_{Ai}) \sum_{k=1}^{nR} D_{II}(\tau|\mathbf{a}_{II,k}, \mathbf{e}_{Mi})/nR \\ &\cong p_A(\mathcal{A}_{II}|\mathbf{e}_{Ai}) \sum_{k=1}^{nR} \left\{ \sum_{j=1}^{nI_k} (N_{jk}/nWP) \hat{D}_{II}(\tau|[1, t_{jk}, nWP], \mathbf{e}_{Mi}) \right\} /nR,\end{aligned}\tag{Eq. J7.2-21}$$

$$\begin{aligned}p_A[D_{II}(\tau|\mathbf{a}, \mathbf{e}_{Mi}) \leq D|\mathbf{e}_{Ai}] &= 1 - p_A[D < D_{II}(\tau|\mathbf{a}, \mathbf{e}_{Mi})|\mathbf{e}_{Ai}] \\ &\cong p_A(\mathcal{A}_{II}|\mathbf{e}_{Ai}) \sum_{k=1}^{nR} \bar{\delta}_D[D_{II}(\tau|\mathbf{a}_{II,k}, \mathbf{e}_{Mi})]/nR \\ &\cong p_A(\mathcal{A}_{II}|\mathbf{e}_{Ai}) \sum_{k=1}^{nR} \bar{\delta}_D \left\{ \sum_{j=1}^{nI_k} (N_{jk}/nWP) \hat{D}_{II}(\tau|[1, t_{jk}, nWP], \mathbf{e}_{Mi}) \right\} /nR\end{aligned}\tag{Eq. J7.2-22}$$

and

$$\begin{aligned}p_A[D < D_{II}(\tau|\mathbf{a}, \mathbf{e}_{Mi})|\mathbf{e}_{Ai}] &\cong p_A(\mathcal{A}_{II}|\mathbf{e}_{Ai}) \sum_{k=1}^{nR} \bar{\delta}_D[D_{II}(\tau|\mathbf{a}_{II,k}, \mathbf{e}_{Mi})]/nR \\ &\cong p_A(\mathcal{A}_{II}|\mathbf{e}_{Ai}) \sum_{k=1}^{nR} \bar{\delta}_D \left\{ \sum_{j=1}^{nI_k} (N_{jk}/nWP) \hat{D}_{II}(\tau|[1, t_{jk}, nWP], \mathbf{e}_{Mi}) \right\} /nR\end{aligned}\tag{Eq. J7.2-23}$$

as indicated in Equations J4.5-19 – J4.5-21 with $C = II$, where (i)

$$\mathbf{a}_{II,k} = [nI_k, \mathbf{a}_{II,1k}, \mathbf{a}_{II,2k}, \dots, \mathbf{a}_{II,nI_k,k}], k = 1, 2, \dots, nR,$$

is a random sample from vectors \mathbf{a}_{II} of the form defined in Equation J7.1-8 generated in consistency with λ_I and $d_{II}(N)$ and with elements

$$\mathbf{a}_{II,jk} = [t_{jk}, N_{jk}]$$

for $j = 1, 2, \dots, nII_k$, (ii) $\hat{D}_{II}(\tau|[1, t_{jk}, nWP], \mathbf{e}_{Mi})$ is obtained by interpolation from the results in Equation J7.2-18 with procedures of the form illustrated in Figure J7.2-2, and (iii) the indicator functions $\bar{\delta}_D(\sim)$ and $\underline{\delta}_D(\sim)$ are defined in Equations J4.2-3 and J4.2-7, respectively. If considered appropriate, the requirement $nII_k = 1$ could be imposed.

As an example, Figure J7.2-8a shows the CCDF for the dose $D_{II}(10^4 \text{ yr}|\mathbf{a}_{II}, \mathbf{e}_{M1})$ to the RMEI at $\tau = 10^4 \text{ yr}$ obtained with LHS element \mathbf{e}_1 . Specifically, the CCDF in Figure J7.2-8a is a plot of the exceedance probabilities $p_A[D < D_{II}(10^4 \text{ yr}|\mathbf{a}, \mathbf{e}_{M1})|\mathbf{e}_{A1}]$ defined in Equation J7.2-23 and obtained with a random sample of size $nR = 10^4$ from \mathcal{A}_{II} . In turn, the sampled results used in the construction of the CCDF in Figure J7.2-8a can be reduced to an estimate for the expected dose $\bar{D}_{II}(10^4 \text{ yr}|\mathbf{e}_1)$ as indicated in Equation J7.2-21 and illustrated in Figure J7.2-8b. Specifically, Figure J7.2-8a shows the expected dose curve $\bar{D}_{II}(\tau|\mathbf{e}_1)$, $0 \leq \tau \leq 20,000 \text{ yr}$, previously presented in Figure J7.2-3 and the expected dose $\bar{D}_{II}(10^4 \text{ yr}|\mathbf{e}_1)$ calculated with the indicated Monte Carlo procedure. As can be seen, the value for $\bar{D}_{II}(10^4 \text{ yr}|\mathbf{e}_1)$ produced by the Monte Carlo procedure is effectively the same as the value for $\bar{D}_{II}(10^4 \text{ yr}|\mathbf{e}_1)$ produced by integration procedures. As a result, repeating the Monte Carlo estimation procedure for a sequence of values for τ would result in an estimate for $\bar{D}_{II}(\tau|\mathbf{e}_1)$ for $0 \leq \tau \leq 20,000 \text{ yr}$ that is effectively the same as the estimate that appears in Figures J7.2-3 and J7.2-8b. The integration-based approach to estimating $\bar{D}_{II}(\tau|\mathbf{e})$ has the advantage of numerical efficiency but does not provide estimates of CCDFs of the form shown in Figure J7.2-8a. In contrast, the sampling-based approach to estimating $\bar{D}_{II}(\tau|\mathbf{e})$ is less efficient numerically but provides CCDFs that summarize the effects of aleatory uncertainty.

The CCDF in Figure J7.2-8a is for a single LHS element. As shown in Figure J7.2-9a,b, a different CCDF results for $D_{II}(10^4 \text{ yr}|\mathbf{a}_{II}, \mathbf{e}_{Mi})$ for each LHS element $\mathbf{e}_i = [\mathbf{e}_{Ai}, \mathbf{e}_{Mi}]$. Collectively, these CCDFs are displaying the epistemic uncertainty associated with the distribution of dose $D_{II}(10^4 \text{ yr}|\mathbf{a}_{II}, \mathbf{e}_{Mi})$ to the RMEI at $\tau = 10^4 \text{ yr}$ that results from the different possible values for \mathbf{a}_{II} . In turn, the epistemic uncertainty associated with these CCDFs can be summarized by an expected (mean) CCDF and quantile curves constructed in a manner analogous to the construction of expected (mean) and quantile curves for expected dose $\bar{D}_{II}(\tau|\mathbf{e})$ (Figure J7.2-9c). The expected (mean) dose $\bar{\bar{D}}_{II}(10^4 \text{ yr})$ appearing in Figures J7.2-4, J7.2-5 and J7.2-7 is the result of reducing all the information in Figure J7.2-9a to single number (i.e., $\bar{\bar{D}}_{II}(10^4 \text{ yr})$).

As discussed in Section J4.10, the numerical stability of results obtained with Latin hypercube sampling can be assessed with replicated sampling. Specifically, the analysis for igneous intrusive events was performed with the $nRL = 3$ replicated LHSs indicated in Equation J4.10-1. In turn, this analysis shows that the numerical error in using Latin hypercube sampling to estimate $\bar{\bar{D}}_{II}(\tau)$ is small relative to the epistemic uncertainty associated with the possible values for $\bar{\bar{D}}_{II}(\tau|\mathbf{e})$ (Figure J7.2-10).

The results presented in Figures J7.2-1 to J7.2-10 are for the time period [0, 20,000 yr]. Corresponding results for the time period [0, 10^6 yr] are presented without discussion in Figures J7.2-11 to J7.2-20.

J7.3 Igneous Eruptive Scenario Class: \mathcal{A}_{IE}

The aleatory futures associated with the igneous eruptive scenario class \mathcal{A}_{IE} are defined by number of eruptive events (nIE) and, for each eruptive event, by event time, number of WPs intersected by vents leading to the surface, fraction of intersected WP content that is ejected into the atmosphere, eruptive power, eruptive velocity, eruption duration, wind speed and wind direction. Specifically, the individual vectors $\mathbf{a}_{IE,j}, j = 1, 2, \dots, nIE$, appearing in the definition of \mathbf{a}_{IE} in Equation J7.1-9 are defined by

$$\mathbf{a}_{IE,j} = [t_j, nWE_j, fP_j, EP_j, EV_j, ED_j, WS_j, WD_j], \quad (\text{Eq. J7.3-1})$$

where

t_j = event time (yr),

nWE_j = number of WPs intersected by vents leading to the surface,

fP_j = fraction of intersected WP content ejected into the atmosphere,

EP_j = eruptive power (watts),

EV_j = eruptive velocity (cm/s),

ED_j = eruption duration (s),

WS_j = wind speed at maximum plume height (cm/s),

WD_j = wind direction at maximum plume height.

In turn, the following quantities define the probabilities associated with \mathcal{A}_{IE} :

$pE \lambda_I$ = rate of occurrence (yr^{-1}) of igneous eruptive events that intersect one or more WPs in the repository, where λ_I is the rate of occurrence (yr^{-1}) of igneous

events that intersect the repository and pE is the conditional probability that an igneous intrusive event will also have an eruptive component that ejects waste into the atmosphere (i.e., pE is the probability that waste will be ejected into the atmosphere given that an igneous intrusive event has occurred).

$d_{IE}(N)$ = density function for number N of WPs intersected by vents leading to the surface (i.e., $N \sim nWE_j$ in Equation J7.3-1),

$d_F(F)$ = density function for fraction F of intersected WP content that is ejected into the atmosphere (i.e., $F \sim fP_j$ in Equation J7.3-1),

$d_P(P)$ = density function (watts^{-1}) for eruptive power P (i.e., $P \sim EP_j$ in Equation J7.3-1),

$d_V(V)$ = density function (s/cm) for eruptive velocity V (i.e., $V \sim EV_j$ in Equation J7.3-1),

$d_D(D|P)$ = density function (s^{-1}) for eruption duration (i.e., $D \sim ED_j$ in Equation J7.3-1),

$d_{WS}(WS|H)$ = density function (s/cm) for wind speed at maximum plume height H (km) (i.e., $WS \sim WS_j$ in Equation J7.3-1),

$d_{WD}(WD|H)$ = density function for wind direction WS at maximum plume height H (km) (i.e., $WD \sim WD_j$ in Equation J7.3-1).

As indicated, the density function $d_D(D|P)$ is conditional on eruptive power P , and the density functions $d_{WS}(WS|H)$ and $d_{WD}(WD|H)$ for wind speed and wind direction are conditional on maximum plume height H . In turn, H is a function $H(P)$ of eruptive power P .

Given pE , λ_I , $d_{IE}(N)$, $d_F(F)$, $d_P(P)$, $d_V(V)$, $d_D(D|P)$, $d_{WS}(WS|H)$, $d_{WD}(WD|H)$ and an LHS element $\mathbf{e}_i = [\mathbf{e}_{Ai}, \mathbf{e}_{Mi}]$ of the form indicated in Equation J4.9-1, then $\bar{D}_{IE}(\tau|\mathbf{e}_i)$ formally has the form

$$\bar{D}_{IE}(\tau|\mathbf{e}_i) = \int_{\mathcal{A}_{IE}} D_{IE}(\tau|\mathbf{a}, \mathbf{e}_{Mi}) d_A(\mathbf{a}|\mathbf{e}_{Ai}) dA, \quad (\text{Eq. J7.3-2})$$

where, in concept, the density $d_A(\mathbf{a}|\mathbf{e}_{Ai})$ derives from pE , λ_I , $d_{IE}(N)$, $d_F(F)$, $d_P(P)$, $d_V(V)$, $d_D(D|P)$, $d_{WS}(WS|H)$, and $d_{WD}(WD)$. The dependence of $d_A(\mathbf{a}|\mathbf{e}_{Ai})$ on \mathbf{e}_{Ai} results in the TSPA-LA because λ_I is an element of \mathbf{e}_A .

In turn, the formal representation for $\bar{D}_{IE}(\tau|\mathbf{e}_i)$ in Equation J7.3-2 can be restated as

$$\begin{aligned} \bar{D}_{IE}(\tau|\mathbf{e}_i) &= \int_0^\tau \left\{ \int_{\mathcal{N}_{IE}} \int_{\mathcal{F}_{IE}} \left[\int_{\mathcal{U}_{IE}} D_{IE}(\tau|[1, t, F, N, \mathbf{u}], \mathbf{e}_{Mi}) d_U(\mathbf{u}) dU \right]_1 d_F(F) d_{IE}(N) dF dN \right\}_2 pE \lambda_{Ii} dt \\ &\quad \text{(Eq. J7.3-3)} \end{aligned}$$

where (i) \mathcal{N}_{IE} , \mathcal{F}_{IE} , \mathcal{P}_{IE} , \mathcal{V}_{IE} , \mathcal{D}_{IE} , \mathcal{WS}_{IE} and \mathcal{WD}_{IE} are the sets of possible values for N , F , P , V , D , WS and WD associated with the density functions $d_{IE}(N)$, $d_F(F)$, $d_P(P)$, $d_V(V)$, $d_D(D|P)$, $d_{WS}(WS|H)$ and $d_{WD}(WD|H)$, (ii) the set \mathcal{U}_{IE} is defined by

$$\begin{aligned} \mathcal{U}_{IE} &= \mathcal{P}_{IE} \times \mathcal{V}_{IE} \times \mathcal{D}_{IE} \times \mathcal{WS}_{IE} \times \mathcal{WD}_{IE} \\ &= \{\mathbf{u}: \mathbf{u} = [P, V, D, WS, WD] \text{ with } p \in \mathcal{P}_{IE}, V \in \mathcal{V}_{IE}, D \in \mathcal{D}_{IE}, WS \in \mathcal{WS}_{IE}, WD \in \mathcal{WD}_{IE}\}, \end{aligned}$$

(iii) $d_U(\mathbf{u})$ is the density function on \mathcal{U}_{IE} that derives from $d_P(P)$, $d_V(V)$, $d_D(D|P)$, $d_{WS}(WS|H)$ and $d_{WD}(WD|H)$, and (iv) $D_{IE}(\tau|[1, t, F, N, \mathbf{u}], \mathbf{e}_{Mi})$ is the dose to the RMEI (mrem/yr) at time τ that results from a single igneous eruptive event at time t that has the properties defined by the components of the vector $\mathbf{u} = [P, V, D, WS, WD]$, intercepts N WPs in the repository, and ejects a fraction F of these WPs into the atmosphere. In the actual calculations performed for the igneous eruptive scenario class, each intercepted WP is assumed to be a “blended” WP that contains a radionuclide content equal to the fraction $1/nWP$ of the entire radionuclide content in the repository.

In Equation J7.3-3, the integral contained in $[\sim]_1$ is the expected dose to the RMEI at time τ from an event that occurs at time t , intercepts N WPs, and ejects a fraction F of the content of these WPs into the atmosphere. Or, put another way, this integral is the expected dose to the RMEI that derives from the distribution of $\mathbf{u} = [P, V, D, WS, WD]$ over the set \mathcal{U} as defined by $d_U(\mathbf{u})$ conditional on t , N and F . In turn, the triple integral contained in $\{\sim\}_2$ is the expected dose to the RMEI at time τ conditional on the occurrence of an igneous eruptive event at time t . Further, the “product” $pE \lambda_{Ii} dt$ of the occurrence rate $pE \lambda_{Ii}$ and the differential on time dt in Equation J7.3-3 results in the conditional expected dose defined by the triple integral in $\{\sim\}_2$ being multiplied by the expected number of igneous eruptive events in a time interval with a length conceptually represented by the differential dt (i.e., in an interval of length Δt_k when a subdivision $0 = t_0 < t_1 < \dots < t_n = \tau$ of $[0, \tau]$ is used in an approximation of the integral over t in Equation J7.3-3). As a result, the representation for $\bar{D}_{IE}(\tau|\mathbf{e}_i)$ in Equation J7.3-3 derives from the approximation

$$\begin{aligned} \bar{D}_{IE}(\tau|\mathbf{e}_i) &\cong \sum_{k=1}^n \left\{ \int_{\mathcal{N}_{IE}} \int_{\mathcal{F}_{IE}} \left[\int_{\mathcal{U}_{IE}} D_{IE}(\tau|[1, t_k, FN, \mathbf{u}], \mathbf{e}_{Mi}) d_U(\mathbf{u}) dU \right]_1 d_F(F) d_{IE}(N) dF dN \right\}_2 \\ &\quad \times pE \lambda_{Ii} \Delta t_k \\ &\quad \text{(Eq. J7.3-4)} \end{aligned}$$

as $\Delta t_k \rightarrow 0$, where $pE \lambda_{Ii} \Delta t_k$ is the expected number of igneous eruptive events in the time interval $[t_{k-1}, t_k]$ and the triple integral contained in $\{\sim\}_2$ is the conditional expected dose to the RMEI given the occurrence of an igneous eruptive event at time t_k .

The dose $D_{IE}(\tau|[1, t, FN, \mathbf{u}], \mathbf{e}_{Mi})$ appearing in Equation J7.3-3 is linear with respect to the term FN . As a result, the simplification

$$\begin{aligned} & \int_{\mathcal{N}_{IE}} \int_{\mathcal{F}_{IE}} \left[\int_{\mathcal{U}_{IE}} D_{IE}(\tau|[1, t_k, FN, \mathbf{u}], \mathbf{e}_{Mi}) d_U(\mathbf{u}) dU \right] d_F(F) d_{IE}(N) dF dN \\ &= \bar{N}_{IE} \bar{F} \int_{\mathcal{U}_{IE}} D_{IE}(\tau|[1, t, 1, \mathbf{u}], \mathbf{e}_{Mi}) d_U(\mathbf{u}) dU \end{aligned} \quad (\text{Eq. J7.3-5})$$

results for the triple integral contained in $\{\sim\}_2$ in Equation J7.3-3, where

$$\bar{N}_{IE} = \int_{\mathcal{N}_{IE}} N d_{IE}(N) dN$$

and

$$\bar{F} = \int_{\mathcal{F}_{IE}} F d_F(F) dF$$

are the expected values for N and F , respectively. In turn, the simpler representation

$$\begin{aligned} \bar{D}_{IE}(\tau|\mathbf{e}_i) &= pE \lambda_{Ii} \bar{N}_{IE} \bar{F} \int_0^\tau \left[\int_{\mathcal{U}_{IE}} D_{IE}(\tau|[1, t, 1, \mathbf{u}], \mathbf{e}_{Mi}) d_U(\mathbf{u}) dU \right] dt \\ &= pE \lambda_{Ii} \bar{N}_{IE} \bar{F} \int_{\mathcal{U}_{IE}} \left[\int_0^\tau D_{IE}(\tau|[1, t, 1, \mathbf{u}], \mathbf{e}_{Mi}) dt \right] d_U(\mathbf{u}) dU \end{aligned} \quad (\text{Eq. J7.3-6})$$

results when the representation in Equation J7.3-5 for the triple integral contained in $\{\sim\}_2$ is substituted into the representation for $D_{IE}(\tau|\mathbf{e}_i)$ in Equation J7.3-3.

The integrals involving \mathcal{U}_{IE} in Equation J7.3-6 can be approximated with a Monte Carlo procedure. Specifically, an LHS

$$\mathbf{u}_l = [P_l, V_l, D_l, WS_l, WD_l], l = 1, 2, \dots, nU, \quad (\text{Eq. J7.3-7})$$

of size nU can be generated from \mathcal{U}_{IE} in consistency with the distributions defined by the density functions $d_P(P)$, $d_V(V)$, $d_D(D|P)$, $d_{WS}(WS|H)$ and $d_{WD}(WD|H)$. In practice, this sample is generated by first constructing an LHS

$$\tilde{\mathbf{u}}_l = [P_l, V_l, p_{1l}, p_{2l}, p_{3l}], l = 1, 2, \dots, nU, \quad (\text{Eq. J7.3-8})$$

from $\tilde{V}_{IE} = \mathcal{P}_{IE} \times \mathcal{V}'_{IE} \times [0, 1] \times [0, 1] \times [0, 1]$ in consistency with the density functions $d_P(P)$ and $d_V(V)$ for P and V and uniform density functions for the pointer variables p_1 , p_2 and p_3 . Then, D_l is determined with the pointer variable p_{1l} from the distribution for D defined by $d_D(D|P_l)$, and once plume height H_l is determined as a function of eruptive power P_l , values for WS_l and WD_l are determined with the pointer variables p_{2l} and p_{3l} from the distributions for WS and WD defined by $d_{WS}(WS|H_l)$ and $d_{WD}(WD|H_l)$.

Once the sample in Equation J7.3-7 is generated, $\bar{D}_{IE}(\tau|\mathbf{e}_i)$ can be approximated by

$$\begin{aligned} \bar{D}_{IE}(\tau|\mathbf{e}_i) &\cong pE \lambda_{Ii} \bar{N}_{IE} \bar{F} \int_0^\tau \left[\sum_{l=1}^{nU} D_{IE}(\tau|[1, t, 1, \mathbf{u}_l], \mathbf{e}_{Mi}) / nU \right] dt \\ &\cong pE \lambda_{Ii} \bar{N}_{IE} \bar{F} \sum_{k=1}^n \left[\sum_{l=1}^{nU} D_{IE}(\tau|[1, t_k, 1, \mathbf{u}_l], \mathbf{e}_{Mi}) / nU \right] \Delta t_k \end{aligned} \quad (\text{Eq. J7.3-9})$$

and also by

$$\begin{aligned} \bar{D}_{IE}(\tau|\mathbf{e}_i) &\cong pE \lambda_{Ii} \bar{N}_{IE} \bar{F} \sum_{l=1}^{nU} \left[\int_0^\tau D_{IE}(\tau|[1, t, 1, \mathbf{u}_l], \mathbf{e}_{Mi}) dt \right] / nU \\ &\cong pE \lambda_{Ii} \bar{N}_{IE} \bar{F} \sum_{l=1}^{nU} \left[\sum_{k=1}^n D_{IE}(\tau|[1, t_k, 1, \mathbf{u}_l], \mathbf{e}_{Mi}) \Delta t_k \right] / nU \\ &= pE \lambda_{Ii} \bar{N}_{IE} \bar{F} \sum_{k=1}^n \left[\sum_{l=1}^{nU} D_{IE}(\tau|[1, t_k, 1, \mathbf{u}_l], \mathbf{e}_{Mi}) / nU \right] \Delta t_k, \end{aligned} \quad (\text{Eq. J7.3-10})$$

where (i) the approximations in Equation J7.3-9 start with the first representation for $\bar{D}_{IE}(\tau|\mathbf{e}_i)$ in Equation J7.3-6, (ii) the approximations in Equation J7.3-10 start with the second representation for $\bar{D}_{IE}(\tau|\mathbf{e}_i)$ in Equation J7.3-6, and (iii) the sequences of approximations in Equations J7.3-9 and J7.3-10 ultimately lead to the same final approximation. The particular approximation for $\bar{D}_{IE}(\tau|\mathbf{e}_i)$ that is used depends on the form in which results from GoldSim are saved.

The TSPA-LA calculates $\bar{D}_{IE}(\tau|\mathbf{e}_i)$ on the basis of the representation in Equation J7.3-9. To support this calculation, $D_{IE}(\tau|[1, t, 1, \mathbf{u}], \mathbf{e}_{Mi})$ is evaluated for a sequence of times and a set of sampled selected values of \mathbf{u} for each time. Two cases are considered in the TSPA-LA: events occurring over the time interval $[0, 2.0 \times 10^4 \text{ yr}]$ and events occurring over the time interval $[0, 1.0 \times 10^6 \text{ yr}]$. For the time interval $[0, 2.0 \times 10^4 \text{ yr}]$, the results

$$D_{IE}(\tau|[1, t_k, 1, \mathbf{u}_l], \mathbf{e}_{Mi}), k = 1, 2, \dots, 10, l = 1, 2, \dots, nU = 40, i = 1, 2, \dots, 300, \quad (\text{Eq. J7.3-11})$$

are calculated for (i) $0 \leq \tau \leq 2.0 \times 10^4$ yr, (ii) $t_k = 10, 100, 600, 1000, 2000, 4000, 6000, 10,000, 14,000$ and $18,000$ yr, and (iii) the \mathbf{u}_l an LHS of size $nU = 40$ from \mathcal{V}_{IE} . For the time interval $[0, 1.0 \times 10^6$ yr], the results in Equation J7.3-11 are calculated for (i) $0 \leq \tau \leq 1.0 \times 10^6$ yr, (ii) $t_k = 250, 600, 1000, 4000, 10,000, 40,000, 100,000, 200,000, 400,000$ and $800,000$ yr, and (iii) the \mathbf{u}_l an LHS of size $nU = 40$ from \mathcal{V}_{IE} .

Because of the interpolations involved, it is more efficient to sum over \mathbf{u}_l and then integrate over time as indicated in Equation J7.3-9 than to integrate on time and then sum on \mathbf{u}_l as indicated in Equation J7.3-10. As a result, the approximations to $\bar{D}_{IE}(\tau|\mathbf{e}_i)$ in the TSPA-LA are of the form

$$\bar{D}_{IE}(\tau|\mathbf{e}_i) \cong pE \lambda_{Ii} \bar{N}_{IE} \bar{F} \sum_{k=1}^n \left[\sum_{l=1}^{nU} \hat{D}_{IE}(\tau|[1, \hat{t}_k, 1, \mathbf{u}_l], \mathbf{e}_{Mi}) / nU \right] \Delta \hat{t}_k, \quad (\text{Eq. J7.3-12})$$

where (i) $0 = \hat{t}_0 < \hat{t}_1 < \dots < \hat{t}_n = \tau$ and (ii) $\hat{D}_{IE}(\tau|[1, \hat{t}_k, 1, \mathbf{u}_l], \mathbf{e}_{Mi})$ is an approximation to $D_{IE}(\tau|[1, \hat{t}_k, 1, \mathbf{u}_l], \mathbf{e}_{Mi})$ obtained by interpolation from the calculated values $D_{IE}(\tau|[1, t_k, 1, \mathbf{u}_l], \mathbf{e}_{Mi})$ indicated in Equation J7.3-11.

For computational efficiency, the quantity

$$\sum_{l=1}^{nU} \hat{D}_{IE}(\tau|[1, \hat{t}_k, 1, \mathbf{u}_l], \mathbf{e}_{Mi}) / nU \quad (\text{Eq. J7.3-13})$$

in Equation J7.3-12 is actually obtained by interpolating on the sums

$$S(\tau|t_k, \mathbf{e}_{Mi}) = \sum_{l=1}^{nU} D_{IE}(\tau|[1, t_k, 1, \mathbf{u}_l], \mathbf{e}_{Mi}) / nU \quad (\text{Eq. J7.3-14})$$

rather than on the individual doses $D_{IE}(\tau|[1, t_k, 1, \mathbf{u}_l], \mathbf{e}_{Mi})$, which reduces the number of required interpolations by a factor of nU . Specifically, the interpolated approximation $\hat{S}(\tau|\hat{t}_k, \mathbf{e}_{Mi})$ to $S(\tau|\hat{t}_k, \mathbf{e}_{Mi})$ is given by

$$\begin{aligned} \hat{S}(\tau|\hat{t}_k, \mathbf{e}_{Mi}) &= S \left[t_{k-1} + (\tau - \hat{t}_k) \middle| t_{k-1}, \mathbf{e}_{Mi} \right] \\ &\quad + \left\{ (\hat{t}_k - t_{k-1}) / (t_k - t_{k-1}) \right\} \left\{ S \left[t_k + (\tau - \hat{t}_k) \middle| t_k, \mathbf{e}_{Mi} \right] - S \left[t_{k-1} + (\tau - \hat{t}_k) \middle| t_{k-1}, \mathbf{e}_{Mi} \right] \right\} \\ &\cong \sum_{l=1}^{nU} D_{IE}(\tau|[1, \hat{t}_k, 1, \mathbf{u}_l], \mathbf{e}_{Mi}) / nU \\ &\cong \int_{\mathcal{V}_{IE}} D_{IE}(\tau|[1, \hat{t}_k, 1, \mathbf{u}], \mathbf{e}_{Mi}) d_U(\mathbf{u}) dU \quad (\text{Eq. J7.3-15}) \end{aligned}$$

for $\hat{t}_k \leq \tau$ and $t_{k-1} < \hat{t}_k < t_k$. In turn,

$$\bar{D}_{IE}(\tau|\mathbf{e}_i) \cong pE \lambda_{fi} \bar{N}_{IE} \bar{F} \sum_{k=1}^n \hat{S}(\tau|\hat{t}_k, \mathbf{e}_{Mi}) \Delta \hat{t}_k \quad (\text{Eq. J7.3-16})$$

is the resultant approximation to $\bar{D}_{IE}(\tau|\mathbf{e}_i)$.

Results are initially illustrated for the 20,000 yr time period. As indicated in conjunction with Equation J7.3-11, the expected dose results are based on the results $D_{IE}(\tau|[1, t_k, 1, \mathbf{u}_l], \mathbf{e}_{Mi})$. As an example, the values obtained for $D_{IE}(\tau|[1, t_k, 1, \mathbf{u}_l], \mathbf{e}_{Mi})$ for $t_k = 100, 1000, 4000$ and $10,000$ yr and LHS element \mathbf{e}_1 are presented in Figure J7.3-1.

As indicated in Equation J7.3-15 and illustrated in Figure J7.3-2 for LHS element \mathbf{e}_1 , the results $D_{IE}(\tau|[1, t_k, 1, \mathbf{u}_l], \mathbf{e}_{Mi})$ are used in an interpolation procedure to obtain the quantities $\hat{S}(\tau|\hat{t}_k, \mathbf{e}_{Mi})$ used in the approximation to $\bar{D}_{IE}(\tau|\mathbf{e}_i)$ in Equation J7.3-16. Specifically, the following results are shown in Figure J7.3-2 for LHS element \mathbf{e}_1 : (i) the quantities $S(\tau|t_k, \mathbf{e}_{Mi})$ defined in Equation J7.3-14 for $k = 1, 2, \dots, 10$ (Figure J7.3-2a), (ii) the approximations $\hat{S}(\tau|\hat{t}_k, \mathbf{e}_{Mi})$ to $S(\tau|t_k, \mathbf{e}_{Mi})$ defined in Equation J7.3-15 for \hat{t}_k between $t_7 = 6000$ yr and $t_8 = 10,000$ yr (Figure J7.3-2b), and (iii) the approximations $\hat{S}(\tau|\hat{t}_k, \mathbf{e}_{Mi})$ defined between 0 and 20,000 yr and used in the approximation to $\bar{D}_{IE}(\tau|\mathbf{e}_i)$ in Equation J7.3-16 (Figure J7.3-2c).

In turn, the results indicated in Equation J7.3-11 can be used to estimate $\bar{D}_{IE}(\tau|\mathbf{e}_i)$ as illustrated in Figure J7.3-3 for LHS element \mathbf{e}_1 . Further, the results obtained with all $nLHS = 300$ LHS elements are summarized in Figure J7.3-4 and presented in a standard format in Figure J7.3-5.

As discussed in conjunction with Equations J5-8 and J6.2-9, dose and expected dose to the RMEI are just two of a large number of results that can be produced and presented in the TSPA-LA. As previously done in Figure J5-4 and other similar figures, a compact summary of the expected (mean) dose results $\bar{\bar{D}}_{IE,r}(\tau)$ for the individual radioactive species is provided in Figure J7.3-6, where $\bar{\bar{D}}_{IE,r}(\tau)$ is the expected (mean) dose to the RMEI at time τ resulting from the atmospheric release of radioactive species r due to igneous eruptive events (see Equation J6.2-9 and associated discussion). In concept, the expected (mean) dose results $\bar{\bar{D}}_{IE,r}(\tau)$ for the individual radioactive species are computed using Equation J7.3-10. However, as indicated by Equation 6.5.2-1, the implementation of this calculation does not produce the intermediate quantities $\bar{D}_{IE,r}(\tau|\mathbf{e}_i)$.

Once the results in Equation J7.3-11 are available, Monte Carlo procedures can also be used to estimate $\bar{D}_{IE}(\tau|\mathbf{e}_i)$, the CDF for $D_{IE}(\tau|\mathbf{a}, \mathbf{e}_{Mi})$, and the CCDF for $D_{IE}(\tau|\mathbf{a}, \mathbf{e}_{Mi})$. Specifically, a sequence

$$\mathbf{a}_{IE,k} = \left[nIE_k, t_{1k}, \mathbf{a}_{IE,1k}, t_{2k}, \mathbf{a}_{IE,2k}, \dots, t_{nIE_k,k}, \mathbf{a}_{IE,nIE_k,k} \right], k = 1, 2, \dots, nR, \quad (\text{Eq. J7.3-17})$$

of random futures can be generated, where

$$\mathbf{a}_{IE,jk} = \left[N_{jk}, F_{jk}, \mathbf{u}_{jk} \right]$$

for $j = 1, 2, \dots, nIE_k$. In generating the indicated sample, the number of igneous eruptive events (nIE_k) would be sampled conditional on the occurrence of one or more events; the number of WPs intersected by vents leading to the surface (N_{jk}) and fraction of intersected WP content ejected into the atmosphere (F_{jk}) would be sampled from their assigned distributions; and the property vectors \mathbf{u}_{jk} would be randomly selected from the vectors \mathbf{u}_l used in the generation of the results in Equation J7.3-11. In practice, the probability that nIE_k will be greater than one is very small. Then,

$$\begin{aligned} \bar{D}_{IE}(\tau|\mathbf{e}_i) &\cong p_A(\mathcal{A}_{IE}|\mathbf{e}_{Ai}) \sum_{k=1}^{nR} D_{IE}(\tau|\mathbf{a}_{IE,k}, \mathbf{e}_{Mi})/nR \\ &\cong p_A(\mathcal{A}_{IE}|\mathbf{e}_{Ai}) \sum_{k=1}^{nR} \left\{ \sum_{j=1}^{nIE_k} (F_{jk} N_{jk}) \hat{D}_{IE}(\tau|[1, t_{jk}, 1, \mathbf{u}_{jk}], \mathbf{e}_{Mi}) \right\} / nR, \end{aligned} \quad (\text{Eq. J7.3-18})$$

$$\begin{aligned} p_A[D_{IE}(\tau|\mathbf{a}, \mathbf{e}_{Mi}) \leq D|\mathbf{e}_{Ai}] &= 1 - p_A[D < D_{IE}(\tau|\mathbf{a}, \mathbf{e}_{Mi})|\mathbf{e}_{Ai}] \\ &\cong p_A(\mathcal{A}_{IE}|\mathbf{e}_{Ai}) \sum_{k=1}^{nR} \delta_D[D_{IE}(\tau|\mathbf{a}_{IE,k}, \mathbf{e}_{Mi})]/nR \\ &\cong p_A(\mathcal{A}_{IE}|\mathbf{e}_{Ai}) \sum_{k=1}^{nR} \delta_D \left\{ \sum_{j=1}^{nIE_k} (F_{jk} N_{jk}) \hat{D}_{IE}(\tau|[1, t_{jk}, 1, \mathbf{u}_{jk}], \mathbf{e}_{Mi}) \right\} / nR \end{aligned} \quad (\text{Eq. J7.3-19})$$

and

$$\begin{aligned} p_A[D < D_{IE}(\tau|\mathbf{a}, \mathbf{e}_{Mi})|\mathbf{e}_{Ai}] &\cong p_A(\mathcal{A}_{IE}|\mathbf{e}_{Ai}) \sum_{k=1}^{nR} \bar{\delta}_D[D_{IE}(\tau|\mathbf{a}_{IE,k}, \mathbf{e}_{Mi})]/nR \\ &\cong p_A(\mathcal{A}_{IE}|\mathbf{e}_{Ai}) \sum_{k=1}^{nR} \bar{\delta}_D \left\{ \sum_{j=1}^{nIE_k} (F_{jk} N_{jk}) \hat{D}_{IE}(\tau|[1, t_{jk}, 1, \mathbf{u}_{jk}], \mathbf{e}_{Mi}) \right\} / nR \end{aligned} \quad (\text{Eq. J7.3-20})$$

as indicated in Equations J4.5-19 – J4.5-21 with $\hat{D}_{IE}[\tau|[1, t_{jk}, 1, \mathbf{u}_{jk}], \mathbf{e}_{Mi}]$ with interpolation procedures from the results in Equation J7.3-11.

Further, the LHS in Equation J4.9-1 can be used to estimate $\bar{\bar{D}}_{IE}(\tau)$, $p_E[\bar{D}_{IE}(\tau|\mathbf{e}) \leq D]$ and $p_E[D < \bar{D}_{IE}(\tau|\mathbf{e})]$. Specifically,

$$\bar{\bar{D}}_{IE}(\tau) \cong \sum_{i=1}^{nLHS} \bar{D}_{IE}(\tau|\mathbf{e}_i) / nLHS, \quad (\text{Eq. J7.3-21})$$

$$p_E[\bar{D}_{IE}(\tau|\mathbf{e}) \leq D] \cong \sum_{i=1}^{nLHS} \delta_D[\bar{D}_{IE}(\tau|\mathbf{e}_i)] / nLHS \quad (\text{Eq. J7.3-22})$$

and

$$p_E[D < \bar{D}_{IE}(\tau|\mathbf{e})] \cong \sum_{i=1}^{nLHS} \bar{\delta}_D[\bar{D}_{IE}(\tau|\mathbf{e}_i)] / nLHS \quad (\text{Eq. J7.3-23})$$

as indicated in Equations J4.9-8 – J4.9-10.

As an example, Figure J7.3-7a shows the CCDF for the dose $D_{IE}(10^4 \text{ yr}|\mathbf{a}_{IE}, \mathbf{e}_{M1})$ to the RMEI at $\tau = 10^4 \text{ yr}$ obtained with LHS element \mathbf{e}_1 . Specifically, the CCDF in Figure J7.3-7 is a plot of the exceedance probabilities $p_A[D < D_{IE}(10^4 \text{ yr}|\mathbf{a}, \mathbf{e}_{M1})|\mathbf{e}_{A1}]$ defined in Equation J7.3-20 and obtained with a random sample of size $nR = 10^4$ from \mathcal{A}_{IE} . In turn, the sampled results used in the construction of the CCDF in Figure J7.3-7a can be reduced to an estimate for the expected dose $\bar{D}_{IE}(10^4 \text{ yr}|\mathbf{e}_1)$ as indicated in Equation J7.3-18 and illustrated in Figure J7.3-7b. Specifically, Figure J7.3-7a shows the expected dose curve $\bar{D}_{IE}(\tau|\mathbf{e}_1)$, $0 \leq \tau \leq 20,000 \text{ yr}$, previously presented in Figure J7.3-3 and the expected dose $\bar{D}_{IE}(10^4 \text{ yr}|\mathbf{e}_1)$ calculated with the indicated Monte Carlo procedure. As can be seen, the value for $\bar{D}_{IE}(10^4 \text{ yr}|\mathbf{e}_1)$ produced by the Monte Carlo procedure is effectively the same as the value for $\bar{D}_{IE}(10^4 \text{ yr}|\mathbf{e}_1)$ produced by integration procedures. As a result, repeating the Monte Carlo estimation procedure for a sequence of values for τ would result in an estimate for $\bar{D}_{IE}(\tau|\mathbf{e}_1)$ for $0 \leq \tau \leq 20,000 \text{ yr}$ that is effectively the same as the estimate that appears in Figures J7.3-3 and J7.3-7b. The integration-based approach to estimating $\bar{D}_{IE}(\tau|\mathbf{e})$ has the advantage of numerical efficiency but does not provide estimates of CCDFs of the form shown in Figure J7.3-7a. In contrast, the sampling-based approach to estimating $\bar{D}_{IE}(\tau|\mathbf{e})$ is less efficient numerically but provides CCDFs that summarize the effects of aleatory uncertainty.

The CCDF in Figure J7.3-7a is for a single LHS element. As shown in Figure J7.3-8a,b, a different CCDF results for $D_{IE}(10^4 \text{ yr}|\mathbf{a}_{IE}, \mathbf{e}_{M1})$ for each LHS element $\mathbf{e}_i = [\mathbf{e}_{Ai}, \mathbf{e}_{Mi}]$. Collectively, these CCDFs are displaying the epistemic uncertainty associated with the distribution of dose $D_{IE}(10^4 \text{ yr}|\mathbf{a}_{IE}, \mathbf{e}_{M1})$ to the RMEI at $\tau = 10^4 \text{ yr}$ that results from the different possible values for \mathbf{a}_{IE} . In turn, the epistemic uncertainty associated with these CCDFs can be

summarized by an expected (mean) CCDF and quantile curves constructed in a manner analogous to the construction of expected (mean) and quantile curves for expected dose $\bar{D}_{IE}(\tau|\mathbf{e})$ (Figure J7.3-8c). The expected (mean) dose $\bar{\bar{D}}_{IE}(10^4 \text{ yr})$ appearing in Figures J7.3-4, J7.3-5, and J7.3-6 is the result of reducing all the information in Figure J7.3-8a to single number (i.e., $\bar{\bar{D}}_{IE}(10^4 \text{ yr})$).

As discussed in Section J4.10, the numerical stability of results obtained with Latin hypercube sampling can be assessed with replicated sampling. Specifically, the analysis for igneous eruptive events was performed with the $nRL = 3$ replicated LHSs indicated in Equation J4.10-1. In turn, this analysis shows that the numerical error in using Latin hypercube sampling to estimate $\bar{\bar{D}}_{IE}(\tau)$ is small relative to the epistemic uncertainty associated with the possible values for $\bar{\bar{D}}_{IE}(\tau)$ (Figure J7.3-9).

The results presented in Figures J7.3-1 to J7.3-9 are for the time period $[0, 2.0 \times 10^4 \text{ yr}]$. Corresponding results for the time period $[0, 10^6 \text{ yr}]$ are presented without discussion in Figures J7.3-10 and J7.3-18.

J7.4 Igneous Scenario Class: \mathcal{A}_I

The results $\bar{D}_{II}(\tau|\mathbf{e}_i)$ and $\bar{\bar{D}}_{II}(\tau)$ obtained for the igneous intrusive scenario class \mathcal{A}_{II} are much larger than the corresponding results $\bar{D}_{IE}(\tau|\mathbf{e}_i)$ and $\bar{\bar{D}}_{IE}(\tau)$ obtained for the igneous eruptive scenario class \mathcal{A}_{IE} . As a result, $\bar{D}_I(\tau|\mathbf{e}_i)$ and $\bar{\bar{D}}_I(\tau)$ for the igneous scenario class \mathcal{A}_I are effectively the same as $\bar{D}_{II}(\tau|\mathbf{e}_i)$ and $\bar{\bar{D}}_{II}(\tau)$ and are not presented as separate figures for this reason.

J7.5 Probabilities Associated with Igneous Scenario Classes

The probabilities $p_A(\mathcal{A}_{II}|\mathbf{e}_A)$, $p_A(\mathcal{A}_{IE}|\mathbf{e}_A)$ and $p_A(\mathcal{A}_I|\mathbf{e}_A)$ for the scenario classes \mathcal{A}_{II} , \mathcal{A}_{IE} and \mathcal{A}_I conditional on the element $\mathbf{e} = [\mathbf{e}_A, \mathbf{e}_M]$ of \mathcal{E} depend on the time interval under consideration. In the TSPA-LA, the time intervals of primary interest are $[0, 20,000 \text{ yr}]$ and $[0, 1,000,000 \text{ yr}]$. However, for generality, a time interval $[0, \tau]$ is assumed to be under consideration and $\mathcal{A}_{II}(0, \tau)$, $\mathcal{A}_{IE}(0, \tau)$ and $\mathcal{A}_I(0, \tau)$ will represent \mathcal{A}_{II} , \mathcal{A}_{IE} and \mathcal{A}_I defined with futures (i.e., igneous event occurrences) restricted to $[0, \tau]$. Formally, this corresponds to restricting the sample spaces (i.e., sets of possible futures) under consideration to futures defined on the time interval $[0, \tau]$.

With the indicated restriction,

$$\begin{aligned} p_A \left[\mathcal{A}_{II}(0, \tau) | \mathbf{e}_A \right] &= p_A \left[\mathcal{A}_I(0, \tau) | \mathbf{e}_A \right] \\ &= 1 - \exp(-\lambda_I \tau) \end{aligned} \quad (\text{Eq. J7.5-1})$$

and

$$p_A \left[A_{IE} (0, \tau) | \mathbf{e}_A \right] = 1 - \exp(-p_E \lambda_I \tau), \quad (\text{Eq. J7.5-2})$$

where λ_I is the element of \mathbf{e}_A that corresponds to the annual frequency of an igneous intrusive event, p_E is the conditional probability that an igneous intrusive event will also have an eruptive component that ejects waste into the atmosphere, and the indicated probabilities are special cases of Equation J3.6-9. In turn, p_E is defined by

$$p_E = p_{EC} p_{IW} = (0.28) (0.2968) = 0.083, \quad (\text{Eq. J7.5-3})$$

where $p_{EC} = 0.28$ is the conditional probability that an igneous intrusive event will have an eruptive component and $p_{IW} = 0.2968$ is the conditional probability that the eruptive component of an igneous intrusive event will intersect waste.

The probabilities $p_A[\mathcal{A}_{II}(0, \tau) | \mathbf{e}_A]$ and $p_A[\mathcal{A}_{IE}(0, \tau) | \mathbf{e}_A]$ defined in Equations J7.5-1 and J7.5-2 are for one or more events. The corresponding probabilities for exactly one event in the time interval $[0, \tau]$ are

$$p_A \left[\tilde{\mathcal{A}}_{II} (0, \tau) | \mathbf{e}_A \right] = (\lambda_I \tau) \exp(-\lambda_I \tau) \quad (\text{Eq. J7.5-4})$$

and

$$p_A \left[\tilde{\mathcal{A}}_{IE} (0, \tau) | \mathbf{e}_A \right] = (p_E \lambda_I \tau) \exp(-p_E \lambda_I \tau), \quad (\text{Eq. J7.5-5})$$

where

$$\tilde{\mathcal{A}}_{II} (0, \tau) = \{ \mathbf{a}_{II} : \mathbf{a}_{II} \in \mathcal{A}_{II} (0, \tau) \text{ and } n_{II} = 1 \},$$

$$\tilde{\mathcal{A}}_{IE} (0, \tau) = \{ \mathbf{a}_{IE} : \mathbf{a}_{IE} \in \mathcal{A}_{IE} (0, \tau) \text{ and } n_{IE} = 1 \}$$

and the indicated probabilities are special cases of Equation J3.6-8.

The values for $p_A[\mathcal{A}_{II}(0, \tau) | \mathbf{e}_{Ai}]$, $p_A[\tilde{\mathcal{A}}_{II}(0, \tau) | \mathbf{e}_{Ai}]$, $p_A[\mathcal{A}_{IE}(0, \tau) | \mathbf{e}_{Ai}]$ and $p_A[\tilde{\mathcal{A}}_{IE}(0, \tau) | \mathbf{e}_{Ai}]$ for the time intervals $[0, 20,000 \text{ yr}]$ and $[0, 1,000,000 \text{ yr}]$ obtained for the LHS in Equation J4.9-1 are summarized in Figure J7.5-1.

J8 SEISMIC SCENARIO CLASSES: \mathcal{A}_S , \mathcal{A}_{SG} AND \mathcal{A}_{SF}

J8.1 Relationships Involving \mathcal{A}_S , \mathcal{A}_{SG} and \mathcal{A}_{SF}

The seismic ground motion scenario class and the seismic fault displacement scenario class are defined by the sets

$$\mathcal{A}_{SG} = \{ \mathbf{a} : \mathbf{a} \in \mathcal{A} \text{ and } n_{SG} \geq 1 \} \quad (\text{Eq. J8.1-1})$$

and

$$\mathcal{A}_{SF} = \{\mathbf{a} : \mathbf{a} \in \mathcal{A} \text{ and } nSF \geq 1\} \quad (\text{Eq. J8.1-2})$$

as indicated in Equations J4.4-17 and J4.4-18. Further, the seismic scenario class \mathcal{A}_S is defined by

$$\mathcal{A}_S = \mathcal{A}_{SG} \cup \mathcal{A}_{SF} = \{\mathbf{a} : \mathbf{a} \in \mathcal{A} \text{ and } nSG \geq 1 \text{ or } nSF \geq 1\} \quad (\text{Eq. J8.1-3})$$

as indicated in Equation J4.4-12. In turn, $p_A(\mathcal{A}_{SG})$ is the probability of one or more seismic ground motion events; $p_A(\mathcal{A}_{SF})$ is the probability of one or more seismic fault displacement events; and $p_A(\mathcal{A}_S)$ is the probability of one or more seismic events.

The scenario classes \mathcal{A}_S , \mathcal{A}_{SG} and \mathcal{A}_{SF} are not disjoint. However, if the question is asked “What is the probability of a seismic event?,” then most likely $p_A(\mathcal{A}_S)$ is the desired answer. If the question is asked “What is the probability of a seismic ground motion event?,” then most likely $p_A(\mathcal{A}_{SG})$ is the desired answer. Similarly, if the question is asked “What is the probability of a seismic fault displacement event?,” then most likely $p_A(\mathcal{A}_{SF})$ is the desired answer. If desired, disjoint scenario classes involving seismic ground motion and their associated probabilities can be defined in the same manner as indicated in Equations J6.1-4 – J6.1-7 for early WP failure and early DS failure.

No synergisms are assumed to exist between the doses that result from the seismic ground motion damage to WPs and the doses that result from seismic fault displacement damage to WPs. Further, as indicated in conjunction with Equation J4.5-1, no synergisms are assumed to exist between doses that result from seismic events and doses that result from other disruptions. As a result,

$$D_S(\tau|\mathbf{a}, \mathbf{e}_M) = D_{SG}(\tau|\mathbf{a}, \mathbf{e}_M) + D_{SF}(\tau|\mathbf{a}, \mathbf{e}_M), \quad (\text{Eq. J8.1-4})$$

where

$D_S(\tau|\mathbf{a}, \mathbf{e}_M)$ = dose to RMEI (mrem/yr) at time τ resulting from seismic events associated with element \mathbf{a} of \mathcal{A} ,

$D_{SG}(\tau|\mathbf{a}, \mathbf{e}_M)$ = dose to RMEI (mrem/yr) at time τ resulting from ground motion damage to WPs for seismic events associated with element \mathbf{a} of \mathcal{A} ,

$D_{SF}(\tau|\mathbf{a}, \mathbf{e}_M)$ = dose to RMEI (mrem/yr) at time τ resulting from fault displacement damage to WPs for seismic events associated with element \mathbf{a} of \mathcal{A} ,

and all results are conditional on the element $\mathbf{e} = [\mathbf{e}_A, \mathbf{e}_M]$ of \mathcal{E} . If \mathbf{a} involves no seismic ground motion damage to WPs, then $D_{SG}(\tau|\mathbf{a}, \mathbf{e}_M) = 0$; similarly, if \mathbf{a} involves no seismic fault displacement damage to WPs, then $D_{SF}(\tau|\mathbf{a}, \mathbf{e}_M) = 0$.

In turn, the expected dose $\bar{D}_S(\tau|\mathbf{e})$ to the RMEI (mrem/yr) at time τ is given by

$$\begin{aligned}
 \bar{D}_S(\tau|\mathbf{e}) &= \int_{\mathcal{A}_S} D_S(\tau|\mathbf{a}, \mathbf{e}_M) d_A(\mathbf{a}|\mathbf{e}_A) dA \\
 &= \int_{\mathcal{A}_S} [D_{SG}(\tau|\mathbf{a}, \mathbf{e}_M) + D_{SF}(\tau|\mathbf{a}, \mathbf{e}_M)] d_A(\mathbf{a}|\mathbf{e}_A) dA \\
 &= \int_{\mathcal{A}_S} D_{SG}(\tau|\mathbf{a}, \mathbf{e}_M) d_A(\mathbf{a}|\mathbf{e}_A) dA + \int_{\mathcal{A}_S} D_{SF}(\tau|\mathbf{a}, \mathbf{e}_M) d_A(\mathbf{a}|\mathbf{e}_A) dA \\
 &= \bar{D}_{SG}(\tau|\mathbf{e}) + \bar{D}_{SF}(\tau|\mathbf{e}), \tag{Eq. J8.1-5}
 \end{aligned}$$

where (i)

$$\begin{aligned}
 \bar{D}_{SG}(\tau|\mathbf{e}) &= \int_{\mathcal{A}_S} D_{SG}(\tau|\mathbf{a}, \mathbf{e}_M) d_A(\mathbf{a}|\mathbf{e}_A) dA \\
 &= \int_{\mathcal{A}_{SG}} D_{SG}(\tau|\mathbf{a}, \mathbf{e}_M) d_A(\mathbf{a}|\mathbf{e}_A) dA \tag{Eq. J8.1-6}
 \end{aligned}$$

is the expected dose to the RMEI (mrem/yr) at time τ resulting from seismic ground motion events, (ii)

$$\begin{aligned}
 \bar{D}_{SF}(\tau|\mathbf{e}) &= \int_{\mathcal{A}_S} D_{SF}(\tau|\mathbf{a}, \mathbf{e}_M) d_A(\mathbf{a}|\mathbf{e}_A) dA \\
 &= \int_{\mathcal{A}_{SF}} D_{SF}(\tau|\mathbf{a}, \mathbf{e}_M) d_A(\mathbf{a}|\mathbf{e}_A) dA \tag{Eq. J8.1-7}
 \end{aligned}$$

is the expected dose to the RMEI (mrem/yr) at time τ resulting from seismic fault displacement events, and (iii) all results are conditional on the element $\mathbf{e} = [\mathbf{e}_A, \mathbf{e}_M]$ of \mathcal{E} . The conversion from an integral over \mathcal{A}_S to an integral over \mathcal{A}_{SG} in Equation J8.1-6 is possible because $D_{SG}(\tau|\mathbf{a}, \mathbf{e}_M) = 0$ if $\mathbf{a} \notin \mathcal{A}_{SG}$; similarly, the conversion from an integral over \mathcal{A}_S to an integral over \mathcal{A}_{SF} in Equation J8.1-7 is possible because $D_{SF}(\tau|\mathbf{a}, \mathbf{e}_M) = 0$ if $\mathbf{a} \notin \mathcal{A}_{SF}$.

The general form of the elements \mathbf{a} of \mathcal{A} is shown in Equations J4.4-1 – J4.4-8. However, because no synergisms between disruptions are assumed in the determination of $\bar{D}_{SG}(\tau|\mathbf{e})$ and $\bar{D}_{SF}(\tau|\mathbf{e})$, the representations for the elements of \mathcal{A}_{SG} and \mathcal{A}_{SF} can be simplified to

$$\mathbf{a}_{SG} = [nSG, \mathbf{a}_{SG,1}, \mathbf{a}_{SG,2}, \dots, \mathbf{a}_{SG,nSG}] \tag{Eq. J8.1-8}$$

and

$$\mathbf{a}_{SF} = [nSF, \mathbf{a}_{SF,1}, \mathbf{a}_{SF,2}, \dots, \mathbf{a}_{SF,nSF}], \tag{Eq. J8.1-9}$$

respectively. With this notation, the elements \mathbf{a}_{SG} of \mathcal{A}_{SG} only contain representations for seismic ground motion events, and the elements \mathbf{a}_{SF} of \mathcal{A}_{SF} only contain representations for seismic fault displacement events.

The expected (mean) dose $\bar{\bar{D}}_S(\tau)$ for the seismic scenario class \mathcal{A}_S over both aleatory and epistemic uncertainty is given by

$$\begin{aligned}
 \bar{\bar{D}}_S(\tau) &= \int_{\mathcal{E}} \bar{D}_S(\tau|\mathbf{e}) d_E(\mathbf{e}) dE \\
 &= \int_{\mathcal{E}} \left[\bar{D}_{SG}(\tau|\mathbf{e}) + \bar{D}_{SF}(\tau|\mathbf{e}) \right] d_E(\mathbf{e}) dE \\
 &= \int_{\mathcal{E}} \bar{D}_{SG}(\tau|\mathbf{e}) d_E(\mathbf{e}) dE + \int_{\mathcal{E}} \bar{D}_{SF}(\tau|\mathbf{e}) d_E(\mathbf{e}) dE \\
 &= \bar{\bar{D}}_{SG}(\tau) + \bar{\bar{D}}_{SF}(\tau), \tag{Eq. J8.1-10}
 \end{aligned}$$

where

$$\bar{\bar{D}}_{SG}(\tau) = \int_{\mathcal{E}} \bar{D}_{SG}(\tau|\mathbf{e}) d_E(\mathbf{e}) dE \tag{Eq. J8.1-11}$$

is the expected (mean) dose for the seismic ground motion scenario class \mathcal{A}_{SG} over both aleatory and epistemic uncertainty and

$$\bar{\bar{D}}_{SF}(\tau) = \int_{\mathcal{E}} \bar{D}_{SF}(\tau|\mathbf{e}) d_E(\mathbf{e}) dE \tag{Eq. J8.1-12}$$

is the expected (mean) dose for the seismic fault displacement scenario class \mathcal{A}_{SF} over both aleatory and epistemic uncertainty.

The CCDF and CDF for $\bar{D}_S(\tau|\mathbf{e})$ over epistemic uncertainty are defined by

$$\begin{aligned}
 p_E \left[D < \bar{D}_S(\tau|\mathbf{e}) \right] &= \int_{\mathcal{E}} \bar{\delta}_D \left[\bar{D}_S(\tau|\mathbf{e}) \right] d_E(\mathbf{e}) dE \\
 &= \int_{\mathcal{E}} \bar{\delta}_D \left[\bar{D}_{SG}(\tau|\mathbf{e}) + \bar{D}_{SF}(\tau|\mathbf{e}) \right] d_E(\mathbf{e}) dE \tag{Eq. J8.1-13}
 \end{aligned}$$

and

$$\begin{aligned}
 p_E \left[\bar{D}_S(\tau|\mathbf{e}) \leq D \right] &= 1 - p_E \left[D < \bar{D}_S(\tau|\mathbf{e}) \right] \\
 &= \int_{\mathcal{E}} \underline{\delta}_D \left[\bar{D}_S(\tau|\mathbf{e}) \right] d_E(\mathbf{e}) dE \\
 &= \int_{\mathcal{E}} \underline{\delta}_D \left[\bar{D}_{SG}(\tau|\mathbf{e}) + \bar{D}_{SF}(\tau|\mathbf{e}) \right] d_E(\mathbf{e}) dE, \tag{Eq. J8.1-14}
 \end{aligned}$$

respectively. However, unlike the result for $\bar{\bar{D}}_S(\tau)$ in Equation J8.1-10, the CCDF and CDF for $\bar{D}_S(\tau|\mathbf{e})$ cannot be decomposed into a sum of separate results for the seismic ground motion scenario class \mathcal{A}_{SG} and the seismic fault displacement scenario class \mathcal{A}_{SF} .

Direct evaluation of the integrals that define $\bar{\bar{D}}_S(\tau)$, $p_E[D < \bar{D}_S(\tau|\mathbf{e})]$ and $p_E[\bar{D}_S(\tau|\mathbf{e}) \leq D]$ is not practicable. However, the approximations

$$\bar{\bar{D}}_S(\tau) \cong \sum_{i=1}^{nLHS} \bar{D}_S(\tau|\mathbf{e}_i) / nLHS, \quad (\text{Eq. J8.1-15})$$

$$p_E[D < \bar{D}_S(\tau|\mathbf{e})] \cong \sum_{i=1}^{nLHS} \bar{\delta}_D[\bar{D}_S(\tau|\mathbf{e}_i)] / nLHS \quad (\text{Eq. J8.1-16})$$

and

$$p_E[\bar{D}_S(\tau|\mathbf{e}) \leq D] \cong \sum_{i=1}^{nLHS} \bar{\delta}_D[\bar{D}_S(\tau|\mathbf{e}_i)] / nLHS \quad (\text{Eq. J8.1-17})$$

result with use of the LHS in Equation J4.9-1 as previously indicated in conjunction with Equations J4.9-8 – J4.9-10.

Further descriptions of the seismic scenario classes \mathcal{A}_S , \mathcal{A}_{SG} and \mathcal{A}_{SF} and sources of additional information are available in Section 6.6.

J8.2 Seismic Ground Motion Scenario Class: \mathcal{A}_{SG}

As discussed in conjunction with Equation J8.1-1, the seismic ground motion scenario class is defined by the subset \mathcal{A}_{SG} of \mathcal{A} . Formally, \mathcal{A}_{SG} contains all elements \mathbf{a} of \mathcal{A} with $n_{SG} > 0$. To fully define \mathcal{A}_{SG} , it is necessary to first define the vector \mathbf{a}_{SG} indicated in Equation (J8.1-8) and its associated components $\mathbf{a}_{SG,j}$, $j = 1, 2, \dots, n_S$.

Each component $\mathbf{a}_{SG,j}$ of \mathbf{a}_{SG} is defined by

$$\mathbf{a}_{SG,j} = [t_j, v_j, VR_j, AW_{1j}, AW_{2j}, AD_j, RW_{1j}, RW_{2j}, FDP_j, FDF_j], \quad (\text{Eq. J8.2-1})$$

where, for seismic event j occurring at time t_j (yr),

v_j = peak ground velocity (PGV, m/s),

VR_j = volume (m^3/m) of rockfall,

AW_{rj} = damaged area (m^2) on WP type r with $r = 1 \sim \text{CSNF WP}$ and $r = 2 \sim \text{CDSP WP}$,

AD_j = damaged area (m^2) on DSs,

RW_{rj} = indicator variable for rupture of WP type r

$$= \begin{cases} 2 & \text{if rupture occurred} \\ 1 & \text{if incipient rupture occurred} \\ 0 & \text{otherwise,} \end{cases}$$

FDP_j = indicator variable for failure of DS plates

$$= \begin{cases} 1 & \text{if DS plates fail} \\ 0 & \text{otherwise,} \end{cases}$$

FDF_j = indicator variable for failure of DS frame

$$= \begin{cases} 1 & \text{if DS frames fail} \\ 0 & \text{otherwise.} \end{cases}$$

In turn, the distributions for the individual elements of $\mathbf{a}_{SG,j}$ are defined by the following quantities:

$$\lambda_G(v) = \text{exceedance frequency (yr}^{-1}\text{) for PGV } v \text{ (i.e., } \lambda_G(v) \text{ is the seismic ground motion hazard curve),} \quad (\text{Eq. J8.2-2})$$

$$pRF(v) = \text{probability of rockfall conditional on the occurrence of a seismic ground motion event with PGV } v, \quad (\text{Eq. J8.2-3})$$

$$d_V(V|v) = \text{density function (m/m}^3\text{) for volume } V \text{ of rock (m}^3\text{/m) that caves into a drift conditional on the occurrence of a seismic ground motion event with PGV } v \text{ (} d_V(V|v) \text{ corresponds to a gamma distribution with a mean } \mu(v) \text{ and a standard deviation } \sigma(v) \text{ that are functions of } v\text{),} \quad (\text{Eq. J8.2-4})$$

$$pWD_r(v|\delta_{I_r}, \delta_{R_r}, WT_r, R) = \text{probability of nonzero damaged area on a WP of type } r \text{ (} r = 1 \sim \text{CSNF WP and } r = 2 \sim \text{CDSP WP) conditional on the occurrence of a seismic ground motion event with PGV } v \text{ given the existence of conditions defined by the following variables: (i) } \delta_{I_r}, \text{ where } \delta_{I_r} = 1 \sim \text{WPs with degraded internals and } \delta_{I_r} = 0 \sim \text{WPs with intact internals, (ii) } \delta_{R_r}, \text{ where } \delta_{R_r} = 1 \sim \text{WPs surrounded by rubble and } \delta_{R_r} = 0 \sim \text{WPs not surrounded by rubble, (iii) } WT_r = \text{outer corrosion barrier thickness (mm) on WP, and (iv) } R = \text{residual stress failure threshold,} \quad (\text{Eq. J8.2-5})$$

$d_{Ar}(A|v, \delta_{Ir}, \delta_{Rr}, WT_r, R)$ = density function (m^{-2}) for damaged area A (m^2) on a WP of type r conditional on the occurrence of a seismic ground motion event with PGV v that results in a nonzero damaged area (see $pWD_r(v|\delta_{Ir}, \delta_{Rr}, WT_r, R)$) given the existence of conditions defined by $\delta_{Ir}, \delta_{Rr}, WT_r, R$, (Eq. J8.2-6)

$d_L(L|v, F)$ = density function (Pa^{-1}) for total dynamic load L (Pa) on a DS conditional on the occurrence of a seismic ground motion event with PGV v given that a fraction F of the drift is filled with rubble ($d_L(L|v, F)$ corresponds to a lognormal distribution with parameters that are functions of v and F), (Eq. J8.2-7)

$d_A(A|L, DT)$ = density function (m^{-2}) for damaged area (m^2) on DS conditional on total dynamic load L on DS and DS thickness DT (mm), (Eq. J8.2-8)

$pIRW_r(v|\delta_{Ir}, \delta_{Rr}, WT_r)$ = probability of incipient rupture of a WP of type r conditional on the occurrence of a seismic ground motion event with PGV v given the existence of conditions defined by $\delta_{Ir}, \delta_{Rr}, WT_r$, (Eq. J8.2-9)

$pRW_r(v|\delta_{Ir}, \delta_{Rr}, WT_r)$ = probability of rupture of a WP of type r conditional on the occurrence of a seismic ground motion event with PGV v given the existence of conditions defined by $\delta_{Ir}, \delta_{Rr}, WT_r$, (Eq. J8.2-10)

$pDP(v|F, DT)$ = probability of DS plate failure conditional on the occurrence of a seismic ground motion event with PGV v given the existence of conditions defined by F and DT , (Eq. J8.2-11)

$pDF(v|F, DT)$ = probability of DS frame failure conditional on the occurrence of a seismic ground motion event with PGV v given the existence of conditions defined by F and DT . (Eq. J8.2-12)

As indicated by the definitions of the components of \mathbf{a}_{SGj} in Equation J8.2-1 and the following definitions in Equations J8.2-2 – J8.2-12 of the quantities that define the distributions for the components of \mathbf{a}_{SGj} , the probabilistic structure for the set \mathcal{A}_{SG} is very complex. This structure is made even more complex by the fact that the distributions for individual components of \mathbf{a}_{SGj} can depend on both the values for components in $\mathbf{a}_{SG,k}$, $k = 1, 2, \dots, j - 1$, and the repository conditions that derive from these values. For example, WP thickness at time t_j affects values for components of \mathbf{a}_{SGj} and derives from both values of components in $\mathbf{a}_{SG,k}$, $k = 1, 2, \dots, j - 1$, and the modeling of WP thickness as a function of these values. In concept, there exists a density

function $d_A(\mathbf{a})$ defined on \mathcal{A} that includes the aleatory uncertainty associated with the occurrence of seismic events. Actually, $d_A(\mathbf{a})$ is more appropriately represented by $d_A(\mathbf{a}|\mathbf{e})$ given that the distributions for components of $\mathbf{a}_{SG,j}$ can depend on calculated quantities that in turn depend on components of $\mathbf{e} = [\mathbf{e}_A, \mathbf{e}_M]$. However, in practice, $d_A(\mathbf{a})$, or more generally $d_A(\mathbf{a}|\mathbf{e})$, is too complex to represent in a closed form.

Formally, the expected dose $\bar{D}_{SG}(\tau|\mathbf{e})$ to the RMEI (mrem/yr) at time τ from the seismic ground motion scenario class \mathcal{A}_{SG} is given by

$$\bar{D}_{SG}(\tau|\mathbf{e}) = \int_{\mathcal{A}_{SG}} D_{SG}(\tau|\mathbf{a}, \mathbf{e}_M) d_A(\tau|\mathbf{e}) dA \quad (\text{Eq. J8.2-13})$$

as indicated in Equation J4.4-13, where

$$D_{SG}(\tau|\mathbf{a}, \mathbf{e}_M) = \text{dose to RMEI (mrem/yr) at time } \tau \text{ resulting from seismic ground motion events associated with element } \mathbf{a} \text{ of } \mathcal{A}_{SG}$$

and all results are conditional on the element $\mathbf{e} = [\mathbf{e}_A, \mathbf{e}_M]$ of \mathcal{E} . In the determination of $D_{SG}(\tau|\mathbf{a}, \mathbf{e}_M)$, no synergisms are assumed to exist with other disruptive events that could be associated with elements of \mathcal{A}_{SG} . Further, as indicated in Equations J4.5-16 and J4.5-18 with $C = SG$, the CCDF and CDF for $D_{SG}(\tau|\mathbf{a}, \mathbf{e}_M)$ are defined by the probabilities $p_A[D_{SG}(\tau|\mathbf{a}, \mathbf{e}_M) \leq D|\mathbf{e}_A]$ and $p_A[D < D_{SG}(\tau|\mathbf{a}, \mathbf{e}_M)|\mathbf{e}_A]$.

In addition, given that $\bar{D}_{SG}(\tau|\mathbf{e})$ can be determined, additional results of the form indicated in Equations J4.9-8 – J4.9-10 with $C = SG$ can also be determined for the seismic ground motion scenario class \mathcal{A}_{SG} . For example, the expected (mean) dose $\bar{\bar{D}}_{SG}(\tau)$ to the RMEI (mrem/yr) at time τ for the seismic ground motion scenario class \mathcal{A}_{SG} over both aleatory and epistemic uncertainty is given by

$$\begin{aligned} \bar{\bar{D}}_{SG}(\tau) &= \int_{\mathcal{E}} \bar{D}_{SG}(\tau|\mathbf{e}) d_E(\mathbf{e}) dE \\ &= \int_{\mathcal{E}} \left[\int_{\mathcal{A}_{SG}} D_{SG}(\tau|\mathbf{a}, \mathbf{e}_M) d_A(\mathbf{a}|\mathbf{e}) dA \right] d_E(\mathbf{e}) dE \\ &\cong \sum_{i=1}^{nLHS} \left[\int_{\mathcal{A}_{SG}} D_{SG}(\tau|\mathbf{a}, \mathbf{e}_{Mi}) d_A(\mathbf{a}|\mathbf{e}_i) dA \right] / nLHS, \quad (\text{Eq. J8.2-14}) \end{aligned}$$

where $\mathbf{e}_i = [\mathbf{e}_{Ai}, \mathbf{e}_{Mi}]$, $i = 1, 2, \dots, nLHS$, corresponds to the LHS indicated in Equation J4.9-1.

J8.3 Seismic Ground Motion Scenario Class: 0 to 20,000 yr

Evaluation of the integral in Equation J8.2-13 that defines $\bar{D}_{SG}(\tau|\mathbf{e})$ for $0 \leq \tau \leq 10^6$ yr with quadrature-based procedures is not possible as a result of the complexity of the futures contained in \mathcal{A}_{SG} and their associated probabilistic structure. However, when τ is restricted to the time interval $[0, 20,000 \text{ yr}]$, the evaluation of $D_{SG}(\tau|\mathbf{e})$ is significantly simplified. This simplification results because (i) significant reduction in the thicknesses of the WPs and DSs does not take place, (ii) significant accumulation of rock fall does not take place, (iii) the probabilities of WP damage and WP rupture for CSNF WPs are sufficiently low that these potential occurrences do not need to be included in the determination of $\bar{D}_{SG}(\tau|\mathbf{e})$, (iv) the probability of rupture for CDSP WPs is sufficiently low that this potential occurrence does not need to be included in the determination of $\bar{D}_{SG}(\tau|\mathbf{e})$, and (v) the probabilities for DS plate damage, DS plate failure and DS frame failure are sufficiently low that these potential occurrences do not need to be included in the determination of $\bar{D}_{SG}(\tau|\mathbf{e})$. As a result, only damage to CDSP WPs under intact DSs needs to be considered in the determination of $\bar{D}_{SG}(\tau|\mathbf{e})$ for $0 \leq \tau \leq 20,000$ yr.

Given that only damage to CDSP WPs under intact DSs needs to be considered in the determination of $\bar{D}_{SG}(\tau|\mathbf{e})$ for $0 \leq \tau \leq 20,000$ yr, the representation for $\mathbf{a}_{SG,j}$ in Equation J8.2-1 simplifies to

$$\mathbf{a}_{SG,j} = [t_j, A_j], \quad (\text{Eq. J8.3-1})$$

where t_j is the time (yr) of seismic event j and A_j is the resultant damaged area (m^2) on a CDSP WP. As a result, a seismic ground motion future \mathbf{a}_{SG} for the time interval $[0, 20,000 \text{ yr}]$ is effectively of the form

$$\mathbf{a}_{SG} = [n_{SG}, t_1, A_1, t_2, A_2, \dots, t_{n_{SG}}, A_{n_{SG}}]. \quad (\text{Eq. J8.3-2})$$

Distributions for t_j and A_j can be derived from quantities characterizing the aleatory uncertainty associated with seismic ground motion events that are given following Equation J8.2-1. The PGV v_j associated with seismic ground motion event j is not included in the definition $\mathbf{a}_{SG,j}$ in Equation J8.3-1. However, the hazard curve defining exceedance probabilities for PGV defines the distribution of event times t_j and also enters into the determination of the distribution of the damaged area A_j given the occurrence of a seismic ground motion event at time t_j .

A distinction is made between WPs with intact internals and WPs with degraded internals. Further, the assumption is made that the internals in a WP degrade as soon as the outer barrier of the WP is damaged. The distinction between WPs with intact internals and degraded internals is potentially important because WPs with degraded internals are assumed to be less resistant to damage than WPs with intact internals. In the context of the representation for \mathbf{a}_{SG} in Equation J8.3-2, the first event at time t_1 involves damage to WPs with intact internals, and the events at times t_2, t_3, \dots, t_{n_S} involve damage to WPs with degraded internals.

Given that seismic ground motion futures \mathbf{a}_{SG} of the form indicated in Equation J8.3-2 are under consideration, the expected dose $\bar{D}_{SG}(\tau|\mathbf{a}, \mathbf{e})$ to the RMEI can be determined with use of the following quantities to characterize the aleatory uncertainty associated with the components of \mathbf{a} that are defined by \mathbf{a}_{SG} :

$$\lambda_1(\mathbf{e}) = \text{occurrence rate (yr}^{-1}\text{) for seismic ground motion events that cause damage to CDSP WPs with intact internals,} \quad (\text{Eq. J8.3-3})$$

$$d_{A1}(A|\mathbf{e}) = \text{density function (m}^{-2}\text{) defined on set } \mathcal{A}1 \text{ for damaged (i.e., diffusive) area on a CDSP WP with intact internals conditional on the occurrence of a damaging seismic ground motion event,} \quad (\text{Eq. J8.3-4})$$

$$\lambda_2(\mathbf{e}) = \text{occurrence rate (yr}^{-1}\text{) for seismic ground motion events that cause damage to CDSP WPs with degraded internals,} \quad (\text{Eq. J8.3-5})$$

$$d_{A2}(A|\mathbf{e}) = \text{density function (m}^{-2}\text{) defined on set } \mathcal{A}2 \text{ for damaged (i.e., diffusive) area on a CDSP WP with degraded internals conditional on the occurrence of a damaging seismic ground motion event.} \quad (\text{Eq. J8.3-6})$$

As indicated, $\lambda_1(\mathbf{e})$, $d_{A1}(A|\mathbf{e})$, $\lambda_2(\mathbf{e})$ and $d_{A2}(A|\mathbf{e})$ are dependent on elements of \mathbf{e} . Derivations of these quantities that incorporate this dependence will be discussed later.

Given the preceding quantities, the expected dose $\bar{D}_{SG}(\tau|\mathbf{e})$ to the RMEI at time τ for $0 \leq \tau \leq 20,000$ yr arising from the aleatory uncertainty associated with seismic ground motion events can be approximated by

$$\begin{aligned} \bar{D}_{SG}(\tau|\mathbf{e}) \cong & \sum_{k=1}^n \left(\left\{ \exp[-\lambda_1(\mathbf{e}) t_{k-1}] \right\}_3 \left\{ \lambda_1(\mathbf{e}) (\Delta t_k) \exp[-\lambda_1(\mathbf{e}) \Delta t_k] \right\}_4 \right)_1 \\ & \times \left(\left\{ \int_{\mathcal{A}1} D_{SG}(\tau|[1, t_k, A], \mathbf{e}_M) d_{A1}(A|\mathbf{e}) dA \right\}_5 \right. \\ & \left. + \left\{ \int_{t_k}^{\tau} \left[\int_{\mathcal{A}2} D_{SG}(\tau|[1, \tilde{t}, A], \mathbf{e}_M) d_{A2}(A|\mathbf{e}) dA \right] \lambda_2(\mathbf{e}) d\tilde{t} \right\}_6 \right)_2 \quad (\text{Eq. J8.3-7}) \end{aligned}$$

where $0 = t_0 < t_1 < \dots < t_n = \tau$, $\Delta t_k = t_{k-1} - t_k$, and $D_{SG}(\tau|[1, t_k, A], \mathbf{e}_M)$ is the dose to the RMEI (mrem/yr) at time τ that results from a damaged (i.e., diffusive) area of size A (m²) on individual WPs associated with a single seismic ground motion event occurring at time t_k .

In the preceding, $\{\sim\}_3$ is the probability that WPs with intact internals are not damaged in the time interval $[0, t_{k-1}]$, and $\{\sim\}_4$ is the probability that WPs with intact internals are damaged in the time interval $[t_{k-1}, t_k]$. As a result, the product $(\{\sim\}_3 \{\sim\}_4)_1$ is the probability that the first

seismic ground motion event causing damage to WPs with intact internals occurs in the time interval $[t_{k-1}, t_k]$. The integral contained in $\{\sim\}_5$ is the expected dose to the RMEI at time τ from a seismic ground motion event at time t_k that damages WPs with intact internals, and the double integral contained in $\{\sim\}_6$ is the expected dose to the RMEI at time τ from seismic ground motion events that occur in the time interval $[t_k, \tilde{\tau}]$ and damage WPs with degraded internals. As a result, the sum $(\{\sim\}_5 + \{\sim\}_6)_2$ is the expected dose to the RMEI at time τ conditional on the occurrence of a seismic ground motion event at time t_k that damages WPs with intact internals; specifically, the conditional expected dose $(\{\sim\}_5 + \{\sim\}_6)_2$ includes both the dose from the event at time k and the dose from additional events that can potentially occur in the time interval $[t_k, \tilde{\tau}]$. Given that the “events” corresponding to occurrence in time interval $[t_{k-1}, t_k]$ of first damage to WPs with intact internals are disjoint, it follows that the sum of the products of the probabilities defined by $(\{\sim\}_3 \{\sim\}_4)_1$ and the conditional expected doses defined by $(\{\sim\}_5 + \{\sim\}_6)_2$ approximates $\bar{D}_{SG}(\tau|\mathbf{e})$. Underlying this approximation is the assumption that the effects of multiple seismic events are additive.

In turn, the integral representation

$$\begin{aligned} \bar{D}_{SG}(\tau|\mathbf{e}) = & \int_0^\tau (\lambda_1(\mathbf{e}) \exp[-\lambda_1(\mathbf{e})t]) \left(\int_{\mathcal{A}1} D_{SG}(\tau|[1, t, A], \mathbf{e}_M) d_{A1}(A|\mathbf{e}) dA \right. \\ & \left. + \int_t^\tau \left[\int_{\mathcal{A}2} D_{SG}(\tau|[1, \tilde{t}, A], \mathbf{e}_M) d_{A2}(A|\mathbf{e}) dA \right] \lambda_2(\mathbf{e}) d\tilde{t} \right) dt \end{aligned} \quad (\text{Eq. J8.3-8})$$

follows from the approximation in Equation J8.3-7 as $\Delta t_k \rightarrow 0$.

The integral defining $\bar{D}_{SG}(\tau|\mathbf{e})$ in Equation J8.3-8 can be efficiently approximated with quadrature-based methods by evaluating $D_{SG}(\tau|[1, t, A], \mathbf{e}_M)$ for selected values of t and A and then using interpolation to obtain $D_{SG}(\tau|[1, t, A], \mathbf{e}_M)$ for additional values of t and A . Specifically, the evaluations

$$D_{SG}(\tau|[1, t_r, A_s], \mathbf{e}_{Mi}), r = 1, 2, \dots, nT, s = 1, 2, \dots, nDA, \quad (\text{Eq. J8.3-9})$$

are carried out for $0 \leq \tau \leq 20,000$ yr, each element $\mathbf{e}_i = [\mathbf{e}_{Ai}, \mathbf{e}_{Mi}]$ of the LHS in Equation J4.9-1 and damage to CDSP WPs. In the TSPA-LA,

$$t_r = 100, 1000, 3000, 6000, 12000, 18000 \text{ yrs} \quad (\text{Eq. J8.3-10})$$

for $r = 1, 2, \dots, nT = 6$ and

$$A_s = 10^{-8+s} (32.6 \text{ m}^2) \quad (\text{Eq. J8.3-11})$$

for $s = 1, 2, \dots, nDA = 5$. Selected results are shown in Figures J8.3-1 and J8.3-2.

In turn, $\bar{D}_{SG}(\tau|\mathbf{e}_i)$ can be approximated by

$$\begin{aligned} \bar{D}_{SG}(\tau|\mathbf{e}_i) \cong & \sum_{j=1}^n \left(\lambda_1(\mathbf{e}_i) \exp[-\lambda_1(\mathbf{e}_i)\hat{t}_{j-1}] \right) \left(\left\{ \sum_{l=1}^{n1} \hat{D}_{SG}(\tau|[1, \hat{t}_j, A_{1l}], \mathbf{e}_{Mi}) d_{A1}(A_{1l}|\mathbf{e}_i) \Delta A_{1l} \right\} \right. \\ & \left. + \left\{ \sum_{k=j+1}^n \left[\sum_{l=1}^{n2} \hat{D}_{SG}(\tau|[1, \hat{t}_{k-1}, A_{2l}], \mathbf{e}_{Mi}) d_{A2}(A_{2l}|\mathbf{e}_i) \Delta A_{2l} \right] \lambda_2(\mathbf{e}_i) \Delta \hat{t}_k \right\} \right) \Delta \hat{t}_j, \end{aligned} \quad (\text{Eq. J8.3-12})$$

where (i) $0 = \hat{t}_0 < \hat{t}_1 < \dots < \hat{t}_n = \tau$ is a subdivision of $[0, \tau]$, (ii) $a_1 = A_{10} < A_{11} < \dots < A_{1,n1} = b_1$ is a subdivision of $\mathcal{A}1 = [a_1, b_1]$, (iii) $a_2 = A_{20} < A_{21} < \dots < A_{2,n2} = b_2$ is a subdivision of $\mathcal{A}2 = [a_2, b_2]$, and (iv) the doses $\hat{D}_{SG}(\tau|[1, \hat{t}_j, A_{1l}], \mathbf{e}_{Mi})$ and $\hat{D}_{SG}(\tau|[1, \hat{t}_{k-1}, A_{2l}], \mathbf{e}_{Mi})$ are approximations to $D_{SG}(\tau|[1, \hat{t}_j, A_{1l}], \mathbf{e}_{Mi})$ and $D_{SG}(\tau|[1, \hat{t}_{k-1}, A_{2l}], \mathbf{e}_{Mi})$ obtained with interpolation procedures from the results indicated in Equation J8.3-9.

An alternative computational strategy that involves fewer interpolations is to approximate $\bar{D}_{SG}(\tau|\mathbf{e}_i)$ by

$$\bar{D}_{SG}(\tau|\mathbf{e}_i) \cong \sum_{j=1}^n \left(\lambda_1(\mathbf{e}_i) \exp[-\lambda_1(\mathbf{e}_i)\hat{t}_{j-1}] \right) \left(\hat{I}_1(\tau|\hat{t}_j, \mathbf{e}_i) + \sum_{k=j+1}^n [\hat{I}_2(\tau|\hat{t}_{k-1}, \mathbf{e}_i)] \lambda_2(\mathbf{e}_i) \Delta \hat{t}_k \right) \Delta \hat{t}_j, \quad (\text{Eq. J8.3-13})$$

where, for a given event time t , $\hat{I}_1(\tau|t, \mathbf{e}_i)$ and $\hat{I}_2(\tau|t, \mathbf{e}_i)$ are approximations to the integrals

$$I_1(\tau|t, \mathbf{e}_i) = \int_{\mathcal{A}1} D_{SG}(\tau|[1, t, A], \mathbf{e}_{Mi}) d_{A1}(A|\mathbf{e}_i) dA \quad (\text{Eq. J8.3-14})$$

and

$$I_2(\tau|t, \mathbf{e}_i) = \int_{\mathcal{A}2} D_{SG}(\tau|[1, t, A], \mathbf{e}_{Mi}) d_{A2}(A|\mathbf{e}_i) dA, \quad (\text{Eq. J8.3-15})$$

respectively. For numerical implementation, the approximations

$$\hat{I}_1(\tau|t_r, \mathbf{e}_i) = \sum_{l=1}^{n1} \hat{D}_{SG}(\tau|[1, t_r, A_{1l}], \mathbf{e}_{Mi}) d_{A1}(A_{1l}|\mathbf{e}_i) \Delta A_{1l} \quad (\text{Eq. J8.3-16})$$

and

$$\hat{I}_2(\tau|t_r, \mathbf{e}_i) = \sum_{l=1}^{n2} \hat{D}_{SG}(\tau|[1, t_r, A_{2l}], \mathbf{e}_{Mi}) d_{A2}(A_{2l}|\mathbf{e}_i) \Delta A_{2l} \quad (\text{Eq. J8.3-17})$$

can be determined for the times $t_r, r = 1, 2, \dots, nT = 6$, in Equation J8.3-10 with the areas A_{1l} and A_{2l} defined the same as in Equation J8.3-12. Once values for $\hat{I}_1(\tau|t_r, \mathbf{e}_i)$ and $\hat{I}_2(\tau|t_r, \mathbf{e}_i), r = 1, 2, \dots, nT = 6$, are determined, the required values for $\hat{I}_1(\tau|\hat{t}_j, \mathbf{e}_i)$ and $\hat{I}_2(\tau|\hat{t}_{k-1}, \mathbf{e}_i)$ in Equation J8.3-13 can be determined by interpolation as illustrated in Figure J8.3-3. Use of the approximation to $\bar{D}_{SG}(\tau|\mathbf{e}_i)$ in Equation J8.3-13 rather than the approximation in Equation J8.3-12 reduces the number of required interpolations by a factor of approximately $nDA = 5$ (see Equation J8.3-11).

As an example, the estimate for $\bar{D}_{SG}(\tau|\mathbf{e}_1)$ obtained for LHS element \mathbf{e}_1 with the procedure indicated in Equation J8.3-13 is shown in Figure J8.3-4. Further, the results obtained with all $nLHS = 300$ LHS elements are summarized in Figure J8.3-5 and presented in a standard format in Figure J8.3-6.

As previously discussed in conjunction with Equations J5-8 and J6.2-9, dose and expected dose to the RMEI are just two of a large number of results that can be produced and presented in the TSPA-LA. As an example, a summary of the dose calculations for ^{99}Tc is given in Figure J8.3-7, which has the same organization as Figure J8.3-5. Overall, ^{99}Tc is one of the largest contributors to the expected (mean) dose $\bar{D}_{SG}(\tau)$ for the 20,000 yr time period. As previously done in Figure J5-4 and other similar figures, a compact summary of the expected (mean) dose results $\bar{D}_{SG,r}(\tau)$ for the individual radioactive species is provided in Figure J8.3-8, where $\bar{D}_{SG,r}(\tau)$ is the expected (mean) dose to the RMEI at time τ resulting from the release of radioactive species r due to seismic ground motion events (see Equation J6.2-9 and associated discussion).

An alternative numerical procedure is to use Monte Carlo techniques to estimate the distribution of the dose function $D_{SG}(\tau|\mathbf{a}, \mathbf{e}_M)$ defined in conjunction with Equation J8.3-8 for futures of the form defined in Equation J8.3-2. Specifically, a random sample of futures

$$\mathbf{a}_{SG,k} = [nSG_k, t_{1k}, A_{1k}, t_{2k}, A_{2k}, \dots, t_{nSG_k,k}, A_{nSG_k,k}], k = 1, 2, \dots, nR, \quad (\text{Eq. J8.3-18})$$

of size nR can be drawn in consistency with the distributions defined by $\lambda_1(\mathbf{e}_i), d_{A1}(A|\mathbf{e}_i), \lambda_2(\mathbf{e}_i)$ and $d_{A2}(A|\mathbf{e}_i)$ for each LHS element $\mathbf{e}_i = [\mathbf{e}_{Ai}, \mathbf{e}_{Mi}]$. Then, $D_{SG}(\tau|\mathbf{a}_{SG,j}, \mathbf{e}_{Mi})$ can be estimated by

$$D_{SG}(\tau|\mathbf{a}_{SG,k}, \mathbf{e}_{Mi}) \cong \sum_{j=1}^{nSG_k} \hat{D}_{SG}(\tau|[1, t_{jk}, A_{jk}], \mathbf{e}_{Mi}) \quad (\text{Eq. J8.3-19})$$

where the individual doses $\hat{D}_{SG}(\tau|[1, t_{jk}, A_{jk}], \mathbf{e}_{Mi})$ are obtained with interpolation procedures from the results indicated in Equation J8.3-9.

Once the results in Equation J8.3-19 are available, $\bar{D}_{SG}(\tau|\mathbf{e}_i)$, the CDF for $D_{SG}(\tau|\mathbf{a}_{SG}, \mathbf{e}_{Mi})$ and the CCDF for $D_{SG}(\tau|\mathbf{a}_{SG}, \mathbf{e}_{Mi})$ can be determined in the same manner as indicated in Equations J4.5-19 – J4.5-21 with $C = SG$. Specifically,

$$\begin{aligned}\bar{D}_{SG}(\tau|\mathbf{e}_i) &\equiv p_A(\mathcal{A}_{SG}|\mathbf{e}_i) \sum_{k=1}^{nR} D_{SG}(\tau|\mathbf{a}_{SG,k}, \mathbf{e}_{Mi})/nR \\ &\equiv p_A(\mathcal{A}_{SG}|\mathbf{e}_i) \sum_{k=1}^{nR} \left\{ \sum_{j=1}^{nSG_k} \hat{D}_{SG}(\tau|[1, t_{jk}, \mathcal{A}_{jk}], \mathbf{e}_{Mi}) \right\} / nR,\end{aligned}\tag{Eq. J8.3-20}$$

$$\begin{aligned}p_A[D_{SG}(\tau|\mathbf{a}, \mathbf{e}_{Mi}) \leq D|\mathbf{e}_i] &= 1 - p_A[D < D_{SG}(\tau|\mathbf{a}, \mathbf{e}_{Mi})|\mathbf{e}_i] \\ &\equiv p_A(\mathcal{A}_{SG}|\mathbf{e}_i) \sum_{k=1}^{nR} \bar{\delta}_D[D_{SG}(\tau|\mathbf{a}_{SG,k}, \mathbf{e}_{Mi})]/nR \\ &\equiv p_A(\mathcal{A}_{SG}|\mathbf{e}_i) \sum_{k=1}^{nR} \bar{\delta}_D \left\{ \sum_{j=1}^{nSG_k} [\hat{D}_{SG}(\tau|[1, t_{jk}, A_{jk}], \mathbf{e}_{Mi})] \right\} / nR\end{aligned}\tag{Eq. J8.3-21}$$

and

$$\begin{aligned}p_A[D < D_{SG}(\tau|\mathbf{a}, \mathbf{e}_{Mi})|\mathbf{e}_i] &\equiv p_A(\mathcal{A}_{SG}|\mathbf{e}_i) \sum_{k=1}^{nR} \delta_D[D_{SG}(\tau|\mathbf{a}_{SG,k}, \mathbf{e}_{Mi})]/nR \\ &\equiv p_A(\mathcal{A}_{SG}|\mathbf{e}_i) \sum_{k=1}^{nR} \delta_D \left\{ \sum_{j=1}^{nSG_k} \hat{D}_{SG}(\tau|[1, t_{jk}, A_{jk}], \mathbf{e}_{Mi}) \right\} / nR,\end{aligned}\tag{Eq. J8.3-22}$$

as indicated in Equations J4.5-19 – J4.5-21 with $C = SG$, where (i)

$$\mathbf{a}_{SG,k} = [nSG_k, \mathbf{a}_{SG,1k}, \mathbf{a}_{SG,2k}, \dots, \mathbf{a}_{SG,nSG_k,k}], k = 1, 2, \dots, nR,$$

is a random sample from vectors \mathbf{a}_{SG} of the form defined in Equation J8.3-18 generated in consistency with $\lambda_I(\mathbf{e}_i)$, $d_{A1}(A|\mathbf{e}_i)$, $\lambda_2(\mathbf{e}_i)$ and $d_{A2}(A|\mathbf{e}_i)$ and with

$$\mathbf{a}_{SG,jk} = [t_{jk}, A_{jk}]$$

for $j = 1, 2, \dots, nSG_k$ and (ii) the indicator functions $\bar{\delta}_D(\sim)$ and $\underline{\delta}_D(\sim)$ are defined in Equations J4.2-3 and J4.2-7, respectively. This process is illustrated in Figures J8.3-9 and J8.3-10.

In the preceding, $p_A(\mathcal{A}_{SG}|\mathbf{e}_i)$, $p_A[D_{SG}(\tau|\mathbf{a}, \mathbf{e}_{Mi}) \leq D|\mathbf{e}_i]$ and $p_A[D < D_{SG}(\tau|\mathbf{a}, \mathbf{e}_{Mi})|\mathbf{e}_i]$ are indicated as being conditional on \mathbf{e}_i because the values for $\lambda_1(\mathbf{e}_i)$, $d_{A1}(A|\mathbf{e}_i)$, $\lambda_2(\mathbf{e}_i)$ and $d_{A2}(A|\mathbf{e}_i)$ are conditional on the value for \mathbf{e}_i . Further, as used in Equations J8.3-20 – J8.3-22, the set (i.e., scenario class) \mathcal{A}_{SG} is assumed to only contain those futures in which one or more CDSP WPs failures occur in the time interval $[0, 20,000 \text{ yr}]$. Because of this restriction,

$$p_A(\mathcal{A}_{SG}|\mathbf{e}_i) = 1 - \exp[-20,000 \lambda_1(\mathbf{e}_i)] \quad (\text{Eq. J8.3-23})$$

in Equations J8.3-20 – J8.3-22 (see Equation J3.6-9).

As discussed in Section J4.10, the numerical stability of results obtained with Latin hypercube sampling can be assessed with replicated sampling. Specifically, the analysis for seismic ground motion events was performed with the $nRL = 3$ replicated LHSs indicated in Equation J4.10-1. In turn, this analysis shows that the numerical error in using Latin hypercube sampling to estimate $\bar{D}_{SG}(\tau)$ is small relative to the epistemic uncertainty associated with the possible values for $\bar{D}_{SG}(\tau)$ (Figure J8.3-11).

J8.4 Seismic Ground Motion Scenario Class: 0 to 10^6 yr

The expected dose $\bar{D}_{SG}(\tau|\mathbf{e})$ is formally defined by the integral in Equation J8.2-13. For the time interval $[0, 10^6 \text{ yr}]$, the structure of the elements \mathbf{a} of \mathcal{A}_{SG} is too complex (see definition of $\mathbf{a}_{SG,j}$ in Equation J8.2-1) to allow a quadrature-based approximation for the defining integral for $\bar{D}_{SG}(\tau|\mathbf{e})$. However, a sampling-based (i.e., Monte Carlo) approximation is possible.

As a result, $\bar{D}_{SG}(\tau|\mathbf{e}_i)$ will be approximated in the TSPA-LA for each element $\mathbf{e}_i = [\mathbf{e}_{Ai}, \mathbf{e}_{Mi}]$ of the LHS in Equation J4.9-1 by

$$\bar{D}_{SG}(\tau|\mathbf{e}_i) \cong \sum_{k=1}^{nR} D_{SG}(\tau|\mathbf{a}_{SG,ik}, \mathbf{e}_{Mi}) / nR, \quad (\text{Eq. J8.4-1})$$

where $\mathbf{a}_{SG,ik}$, $k = 1, 2, \dots, nR$, is a random sample from \mathcal{A}_{SG} generated in consistency with the conceptual, but undefined, density function $d_{SG}(\mathbf{a}|\mathbf{e}_i)$. Owing to the complexity of the distributions that define the properties of individual seismic ground motion events, the properties of each seismic ground motion event must be sampled internal to the evaluation of $D_{SG}(\tau|\mathbf{a}_{SG,ik}, \mathbf{e}_{Mi})$ as the properties of the disposal system and the resultant distributions for some of elements of $\mathbf{a}_{SG,ik}$ change through time.

In concept, the following results can be sampled for each future $\mathbf{a}_{SG,ik}$ before the calculation of $D_{SG}(\tau|\mathbf{a}_{SG,ik}, \mathbf{e}_{Mi})$ is initiated: (i) number nSG_{ik} of seismic ground motion events associated with $\mathbf{a}_{SG,ik}$, (ii) times

$$0 \leq t_{i1k} \leq t_{i2k} \leq \dots \leq t_{i,nSG_{ik},k} \leq 10^6 \text{ yr} \quad (\text{Eq. J8.4-2})$$

of seismic ground motion events associated with $\mathbf{a}_{SG,ik}$, (iii) PGVs

$$v_{i1k}, v_{i2k}, \dots, v_{i,nSG_{ik},k} \quad (\text{Eq. J8.4-3})$$

for seismic ground motion events associated with $\mathbf{a}_{SG,ik}$, and (iv) rock fall volumes

$$VR_{i1k}, VR_{i2k}, \dots, VR_{i,nSG_{ik},k} \quad (\text{Eq. J8.4-4})$$

for seismic ground motion events associated with $\mathbf{a}_{SG,ik}$. The remaining properties associated with individual seismic ground motion events (i.e., AW_{1ijk} , AW_{2ijk} , AD_{ijk} , RW_{1ijk} , RW_{2ijk} , FDP_{ijk} , FDF_{ijk} for $j = 1, 2, \dots, nSG_{ik}$; see Equation J8.2-1) have distributions that are conditional on repository properties and can only be sampled once these conditions are calculated within the computational structure that underlies the determination of $D_{SG}(\tau|\mathbf{a}_{SG,ik}, \mathbf{e}_{Mi})$.

When the same hazard curve (i.e., the function $\lambda_G(v)$) is used for all LHS elements, an initial set of high-level futures defined by

$$\tilde{\mathbf{a}}_{SG,k} = \left[nSG_{1k}, t_{1k}, v_{1k}, VR_{1k}, t_{2k}, v_{2k}, VR_{2k}, \dots, t_{nSG_k,k}, v_{nSG_k,k}, VR_{nSG_k,k} \right] \quad (\text{Eq. J8.4-5})$$

can be sampled for $k = 1, 2, \dots, nR$. Then, for each LHS element \mathbf{e}_i , the corresponding future $\mathbf{a}_{SG,k}$ can be generated by using the seismic ground motion properties defined by $\tilde{\mathbf{a}}_{SG,k}$ and sampling the additional properties indicated in Equation J8.2-1 on the basis of distributions that are conditional on calculated repository properties at the times $t_{jk}, j = 1, 2, \dots, nSG_k$. The result is a sequence of futures

$$\mathbf{a}_{SG,ik}, i = 1, 2, \dots, nLHS, k = 1, 2, \dots, nR, \quad (\text{Eq. J8.4-6})$$

where the seismic ground motion properties associated with $\tilde{\mathbf{a}}_{SG,k}$ are used in the definition of $\mathbf{a}_{SG,ik}$ for each LHS element \mathbf{e}_i . This approach has the positive feature that it permits uncertainty and sensitivity analysis results to be obtained conditional on the occurrence of each high level future $\tilde{\mathbf{a}}_{SG,k}$. However, if the hazard curve $\lambda_G(v)$ is treated as being uncertain (i.e., as an element of \mathbf{e}_A), the sampled futures $\mathbf{a}_{SG,ik}$ used in the approximation to $\bar{D}_{SG}(\tau|\mathbf{e}_i)$ in Equation J8.4-1 cannot be generated in this manner and the sequences of properties in Equations J8.4-2 – J8.4-3 will change for each LHS element \mathbf{e}_i . Similarly, this change would also occur if any of the other distributions that characterize aleatory uncertainty associated with seismic events were treated as being uncertain in an epistemic sense.

However, a negative feature of the preceding approach is that it results in less stable estimates for the expected (mean) dose $\bar{\bar{D}}_{SG}(\tau)$ than is the case when the futures $\mathbf{a}_{SG,ik}$ in Equation J8.4-6 are sampled independently for each LHS element. For this reason, the futures $\mathbf{a}_{SG,ik}$ used in the approximations to $\bar{D}_{SG}(\tau|\mathbf{e}_i)$ in Equation J8.4-1, and hence in the approximation $\bar{\bar{D}}_{SG}(\tau)$, in the TSPA-LA are sampled independently for each LHS element. Specifically, the TSPA-LA uses an independently generated sample

$$\mathbf{a}_{SG,ik}, k = 1, 2, \dots, nR = 30, \quad (\text{Eq. J8.4-7})$$

of seismic futures of the form defined in Equations J4.4-7 and J8.2-1 for each LHS element $\mathbf{e}_i = [\mathbf{e}_{Ai}, \mathbf{e}_{Mi}]$ in the approximation $\bar{D}_{SG}(\tau|\mathbf{e}_i)$.

The dose function $D_{SG}(\tau|\mathbf{a}_{SG,ik}, \mathbf{e}_{Mi})$ is evaluated for each seismic future indicated in Equation J8.4-7. As illustrated in Figure J8.4-1, this results in $nR = 30$ dose curves for each LHS element. In turn, vertical averaging of the $nR = 30$ dose curves associated with LHS element \mathbf{e}_i results in the estimate of $\bar{D}_{SG}(\tau|\mathbf{e}_i)$ defined in Equation J8.4-1 (Figure J8.4-1). Further, the results obtained with all $nLHS = 300$ LHS elements are summarized in Figure J8.4-2 and presented in a standard format in Figure J8.4-3.

As previously discussed in conjunction with Equations J5-8 and J6.2-9, dose and expected dose to the RMEI are just two of a large number of results that can be produced and presented in the TSPA-LA. As an example, a summary of the dose calculations for ^{99}Tc is given in Figure J8.4-4, which has the same organization as Figure J8.4-2. Overall, ^{99}Tc is one of the largest contributors to the expected (mean) dose $\bar{\bar{D}}_{SG}(\tau)$ for the 10^6 yr time period. As previously done in Figure J5-4 and other similar figures, a compact summary of the expected (mean) dose results $\bar{\bar{D}}_{SG,r}(\tau)$ for the individual radioactive species is provided in Figure J8.4-5, where $\bar{\bar{D}}_{SG,r}(\tau)$ is the expected (mean) dose to the RMEI at time τ resulting from the release of radioactive species r due to seismic ground motion events over 10^6 yr (see Equation J6.2-9 and associated discussion).

As discussed in Section J4.10, the numerical stability of results obtained with Latin hypercube sampling can be assessed with replicated sampling. Specifically, the analysis for seismic ground motion was performed with the $nRL = 3$ replicated LHSs indicated in Equation J4.10-1. In turn, this analysis shows that the numerical error in using Latin hypercube sampling to estimate $\bar{\bar{D}}_{SG}(\tau)$ is small relative to the epistemic uncertainty associated with the possible values for $\bar{D}_{SG}(\tau|\mathbf{e})$ (Figure J8.4-6). However, a large amount of numerical noise is present in the sampling-based integration over aleatory uncertainty for each LHS element. Thus, the estimates for $\bar{D}_{SG}(\tau|\mathbf{e}_i)$ are not fully converged; specifically, $\bar{D}_{SG}(\tau|\mathbf{e}_i)$ will be a smooth curve when the estimation process is fully converged. In concept, convergence can be achieved by using a sample size larger than $nR = 30$ for each LHS element. Other numerical strategies to make more efficient use of the evaluations of $D_{SG}(\tau|\mathbf{a}_{SG}, \mathbf{e}_{Mi})$ are also possible. For example, an obvious

possibility is to use an appropriate smoothing technique (e.g., a running average with a Gaussian kernel) in the estimation of $\bar{D}_{SG}(\tau|\mathbf{e}_i)$ from the results $D_{SG}(\tau|\mathbf{a}_{SG,ik}, \mathbf{e}_{Mi})$, $k = 1, 2, \dots, nR$, for each LHS element. There is less numerical noise in the estimation of $\bar{\bar{D}}_{SG}(\tau)$ than in the estimation of the individual expected dose curves $\bar{D}_{SG}(\tau|\mathbf{e}_i)$ because the averaging process used to obtain $\bar{\bar{D}}_{SG}(\tau)$ results in a cancellation of some of the random noise associated with the individual expected dose curves $\bar{D}_{SG}(\tau|\mathbf{e}_i)$; in essence, a much larger random sample of futures is used in the estimation of $\bar{\bar{D}}_{SG}(\tau)$ than is used in the estimation of the individual expected dose curves $\bar{D}_{SG}(\tau|\mathbf{e}_i)$.

J8.5 Representation of Aleatory Uncertainty Associated with Seismic Ground Motion Scenario Class \mathcal{A}_{SG}

As indicated in conjunction with Equation J8.2-1, a large number of probability distributions are used to characterize the aleatory uncertainty associated with the occurrence of seismic ground motion events. As described in this section, representational and computational simplifications can be achieved by coalescing multiple distributions into a single distribution. These representations are used explicitly in the quadrature method for the time interval $[0, 2 \times 10^4 \text{ yr}]$ but not in the sampling-based method for the time interval $[0, 1 \times 10^6 \text{ yr}]$.

J8.5.1 Occurrence Rates for WP Damage

The occurrence rates (yr^{-1}) for seismic ground motion events that damage WPs derive from the quantities $\lambda_G(v)$ and $pWD_r(v|\delta_{I_r}, \delta_{R_r}, WT_r, R)$ defined in Equations J8.2-2 and J8.2-5, respectively. Specifically,

$$\lambda_G(v) = \text{exceedance frequency (yr}^{-1}\text{) for PGV } v \text{ (i.e., } \lambda_G(v) \text{ is the seismic ground motion hazard curve)} \quad (\text{Eq. J8.5.1-1})$$

and

$$pWD_r(v|\delta_{I_r}, \delta_{R_r}, WT_r, R) = \text{probability of nonzero damaged area on a WP of type } r \text{ (} r = 1 \sim \text{CSNF WP and } r = 2 \sim \text{CDSP WP) conditional on the occurrence of a seismic ground motion event with PGV } v \text{ given the existence of conditions defined by the following variables: (i) } \delta_{I_r}, \text{ where } \delta_{I_r} = 1 \sim \text{WPs with degraded internals and } \delta_{I_r} = 0 \sim \text{WPs with intact internals, (ii) } \delta_{R_r}, \text{ where } \delta_{R_r} = 1 \sim \text{WPs surrounded by rubble and } \delta_{R_r} = 0 \sim \text{WPs not surrounded by rubble, (iii) } WT_r = \text{outer corrosion barrier thickness (mm) on WP, and (iv) } R = \text{residual stress failure threshold.} \quad (\text{Eq. J8.5.1-2})$$

For notational convenience in the following derivation of occurrence rate for WP damage, the dependence of $pWD_r(v|\delta_{I_r}, \delta_{R_r}, WT_r, R)$ on r , δ_{I_r} , δ_{R_r} , WT_r , and R will be suppressed and $pWD_r(v|\delta_{I_r}, \delta_{R_r}, WT_r, R)$ will simply be represented by $pWD(v)$.

Given $\lambda_G(v)$ and $pWD(v)$, the occurrence rate λ_D (yr^{-1}) of seismic ground motion events that damage WPs is approximated by

$$\begin{aligned}\lambda_D &\equiv \sum_{j=1}^n pWD(v_{j-1}) [\lambda_G(v_{j-1}) - \lambda_G(v_j)] \\ &= \sum_{j=1}^n (-1) pWD(v_{j-1}) [\lambda_G(v_j) - \lambda_G(v_{j-1})],\end{aligned}\quad (\text{Eq. J8.5.1-3})$$

where $[v_{mn}, v_{mx}]$ is the range of values for PGV over which $\lambda_G(v)$ is defined and $v_{mn} = v_0 < v_1 < \dots < v_n = v_{mx}$. In turn, the representations

$$\begin{aligned}\lambda_D &= \int_{v_{mn}}^{v_{mx}} (-1) pWD(v) d\lambda_G(v) \\ &= \int_{v_{mn}}^{v_{mx}} (-1) pWD(v) [d\lambda_G(v)/dv] dv \\ &= \int_{\lambda_G(v_{mn})}^{\lambda_G(v_{mx})} (-1) pWD[\lambda_G^{-1}(\lambda)] d\lambda \\ &= \int_{\lambda_{mx}}^{\lambda_{mn}} (-1) pWD[\lambda_G^{-1}(\lambda)] d\lambda \\ &= \int_{\lambda_{mn}}^{\lambda_{mx}} pWD[\lambda_G^{-1}(\lambda)] d\lambda\end{aligned}\quad (\text{Eq. J8.5.1-4})$$

result as $\Delta v_j \rightarrow 0$, where (i) the first integral is a Stieltjes integral, (ii) the second integral is the corresponding Riemann integral, (iii) the third integral is the result of a change of variables from an integral on v to an integral on λ , (iv) the fourth integral is a notational change in the limits of integration based on the equalities $\lambda_{mx} = \lambda_G(v_{mn})$ and $\lambda_{mn} = \lambda_G(v_{mx})$, and (v) the fifth and final integral results from an interchange of the upper and lower limits of integration.

The residual stress failure threshold R appearing in $pWD_r(v|\delta_{I_r}, \delta_{R_r}, WT_r, R)$ affects the definition of probability distributions that characterize aleatory uncertainty and, in particular, affects the definition of λ_D in Equation J8.5.1-4. However, R is fundamentally a physical property of the WPs. Therefore, given that R is treated as being epistemically uncertain in the TSPA-LA, it seems most natural to identify R as an element of \mathbf{e}_M although a case could be made R should be identified as an element of \mathbf{e}_A . Computationally, this has no effect on the outcome of the TSPA-LA because, with either identification, R is an element of the vector $\mathbf{e} = [\mathbf{e}_A, \mathbf{e}_M]$ of epistemically uncertain quantities sampled in the LHS indicated in Equation J4.9-1. However, in general although not implemented in the TSPA-LA, the hazard

curve $\lambda_G(v)$ is epistemically uncertain (i.e., $\lambda_G(v)$ is an important analysis input that can never be known with certainty) and thus is appropriately viewed as an element of \mathbf{e}_A . As a result, the rate λ_D defined in Equation J8.5.1-4 is actually a function $\lambda_D(\mathbf{e})$ of epistemically uncertain analysis inputs.

The occurrence rates $\lambda_1(\mathbf{e})$ and $\lambda_2(\mathbf{e})$ defined in Equations J8.3-3 and J8.3-5 and appearing in Equations J8.3-7 and J8.3-8 are rates of the form defined in Equation J8.5.1-4. Specifically,

$$\lambda_1(\mathbf{e}) = \int_{\lambda_{mn}}^{\lambda_{mx}} pWD_2 \left[\lambda_G^{-1}(\lambda) \mid \delta_{I2} = 0, \delta_{R2} = 0, WT_2 = 23 \text{ mm}, R \right] d\lambda \quad (\text{Eq. J8.5.1-5})$$

with (i) $r = 2$ indicating CDSP WPs, (ii) $\delta_{I2} = 0$ indicating intact internals, (iii) $\delta_{R2} = 0$ indicating WPs that are free to move beneath the DS, (iv) $WT_2 = 23$ mm corresponding to an essentially undiminished outer corrosion barrier, and (v) R and possibly $\lambda_G(v)$ elements of \mathbf{e} . Similarly,

$$\lambda_2(\mathbf{e}) = \int_{\lambda_{mn}}^{\lambda_{mx}} pWD_2 \left[\lambda_G^{-1}(\lambda) \mid \delta_{I2} = 1, \delta_{R2} = 0, WT_2 = 23 \text{ mm}, R \right] d\lambda, \quad (\text{Eq. J8.5.1-6})$$

with (i) r , δ_{R2} , WT_2 , R and $\lambda_G(v)$ defined the same as in Equation J8.5.1-5 and (ii) $\delta_{I2} = 1$ indicating degraded internals.

The preceding representations for $\lambda_1(\mathbf{e})$ and $\lambda_2(\mathbf{e})$ use the final integral representation for λ_D in Equation J8.5.1-4; however, the other integral representations for λ_D in Equation J8.5.1-4 provide equally valid representations for $\lambda_1(\mathbf{e})$ and $\lambda_2(\mathbf{e})$. For example, use of the second integral representation in Equation J8.5.1-4 results in

$$\lambda_1(\mathbf{e}) = \int_{v_{mn}}^{v_{mx}} (-1) pWD_2(v \mid \delta_{I2} = 0, \delta_{R2} = 0, WT_2 = 23 \text{ mm}, R) \left[d\lambda_G(v)/dv \right] dv \quad (\text{Eq. J8.5.1-7})$$

and

$$\lambda_2(\mathbf{e}) = \int_{v_{mn}}^{v_{mx}} pWD_2(v \mid \delta_{I2} = 1, \delta_{R2} = 0, WT_2 = 23 \text{ mm}, R) \left[d\lambda_G(v)/dv \right] dv, \quad (\text{Eq. J8.5.1-8})$$

which avoids the use of the inverse function $\lambda_G^{-1}(\lambda)$ but requires the determination of the derivative $d\lambda_G(v)/dv$. In many ways, the initial Stieltjes integral in Equation J8.5.1-4 provides the simplest representation for $\lambda_1(\mathbf{e})$ and $\lambda_2(\mathbf{e})$.

J8.5.2 Distributions for PGV

The hazard curve $\lambda_G(v)$ is defined for $v_{mn} \leq v \leq v_{mx}$, where v_{mn} is the smallest PGV included in the analysis (i.e., the smallest PGV with the potential to affect repository behavior) and v_{mx} is the largest PGV that merits inclusion in the analysis on the basis of probabilistic considerations. In

turn, $\lambda_{mx} = \lambda_G(v_{mn})$ and $\lambda_{mn} = \lambda_G(v_{mx})$ are the exceedance frequencies associated with v_{mn} and v_{mx} as previously used in Section J8.5.1. With $\lambda_G(v)$, it is possible to determine the distribution for PGV conditional on the occurrence of a potentially damaging seismic ground motion event (i.e., an event with a PGV $\geq v_{mn}$). Further, with both $\lambda_G(v)$ and the conditional probability of nonzero damage $pWD_r(v|\delta_{I_r}, \delta_{R_r}, WT_r, R)$ defined in Equation J8.5.1-2, it is possible to determine the distributions for PGV conditional on the occurrence of a damaging seismic ground motion event.

The CDF for PGV given a potentially damaging seismic event is defined by probabilities of the form

$$\begin{aligned} \text{prob}(\tilde{v} \leq v | v_{mn} \leq v \leq v_{mx}) &\cong \sum_{j=1}^n \left[\lambda_G(v_{j-1}) - \lambda_G(v_j) \right] / (\lambda_{mx} - \lambda_{mn}) \\ &= \sum_{j=1}^n (-1) \left[\lambda_G(v_j) - \lambda_G(v_{j-1}) \right] / (\lambda_{mx} - \lambda_{mn}), \quad (\text{Eq. J8.5.2-1}) \end{aligned}$$

where $v_{mn} = v_0 < v_1 < \dots < v_n = v$ and $\text{prob}(\tilde{v} \leq v | v_{mn} \leq v \leq v_{mx})$ represents the probability of a PGV that is less than or equal to v given the occurrence of a seismic event with a PGV between v_{mn} and v_{mx} . In turn,

$$\begin{aligned} \text{prob}(\tilde{v} \leq v | v_{mn} \leq v \leq v_{mx}) &= \frac{1}{\lambda_{mx} - \lambda_{mn}} \int_{v_{mn}}^v (-1) d\lambda_G(\tilde{v}) \\ &= \frac{1}{\lambda_{mx} - \lambda_{mn}} \int_{v_{mn}}^v (-1) [d\lambda_G(\tilde{v})/d\tilde{v}] d\tilde{v} \\ &= \frac{1}{\lambda_{mx} - \lambda_{mn}} \int_{\lambda_G(v_{mn})}^{\lambda_G(v)} (-1) d\lambda \\ &= \frac{1}{\lambda_{mx} - \lambda_{mn}} \int_{\lambda_G(v)}^{\lambda_{mx}} d\lambda \\ &= [\lambda_{mx} - \lambda_G(v)] / [\lambda_{mx} - \lambda_{mn}] \quad (\text{Eq. J8.5.2-2}) \end{aligned}$$

as $\Delta v_i \rightarrow 0$.

The density function $d_v(v|P)$ for PGV given a potentially damaging seismic ground motion event (i.e., indicated by the conditionality notation “|P”) can now be obtained by differentiating the cumulative probability $\text{prob}(\tilde{v} \leq v | v_{mn} \leq v \leq v_{mx})$ defined in Equation J8.5.2-2. Specifically,

$$\begin{aligned}
 d_v(v|P) &= \frac{d}{dv} \left[\text{prob}(\tilde{v} \leq v | v_{mn} \leq v \leq v_{mx}) \right] \\
 &= \frac{d}{dv} \left(\frac{[\lambda_{mx} - \lambda_G(v)]}{[\lambda_{mx} - \lambda_{mn}]} \right) \\
 &= - \left[d\lambda_G(v)/dv \right] / [\lambda_{mx} - \lambda_{mn}] \quad (\text{Eq. J8.5.2-3})
 \end{aligned}$$

is the density function for PGV given a potentially damaging seismic ground motion event.

The distributions for PGV given a damaging seismic ground motion event are now considered. This development requires use of both $\lambda_G(v)$ and the conditional probability of nonzero damage $pWD_r(v|\delta_{I_r}, \delta_{R_r}, WT_r, R)$ defined in Equation J8.5.1-2. As in Section J8.5.1, the dependence of $pWD_r(v|\delta_{I_r}, \delta_{R_r}, WT_r, R)$ on r , δ_{I_r} , δ_{R_r} , WT_r and R will be suppressed for notational convenience and $pWD_r(v|\delta_{I_r}, \delta_{R_r}, WT_r, R)$ will simply be represented by $pWD(v)$.

The CDF for PGV given a damaging seismic ground motion event is defined by probabilities of the form

$$\begin{aligned}
 \text{prob}(\tilde{v} \leq v|D) &= \int_{v_{mn}}^v pWD(\tilde{v}) d_v(\tilde{v}|P) d\tilde{v} / \int_{v_{mn}}^{v_{mx}} pWD(\tilde{v}) d_v(\tilde{v}|P) d\tilde{v} \\
 &= \int_{v_{mn}}^v pWD(\tilde{v}) [d\lambda_G(\tilde{v})/d\tilde{v}] d\tilde{v} / \int_{v_{mn}}^{v_{mx}} pWD(\tilde{v}) [d\lambda_G(\tilde{v})/d\tilde{v}] d\tilde{v} \\
 &= (1/\lambda_D) \int_{v_{mn}}^v (-1) pWD(\tilde{v}) [d\lambda_G(\tilde{v})/d\tilde{v}] d\tilde{v}, \quad (\text{Eq. J8.5.2-4})
 \end{aligned}$$

where $\text{prob}(\tilde{v} \leq v|D)$ represents the probability of a PGV less than or equal to v given the occurrence of a seismic ground motion event with a PGV between v_{mn} and v_{mx} that causes WP damage (i.e., indicated by the conditionality notation “|D”) and λ_D is the frequency of damaging events defined in Equation J8.5.1-4. In turn,

$$\begin{aligned}
 d_v(v|D) &= \frac{d}{dv} \left[\text{prob}(\tilde{v} \leq v|D) \right] \\
 &= \frac{d}{dv} \left\{ (1/\lambda_D) \int_{v_{mn}}^v (-1) pWD(\tilde{v}) [d\lambda_G(\tilde{v})/d\tilde{v}] d\tilde{v} \right\} \\
 &= (-1/\lambda_D) pWD(v) [d\lambda_G(v)/dv] \quad (\text{Eq. J8.5.2-5})
 \end{aligned}$$

is the density function for PGV conditional on the occurrence of a seismic ground motion event with a PGV between v_{mn} and v_{mx} that causes WP damage.

As a reminder, $d_v(v|D)$ is actually of the form $d_{v_r}(v|\delta_{I_r}, \delta_{R_r}, WT_r, R, D)$ because of the dependence on $pWD_r(v|\delta_{I_r}, \delta_{R_r}, WT_r, R)$. Further, $d_v(v|P)$ and $d_v(v|D)$ are generally of the form $d_v(v|P, \mathbf{e})$ and $d_v(v|D, \mathbf{e})$ because of dependencies on epistemically uncertain quantities contained in \mathbf{e} .

J8.5.3 Distributions for Damaged Area on WPs

The distributions for damaged area on WPs conditional on the occurrence of a damaging seismic ground motion event derive from the hazard curve $\lambda_G(v)$ (see Equation J8.5.1-1) and the conditional density functions $d_{Ar}(A|v, \delta_{Ir}, \delta_{Rr}, WT_r, R)$, where

$$d_{Ar}(A|v, \delta_{Ir}, \delta_{Rr}, WT_r, R) = \text{density function (m}^{-2}\text{) for damaged area } A \text{ (m}^2\text{) on a WP of type } r \text{ conditional on the occurrence of a seismic ground motion event with PGV } v \text{ that results in a nonzero damaged area (see } pWD_r(v|\delta_{Ir}, \delta_{Rr}, WT_r, R)\text{) given the existence of conditions defined by } \delta_{Ir}, \delta_{Rr}, WT_r \text{ and } R. \quad (\text{Eq. J8.5.3-1})$$

For notational convenience, the dependence of $d_{Ar}(A|v, \delta_{Ir}, \delta_{Rr}, WT_r, R)$ on $r, \delta_{Ir}, \delta_{Rr}, WT_r$ and R will be suppressed and $d_{Ar}(A|v, \delta_{Ir}, \delta_{Rr}, WT_r, R)$ will simply be represented by $d_A(A|v, D)$, with the conditionality indicated by the notation “ $|v, D$ ”.

The CDF for damaged area on a WP given a damaging seismic ground motion event is defined by probabilities of the form

$$\begin{aligned} \text{prob}(\tilde{A} \leq A|D) &\equiv \sum_{j=1}^n \text{prob}(\tilde{A} \leq A|v_j, D) d_v(v_j|D) \Delta v_j \\ &= \sum_{j=1}^n \left[\int_0^A d_A(\tilde{A}|v_j, D) d\tilde{A} \right] d_v(v_j|D) \Delta v_j, \quad (\text{Eq. J8.5.3-2}) \end{aligned}$$

where $v_{mn} = v_0 < v_1 < \dots < v_n = v_{mx}$, $\text{prob}(\tilde{A} \leq A|D)$ represents the probability of a damaged area less than or equal to A given the occurrence of a damaging seismic ground motion event, and $\text{prob}(\tilde{A} \leq A|v_j, D)$ represents the probability of a damaged area less than or equal to A given the occurrence a damaging seismic ground motion event with PGV v_j . In turn,

$$\begin{aligned} \text{prob}(\tilde{A} \leq A|D) &\equiv \int_{v_{mn}}^{v_{mx}} \left[\int_0^A d_A(\tilde{A}|v, D) d\tilde{A} \right] d_v(v|D) dv \\ &= \int_0^A \left[\int_{v_{mn}}^{v_{mx}} d_A(\tilde{A}|v, D) d_v(v|D) dv \right] d\tilde{A} \quad (\text{Eq. J8.5.3-3}) \end{aligned}$$

as $\Delta v_j \rightarrow 0$.

The density function $d_A(A|D)$ for damaged area given a damaging seismic ground motion event can now be obtained by differentiating the cumulative probability $\text{prob}(\tilde{A} \leq A|D)$ defined in Equation J8.5.3-3. Specifically,

$$\begin{aligned}
 d_A(A|D) &= \frac{d}{dA} \left\{ \int_0^A \left[\int_{v_{mn}}^{v_{mx}} d_A(\tilde{A}|v, D) d_v(v|D) dv \right] d\tilde{A} \right\} \\
 &= \int_{v_{mn}}^{v_{mx}} d_A(A|v, D) d_v(v|D) dv \quad (\text{Eq. J8.5.3-4})
 \end{aligned}$$

is the density function for damaged area on a WP given a damaging seismic ground motion event.

As a reminder, $pWD_r(v|\delta_{I_r}, \delta_{R_r}, WT_r, R)$ and $d_{A_r}(A|v, \delta_{I_r}, \delta_{R_r}, WT_r, R)$ underlie the derivation of $d_A(A|D)$. Further, quantities such as R and $\lambda_G(v)$ that are either actually or potentially elements of \mathbf{e} are also involved. Thus, when a representation of the underlying conditionalities is included, the complete notation for $d_A(A|D)$ in Equation J8.5.3-4 becomes $d_{A_r}(A|\delta_{I_r}, \delta_{R_r}, WT_r, R, \mathbf{e}, D)$.

The density functions $d_{A1}(A|\mathbf{e})$ and $d_{A2}(A|\mathbf{e})$ defined in Equations J8.3-4 and J8.3-6 and appearing in Equations J8.3-7 and J8.3-8 are density functions of the form defined in Equation J8.5.3-4. Specifically,

$$\begin{aligned}
 d_{A1}(A|\mathbf{e}) &= \int_{v_{mn}}^{v_{mx}} d_{A2}(A|v, \delta_{I2} = 0, \delta_{R2} = 0, WT_2 = 23 \text{ mm}, R) \\
 &\quad \times d_{D2}(v|\delta_{I2} = 0, \delta_{R2} = 0, WT_2 = 23 \text{ mm}, R) dv \quad (\text{Eq. J8.5.3-5})
 \end{aligned}$$

and

$$\begin{aligned}
 d_{A2}(A|\mathbf{e}) &= \int_{v_{mn}}^{v_{mx}} d_{A2}(A|v, \delta_{I2} = 1, \delta_{R2} = 0, WT_2 = 23 \text{ mm}, R) \\
 &\quad \times d_{D2}(v|\delta_{I2} = 1, \delta_{R2} = 0, WT_2 = 23 \text{ mm}, R) dv. \quad (\text{Eq. J8.5.3-6})
 \end{aligned}$$

where (i) $d_{A2}(A|v, \delta_{I2}, \delta_{R2}, WT_2, R)$ is defined in Equation J8.2-6 and corresponds to $d_A(A|v, D)$ in Equation J8.5.3-4 and (ii) $d_{D2}(v|\delta_{I2}, \delta_{R2}, WT_2, R)$ is defined by

$$d_{D2}(v|\delta_{I2}, \delta_{R2}, WT_2, R) = \frac{pWD_2(v|\delta_{I2}, \delta_{R2}, WT_2, R) [d\lambda_G(v)/dv]}{\int_{v_{mn}}^{v_{mx}} pWD_2(\tilde{v}|\delta_{I2}, \delta_{R2}, WT_2, R) [d\lambda_G(\tilde{v})/d\tilde{v}] d\tilde{v}} \quad (\text{Eq. J8.5.3-7})$$

as indicated in Equations J8.5.2-5 and J8.5.1-4 with $\lambda_G(v)$ and $pWD_2(v|\delta_{I2}, \delta_{R2}, WT_2, R)$ defined in Equations J8.5.1-1 and J8.5.1-2 and corresponds to $d_v(v|D)$ in Equation J8.5.3-4. In the preceding, R and potentially $\lambda_G(v)$ are elements of \mathbf{e} .

The density functions $d_{A_r}(A|v, \delta_{I_r}, \delta_{R_r}, WT_r, R)$ for damaged area are not defined directly as input to the TSPA-LA. Rather, density functions $\tilde{d}_{A_r}(A|v, \delta_{I_r}, \delta_{R_r}, WT_r, R)$ for stressed area are defined as input. Then, within the computational implementation of the TSPA-LA, an

epistemically uncertain multiplicative scale factor SF (i.e., SF is an element of \mathbf{e}) is used to convert from stressed area A_S to damaged area A_D (i.e., $A_D = SF \times A_S$). As a result,

$$d_{Ar}(A|v, \delta_{Ir}, \delta_{Rr}, WT_r, R) = (1/SF) \tilde{d}_{Ar}(A/SF|v, \delta_{Ir}, \delta_{Rr}, WT_r, R). \quad (\text{Eq. J8.5.3-8})$$

The preceding equality follows from the relationship

$$d_w(w) = f_x \left[h^{-1}(w) \right] \left| dh^{-1}(w)/dw \right|, \quad (\text{Eq. J8.5.3-9})$$

where (i) x has a probability distribution defined over an interval (i.e., the values of x are continuous) with density function $f_x(x)$, (ii) $h(x)$ is a strictly monotonic function such that $w = h(x)$, and (iii) $d_w(w)$ is the density function for the resultant probability space for w (Hahn and Shapiro 1967 [DIRS 146529], Equation 5-7, p. 177). In the context of Equation J8.5.3-8,

$$h(A_S) = SF \times A_S = A_D, \quad h^{-1}(A_D) = A_D/SF, \quad dh^{-1}(A_D)/dA_D = 1/SF. \quad (\text{Eq. J8.5.3-10})$$

In terms of computational implementation, the density functions $d_{A1}(A|\mathbf{e})$ and $d_{A2}(A|\mathbf{e})$ in Equations J8.5.3-5 and J8.5.3-6 can either be (i) defined with $d_{Ar}(A|v, \delta_{Ir}, \delta_{Rr}, WT_r, R)$ as specified in Equation J8.5.3-8, with the result that damaged areas for use in Equations J8.3-7 and J8.3-8 are produced directly or (ii) defined with $\tilde{d}_{Ar}(A|v, \delta_{Ir}, \delta_{Rr}, WT_r, R)$, with the result that stressed areas are produced and the area A indicated in Equations J8.3-7 and J8.3-8 must be replaced by $SF \times A$.

J8.5.4 Distribution of Cumulative Rockfall Volume

The distribution of cumulative rockfall volume (m^3/m) as a function of time derives from the exceedance frequency $\lambda_G(v)$ for PGV v (see Equation J8.2-2), the probability of rockfall $pRV(v)$ conditional on the occurrence of a seismic ground motion event with PGV v (see Equation J8.2-3), and the density function $d_V(V|v)$ for volume V of rock that caves into a drift conditional on PGV v and the occurrence of rockfall (see Equation J8.2-4). Further, $d_V(V|v)$ is assumed to correspond to a gamma distribution with a mean $\mu(v)$ and standard deviation $\sigma(v)$ that are functions of PGV v .

In concept, it is desirable to determine $d_V(V_c|t)$, where $d_V(V_c|t)$ is the density function for cumulative rockfall V_c at time t . However, owing to the complexity of the interplay of $\lambda_G(v)$, $pRV(v)$ and $d_V(V|v)$, a closed form determination for $d_V(V_c|t)$ is difficult. However, the expected value $E_A(V_c|t)$ and variance $V_A(V_c|t)$ of cumulative rockfall volume V_c at time t are relatively easy to determine and so will be determined. Then, by recourse to the Central Limit Theorem, $E_A(V_c|t)$ and $V_A(V_c|t)$ can be used to estimate the distribution for rockfall volume $V_c(t)$ at time t . In the preceding, the subscript “A” on $E_A(V_c|t)$ and $V_A(V_c|t)$ indicates that the mean and variance for V_c derive from aleatory uncertainty.

Rockfall is assumed to follow what is known as a compound Poisson process. In such a process, events occur at a rate λ_R (yr^{-1}) with each event having the same distribution of possible values for an outcome V . Then, if $V_c(t)$ is the cumulative outcome of these events at time t (e.g., cumulative rockfall), the expected value $E_A(V_c|t)$ and variance $V_A(V_c|t)$ at time t for events occurring over the time interval $[0, t]$ is

$$E_A(V_c|t) = \lambda_R t E(V) \quad (\text{Eq. J8.5.4-1})$$

and

$$V_A(V_c|t) = \lambda_R t E(V^2), \quad (\text{Eq. J8.5.4-2})$$

where $E(V)$ and $E(V^2)$ denote the expectation of V and V^2 (Ross1993 [DIRS 172064], pp. 239-241). In this section, the outcomes of interest are rockfall volume V and the associated expected value $E_A(V_c|t)$ and variance $V_A(V_c|t)$ for cumulative rockfall V_c at time t . The subscript A is used to indicate $E_A(V_c|t)$ and $V_A(V_c|t)$ derive from aleatory uncertainty associated with the occurrence of seismic events.

The expectation $E(V)$ is given by

$$E(V) = \int_{v_{R,mn}}^{v_{R,mx}} \mu(v) d_v(v|R) dv, \quad (\text{Eq. J8.5.4-3})$$

where (i) $[v_{R,mn}, v_{R,mx}]$ is the range of PGVs that have the potential to cause rockfall, (ii)

$$\lambda_R = \int_{v_{R,mn}}^{v_{R,mx}} (-1) pRF(v) d\lambda_G(v) \quad (\text{Eq. J8.5.4-4})$$

is the occurrence rate (yr^{-1}) of rockfall events, and (iii)

$$d_v(v|R) = (-1/\lambda_R) pRF(v) [d\lambda_G(v)/dv] \quad (\text{Eq. J8.5.4-5})$$

is the density function for PGV conditional on the occurrence of rockfall. The derivations for λ_R and $d_v(v|R)$ are analogous to the derivations for λ_D and $d_v(v|D)$ in Equations J8.5.1-4 and J8.5.2-5. In turn, the representation

$$E_A(V_c|t) = t \left[\int_{v_{R,mn}}^{v_{R,mx}} (-1) \mu(v) pRF(v) [d\lambda_G(v)/dv] dv \right] \quad (\text{Eq. J8.5.4-6})$$

results when the values for $E(V)$, λ_R and $d_v(v|R)$ in Equations J8.5.4-3 – J8.5.4-5 are substituted into Equation J8.5.4-1.

The determination of $E(V^2)$ requires the density function $d_V(V|R)$ for rockfall volume V given the occurrence of rockfall. Specifically, $d_V(V|R)$ is given by

$$d_V(V|R) = \int_{v_{R,mn}}^{v_{R,mx}} d_V(V|v) d_v(v|R) dv, \quad (\text{Eq. J8.5.4-7})$$

where $d_V(V|v)$ is the density function for rockfall volume V given the occurrence of a rockfall at a PGV of v (i.e., a gamma distribution with mean $\mu(v)$ and standard deviation $\sigma(v)$ as previously indicated) and $d_v(v|R)$ is the density function for PGV v defined in Equation J8.5.4-5 given the occurrence of rockfall. In turn, $E(V^2)$ is given by

$$\begin{aligned} E(V^2) &= \int_{V_{R,mn}}^{V_{R,mx}} V^2 d_V(V|R) dV \\ &= \int_{V_{R,mn}}^{V_{R,mx}} V^2 \left\{ \int_{v_{R,mn}}^{v_{R,mx}} d_V(V|v) d_v(v|R) dv \right\} dV \\ &= \int_{V_{R,mn}}^{V_{R,mx}} V^2 \left\{ \int_{v_{R,mn}}^{v_{R,mx}} d_V(V|v) (-1/\lambda_R) pRF(v) [d\lambda_G(v)/dv] dv \right\} dV \\ &= (-1/\lambda_R) \int_{V_{R,mn}}^{V_{R,mx}} \int_{v_{R,mn}}^{v_{R,mx}} V^2 d_V(V|v) pRF(v) [d\lambda_G(v)/dv] dv dV, \quad (\text{Eq. J8.5.4-8}) \end{aligned}$$

where (i) the first integral corresponds to the definition of $E(V^2)$ with $[V_{R,mn}, V_{R,mx}]$ the range of possible values for V , (ii) the second integral results from the replacement of $d_V(V|v)$ by its representation in Equation J8.5.4-7, (iii) the third integral results from the replacement of $d_v(v|R)$ by its representation in Equation J8.5.4-5, and (iv) the final integral is an algebraic rearrangement of the third integral. Once $E(V^2)$ is determined, $V_A(V_c|t)$ can be determined as indicated in Equation J8.5.4-2.

J8.5.5 Probability of CDSP WP Rupture in 10^4 yr

The probability of the rupture of a CDSP WP in the time interval $[0, 10^4 \text{ yr}]$ is now considered. The probability of a rupture of a CDSP WP with a 23 mm thick outer corrosion barrier (OCB) and intact internals is zero. Thus, as there will be little reduction of OCB thickness in the $[0, 10^4 \text{ yr}]$ time interval, the probability that an initial seismic ground motion event in this time interval will result in a rupture is zero.

The first seismic ground motion event that damages the OCB is assumed to instantly result in degraded internals (an obviously conservative assumption). Thus, only second and subsequent seismic ground motions events have the potential to cause WP rupture. Such events have the potential to cause two types of damage relevant to the occurrence of rupture: (i) incipient rupture, and (ii) rupture. Incipient rupture corresponds to a condition in which the WP is weakened and thus more susceptible to rupture should additional events occur.

For a CDSP WP with degraded internals, a 23 mm thick OCB and freedom to move beneath the DS that experiences a seismic ground motion event with PGV v , the probabilities of incipient rupture and rupture are

$$pIRW(v) = \begin{cases} (0.0158)(v-1.05)^{1.8586} & \text{if } v \geq 1.05 \text{ m/s} \\ 0 & \text{otherwise} \end{cases} \quad (\text{Eq. J8.5.5-1})$$

and

$$pRW(v) = \begin{cases} (0.0474)(v-2.44)^{1.8586} & \text{if } v \geq 2.44 \text{ m/s} \\ 0 & \text{otherwise,} \end{cases} \quad (\text{Eq. J8.5.5-2})$$

respectively. The probabilities $pIRW(v)$ and $pRW(v)$ correspond to $pIRW_2(v|\delta_{I2} = 1, \delta_{R2} = 0, WT_2 = 23 \text{ mm})$ and $pRW_2(v|\delta_{I2} = 1, \delta_{R2} = 0, WT_2 = 23 \text{ mm})$ in Equations J8.2-9 and J8.2-10. In turn, the corresponding frequencies (yr^{-1}) of incipient rupture and rupture are

$$\lambda_{IR} = \int_{1.05}^{4.07} pIRW(v)(-1) d\lambda_G(v) \quad (\text{Eq. J8.5.5-3})$$

and

$$\lambda_R = \int_{2.44}^{4.07} pRW(v)(-1) d\lambda_G(v), \quad (\text{Eq. J8.5.5-4})$$

respectively.

Given λ_R , the probability $pR2(\tau)$ of the rupture of a CDSP WP due to two seismic events in the time interval $[0, \tau]$ with the first event causing WP damage and the second event causing WP rupture is

$$pR2(\tau) = \int_0^\tau \left(\exp[-\lambda_1(R)t] \right) \lambda_1(R) \{1 - \exp[-\lambda_R(\tau-t)]\} dt, \quad (\text{Eq. J8.5.5-5})$$

where $\lambda_1(R)$ corresponds to the rate term $\lambda_1(\mathbf{e})$ in Equation J8.3-3 with \mathbf{e} replaced by the residual stress threshold R , which is the only variable in \mathbf{e} that affects the definition of $\lambda_1(\mathbf{e})$ in the TSPA-LA. The rate $\lambda_1(R) = \lambda_1(\mathbf{e})$ is defined in Equation J8.5.1-5.

The preceding representation for $pR2(\tau)$ follows from the approximation

$$\begin{aligned}
 pR2 &\equiv \sum_{i=1}^n \left\{ \left(\exp[-\lambda_1(R)t_{i-1}] \right)_1 \left(1 - \exp[-\lambda_1(R)\Delta t_i] \right)_2 \right\}_1 \left\{ 1 - \exp[-\lambda_R(\tau - t_i)] \right\}_2 \\
 &\equiv \sum_{i=1}^n \left\{ \left(\exp[-\lambda_1(R)t_{i-1}] \right)_1 \left(\lambda_1(R)\Delta t_i \right)_3 \right\}_3 \left\{ 1 - \exp[-\lambda_R(\tau - t_i)] \right\}_2, \quad (\text{Eq. J8.5.5-6})
 \end{aligned}$$

where (i) $0 = t_0 < t_1 < \dots < t_n = \tau$, (ii) $(\sim)_1$ is the probability that no WP damage occurs in the time interval $[0, t_{i-1}]$, (iii) $(\sim)_2$ is the probability that WP damage occurs in the time interval $[t_{i-1}, t_i]$, (iv) $\{(\sim)_1, (\sim)_2\}_1$ is the probability that the first WP damage occurs in the time interval $[t_{i-1}, t_i]$, (v) $\{(\sim)_1, (\sim)_2\}_1 \{(\sim)_2\}_2$ is the probability that the first damaging event occurs in the time interval $[t_{i-1}, t_i]$ and is followed by an event that causes rupture in the time interval $[t_i, \tau]$, and (vi) $(\sim)_3$ is an approximation to $(\sim)_2$. The representation for $pR2(\tau)$ in Equation J8.5.5-6 then follows in the limit as $\Delta t_i \rightarrow 0$.

Similarly, the probability $pR3(\tau)$ of the rupture of a CDSP WP due to three seismic events in the time interval $[0, \tau]$ with the first event causing WP damage and the next two events causing incipient ruptures (which corresponds to the third event causing rupture) is

$$pR3(\tau) = \int_0^\tau \left(\exp[-\lambda_1(R)t] \right) \lambda_1(R) \left(\int_t^\tau \exp[-\lambda_{IR}(\tilde{t} - t)] \lambda_{IR} \left\{ 1 - \exp[-(\tau - \tilde{t})\lambda_{IR}] \right\} d\tilde{t} \right) dt. \quad (\text{J8.5.5-7})$$

The derivation of $pR3(\tau)$ is similar to the derivation of $pR2(\tau)$.

As an example, the values of $pR2(\tau)$ for $R = 90$ (i.e., 90 percent of the stress threshold) and $\tau = 10,000$ and $20,000$ yrs are estimated to be

$$pR2(10,000) = 8.3 \times 10^{-5} \quad (\text{J8.5.5-8})$$

and

$$pR2(20,000) = 1.7 \times 10^{-4} \quad (\text{J8.5.5-9})$$

respectively.

J8.6 Seismic Fault Displacement Scenario Class: \mathcal{A}_{SF}

As discussed in conjunction with Equation J8.1-2, the seismic fault displacement scenario class is defined by the subset \mathcal{A}_{SF} of \mathcal{A} . Formally, \mathcal{A}_{SF} contains all elements \mathbf{a} of \mathcal{A} with $nSF > 0$. To fully define \mathcal{A}_{SF} , it is necessary to first define the vector \mathbf{a}_{SF} indicated in Equation J8.1-9 and its associated components $\mathbf{a}_{SF,j}, j = 1, 2, \dots, nSF$.

Each component $\mathbf{a}_{SF,j}$ of \mathbf{a}_{SF} is defined by

$$\mathbf{a}_{SF,j} = [t_j, N_{1j}, N_{2j}, A_{1j}, A_{2j}, b_j, d_j] \quad (\text{Eq. J8.6-1})$$

where, for fault displacement event j ,

t_j = event time (yr),

N_{rj} = number of WPs of type r damaged (i.e., $r = 1 \sim$ CSNF WPs, $r = 2 \sim$ CDSP WPs),

A_{rj} = damaged area on a WP of type r ,

b_j = indicator variable for percolation bin containing damaged WPs (e.g., $b_j = k \sim$ location of failed WPs in percolation bin k for $k = 1, 2, 3, 4, 5$),

d_j = indicator variable for dripping/nondripping conditions experienced by damaged WPs

$$= \begin{cases} 1 & \text{if dripping conditions} \\ 0 & \text{if nondripping conditions.} \end{cases}$$

The following quantities are used to characterize the aleatory uncertainty associated with the elements of $\mathbf{a}_{SF,j}$:

$\lambda_{SF,r}$ = occurrence rate (yr^{-1}) for fault displacement events that damage WPs of type r , (Eq. J8.6-2)

$d_{N_r}(N_r)$ = density function defined on set \mathcal{N}_r for number of damaged WPs of type r given the occurrence of a fault displacement event, (Eq. J8.6-3)

$d_{A_r}(A_r)$ = density function (m^{-2}) defined on set \mathcal{A}_r for damaged area on a WP of type r damaged by a fault displacement event, (Eq. J8.6-4)

pBN_k = probability that damaged WPs are located in percolation bin k , $k = 1, 2, \dots, nBN$, given the occurrence of a fault displacement event, (Eq. J8.6-5)

$pDRP_{kl}$ = probability that damaged WPs in percolation bin k experience dripping condition l , $l = 0, 1$, with $l = 0 \sim$ nondripping conditions and $l = 1 \sim$ dripping conditions. (Eq. J8.6-6)

An alternate formulation is to specify $\lambda_{SF,r}$ and $d_{N_r}(N_r)$ through a hazard curve $\lambda_{SF,r}(N_r)$ defined for $0 < N_{mn,r} \leq N_r \leq N_{mx,r}$, where $\lambda_{SF,r}(N_r)$ is the frequency (yr^{-1}) of fault displacement events that damage N_r or more WPs of type r and $[N_{mn,r}, N_{mx,r}]$ is the range of possible values for N_r . Then,

$$\lambda_{SF,r} = \lambda_{SF,r}(N_{mn,r}), \quad (\text{Eq. J8.6-7})$$

$$d_{N_r}(N_r) = \left[-d\lambda_{SF,r}(N_r)/dN_r \right] / \left[\lambda_{SF,r}(N_{mn,r}) - \lambda_{SF,r}(N_{mx,r}) \right] \quad (\text{Eq. J8.6-8})$$

provided $\lambda_{SF,r}(N_r)$ is differentiable, and

$$\mathcal{N}_r = \{N_r : N_{mn,r} \leq N_r \leq N_{mx,r}\}. \quad (\text{Eq. J8.6-9})$$

If the hazard curve $\lambda_{SF,r}(N_r)$ is not continuous over the set \mathcal{N}_r , then a modification to the definition of $d_{N_r}(N_r)$ is necessary (e.g., if $\lambda_{SF,r}(N_r)$ is piecewise constant or, equivalently, if \mathcal{N}_r contains a finite number of elements).

Because multiple fault displacement events would damage different WPs at different locations and times, the dose $D_{SF}(\tau|\mathbf{a}_{SF}, \mathbf{e}_M)$ to the RMEI (mrem/yr) at time τ associated with the fault displacement future defined by

$$\mathbf{a}_{SF} = [nSF, \mathbf{a}_{SF,1}, \mathbf{a}_{SF,2}, \dots, \mathbf{a}_{SF,nSF}] \quad (\text{Eq. J8.6-10})$$

and the vector \mathbf{e}_M of epistemically uncertain quantities can be represented by

$$D_{SF}(\tau|\mathbf{a}_{SF}, \mathbf{e}_M) = \sum_{j=1}^{nSF} D_{SF}(\tau|[1, \mathbf{a}_{SF,j}], \mathbf{e}_M), \quad (\text{Eq. J8.6-11})$$

where

$$D_{SF}(\tau|[1, \mathbf{a}_{SF,j}], \mathbf{e}_M) = D_{SF}(\tau|[1, t_j, N_{1j}, N_{2j}, A_{1j}, A_{2j}, b_j, d_j], \mathbf{e}_M)$$

is the dose to the RMEI (mrem/yr) that derives from the fault displacement event characterized by $\mathbf{a}_{SF,j}$.

Further, given the occurrence of the event characterized by $\mathbf{a}_{SF,j}$, there are no synergisms between the doses that derive from the individual N_{1j} damaged CSNF WPs and the individual N_{2j} damaged CDSP WPs. As a result, the further simplification

$$\begin{aligned}
 D_{SF} \left(\tau \left[1, t_j, N_{1j}, N_{2j}, A_{1j}, A_{2j}, b_j, d_j \right], \mathbf{e}_M \right) \\
 &= \sum_{r=1}^2 D_{SF,r} \left(\tau \left[1, t_j, N_{rj}, A_{rj}, b_j, d_j \right], \mathbf{e}_M \right) \\
 &= \sum_{r=1}^2 \left(N_{rj} / \tilde{N}_r \right) D_{SF,r} \left(\tau \left[1, t_j, \tilde{N}_r, A_{rj}, b_j, d_j \right], \mathbf{e}_M \right) \quad (\text{Eq. J8.6-12})
 \end{aligned}$$

is possible, where

$$\begin{aligned}
 D_{SF,1} \left(\tau \left[1, t_j, N, A_{1j}, b_j, d_j \right], \mathbf{e}_M \right) &= D_{SF} \left(\tau \left[1, t_j, N, 0, A_{1j}, 0, b_j, d_j \right], \mathbf{e}_M \right), \\
 D_{SF,2} \left(\tau \left[1, t_j, N, A_{2j}, b_j, d_j \right], \mathbf{e}_M \right) &= D_{SF} \left(\tau \left[1, t_j, 0, N, 0, A_{2j}, b_j, d_j \right], \mathbf{e}_M \right),
 \end{aligned}$$

and \tilde{N}_r , $r = 1, 2$, is some computationally convenient number of damaged WPs (e.g., 1 or 100). The factoring of N_{rj} in Equation J8.6-12 is possible because dose is linear with respect to the number of damaged WPs.

In concept, the expected dose $\bar{D}_{SF}(\tau|\mathbf{e})$ to the RMEI is defined by the integral

$$\bar{D}_{SF}(\tau|\mathbf{e}) = \int_{\mathcal{A}_{SF}} D_{SF}(\tau|\mathbf{a}_{SF}, \mathbf{e}_M) d_A(\mathbf{a}_{SF}|\mathbf{e}_A) dA. \quad (\text{Eq. J8.6-13})$$

In turn, the representations for $D_{SF}(\tau|\mathbf{a}_{SF}, \mathbf{e}_M)$ and $D_{SF}(\tau[1, t_j, N_{1j}, N_{2j}, A_{1j}, A_{2j}, b_j, d_j], \mathbf{e}_M)$ in Equations J8.6-11 and J8.6-12 permit a more explicit and computationally tractable representation for the defining integral for $\bar{D}_{SF}(\tau|\mathbf{e})$. Specifically, $\bar{D}_{SF}(\tau|\mathbf{e})$ can be represented by

$$\begin{aligned}
 \bar{D}_{SF}(\tau|\mathbf{e}) &= \sum_{r=1}^2 \sum_{k=1}^{nBN} \sum_{l=0}^1 (pBN_k pDRP_{kl}) \\
 &\times \left(\int_0^\tau \left\{ \int_{\mathcal{A}_r} \left[\int_{\mathcal{N}_r} D_{SF,r}(\tau[1, t, N_r, A_r, b_k, d_l], \mathbf{e}_M) d_{N_r}(N_r) dN_r \right]_{-1} d_{A_r}(A_r) dA_r \right\}_2 \lambda_{SF,r} dt \right)_3, \quad (\text{Eq. J8.6-14})
 \end{aligned}$$

where (i) the integral in $[-]_1$ is expected dose at time τ from WP package type r conditional on $A_r, b_k, d_l, \mathbf{e}_M$ and t , (ii) the double integral in $\{\sim\}_2$ is the expected dose at time τ from WP type r conditional on b_k, d_l, \mathbf{e}_M and t , (iii) the triple integral in $(\sim)_3$ is the expected dose at time τ from WP type r conditional on b_k, d_l and \mathbf{e}_M . Then, the summations on k and l and the associated

multiplication of $(\sim)_3$ by $pBN_k pDRP_{kl}$ removes the conditionality on b_k and d_l for WP type r . Finally, the summation on r combines the expected doses for the individual WP types and leaves only the conditionality on \mathbf{e}_M .

In turn, the simpler representation

$$\begin{aligned} \bar{D}_{SF}(\tau|\mathbf{e}) &= \sum_{r=1}^2 \left[\bar{N}_r \lambda_{SF,r} / \tilde{N}_r \right] \left[\sum_{k=1}^{nBN} \sum_{l=0}^1 (pBN_k pDRP_{kl}) \right] \\ &\times \left(\int_0^\tau \left\{ \int_{\mathcal{A}_r} D_{SF,r}(\tau|[1, t, \tilde{N}_r, A_r, b_k, d_l], \mathbf{e}_M) d_{A_r}(A_r) dA_r \right\} dt \right) \quad (\text{Eq. J8.6-15}) \end{aligned}$$

results from the linear relationship between dose and number of damaged WPs indicated in Equation J8.6-12, where

$$\bar{N}_r = \int_{\mathcal{N}_r} N_r d_{N_r}(N_r) dN_r \quad (\text{Eq. J8.6-16})$$

is the expected number of damaged WPs of type r .

For implementation in the TSPA-LA, the division of the repository into multiple percolation bins is not considered for fault displacement events. Rather, the entire repository is treated as a single percolation bin with 100 failed WPs of a given type spread over this “bin.” In this implementation, the number nB_k of WPs assigned to each of the $k = 1, 2, 3, 4, 5$ original percolation bins is $nB_k = pBN_k(100)$. Further, the numbers nB_{kl} , $l = 0, 1$, of WPs assigned to nondripping ($\sim l = 0$) and dripping ($\sim l = 1$) conditions in percolation bin k are $nB_{kl} = pDRP_{kl} nB_k$ for $l = 0, 1$. With this simplification, the representation for $\bar{D}_{SF}(\tau|\mathbf{e})$ in Equation J8.6-15 reduces to

$$\begin{aligned} \bar{D}_{SF}(\tau|\mathbf{e}) &= \sum_{r=1}^2 (\bar{N}_r \lambda_{SF,r} / 100) \left(\int_0^\tau \left\{ \int_{\mathcal{A}_r} D_{SF,r}(\tau|[1, t, 100, A_r, 1, \sim], \mathbf{e}_M) d_{A_r}(A_r) dA_r \right\} dt \right) \\ &= \sum_{r=1}^2 \bar{D}_{SF,r}(\tau|\mathbf{e}), \quad (\text{Eq. J8.6-17}) \end{aligned}$$

where the “ d_l ” has been replaced by “ \sim ” to indicate that the presence of nondripping and dripping conditions is now incorporated into the locations assigned to the individual WPs and

$$\bar{D}_{SF,r}(\tau|\mathbf{e}) = (\bar{N}_r \lambda_{SF,r} / 100) \left(\int_0^\tau \left\{ \int_{\mathcal{A}_r} D_{SF,r}(\tau|[1, t, 100, A_r, 1, \sim], \mathbf{e}_M) d_{A_r}(A_r) dA_r \right\} dt \right).$$

In turn, evaluation of the preceding representation for $\bar{D}_{SF}(\tau|\mathbf{e})$ requires the evaluation of two double integrals; specifically, one double integral for CSNF WPs (i.e., for $r = 1$) and one double integral for CDSP WPs (i.e., for $r = 2$).

The preceding integrations must be carried out for each element of the LHS indicated in Equation J4.9-1. To support these integrations,

$$D_{SF,r} \left(\tau \left| \left[1, t_j, 100, A_{rk}, 1, \sim \right], \mathbf{e}_{Mi} \right. \right) \quad (\text{Eq. J8.6-18})$$

must be evaluated for (i) $r = 1, 2$, (ii) $0 \leq \tau \leq 20,000$ yr or $0 \leq \tau \leq 10^6$ yr, (iii) a sequence of event times $0 < t_1 < t_2 < \dots < t_m$ from the intervals $[0, 20,000$ yr] and $[0, 10^6$ yr], (iv) a sequence of damaged areas $0 < A_{r1} < A_{r2} < \dots < A_{rm}$, where A_{rm} is an upper bound for the set \mathcal{A}_r , and (v) \mathbf{e}_{Mi} , $i = 1, 2, \dots, nLHS$.

In the TSPA-LA for the $[0, 20,000$ yr] time interval, the $m = 6$ event times t_1, t_2, \dots, t_m are

$$200, 800, 2000, 4000, 8000, 18,000 \text{ yrs}; \quad (\text{Eq. J8.6-19})$$

the $n = 3$ areas A_{11}, A_{12}, A_{13} are

$$A_1/3, 2A_1/3, A_1, \quad (\text{Eq. J8.6-20})$$

where $A_1 = 2.78 \text{ m}^2$ is the cross-sectional area (m^2) of a CSNF WP; and the $n = 3$ areas A_{21}, A_{22}, A_{23} are

$$A_2/3, 2A_2/3, A_2, \quad (\text{Eq. J8.6-21})$$

where $A_2 = 3.28 \text{ m}^2$ is the cross-sectional area of a CDSP WP. For the $[0, 10^6$ yr] time interval, the $m = 6$ times t_1, t_2, \dots, t_m are

$$1000, 20,000, 80,000, 200,000, 400,000, 800,000 \text{ yrs}; \quad (\text{Eq. J8.6-22})$$

and the cross-sectional areas for CSNF and CDSP WPs are the same as in Equations J8.6-20 and J8.6-21, respectively. Selected results for the $[0, 20,000$ yr] time interval are shown in Figures J8.6-1 and J8.6-2.

Once the preceding results are available, quadrature procedures can be used to evaluate $\bar{D}_{SF}(\tau|\mathbf{e}_{Mi})$ for $i = 1, 2, \dots, nLHS$. Specifically, the double integral in Equation J8.6-17 is approximated by

$$\int_0^\tau \left\{ \int_{\mathcal{A}_r} D_{SF,r}(\tau|[1, t, 100, A_r, 1, \sim], \mathbf{e}_{Mi}) d_{A_r}(A_r) dA_r \right\} dt$$

$$\cong \sum_{k=1}^n \left\{ \sum_{l=1}^m \hat{D}_{SF,r}(\tau|[1, \hat{t}_k, 100, \hat{A}_{rl}, 1, \sim], \mathbf{e}_{Mi}) \Delta \hat{A}_{rl} \right\} \Delta \hat{t}_k, \quad (\text{Eq. J8.6-23})$$

where $0 = \hat{t}_0 < \hat{t}_1 < \dots < \hat{t}_n = \tau$ is a subdivision of $[0, \tau]$, (ii) $A_{mn,r} = \hat{A}_{r0} < \hat{A}_{r1} < \dots < \hat{A}_{rm} = A_{mx,r}$ is a subdivision of $\mathcal{A}_r = [A_{mn,r}, A_{mx,r}]$, and (iii) $\hat{D}(\tau|[1, \hat{t}_k, 100, \hat{A}_{rl}, 1, \sim], \mathbf{e}_{Mi})$ is an approximation to $D(\tau|[1, \hat{t}_k, 100, \hat{A}_{rl}, 1, \sim], \mathbf{e}_{Mi})$ obtained with interpolation procedures from the results in Equation J8.6-18. Then,

$$\bar{D}_{SF}(\tau|\mathbf{e}_i) \cong \sum_{r=1}^2 (\bar{N}_r, \lambda_{SF,r}/100) \left(\sum_{k=1}^n \left\{ \sum_{l=1}^m \hat{D}_{SF,r}(\tau|[1, \hat{t}_k, 100, \hat{A}_{rl}, 1, \sim], \mathbf{e}_{Mi}) \Delta \hat{A}_{rl} \right\} \Delta \hat{t}_k \right)$$

(Eq. J8.6-24)

is the desired approximation to $\bar{D}_{SF}(\tau|\mathbf{e}_i)$.

An alternative computational strategy that involves fewer interpolations is to approximate $\bar{D}_{SF}(\tau|\mathbf{e}_i)$ by

$$\bar{D}_{SF}(\tau|\mathbf{e}_i) \cong \sum_{r=1}^2 [\bar{N}_r \lambda_{SF,r}/100] \left[\sum_{k=1}^n \hat{I}_r(\tau|\hat{t}_k, \mathbf{e}_{Mi}) \Delta \hat{t}_k \right], \quad (\text{Eq. J8.6-25})$$

where, for a given time t , $\hat{I}_r(\tau|t, \mathbf{e}_{Mi})$ is an approximation to the integral

$$I_r(\tau|t, \mathbf{e}_{Mi}) = \int_{\mathcal{A}_r} D_{SF,r}(\tau|[1, t, A_r, 1, \sim], \mathbf{e}_{Mi}) d_{A_r}(A_r) dA_r \quad (\text{Eq. J8.6-26})$$

for $r = 1, 2$. For numerical implementation, the approximations

$$\hat{I}_r(\tau|t_j, \mathbf{e}_{Mi}) = \sum_{l=1}^m \hat{D}_{SF,r}(\tau|[1, t_j, 100, \hat{A}_{rl}, 1, \sim], \mathbf{e}_{Mi}) \Delta \hat{A}_{rl} \quad (\text{Eq. J8.6-27})$$

can be determined for the times $t_j, j = 1, 2, \dots, 6$, in Equation J8.6-19 with the areas \hat{A}_{rl} determined the same as in Equation J8.6-23. Once the values for $\hat{I}_r(\tau|t_j, \mathbf{e}_{Mi})$ are determined for $r = 1, 2$ and $j = 1, 2, \dots, 6$, the required values for $\hat{I}_r(\tau|\hat{t}_k, \mathbf{e}_{Mi})$ in Equation J8.6-25 can be determined by interpolation as illustrated in Figure J8.6-3. In addition, the expected doses from the individual WP types are approximated by

$$\bar{D}_{SF,r}(\tau|\mathbf{e}_i) \cong \left[\bar{N}_r \lambda_{SF,r} / 100 \right] \left[\sum_{k=1}^n \hat{I}_r(\tau|\hat{t}_k, \mathbf{e}_{Mi}) \right] \quad (\text{Eq. J8.6-28})$$

for $r = 1, 2$. Use of the approximation to $\bar{D}_{SF}(\tau|\mathbf{e}_i)$ in Equation J8.6-25 rather than the approximation in Equation J8.6-24 reduces the number of required interpolations by a factor of approximately 3 (see Equation J8.6-20).

Some additional elaboration on Figure J8.6-3 follows. As noted in the caption for Figure J8.6-3, the results for the three damaged areas under consideration (see Equations J8.6-20 and J8.6-21) are the same for each event time. As a result, the three dose curves for the three damaged areas for each event time exactly overlay in Figure J8.6-3a; if this was not the case, Figure J8.6-3a would look like Figure J8.3-3a but with three rather than five dose curves for each event time. As a result, the integral $I_1(\tau|t_j, \mathbf{e}_{M1})$ in Equation J8.6-26 and its approximation $\hat{I}_1(\tau|t_j, \mathbf{e}_{Mi})$ in Equation J8.6-27 are effectively the same as the dose curves in Figure J8.6-3a. Further, again as noted in the caption to Figure J8.6-3, the results for t_1 and t_2 overlay; thus, Figure J8.6-3a appears to contain five curves when, in actuality, it contains eighteen curves. The results in Figure J8.6-3b,c illustrate interpolated values $\hat{I}_1(\tau|\hat{t}_k, \mathbf{e}_{Mi})$ obtained from $\hat{I}_1(\tau|t_j, \mathbf{e}_{Mi})$. Finally, the expected doses $\bar{D}_{SF,1}(\tau|\mathbf{e}_1)$ and $\bar{D}_{SF,2}(\tau|\mathbf{e}_1)$ for CSNF and CDSP WPs, respectively, defined in Equation J8.6-28 and the expected dose $\bar{D}_{SF}(\tau|\mathbf{e}_1)$ for CSNF and CDSP WPs defined in Equation (J8.6-25) are shown in Figure J8.6-3d.

As an example, the estimate for $\bar{D}_{SF}(\tau|\mathbf{e}_1)$ obtained for LHS element \mathbf{e}_1 with the procedure indicated in Equation J8.6-25 is shown in Figure J8.6-4. Further, the results obtained with all $nLHS = 300$ LHS elements are summarized in Figure J8.6-5 and presented in a standard format in Figure J8.6-6.

As previously discussed in conjunction with Equations J5-8 and J6.2-9, dose and expected dose to the RMEI are just two of a large number of results that can be produced and presented in the TSPA-LA. As an example, a summary of the dose calculations for ^{99}Tc is given in Figure J8.6-7, which has the same organization as Figure J8.6-5. Overall, ^{99}Tc is one of the largest contributors to the expected (mean) dose $\bar{\bar{D}}_{SF}(\tau)$ for the 20,000 yr time period. As previously done in Figure J5-4 and other similar figures, a compact summary of the expected (mean) dose results $\bar{\bar{D}}_{SF,r}(\tau)$ for the individual radioactive species is provided in Figure J8.6-8, where $\bar{\bar{D}}_{SF,r}(\tau)$ is the expected (mean) dose to the RMEI at time τ resulting from the release of radioactive species r due to fault displacement events (see Equation J6.2-9 and associated discussion).

The results in Equation J8.6-18 can also be used in a Monte Carlo procedure to provide both (i) an alternate calculation of $\bar{D}_{SF}(\tau|\mathbf{e}_i)$ and (ii) distributions for $D_{SF}(\tau|\mathbf{a}, \mathbf{e}_{Mi})$ at a sequence of values for τ . It is not necessary to consider correlations between the numbers of damaged CSNF

and CDSP WPs in the determination of $\bar{D}_{SF}(\tau|\mathbf{e})$. However, such correlations are potentially important in the determination of distributions for $D_{SF}(\tau|\mathbf{a}, \mathbf{e}_{Mi})$ for individual values of τ .

In the TSPA-LA, the occurrence of fault displacement events is characterized by hazard curves of the form discussed in conjunction with Equations J8.6-7 – J8.6-9. Further, it is specified that there is a perfect correlation between the numbers of damaged WPs obtained from the hazard curves for individual WP types (i.e., CSNF and CDSP WPs in the TSPA-LA). What perfect correlation means with respect to the indicated hazard curves is that the specific numbers of damaged WPs for a given fault displacement event is obtained by selecting a random number on the ordinate of a plot containing the hazard curves and then moving horizontally across the plot to determine the number of damaged WPs of each type.

When the hazard curves are piecewise constant, the sampling procedure indicated in the preceding paragraph results in a finite number of pairs of values $(N_{1j}, N_{2j}), j = 1, 2, \dots, m$, for the numbers of damaged WPs given the occurrence of a damaging fault displacement event, where N_{1j} is the number of damaged CSNF WPs and N_{2j} is the number of damaged CDSP WPs. Further, each pair (N_{1j}, N_{2j}) has a conditional probability pN_j given the occurrence of a damaging fault displacement event.

In the TSPA-LA, the hazard curves for WP damage from fault displacement are piecewise constant. As a result, the possible combinations of damaged WPs given by a fault displacement event can be described by a sequence of the form

$$\left[pN_j, (N_{1j}, N_{2j}) \right], j = 1, 2, \dots, m. \quad (\text{Eq. J8.6-29})$$

More specifically, the occurrence rate for damaging fault displacement events is

$$\lambda_{SF} = \max \{ \lambda_{SF,1}, \lambda_{SF,2} \} = 2.5 \times 10^{-7} \text{ yr}^{-1}. \quad (\text{Eq. J8.6-30})$$

Further, the specified hazard curves for CSNF and CDSP WPs result in the following $m = 8$ results in the sequence in Equation J8.6-29: $[0.12, (0, 6.5)]$, $[0.24, (19.5, 6.5)]$, $[0.08, (19.5, 9.3)]$, $[0.216, (27.7, 9.3)]$, $[0.032, (27.7, 10.3)]$, $[0.196, (30.7, 10.3)]$, $[0.004, (30.7, 53.2)]$, $[0.112, (158.8, 53.2)]$.

Given the results in Equation J8.6-29 and the frequency λ_{SF} in Equation J8.6-30, the generation of a sampling based distribution for $D_{SF}(\tau|\mathbf{a}, \mathbf{e}_{Mi})$ and an associated estimate for $\bar{D}_{SF}(\tau|\mathbf{e}_i)$ is straightforward. The probability of a fault displacement event in the time interval $[0, \tau]$ is small. Thus, the appropriate computational strategy is to directly calculate

$$\text{prob}_A \left[\mathcal{A}_{SF}(0, \tau) | \mathbf{e}_{Ai} \right] = 1 - \exp(-\lambda_{SF} \tau), \quad (\text{Eq. J8.6-31})$$

which is the probability that one or more WPs will be damaged by one or more fault displacement events in the time interval $[0, \tau]$ (i.e., the notation $\mathcal{A}_{SF}(0, \tau)$ indicates a restriction

to fault displacement events occurring in the time interval $[0, \tau]$). In turn, the probability of exceeding a dose of size D given a damaging fault displacement event is given by

$$prob_A \left[D < D_{SF}(\tau | \mathbf{a}_{SF}) \middle| \mathcal{A}_{SF}(0, \tau), \mathbf{e}_i \right] \cong \sum_{k=1}^{nR} \bar{\delta}_D \left[D_{SF}(\tau | \mathbf{a}_{SF,k}, \mathbf{e}_{Mi}) \right] / nR, \quad (\text{Eq. J8.6-32})$$

where each sampled future $\mathbf{a}_{SF,k}$ is a future of the form \mathbf{a}_{SF} defined in Equation J4.4-8 with components $\mathbf{a}_{SF,jk}$ of the form indicated in Equation J8.6-1 generated under the assumption that one or more damaging fault displacement events have occurred in the time interval. Specifically, the component vectors

$$\mathbf{a}_{SF,jk} = [t_j, N_{1j}, N_{2j}, A_{1j}, A_{2j}, 1, d_j], \quad j = 1, 2, \dots, nSF_k, \quad (\text{Eq. J8.6-33})$$

for a sampled future

$$\mathbf{a}_{SF,k} = [nSF_k, \mathbf{a}_{SF,1k}, \mathbf{a}_{SF,2k}, \dots, \mathbf{a}_{SF,nSF_k,k}] \quad (\text{Eq. J8.6-34})$$

are generated by (i) sampling the event times $0 < t_1 < t_2 < \dots < t_{nSF_k} < \tau$ in consistency with λ_{SF} and the assumption that one or more damaging fault displacement events have occurred in the time interval $[0, \tau]$, (ii) sampling the pairs $(N_{1j}, N_{2j}), j = 1, 2, \dots, nSF_k$, in consistency with the probabilities pN_j indicated in Equation J8.6-29, and (iii) sampling the quantities A_{1j}, A_{2j} and d_j in consistency with their assigned distributions for $j = 1, 2, \dots, nSF_k$. When $\lambda_{SF}\tau$ is substantially less than one, $\mathbf{a}_{SF,k}$ will have the form $\mathbf{a}_{SF,k} = [t, N_1, N_2, A_1, A_2, 1, d]$ for almost all sampled futures with (i) t having a uniform distribution on $[0, \tau]$, (ii) the pair (N_1, N_2) sampled in consistency with the probabilities pN_j indicated in Equation J8.6-29, and (iii) and areas A_1 and A_2 and the dripping indicator sampled in consistency with their assigned distributions. In the current TSPA-LA analysis, the indicator d is not sampled because the effects of dripping/nondripping conditions are incorporated directly into the determination of $D_{SF,r}(\tau | [1, t, 100, A_r, 1, \sim], \mathbf{e}_M)$ as indicated in conjunction with Equation J8.6-17.

The required evaluation of $D_{SF}(\tau | \mathbf{a}_{SF,k}, \mathbf{e}_{Mi})$ in Equation J8.6-32 follows from the relationships

$$\begin{aligned} D_{SF}(\tau | \mathbf{a}_{SF,k}, \mathbf{e}_{Mi}) &= \sum_{j=1}^{nSF_k} D_{SF}(\tau | [1, \mathbf{a}_{SF,jk}], \mathbf{e}_{Mi}) \\ &= \sum_{j=1}^{nSF_k} \sum_{r=1}^2 (N_{rj}/100) D_{SF,r}(\tau | [1, t_j, 100, A_{rj}, 1, \sim], \mathbf{e}_{Mi}), \end{aligned} \quad (\text{Eq. J8.6-35})$$

where $D_{SF,r}(\tau | [1, t_j, 100, A_{rj}, 1, \sim], \mathbf{e}_{Mi})$ is defined in conjunction with (J8.6-17) for $r = 1$ and 2 . The specific values for $D_{SF,r}(\tau | [1, t_j, 100, A_{rj}, 1, \sim], \mathbf{e}_{Mi})$ required in the evaluation of

$D_{SF}(\tau|\mathbf{a}_{SF,k}, \mathbf{e}_{Mi})$ in Equation J8.6-35 and hence in Equation J8.6-28 can be obtained with interpolation procedures from the precalculated results indicated in Equations J8.6-18 – J8.6-22 and are denoted by $\hat{D}_{SF,r}(\tau|[1, t_j, 100, A_{rj}, 1, \sim], \mathbf{e}_{Mi})$.

Together, the results in Equations J8.6-31 and J8.6-32 define the CCDF for dose to the RMEI (mrem/yr) at time τ from fault displacement events. Specifically, the probability of exceeding dose D at time τ is given by

$$\begin{aligned} & \text{prob}_A \left[D < D_{SF}(\tau|\mathbf{a}_{SF}) \middle| \mathbf{e}_i \right] \\ &= \text{prob}_A \left[A_{SF}(0, \tau) \middle| \mathbf{e}_{Ai} \right] \text{prob}_A \left[D < D_{SF}(\tau|\mathbf{a}_{SF}) \middle| A_{SF}(0, \tau), \mathbf{e}_i \right] \text{ (Eq. J8.6-36)} \end{aligned}$$

with $\text{prob}_A[A_{SF}(0, \tau)|\mathbf{e}_{Ai}]$ and $\text{prob}_A[D < D_{SF}(\tau|\mathbf{a}_{SF})|A_{SF}(0, \tau), \mathbf{e}_i]$ defined in Equations J8.6-31 and J8.6-32, respectively. The preceding corresponds to the calculation described in conjunction with Equation J4.5-19 with $C = SF$. A similar calculation leads to the CDF for dose to the RMEI for fault displacements as described in conjunction with Equation J4.5-21 for $C = SF$. This process is illustrated in Figures J8.6-9 and J8.6-10.

As discussed in Section J4.10, the numerical stability of results obtained with Latin hypercube sampling can be assessed with replicated sampling. Specifically, the analysis for fault displacement events was performed with the $nRL = 3$ replicated LHSs indicated in Equation J4.10-1. In turn, this analysis shows that the numerical error in using Latin hypercube sampling to estimate $\bar{D}_{SF}(\tau)$ is small relative to the epistemic uncertainty associated with the possible values for $\bar{D}_{SF}(\tau|\mathbf{e})$ (Figure J8.6-11).

The results presented in Figures J8.6-1 to J8.6-11 are for the time period [0, 20,000 yr]. Corresponding results for the time period [0, 10^6 yr] are presented without discussion in Figures J8.6-12 to J8.6-22.

J8.7 Seismic Scenario Class: \mathcal{A}_S

The results $\bar{D}_{SG}(\tau|\mathbf{e}_i)$ and $\bar{D}_{SG}(\tau)$ obtained for the seismic ground motion scenario class \mathcal{A}_{SG} are generally much larger than the corresponding results $\bar{D}_{SF}(\tau|\mathbf{e}_i)$ and $\bar{D}_{SF}(\tau)$ obtained for the seismic fault displacement scenario class \mathcal{A}_{SF} . The only exceptions to this occur for LHS elements that result in very small values for $\bar{D}_{SG}(\tau|\mathbf{e}_i)$, in which case $\bar{D}_{SG}(\tau|\mathbf{e}_i)$ and $\bar{D}_{SF}(\tau|\mathbf{e}_i)$ have similar values. As a result, $\bar{D}_S(\tau|\mathbf{e}_i)$ and $\bar{D}_S(\tau)$ for the seismic scenario class \mathcal{A}_S are effectively the same as $\bar{D}_{SG}(\tau|\mathbf{e}_i)$ and $\bar{D}_{SG}(\tau)$ and are not presented as separate figures for this reason.

J8.8 Probabilities Associated with Seismic Scenario Classes

The probabilities $p_A(\mathcal{A}_{SG})$, $p_A(\mathcal{A}_{SF})$ and $p_A(\mathcal{A}_S)$ for the scenario classes \mathcal{A}_{SG} , \mathcal{A}_{SF} and \mathcal{A}_S depend on the time interval under consideration. In the TSPA-LA, the time intervals of primary interest are $[0, 20,000 \text{ yr}]$ and $[0, 1,000,000 \text{ yr}]$. However, for generality, a time interval $[0, \tau]$ is assumed to be under consideration and $\mathcal{A}_{SG}(0, \tau)$, $\mathcal{A}_{SF}(0, \tau)$ and $\mathcal{A}_S(0, \tau)$ will represent \mathcal{A}_{SG} , \mathcal{A}_{SF} and \mathcal{A}_S defined with futures (i.e., seismic event occurrences) restricted to $[0, \tau]$. Formally, this corresponds to restricting the sample spaces (i.e., sets of possible futures) under consideration to futures defined on the time interval $[0, \tau]$. The notation for $p_A(\mathcal{A}_{SG})$, $p_A(\mathcal{A}_{SF})$ and $p_A(\mathcal{A}_S)$ does not include a dependence on the vector \mathbf{e} of epistemically uncertain analysis inputs because the TSPA-LA does not include any uncertain analysis inputs (i.e., elements of \mathbf{e}) that affect the values of these probabilities.

The seismic ground motion scenario class $\mathcal{A}_{SG}(0, \tau)$ is assumed to be defined by the properties of seismic ground motion events that have a PGV greater than or equal to 0.219 m/s and an associated exceedance frequency of $4.287 \times 10^{-4} \text{ yr}^{-1}$ (i.e., $v_{mn} = 0.219 \text{ m/s}$ and $\lambda_{mx} = 4.287 \times 10^{-4} \text{ yr}^{-1}$ in previously used notation). In turn,

$$\begin{aligned}
 p_A[\mathcal{A}_{SG}(0, \tau)] &= 1 - \exp(-\lambda_{mx}\tau) \\
 &= \begin{cases} 0.99 & \text{for } \tau = 10^4 \text{ yr} \\ 1.00 & \text{for } \tau = 2 \times 10^4 \text{ yr} \\ 1.00 & \text{for } \tau = 10^6 \text{ yr} \end{cases} \quad (\text{Eq. J8.8-1})
 \end{aligned}$$

as indicated in Equation J3.6-9.

The seismic fault displacement scenario class $\mathcal{A}_{SF}(0, \tau)$ is assumed to be defined by the properties of fault displacement events that have an occurrence frequency of $\lambda_{SF} = 2.5 \times 10^{-7} \text{ yr}^{-1}$. In turn,

$$\begin{aligned}
 p_A[\mathcal{A}_{SF}(0, \tau)] &= 1 - \exp(-\lambda_{SF}\tau) \\
 &= \begin{cases} 2.50 \times 10^{-3} & \text{for } \tau = 10^4 \text{ yr} \\ 4.99 \times 10^{-3} & \text{for } \tau = 2 \times 10^4 \text{ yr} \\ 0.22 \times 10^0 & \text{for } \tau = 10^6 \text{ yr} \end{cases} \quad (\text{Eq. J8.8-2})
 \end{aligned}$$

as indicated in Equation J3.6-9.

If the occurrence of fault displacement events is included in the determination of λ_{mx} for seismic ground motion events, then $p_A[\mathcal{A}_S(0, \tau)] = p_A[\mathcal{A}_{SG}(0, \tau)]$. If the occurrence of fault displacement events is not included in the determination of λ_{mx} , then the occurrence rate λ_S for seismic events

is given by $\lambda_S = \lambda_{mx} + \lambda_{SF}$ as indicated in Equation J3.6-13. However, given that $\lambda_{mx} = 4.287 \times 10^{-4} \text{ yr}^{-1}$ and $\lambda_{SF} = 2.5 \times 10^{-7} \text{ yr}^{-1}$, λ_S in this case is effectively the same as λ_{mx} . As a result, there is no meaningful difference between $p_A[\mathcal{A}_S(0, \tau)]$ and $p_A[\mathcal{A}_{SG}(0, \tau)]$.

J9 EXPECTED DOSE FROM ALL SCENARIO CLASSES

J9.1 Expected Dose from All Scenario Classes: Preliminaries

As indicated in Equation J4.5-1, the TSPA-LA assumes that expected dose to the RMEI at time τ from aleatory uncertainty can be approximated by

$$\begin{aligned} \bar{D}(\tau|\mathbf{e}) \cong & D_N(\tau|\mathbf{a}_N, \mathbf{e}_M) + \bar{D}_{EW}(\tau|\mathbf{e}) + \bar{D}_{ED}(\tau|\mathbf{e}) + \bar{D}_{II}(\tau|\mathbf{e}) \\ & + \bar{D}_{IE}(\tau|\mathbf{e}) + \bar{D}_{SG}(\tau|\mathbf{e}) + \bar{D}_{SF}(\tau|\mathbf{e}) \end{aligned} \quad (\text{Eq. J9.1-1})$$

conditional on the element $\mathbf{e} = [\mathbf{e}_A, \mathbf{e}_M]$ of \mathcal{E} . In turn, the expected (mean) dose to the RMEI at time τ from aleatory and epistemic uncertainty is approximated by

$$\bar{\bar{D}}(\tau) \cong \bar{\bar{D}}_N(\tau) + \bar{\bar{D}}_{EW}(\tau) + \bar{\bar{D}}_{ED}(\tau) + \bar{\bar{D}}_{II}(\tau) + \bar{\bar{D}}_{IE}(\tau) + \bar{\bar{D}}_{SG}(\tau) + \bar{\bar{D}}_{SF}(\tau) \quad (\text{Eq. J9.1-2})$$

as indicated in Equation J4.6-3.

In the TSPA-LA, $\bar{D}_N(\tau|\mathbf{e}) = 0$ for $0 \leq \tau \leq 20,000 \text{ yr}$. Further, for $0 \leq \tau \leq 1,000,000 \text{ yr}$, the effects of nominal processes are incorporated into the determination of $\bar{D}_{SG}(\tau|\mathbf{e})$. As a result, $\bar{D}(\tau|\mathbf{e})$ and $\bar{\bar{D}}(\tau)$ effectively have the forms

$$\bar{D}(\tau|\mathbf{e}) \cong \bar{D}_{EW}(\tau|\mathbf{e}) + \bar{D}_{ED}(\tau|\mathbf{e}) + \bar{D}_{II}(\tau|\mathbf{e}) + \bar{D}_{IE}(\tau|\mathbf{e}) + \bar{D}_{SG}(\tau|\mathbf{e}) + \bar{D}_{SF}(\tau|\mathbf{e}) \quad (\text{Eq. J9.1-3})$$

and

$$\bar{\bar{D}}(\tau) \cong \bar{\bar{D}}_{EW}(\tau) + \bar{\bar{D}}_{ED}(\tau) + \bar{\bar{D}}_{II}(\tau) + \bar{\bar{D}}_{IE}(\tau) + \bar{\bar{D}}_{SG}(\tau) + \bar{\bar{D}}_{SF}(\tau) \quad (\text{Eq. J9.1-4})$$

for both the 20,000 yr and 1,000,000 yr calculations.

The same LHS $\mathbf{e}_i = [\mathbf{e}_{Ai}, \mathbf{e}_{Mi}]$, $i = 1, 2, \dots, nLHS = 300$, is used for all scenario classes. As a result,

$$\bar{D}(\tau|\mathbf{e}_i) \cong \bar{D}_{EW}(\tau|\mathbf{e}_i) + \bar{D}_{ED}(\tau|\mathbf{e}_i) + \bar{D}_{II}(\tau|\mathbf{e}_i) + \bar{D}_{IE}(\tau|\mathbf{e}_i) + \bar{D}_{SG}(\tau|\mathbf{e}_i) + \bar{D}_{SF}(\tau|\mathbf{e}_i) \quad (\text{Eq. J9.1-5})$$

for $i = 1, 2, \dots, nLHS = 300$ and

$$\bar{\bar{D}}(\tau) \equiv \sum_{i=1}^{300} \bar{D}(\tau|\mathbf{e}_i)/300. \quad (\text{Eq. J9.1-6})$$

Further, quantiles $Q_q[\bar{D}(\tau|\mathbf{e})]$ for $\bar{D}(\tau|\mathbf{e})$ are defined as indicated in Equation J4.2-10 and are approximated by the value D such that

$$q \equiv \sum_{i=1}^{300} \underline{\delta}_D [\bar{D}(\tau|\mathbf{e}_i)]/300, \quad (\text{Eq. J9.1-7})$$

where

$$\underline{\delta}_D [\bar{D}(\tau|\mathbf{e}_i)] = \begin{cases} 1 & \text{if } \bar{D}(\tau|\mathbf{e}_i) \leq D \\ 0 & \text{otherwise.} \end{cases} \quad (\text{Eq. J9.1-8})$$

Specifically, $Q_q[\bar{D}(\tau|\mathbf{e})]$ is the q quantile value (e.g., 0.05, 0.5, 0.95) for $\bar{D}(\tau|\mathbf{e})$ and is equal to the value of D that most closely satisfies Equation J9.1-7.

The results $\bar{D}_r(\tau|\mathbf{e}_i)$ and $\bar{\bar{D}}_r(\tau)$ for individual radioactive species designated by r can be determined in the same manner as $\bar{D}(\tau|\mathbf{e}_i)$ and $\bar{\bar{D}}(\tau)$ in Equations J9.1-5 and J9.1-6. Specifically,

$$\bar{D}_r(\tau|\mathbf{e}_i) \equiv \bar{D}_{EW,r}(\tau|\mathbf{e}_i) + \bar{D}_{ED,r}(\tau|\mathbf{e}_i) + \bar{D}_{II,r}(\tau|\mathbf{e}_i) + \bar{D}_{IE,r}(\tau|\mathbf{e}_i) + \bar{D}_{SG,r}(\tau|\mathbf{e}_i) + \bar{D}_{SF,r}(\tau|\mathbf{e}_i) \quad (\text{Eq. J9.1-9})$$

and

$$\bar{\bar{D}}_r(\tau) \equiv \sum_{i=1}^{300} \bar{D}_r(\tau|\mathbf{e}_i)/300, \quad (\text{Eq. J9.1-10})$$

where $\bar{D}_{EW,r}(\tau|\mathbf{e}_i)$ is the expected dose to the RMEI (mrem/yr) at time τ for radioactive species r resulting from early WP failure conditional on \mathbf{e}_i and the other expected doses in Equation J9.1-9 are defined similarly.

J9.2 Expected Dose from All Scenario Classes: 0 to 20,000 yr

The outcomes of the calculation to determine $\bar{D}(\tau|\mathbf{e}_i)$, $Q_q[\bar{D}(\tau|\mathbf{e})]$ for $q = 0.05, 0.5$ and 0.95 , and $\bar{\bar{D}}(\tau)$ for $0 \leq \tau \leq 20,000$ yr are summarized in Figure J9.2-1. Further, the standard presentation format used for these results is shown in Figure J9.2-2. In addition, the expected (mean) results for the individual radioactive species are presented in Figure J9.2-3.

As described in Section J4.10, the analyses leading to the results in Figures J9.2-1 to J9.2-3 were replicated with three independently generated LHSs to test for stability (Figure J9.2-4). This replication shows that an LHS of size 300 is adequate for the estimation of $Q_q[\bar{D}(\tau|\mathbf{e})]$ and $\bar{\bar{D}}(\tau)$ in this analysis for the 0 to 20,000 yr time interval.

J9.3 Expected Dose from All Scenario Classes: 0 to 1,000,000 yr

The same analyses that lead to Figures J9.2-1 to J9.2-4 for the 20,000 yr time interval were also carried out for the 1,000,000 yr time interval (Figures J9.3-1 to J9.3-4).

J10 JUSTIFICATION FOR ANALYSIS DECOMPOSITION

As discussed in Sections J4.5 and J4.6 and explicitly represented in Equations J4.5-1 and (J4.6-1), the computational structure of the TSPA-LA is based on the assumption that there are no significant synergisms between results conditional on the occurrence of individual scenario classes that materially affect the expected dose $\bar{D}(\tau|\mathbf{e})$ over all scenario classes (i.e., over all possible futures \mathbf{a}). Specifically, the assumption is made that

$$\begin{aligned} \bar{D}(\tau|\mathbf{e}) = & D_N(\tau|\mathbf{a}_N, \mathbf{e}_M) + \bar{D}_{EW}(\tau|\mathbf{e}) + \bar{D}_{ED}(\tau|\mathbf{e}) + \bar{\bar{D}}_{II}(\tau|\mathbf{e}) \\ & + \bar{D}_{IE}(\tau|\mathbf{e}) + \bar{D}_{SG}(\tau|\mathbf{e}) + \bar{D}_{SG}(\tau|\mathbf{e}), \end{aligned} \quad (\text{Eq. J10-1})$$

where, conditional on the element $\mathbf{e} = [\mathbf{e}_A, \mathbf{e}_M]$ of \mathcal{E} ,

$$\begin{aligned} D_N(\tau|\mathbf{a}, \mathbf{e}_M) = & \text{dose to RMEI (mrem/yr) at time } \tau \text{ resulting from nominal conditions for} \\ & \text{future } \mathbf{a} \in \mathcal{A} \\ = & D_N(\tau|\mathbf{a}_N, \mathbf{e}_M), \end{aligned} \quad (\text{Eq. J10-2})$$

$$\begin{aligned} D_{EW}(\tau|\mathbf{a}, \mathbf{e}_M) = & \text{dose to RMEI (mrem/yr) at time } \tau \text{ resulting from early WP failure for} \\ & \text{future } \mathbf{a} \in \mathcal{A} \\ = & D_{EW}(\tau|\mathbf{a}_{EW}, \mathbf{e}_M), \end{aligned} \quad (\text{Eq. J10-3})$$

$$\begin{aligned} D_{ED}(\tau|\mathbf{a}, \mathbf{e}_M) = & \text{dose to RMEI (mrem/yr) at time } \tau \text{ resulting from early DS failure for} \\ & \text{future } \mathbf{a} \in \mathcal{A} \\ = & D_{ED}(\tau|\mathbf{a}_{ED}, \mathbf{e}_M), \end{aligned} \quad (\text{Eq. J10-4})$$

$$\begin{aligned} D_{II}(\tau|\mathbf{a}, \mathbf{e}_M) = & \text{dose to RMEI (mrem/yr) at time } \tau \text{ resulting from igneous intrusive events} \\ & \text{for future } \mathbf{a} \in \mathcal{A} \\ = & D_{II}(\tau|\mathbf{a}_{II}, \mathbf{e}_M), \end{aligned} \quad (\text{Eq. J10-5})$$

$$\begin{aligned}
 D_{IE}(\tau|\mathbf{a}, \mathbf{e}_M) &= \text{dose to RMEI (mrem/yr) at time } \tau \text{ resulting from igneous eruptive events} \\
 &\quad \text{for future } \mathbf{a} \in \mathcal{A} \\
 &= D_{IE}(\tau|\mathbf{a}_{IE}, \mathbf{e}_M), \quad (\text{Eq. J10-6})
 \end{aligned}$$

$$\begin{aligned}
 D_{SG}(\tau|\mathbf{a}, \mathbf{e}_M) &= \text{dose to RMEI (mrem/yr) at time } \tau \text{ resulting from seismic ground motion} \\
 &\quad \text{events for future } \mathbf{a} \in \mathcal{A} \\
 &= D_{SG}(\tau|\mathbf{a}_{SG}, \mathbf{e}_M), \quad (\text{Eq. J10-7})
 \end{aligned}$$

$$\begin{aligned}
 D_{SF}(\tau|\mathbf{a}, \mathbf{e}_M) &= \text{dose to RMEI (mrem/yr) at time } \tau \text{ resulting from seismic fault} \\
 &\quad \text{displacement events for future } \mathbf{a} \in \mathcal{A} \\
 &= D_{SF}(\tau|\mathbf{a}_{SF}, \mathbf{e}_M), \quad (\text{Eq. J10-8})
 \end{aligned}$$

and in turn

$$\begin{aligned}
 \bar{D}_{EW}(\tau|\mathbf{e}) &= \text{expected dose to RMEI (mrem/yr) at time } \tau \text{ resulting from early WP failure} \\
 &= E_A \left[D_{EW}(\tau|\mathbf{a}, \mathbf{e}_M) | \mathbf{e}_A \right] \\
 &= \int_{\mathcal{A}} D_{EW}(\tau|\mathbf{a}, \mathbf{e}_M) d_A(\mathbf{a}|\mathbf{e}_A) dA \\
 &= \int_{\mathcal{A}_{EW}} D_{EW}(\tau|\mathbf{a}_{EW}, \mathbf{e}_M) d_A(\mathbf{a}|\mathbf{e}_A) dA, \text{ reminder } \mathbf{a} = [\dots \mathbf{a}_{EW} \dots], \quad (\text{Eq. J10-9})
 \end{aligned}$$

$$\begin{aligned}
 \bar{D}_{ED}(\tau|\mathbf{e}) &= \text{expected dose to RMEI (mrem/yr) at time } \tau \text{ resulting from early DS failure} \\
 &= E_A \left[D_{ED}(\tau|\mathbf{a}, \mathbf{e}_M) | \mathbf{e}_A \right] \\
 &= \int_{\mathcal{A}} D_{ED}(\tau|\mathbf{a}, \mathbf{e}_M) d_A(\mathbf{a}|\mathbf{e}_A) dA \\
 &= \int_{\mathcal{A}_{ED}} D_{ED}(\tau|\mathbf{a}_{ED}, \mathbf{e}_M) d_A(\mathbf{a}|\mathbf{e}_A) dA, \text{ reminder } \mathbf{a} = [\dots \mathbf{a}_{ED} \dots], \quad (\text{Eq. J10-10})
 \end{aligned}$$

$$\begin{aligned}
 \bar{D}_{II}(\tau|\mathbf{e}) &= \text{expected dose to RMEI (mrem/yr) at time } \tau \text{ resulting from igneous intrusive} \\
 &\quad \text{events} \\
 &= E_A \left[D_{II}(\tau|\mathbf{a}, \mathbf{e}_M) | \mathbf{e}_A \right] \\
 &= \int_{\mathcal{A}} D_{II}(\tau|\mathbf{a}, \mathbf{e}_M) d_A(\mathbf{a}|\mathbf{e}_A) dA \\
 &= \int_{\mathcal{A}_{II}} D_{II}(\tau|\mathbf{a}_{II}, \mathbf{e}_M) d_A(\mathbf{a}|\mathbf{e}_A) dA, \text{ reminder } \mathbf{a} = [\dots \mathbf{a}_{II} \dots], \quad (\text{Eq. J10-11})
 \end{aligned}$$

$$\begin{aligned}
 \bar{D}_{IE}(\tau|\mathbf{e}) &= \text{expected dose to RMEI (mrem/yr) at time } \tau \text{ resulting from igneous eruptive} \\
 &\quad \text{events} \\
 &= E_A \left[D_{IE}(\tau|\mathbf{a}, \mathbf{e}_M) | \mathbf{e}_A \right] \\
 &= \int_{\mathcal{A}} D_{IE}(\tau|\mathbf{a}, \mathbf{e}_M) d_A(\mathbf{a}|\mathbf{e}_A) dA \\
 &= \int_{\mathcal{A}_{IE}} D_{IE}(\tau|\mathbf{a}_{IE}, \mathbf{e}_M) d_A(\mathbf{a}|\mathbf{e}_A) dA, \text{ reminder } \mathbf{a} = [\dots \mathbf{a}_{IE} \dots], \quad (\text{Eq. J10-12})
 \end{aligned}$$

$$\begin{aligned}
 \bar{D}_{SG}(\tau|\mathbf{e}) &= \text{expected dose to RMEI (mrem/yr) at time } \tau \text{ resulting from seismic ground} \\
 &\quad \text{motion events} \\
 &= E_A \left[D_{SG}(\tau|\mathbf{a}, \mathbf{e}_M) | \mathbf{e}_A \right] \\
 &= \int_{\mathcal{A}} D_{SG}(\tau|\mathbf{a}, \mathbf{e}_M) d_A(\mathbf{a}|\mathbf{e}_A) dA \\
 &= \int_{\mathcal{A}_{SG}} D_{SG}(\tau|\mathbf{a}_{SG}, \mathbf{e}_M) d_A(\mathbf{a}|\mathbf{e}_A) dA, \text{ reminder: } \mathbf{a} = [\dots \mathbf{a}_{SG} \dots], \quad (\text{Eq. J10-13})
 \end{aligned}$$

$$\begin{aligned}
 \bar{D}_{SF}(\tau|\mathbf{e}) &= \text{expected dose to RMEI (mrem/yr) at time } \tau \text{ resulting from seismic fault} \\
 &\quad \text{displacement events} \\
 &= E_A \left[D_{SF}(\tau|\mathbf{a}, \mathbf{e}_M) | \mathbf{e}_A \right] \\
 &= \int_{\mathcal{A}} D_{SF}(\tau|\mathbf{a}, \mathbf{e}_M) d_A(\mathbf{a}|\mathbf{e}_A) dA \\
 &= \int_{\mathcal{A}_{SF}} D_{SF}(\tau|\mathbf{a}_{SF}, \mathbf{e}_M) d_A(\mathbf{a}|\mathbf{e}_A) dA, \text{ reminder } \mathbf{a} = [\dots \mathbf{a}_{SF} \dots]. \quad (\text{Eq. J10-14})
 \end{aligned}$$

In the preceding, $D_{EW}(\tau|\mathbf{a}, \mathbf{e}_M)$ is equivalent to $D_{EW}(\tau|\mathbf{a}_{EW}, \mathbf{e}_M)$ because only dose from early WP failure is under consideration; for the same reason, the integrals over \mathcal{A} and \mathcal{A}_{EW} in Equation J.4.4-20 are equivalent. Specifically, possible synergisms between occurrences associated with different scenario classes are not being considered. Analogous equivalencies hold $D_{ED}(\tau|\mathbf{a}, \mathbf{e}_M)$, $D_{II}(\tau|\mathbf{a}, \mathbf{e}_M)$, $D_{IE}(\tau|\mathbf{a}, \mathbf{e}_M)$, $D_{SG}(\tau|\mathbf{a}, \mathbf{e}_M)$, $D_{SF}(\tau|\mathbf{a}, \mathbf{e}_M)$ and associated integrals.

The appropriateness of the approximation in Equation J10-1 is now considered. In general, this appropriateness depends on both scenario class probability and the expected doses to the RMEI that result from the futures associated with individual scenario classes.

Nominal processes result in $\bar{D}_N(\tau|\mathbf{a}_N, \mathbf{e}_M) = 0$ mrem/yr prior to 20,000 yr (Figures J5-1 and J5-2). Thus, the separation of $\bar{D}_N(\tau|\mathbf{a}_N, \mathbf{e}_M)$ from the other expected doses in Equation J10-1 has no consequence for the [0, 20,000 yr] time interval. For the determination of $\bar{D}(\tau|\mathbf{e})$ for the

time interval $[0, 10^6 \text{ yr}]$, releases associated with WP failures that derive from nominal processes are included with releases that derive from seismic ground motion events. As a result, the expected dose $\bar{D}_{SG}(\tau|\mathbf{e})$ for the seismic ground motion scenario class \mathcal{A}_{SG} contains the dose $D_N(\tau|\mathbf{a}_N, \mathbf{e}_M)$ associated with the nominal scenario class. In the determination of the doses $D_{SG}(\tau|\mathbf{a}, \mathbf{e}_M)$ that give rise to $\bar{D}_{SG}(\tau|\mathbf{e})$ for the $[0, 10^6 \text{ yr}]$ time interval, the synergisms (e.g., effects of WP thinning, inventory depletion, ...) between the effects of nominal processes and seismic events are incorporated into the analysis. Thus, $\bar{D}_{SG}(\tau|\mathbf{e})$ appropriately contains the effects of both nominal processes and seismic ground motion events.

The early failure scenario classes \mathcal{A}_{EW} and \mathcal{A}_{ED} involve failures of small numbers of WPs (Figure J6.2-1) and DSs (Figure J6.3-1) randomly spread through the repository. Because of the small numbers of WPs and DSs involved, there should be no synergisms between early WP failures and early DS failures. As a result, the separation of $\bar{D}_{EW}(\tau|\mathbf{e})$ and $\bar{D}_{ED}(\tau|\mathbf{e})$ is reasonable. Similarly, the fault displacement scenario class \mathcal{A}_{SF} involves the failure of a small number of WPs (see Equation J8.6-29 and associated discussion) as does the igneous eruptive scenario class \mathcal{A}_{IE} . As a result, the separation of $\bar{D}_{SF}(\tau|\mathbf{e})$, $\bar{D}_{IE}(\tau|\mathbf{e})$, $\bar{D}_{EW}(\tau|\mathbf{e})$ and $\bar{D}_{ED}(\tau|\mathbf{e})$ is also reasonable. Specifically, the likelihood that a given WP would be affected in a given future \mathbf{a} by events associated with more than one of these scenario classes is small. Further, as the analysis is designed, the ignoring of this potential interaction results in a small, and insignificant, upward shift in the values for $\bar{D}_{SF}(\tau|\mathbf{e})$, $\bar{D}_{IE}(\tau|\mathbf{e})$, $\bar{D}_{EW}(\tau|\mathbf{e})$ and $\bar{D}_{ED}(\tau|\mathbf{e})$ as a result of slightly overcounting the releases associated with the WPs affected by more than one event.

The seismic ground motion scenario class \mathcal{A}_{SG} involves damage to large numbers of WPs. Specifically, a seismic ground motion event that damages one WP of a given type (i.e., CSNF or CDSP) will generally damage all WPs of that type. As a result, the fraction of WPs damaged by a seismic ground motion event that have been previously affected by an early WP failure, an early DS failure, an igneous eruptive event or a seismic fault displacement event is small. Because of this, correcting for the inventory reduction associated with such precursor events would have little effect on $\bar{D}_{SG}(\tau|\mathbf{e})$. Specifically, ignoring the effects of this inventory correction produces a small, but not significant, upward shift in $\bar{D}_{SG}(\tau|\mathbf{e})$. For the $[0, 10^6 \text{ yr}]$ time interval, WP failure by nominal processes is included in the determination of $\bar{D}_{SG}(\tau|\mathbf{e})$. With increasing time, many more WPs fail by nominal processes (Figures K4.2-2 and K4.2-4) than fail by early WP failure, early DS failure, seismic fault displacement or igneous eruption. Thus, again, including a correction for the indicated potential precursor events would have little effect on $\bar{D}_{SG}(\tau|\mathbf{e})$ for the $[0, 10^6 \text{ yr}]$ time interval. As a result, the value for $\bar{D}_{SG}(\tau|\mathbf{e})$ is not significantly affected by precursor events associated with the scenario classes \mathcal{A}_{EW} , \mathcal{A}_{ED} , \mathcal{A}_{IE} and \mathcal{A}_{SF} .

The potential effects of seismic ground motion events on $\bar{D}_{EW}(\tau|\mathbf{e})$ and $\bar{D}_{ED}(\tau|\mathbf{e})$ are limited because the affected WPs are destroyed at the start of the calculation for the early WP failure

scenario class \mathcal{A}_{EW} and both the DS and the WP are destroyed at the start of the calculation for the early DS failure scenario class \mathcal{A}_{ED} . Thus, including the potential effects of seismic ground motion events would have little incremental effect on $\bar{D}_{EW}(\tau|\mathbf{e})$ and $\bar{D}_{ED}(\tau|\mathbf{e})$. The most likely effect would be to increase $\bar{D}_{EW}(\tau|\mathbf{e})$ as a result of seismically-induced DS failure. However, this would induce so many more DS failures over additional previously unfailed WPs that the incremental effect on $\bar{D}(\tau|\mathbf{e})$ would be small.

At later times, it is possible that seismic events could reduce the WP inventories that give rise to $\bar{D}_{IE}(\tau|\mathbf{e})$ and $\bar{D}_{SF}(\tau|\mathbf{e})$. However, the values for $\bar{D}_{IE}(\tau|\mathbf{e})$ (Figures J7.3-4 and J7.3-12) and $\bar{D}_{SF}(\tau|\mathbf{e})$ (Figures J8.6-5 and J8.6-16) are already small. As a result, any reductions in $\bar{D}_{IE}(\tau|\mathbf{e})$ and $\bar{D}_{SF}(\tau|\mathbf{e})$ that might occur as a result of correcting for the effects of prior seismic ground motion events would have little effect on $\bar{D}(\tau|\mathbf{e})$.

The potential interactions between seismic ground motion events and igneous intrusive events are now considered. An igneous intrusive event is assumed to destroy all WPs in the repository. When $\bar{D}_{SG}(\tau|\mathbf{e})$ and $\bar{D}_{II}(\tau|\mathbf{e})$ are calculated under the assumptions that $\bar{D}_{SG}(\tau|\mathbf{e})$ is not affected by potential igneous intrusive events and $\bar{D}_{II}(\tau|\mathbf{e})$ is not affected by potential ground motion events, the result is that $\bar{D}_{SG}(\tau|\mathbf{e})$ is slightly overestimated as a result of assuming that seismically-induced releases continue after an igneous intrusion has destroyed all WPs in the repository and $\bar{D}_{II}(\tau|\mathbf{e})$ is slightly overestimated as a result of not correcting for inventory reduction in the WPs that result from the seismically-induced releases.

Because the probability of the seismic ground motion scenario class \mathcal{A}_{SG} is effectively one (Equation J8.8-1) and the probability of the igneous intrusive scenario class is much smaller (Figure J7.5-1), omitting a correction for the effects of igneous intrusive events has a relatively small effect on $\bar{D}_{SG}(\tau|\mathbf{e})$.

In contrast, igneous intrusive events will almost always be preceded by one or more seismic ground motion events. The extent to which these events affect dose from igneous intrusive events depends on the amount of WP inventory released before the igneous intrusive event. At early times (e.g., prior to 10^5 yr), the amount of material released from WPs as a result of seismic ground motion events is likely to be small, with the result that $\bar{D}_{II}(\tau|\mathbf{e})$ will be little affected by prior seismic ground motion events. As time increases, the effect will be larger because of increasing seismic damage, increasing DS and WP failures from nominal processes, and increasing time for radionuclide transport from the WPs and the EBS. To a great extent, this effect will be linear with respect to the amount of radioactive material removed from the WPs and the EBS. As a result, unless prior seismic events result in the release of substantial amounts of radioactive material (e.g., >50 percent of the inventory in the repository), the effect on $\bar{D}_{II}(\tau|\mathbf{e})$ will not be large relative to the epistemic uncertainty in $\bar{D}_{II}(\tau|\mathbf{e})$ that results from the uncertainty associated with \mathbf{e} (Figures J7.2-4 and J7.2-14). As comparison of the igneous dose results in Figures J7.2-1 and J7.2-11 with the seismic dose results in Figures J8.3-1, J8.3-2 and J8.4-1 shows, the doses from igneous intrusive events tend to be much larger than the doses from

seismic events. This observation includes the combined effects of nominal processes and multiple seismic events shown in Figure J8.4-1 for the $[0, 10^6 \text{ yr}]$ time interval. Because dose is proportional to released inventory, this comparison indicates that correcting WP inventory for the effects of nominal processes and prior seismic events would have little effect on $\bar{D}_{II}(\tau|\mathbf{e})$. In any event, the effect of not correcting for the effects of prior seismic ground motion events results in an overestimate for $\bar{D}_{II}(\tau|\mathbf{e})$.

As previously discussed, the scenario classes \mathcal{A}_{EW} , \mathcal{A}_{ED} and \mathcal{A}_{IE} involve damage to small numbers of WPs. In contrast, the igneous intrusive scenario class \mathcal{A}_{II} is assumed to involve damage to all WPs in the repository. As a result, a correction to $\bar{D}_{II}(\tau|\mathbf{e})$ to account for the potential effects of events associated with the scenario classes \mathcal{A}_{EW} , \mathcal{A}_{ED} and \mathcal{A}_{IE} would have no discernable effect.

In summary, the only potentially significant synergisms between events associated with individual scenario classes involve the nominal scenario class \mathcal{A}_N and the seismic ground motion scenario class \mathcal{A}_{SG} for the $[0, 10^6 \text{ yr}]$ time interval. For these two scenario classes, the potential effects of such synergisms are directly incorporated into the determination of $\bar{D}_{SG}(\tau|\mathbf{e})$ for the $[0, 10^6 \text{ yr}]$ time interval. For the remaining scenario classes, no significant synergisms exist that materially affect the estimation of $\bar{D}(\tau|\mathbf{e})$ by first determining the expected doses $\bar{D}_{EW}(\tau|\mathbf{e})$, $\bar{D}_{ED}(\tau|\mathbf{e})$, $\bar{D}_{II}(\tau|\mathbf{e})$, $\bar{D}_{IE}(\tau|\mathbf{e})$, $\bar{D}_{SG}(\tau|\mathbf{e})$ and $\bar{D}_{SF}(\tau|\mathbf{e})$ and then summing these expected doses as indicated in Equation J10-1. As a reminder, $\bar{D}_N(\tau|\mathbf{a}_N, \mathbf{e}_M) = 0 \text{ mrem/yr}$ for the $[0, 20,000 \text{ yr}]$ time interval, and the effects of nominal processes are directly incorporated into the determination of $\bar{D}_{SG}(\tau|\mathbf{e})$ for the $[0, 10^6 \text{ yr}]$ time interval. The result of ignoring inventory corrections for the effects of events associated with individual scenario classes is a slight upward shift in the values for $\bar{D}_{EW}(\tau|\mathbf{e})$, $\bar{D}_{ED}(\tau|\mathbf{e})$, $\bar{D}_{II}(\tau|\mathbf{e})$, $\bar{D}_{IE}(\tau|\mathbf{e})$, $\bar{D}_{SG}(\tau|\mathbf{e})$ and $\bar{D}_{SF}(\tau|\mathbf{e})$ and hence in the value for $\bar{D}(\tau|\mathbf{e})$. However, this effect is small relative to the epistemic uncertainty in $\bar{D}(\tau|\mathbf{e})$ that results from the uncertainty in \mathbf{e} (Figures J9.2-1 and J9.3-1). As a result, the decomposition in Equation J10-1 provides a reasonable and numerically practicable approximation to $\bar{D}(\tau|\mathbf{e})$.

J11 HUMAN INTRUSION SCENARIO

J11.1 Human Intrusion Scenario: Preliminaries

The Human Intrusion Scenario is proscribed by the U.S. Nuclear Regulatory Commission (NRC) proposed rule in 10 CFR 63.322 [DIRS 180319], as follows:

§ 63.322 Human intrusion scenario. For the purposes of the analysis of human intrusion, DOE must make the following assumptions:

- (a) There is a single human intrusion as a result of exploratory drilling for groundwater.

- (b) The intruders drill a borehole directly through a degraded waste package (WP) into the uppermost aquifer underlying the Yucca Mountain repository.
- (c) The drillers use the common techniques and practices that are currently employed in exploratory drilling for groundwater in the region surrounding Yucca Mountain.
- (d) Careful sealing of the borehole does not occur; instead natural degradation processes gradually modify the borehole.
- (e) No particulate waste material falls into the borehole.
- (f) The exposure scenario includes only those radionuclides transported to the saturated Zone (SZ) by water (e.g., water enters the WP, releases radionuclides, and transports radionuclides by way of the borehole to the SZ).
- (g) No releases are included that are caused by unlikely natural processes and events.

The results of this scenario are compared with the individual protection standard for a human intrusion of the repository defined in 10 CFR 63.321 [DIRS 178394]:

§ 63.321 Individual protection standard for human intrusion. DOE must determine the earliest time after disposal that the waste package would degrade sufficiently that a human intrusion could occur without recognition by the drillers. DOE must:

- (a) Provide the analyses and its technical bases used to determine the time of occurrence of human intrusion (§ 63.322) without recognition by the drillers.
- (b) If complete waste package penetration is projected to occur at or before 10,000 years after disposal:
 - (1) Demonstrate that there is a reasonable expectation that the reasonably maximally exposed individual receives no more than an annual dose of 0.15 mSv (15 mrem) as a result of a human intrusion, at or before 10,000 years after disposal. The analysis must include all potential environmental pathways of radionuclide transport and exposure subject to the requirements at § 63.322; and
 - (2) If exposures to the reasonably maximally exposed individual occur more than 10,000 years after disposal, include the results of the analysis and its bases in the environmental impact statement for Yucca Mountain as an indicator of long-term disposal system performance.

- (c) Include the results of the analysis and its bases in the environmental impact statement for Yucca Mountain as an indicator of long-term disposal system performance, if the intrusion is not projected to occur before 10,000 years after disposal.

The NRC specifies that the U.S. Department of Energy (DOE) must determine the earliest time after disposal that the WP would degrade sufficiently that a human intrusion could occur without recognition by the drillers. In addition, by way of explanation and corroboration per 10 CFR 63.321(a) [DIRS 178394], the DOE must provide the analyses and its technical basis used to determine the time of occurrence of human intrusion, as described in NRC proposed rule in 10 CFR 63.322 [DIRS 180319], without recognition by the drillers. Analysis presented in Section 6.7.2 selects 200,000 yrs after closure as the earliest time of intrusion.

J11.2 Human Intrusion Scenario: Analysis

Conceptually, the Human Intrusion Scenario is structured using the same principles as the other scenario classes in the PA for the Yucca Mountain facility. The Human Intrusion Scenario differs only in the uncertainties considered in the scenario, and in the regulation that the scenario answers. As described in Section J3, the same three basic entities underlie the conceptual structure of this scenario: (i) EN1, a probabilistic characterization of what could occur at the facility under consideration; (ii) EN2, mathematical models for estimating the consequences of what could occur; and (iii) EN3, a probabilistic characterization of the uncertainty in the parameters used in the definitions of EN1 and EN2. In the case of the Human Intrusion Scenario, EN1 is comprised of the probability space describing the uncertainty in the location of the intrusion (because the time of intrusion and number of intrusions are not uncertain, location of the intrusion is the only uncertainty described by EN1); EN2 defines the models used to estimate radionuclide transport after the intrusion occurs; and EN3 provides the possible values of parameters that are used in EN1 and EN2.

In the Human Intrusion Scenario, each aleatory future, $\mathbf{a}_j, j = 1, 2, \dots, nHI$, is a sample element from a sample space \mathcal{A}_{HI} , an element of which can be represented by

$$\mathbf{a}_j = [r_j, q_j(\mathbf{e}_{Mi}), SR_j] \quad (\text{Eq. J11.2-1})$$

where nHI is the number of aleatory realizations generated to evaluate the consequences of the Human Intrusion Scenario, r_j designates the type of WP (CDSP WP or transportation, aging, and disposal canister CSNF WP) intersected in the j^{th} aleatory realization, $q_j(\mathbf{e}_{Mi})$ is the percolation rate (mm/yr) in the percolation bin selected in the j^{th} aleatory realization (Section 6.3.2) which depends on the LHS element $\mathbf{e}_i = [\mathbf{e}_{Ai}, \mathbf{e}_{Mi}]$, and SR_j is the SZ source region selected in the j^{th} aleatory realization (Section 6.3.9). The borehole is conceptually represented as a conduit for fluid flow through a WP, through to UZ and into the SZ. The type of WP intersected is determined randomly with the probability of selecting waste package type r_j given by the fraction of WPs of type r_j .

The location of the borehole is described in terms of the percolation bin and the entry point into the SZ. The probability of selecting a percolation bin corresponds to the percentage of WPs located in each bin. Specifically, percolation bins 1 and 5 each contain 5 percent of WPs and are assigned probabilities of 0.05, percolation bins 2 and 4 each contain 25 percent of WPs and are assigned probabilities of 0.25, and percolation bin 3 contains 40 percent of WPs and is assigned probability of 0.40. After selection of a percolation bin into which the intrusion occurs, a UZ node to which mass from the EBS flows is randomly selected, and the percolation rate $q_i(\mathbf{e}_{Ai})$ (mm/yr) at the selected location is determined. Figure 6.3.9-6 illustrates the relationship between percolation bins and their constituent nodes. The percolation rate at a node depends on a number of epistemic uncertainties defined by \mathbf{e}_{Mi} .

As described in Section 6.3.9, flow from the UZ into the SZ is numerically represented by use of four SZ source regions, shown in Figure 6.3.10-6. An SZ source region is randomly selected in conjunction with the selection of the percolation bin. The probability of selecting each region is determined by the fraction of the UZ nodes comprising the selected percolation bin that fall within the SZ source region. Figure 6.3.9-6 combined with Figure 6.3.10-6 illustrates the mapping from UZ nodes to SZ source regions.

For a given LHS element $\mathbf{e}_i = [\mathbf{e}_{Ai}, \mathbf{e}_{Mi}]$ of the form indicated in Equation J4.9-1, the expected dose $\bar{D}_{HI}(\tau|\mathbf{e}_i)$ (mrem/yr) is now given by

$$\bar{D}_{HI}(\tau|\mathbf{e}_i) = \sum_{j=1}^{nHI} D_{HI}(\tau|[1, r_j, q_j(\mathbf{e}_{Mi}) SR_j], \mathbf{e}_i) / nHI \quad (\text{Eq. J11.2-2})$$

where $D_{HI}(\tau|[1, r_j, q_j(\mathbf{e}_{Mi}), SB_j], \mathbf{e}_i)$ denotes the dose (mrem/yr) resulting at time τ from a human intrusion that intersects 1 WP of type r_j that experiences percolation rate $q_j(\mathbf{e}_{Mi})$ (mm/yr) and intersects the SZ in source region SR_j . In turn, the estimates for $\bar{D}_{HI}(\tau|\mathbf{e}_i)$ can be used to estimate $\bar{\bar{D}}_{HI}(\tau)$, $p_E[\bar{D}_{HI}(\tau|\mathbf{e}_i) \leq D]$ and $p_E[D < \bar{D}_{HI}(\tau|\mathbf{e}_i)]$. Specifically,

$$\bar{\bar{D}}_{HI}(\tau) \cong \sum_{i=1}^{nLHS} \bar{D}_{HI}(\tau|\mathbf{e}_i) / nLHS, \quad (\text{Eq. J11.2-3})$$

$$p_E[\bar{D}_{HI}(\tau|\mathbf{e}_i) \leq D] \cong \sum_{i=1}^{nLHS} \delta_D[\bar{D}_{HI}(\tau|\mathbf{e}_i)] / nLHS \quad (\text{Eq. J11.2-4})$$

and

$$p_E[D < \bar{D}_{HI}(\tau|\mathbf{e}_i)] \cong \sum_{i=1}^{nLHS} \bar{\delta}_D[\bar{D}_{HI}(\tau|\mathbf{e}_i)] / nLHS \quad (\text{Eq. J11.2-5})$$

as indicated in Equations J4.9-8 – J4.9-10, where $\bar{\delta}_D(\sim)$ and $\underline{\delta}_N(\sim)$ are defined in Equations J4.2-3 and J4.2-7, respectively. Further, quantiles $Q_q[\bar{D}_{HI}(\tau|\mathbf{e})]$ for $\bar{D}_{HI}(\tau|\mathbf{e})$ can be obtained by solving either

$$q = \int_{\mathcal{A}_{HI}} \underline{\delta}_D [\bar{D}_{HI}(\tau|\mathbf{e})] d_E(\mathbf{e}) dE \quad (\text{Eq. J11.2-6})$$

or

$$1 - q = \int_{\mathcal{A}_{HI}} \bar{\delta}_D [\bar{D}_{HI}(\tau|\mathbf{e})] d_E(\mathbf{e}) dE \quad (\text{Eq. J11.2-7})$$

for D . In practice, the solution of Equation J11.2-6 or Equation J11.2-7 to determine D , and hence $Q_q[\bar{D}_{HI}(\tau|\mathbf{e})]$, is based on the approximating sums in Equations J11.2-4 and J11.2-5.

The determination of $\bar{D}_{HI}(\tau|\mathbf{e}_i)$ as indicated in Equation J11.2-2 requires the evaluation of

$$D_{HI}(\tau | [1, r_j, q_j(\mathbf{e}_{Mi}), SR_j], \mathbf{e}_i) \quad (\text{Eq. J11.2-8})$$

in GoldSim for selected values of τ , $\mathbf{a}_j = [r_j, q_j(\mathbf{e}_{Mi}), SR_j]$, $j = 1, 2, \dots, nHI$, and $\mathbf{e}_i = [\mathbf{e}_{Ai}, \mathbf{e}_{Mi}]$, $i = 1, 2, \dots, nLHS$. Further, a large number of intermediate results are also generated and saved.

The results indicated in conjunction with Equation J11.2-8 were calculated for the time interval $[0, 10^6 \text{ yr}]$ using timesteps of 4,000 yr after the intrusion event. Section 7.3.3 describes the numerical stability of the GoldSim results with respect to the timesteps. For each sample \mathbf{e}_i , $i = 1, 2, \dots, nLHS = 300$, an aleatory sample $\mathbf{a}_j = [r_j, q_j(\mathbf{e}_{Mi}), SR_j]$, $j = 1, 2, \dots, nHI = 30$, was independently generated, and the quantities $D_{HI}(\tau | [1, r_j, q_j(\mathbf{e}_{Mi}), SR_j], \mathbf{e}_i)$ were computed by GoldSim, for a total of 9000 individual dose calculations. Expected dose and expected (mean) dose were computed as defined by Equations J11.2-2 and J11.2-3, respectively (Figure J11.2-1).

As discussed in Section J4.10, the numerical stability of results obtained with Latin hypercube sampling can be assessed with replicated sampling. Specifically, the analysis for human intrusion failure was performed with the $nRL = 3$ replicated LHSs indicated in Equation J4.10-1. In turn, this analysis shows that the numerical error in using Latin hypercube sampling to estimate $\bar{D}_{HI}(\tau)$ is small relative to the epistemic uncertainty associated with the possible values for $\bar{D}_{HI}(\tau|\mathbf{e})$ (Figure J11.2-2).

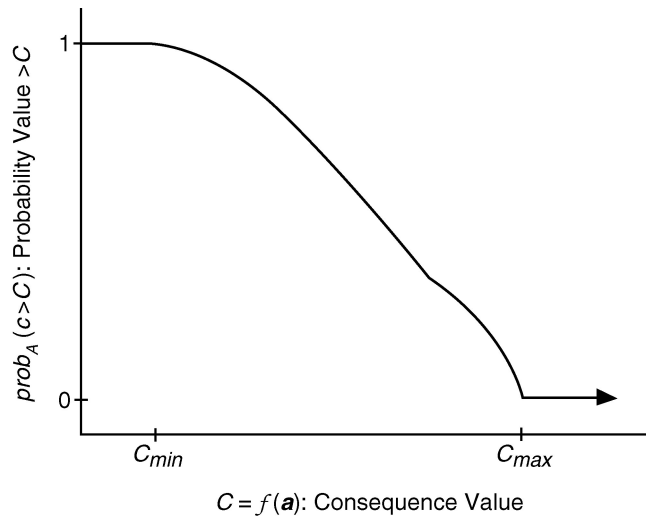


Figure J3.4-1. Example CCDF: plot of probability $prob_A(c > C)$ that a consequence with a value larger than C will occur.

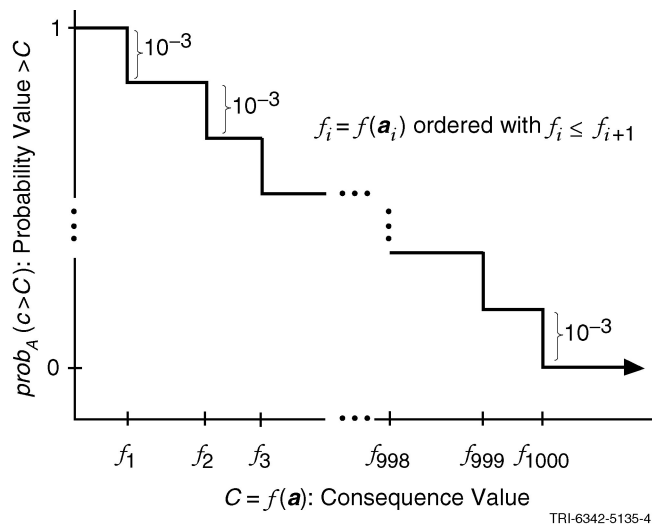


Figure J3.4-2. Approximation of a CCDF with a random sample of size 1,000

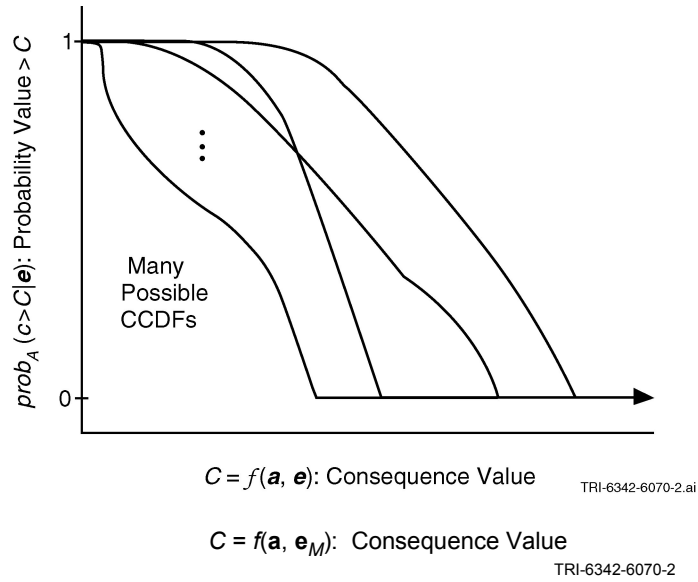


Figure J3.5-1. Different values of CCDF defined by Equation J3.4-5 that derive from different values of e .

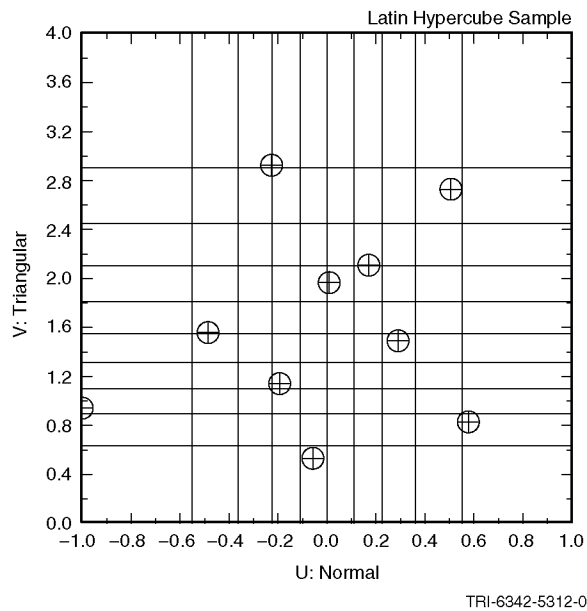
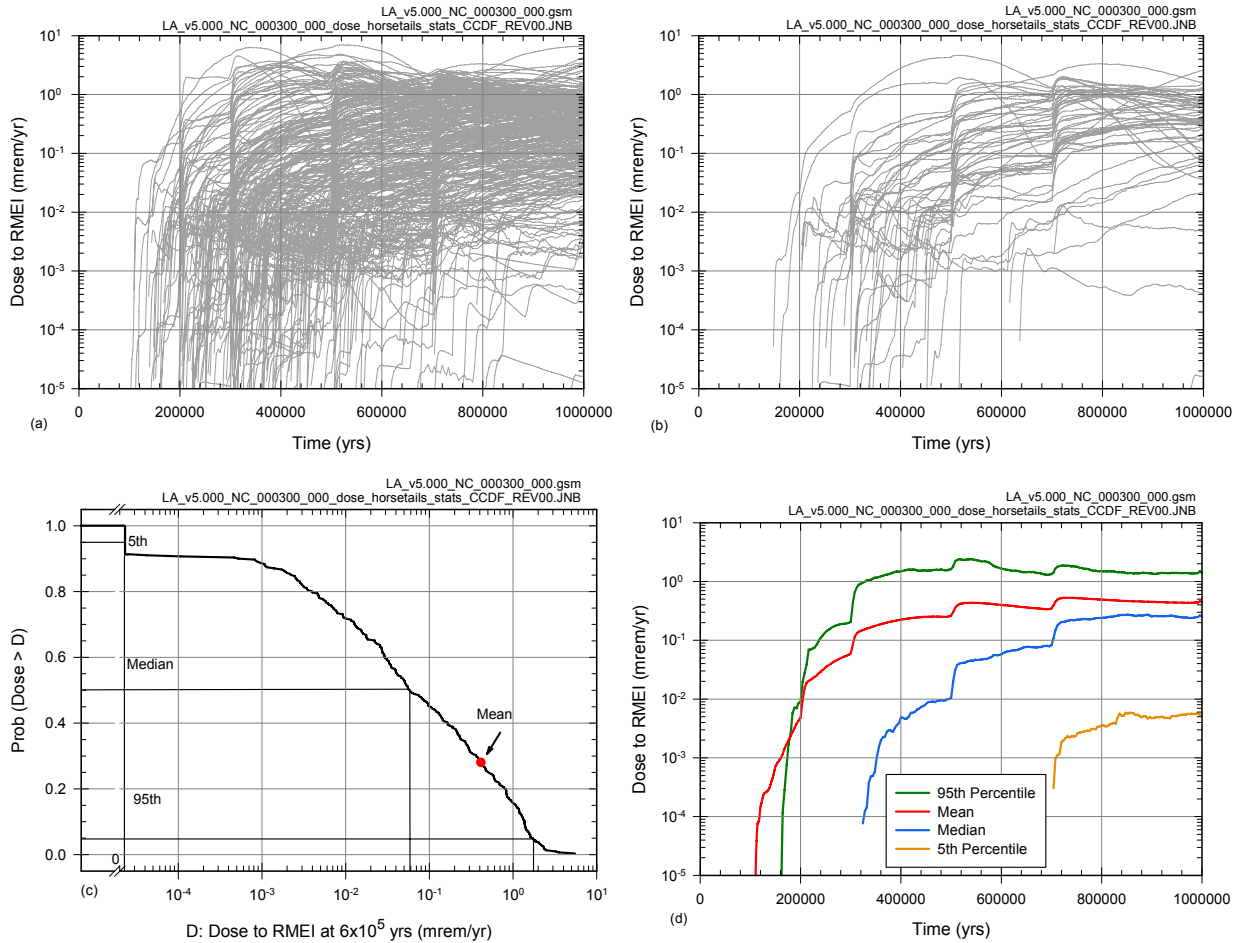
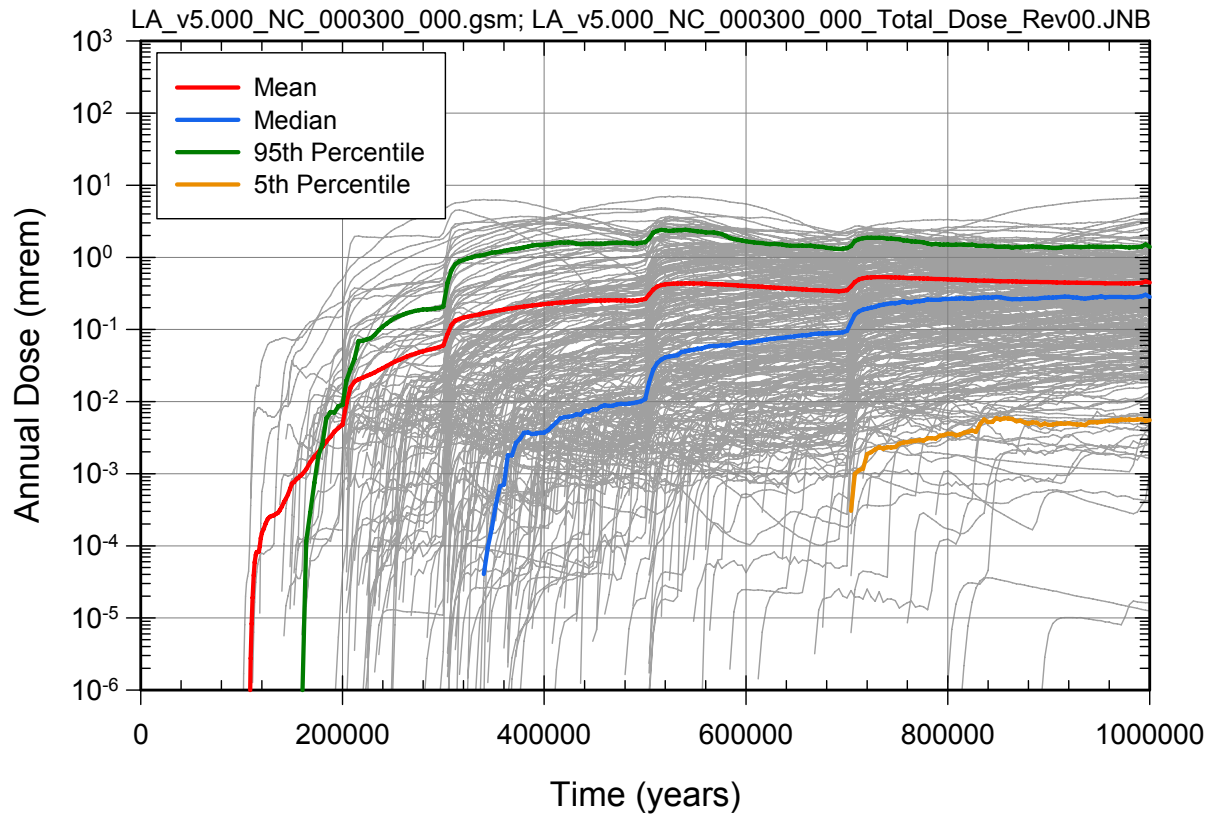


Figure J3.5-2. Example of an LHS of size $nLHS = 10$ from variables U and V with U normal on $[-1, 1]$ (mean = 0, 0.01 quantile = -1, 0.99 quantile = 1) and V triangular on $[0, 4]$ (mode = 1) (Figure 4, Helton 1999 [DIRS 159042])



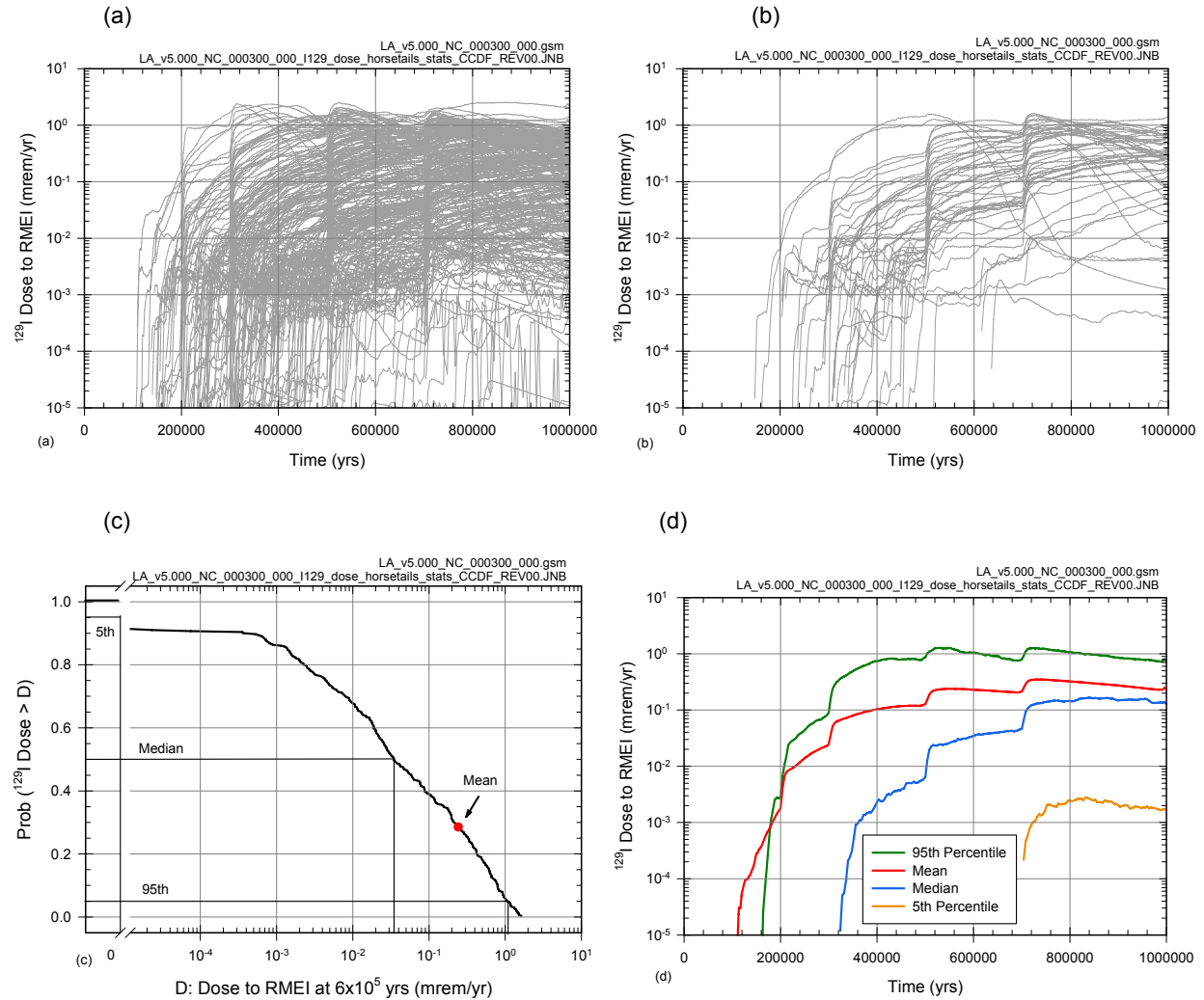
Source: Ouput DTNs: MO0709TSPAPLOT.000 [DIRS 183010]; and MO0709TSPAREGS.000 [DIRS 182976].

Figure J5-1. Estimate obtained with LHS of size $nLHS = 300$ showing epistemic uncertainty in dose $D_N(\tau|\mathbf{a}_N, \mathbf{e}_M)$ to RMEI for $0 \leq \tau \leq 10^6$ yr that results when only nominal conditions are considered: (a) $D_N(\tau|\mathbf{a}_N, \mathbf{e}_{Mi})$, $i = 1, 2, \dots, nLHS = 300$, (b) dose $D_N(\tau|\mathbf{a}_N, \mathbf{e}_{Mi})$, $i = 1, 2, \dots, 50$, (c) exceedance probabilities $p_E[D < D_N(\tau|\mathbf{a}_N, \mathbf{e}_M)]$ and quantiles $Q_q[D_N(\tau|\mathbf{a}_N, \mathbf{e}_M)]$, $q = 0.05, 0.5, 0.95$, for $\tau = 6.0 \times 10^5$ yr, and (d) expected (mean) dose $\bar{D}_N(\tau)$ and quantiles $Q_q[D_N(\tau|\mathbf{a}_N, \mathbf{e}_M)]$, $q = 0.05, 0.5, 0.95$.



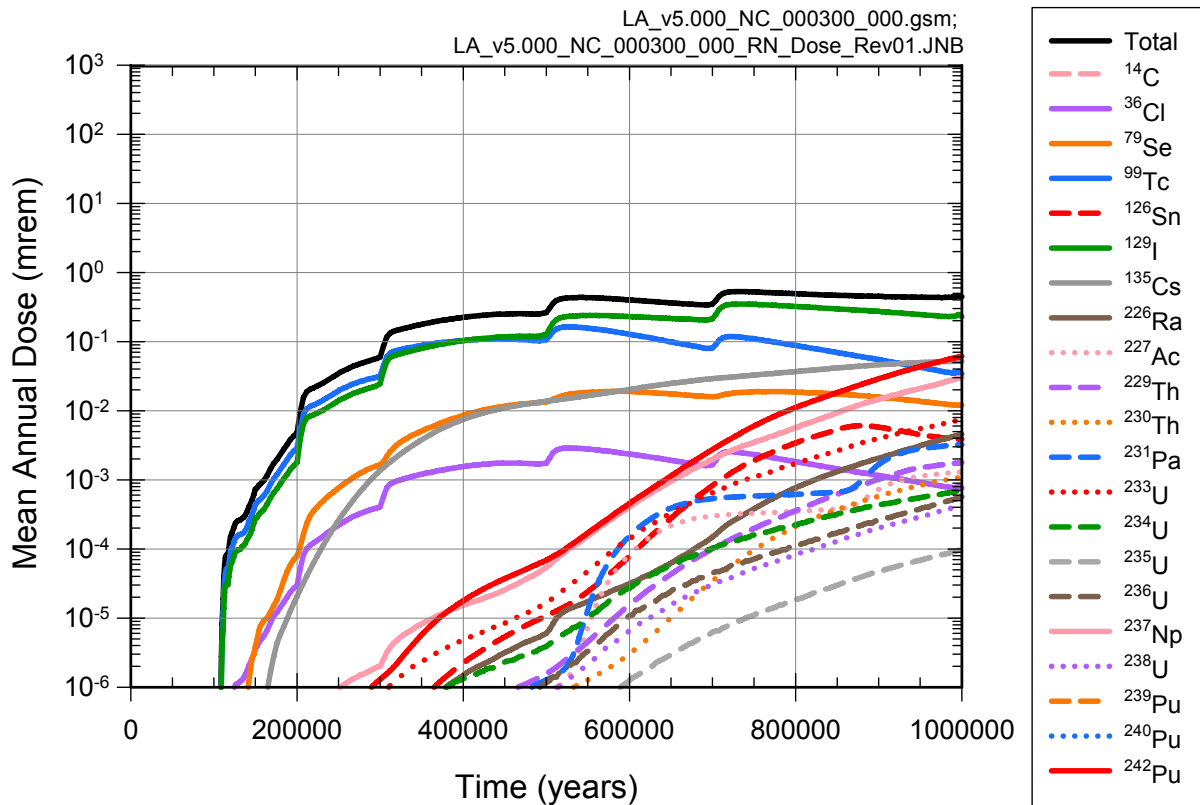
Source: Ouput DTNS: MO0709TSPAPLOT.000 [DIRS 183010]; and MO0709TSPAREGS.000 [DIRS 182976].

Figure J5-2. Summary of results obtained with LHS of size $nLHS = 300$ showing epistemic uncertainty in dose $D_M(\tau|\mathbf{a}_N, \mathbf{e}_M)$ to RMEI for $0 \leq \tau \leq 10^6$ yr that results when only nominal conditions are considered.



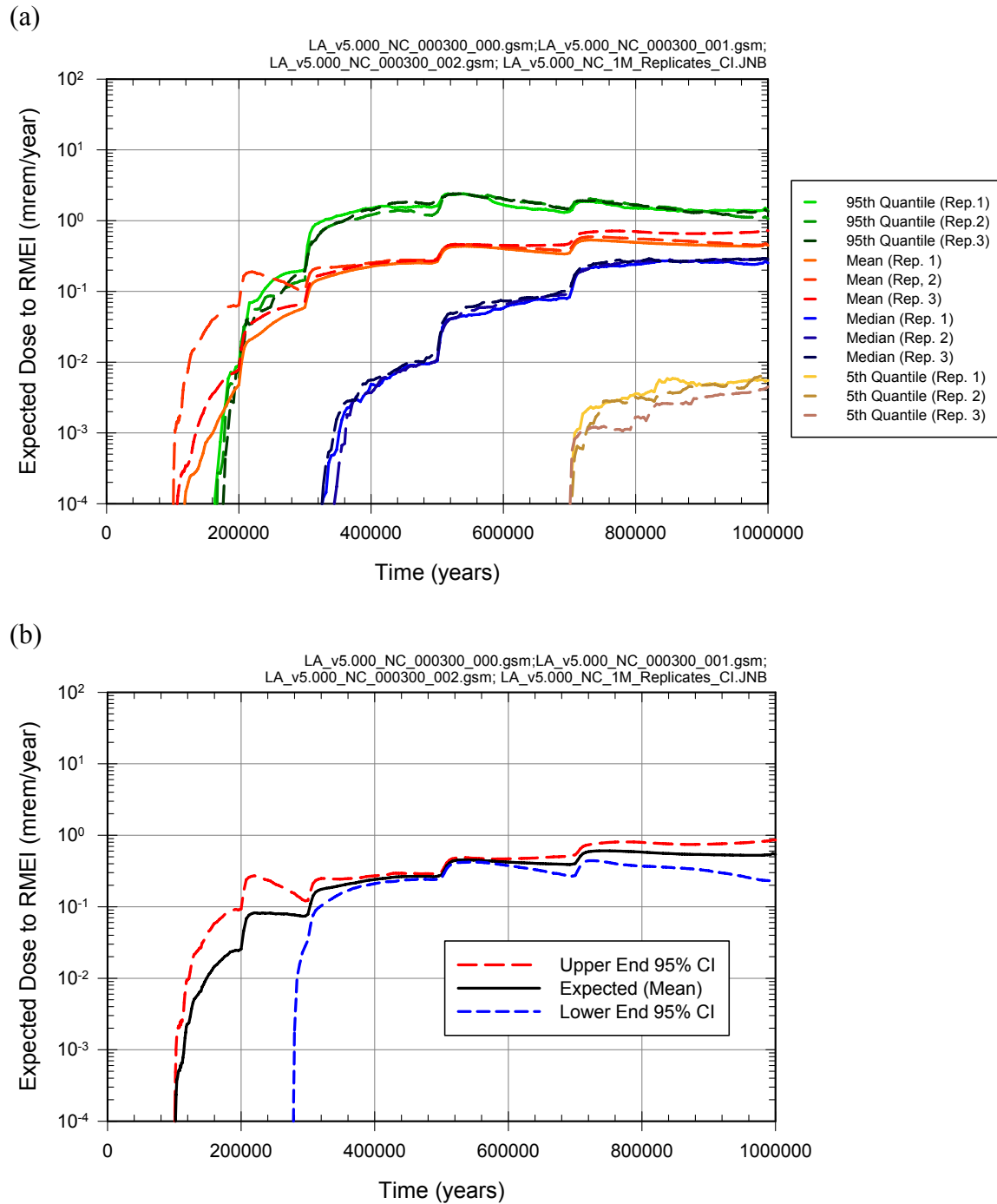
Source: Ouput DTNs: MO0709TSPAPLOT.000 [DIRS 183010]; and MO0709TSPAREGS.000 [DIRS 182976].

Figure J5-3. Estimate obtained with LHS of size $nLHS = 300$ of epistemic uncertainty in dose $D_{Nr}(\tau|\mathbf{a}_N, \mathbf{e}_M)$ to RMEI for $0 \leq \tau \leq 10^6$ yr with r corresponding to ^{129}I that results when only nominal conditions are considered: (a) dose $D_{Nr}(\tau|\mathbf{a}_N, \mathbf{e}_{Mi})$, $i = 1, 2, \dots, nLHS = 300$, (b) dose $D_{Nr}(\tau|\mathbf{a}_N, \mathbf{e}_{Mi})$, $i = 1, 2, \dots, 50$, (c) exceedance probabilities $p_E[D < D_{Nr}(\tau|\mathbf{a}_N, \mathbf{e}_M)]$ and quantiles $Q_q[D_{Nr}(\tau|\mathbf{a}_N, \mathbf{e}_M)]$, $q = 0.05, 0.5$ and 0.95 , for $\tau = 6.0 \times 10^5$ yr, and (d) expected (mean) dose $\bar{D}_{Nr}(\tau)$ and quantiles $Q_q[D_{Nr}(\tau|\mathbf{a}_N, \mathbf{e}_M)]$, $q = 0.05, 0.5, 0.95$.



Source: Ouput DTNs: MO0709TSPAPLOT.000 [DIRS 183010]; and MO0709TSPAREGS.000 [DIRS 182976].

Figure J5-4. Estimates obtained with LHS of size $n_{LHS} = 300$ of expected (mean) dose $\bar{D}_{Nr}(\tau|\mathbf{a}_N)$ to RMEI for $0 \leq \tau \leq 10^6$ yr for individual radioactive species that result when only nominal conditions are considered.

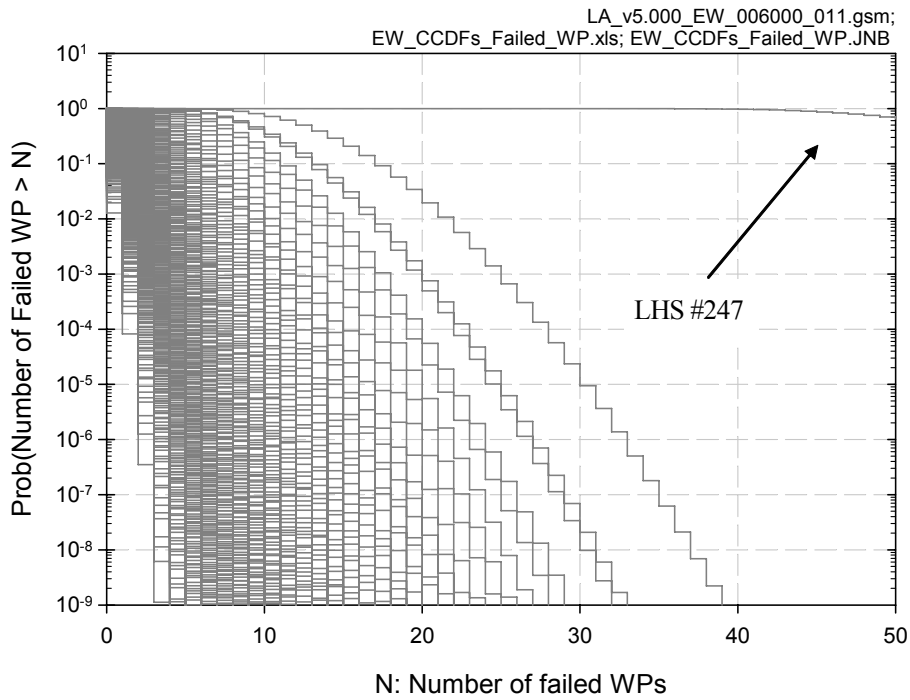


Source: Ouput DTNs: MO0709TSPAPLOT.000 [DIRS 183010]; MO0709TSPAREGS.000 [DIRS 182976]; and MO0709TSPASTAB.000 [DIRS 182983].

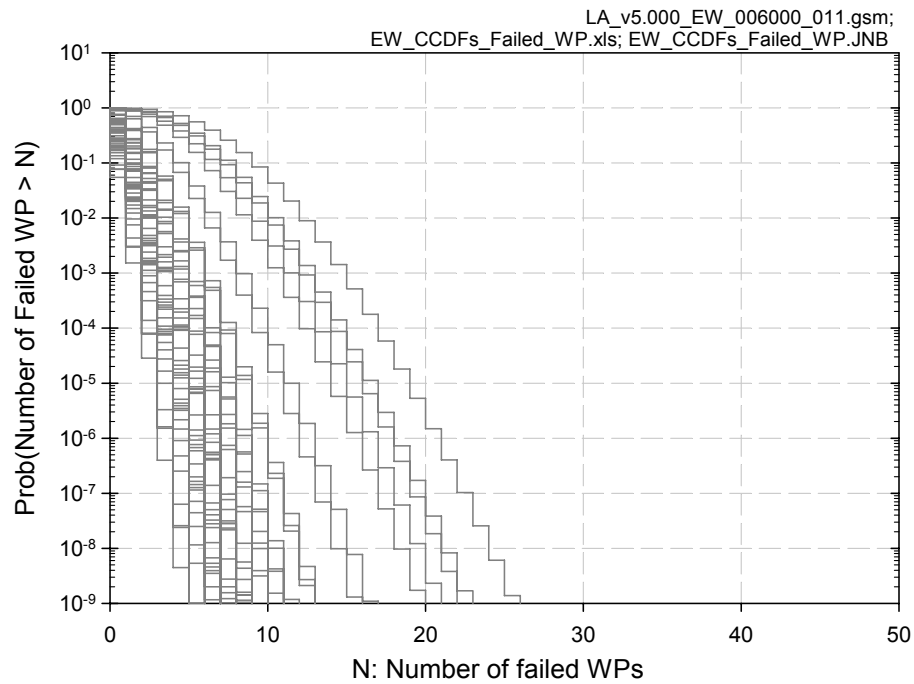
Figure J5-5. Assessment with replicated sampling of numerical error associated with use of an LHS of size $n_{LHS} = 300$ to determine epistemic uncertainty in dose $D_N(\tau | \mathbf{a}_N, \mathbf{e}_M)$ to RMEI for $0 \leq \tau \leq 10^6$ yr that results when only nominal conditions are considered: (a) Replicated estimates of expected (mean) dose $\bar{D}_N(\tau | \mathbf{a}_N)$ and quantiles $Q_q[D_N(\tau | \mathbf{a}_N, \mathbf{e}_M)]$, $q = 0.05, 0.5, 0.95$, and (b) confidence intervals for estimates of expected (mean) dose $\bar{D}_N(\tau | \mathbf{a}_N)$.

INTENTIONALLY LEFT BLANK

(a)

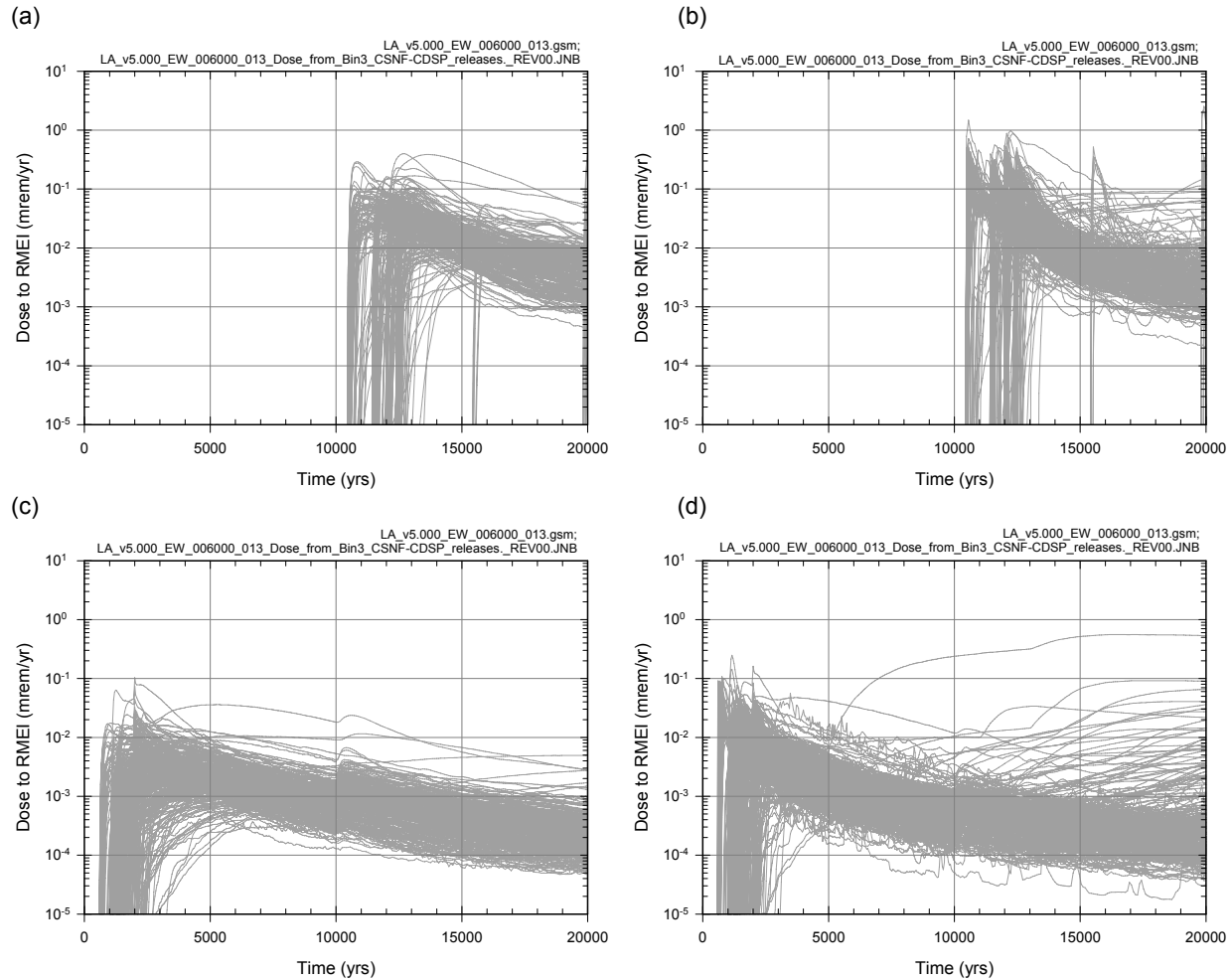


(b)



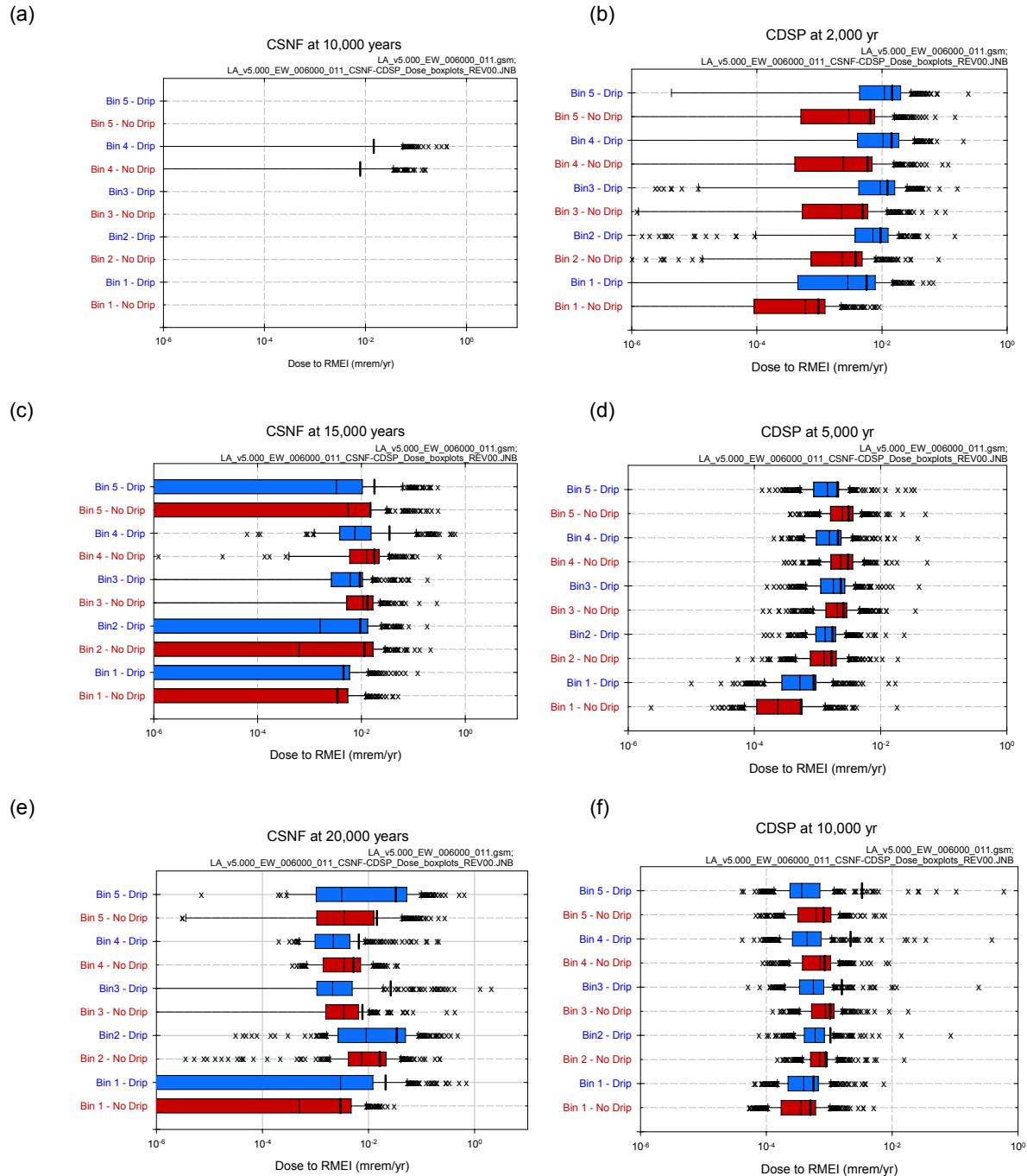
Source: Ouput DTNs: MO0709TSPAPLOT.000 [DIRS 183010]; and MO0709TSPAREGS.000 [DIRS 182976].

Figure J6.2-1. Complementary cumulative distribution functions (CCDFs) for number n_{EW} of WPs with early failure associated with individual elements of LHS of size $n_{LHS} = 300$ in Equation J.4.9-1: (a) CCDFs for all 300 LHS elements, and (b) CCDFs for first 50 LHS elements.



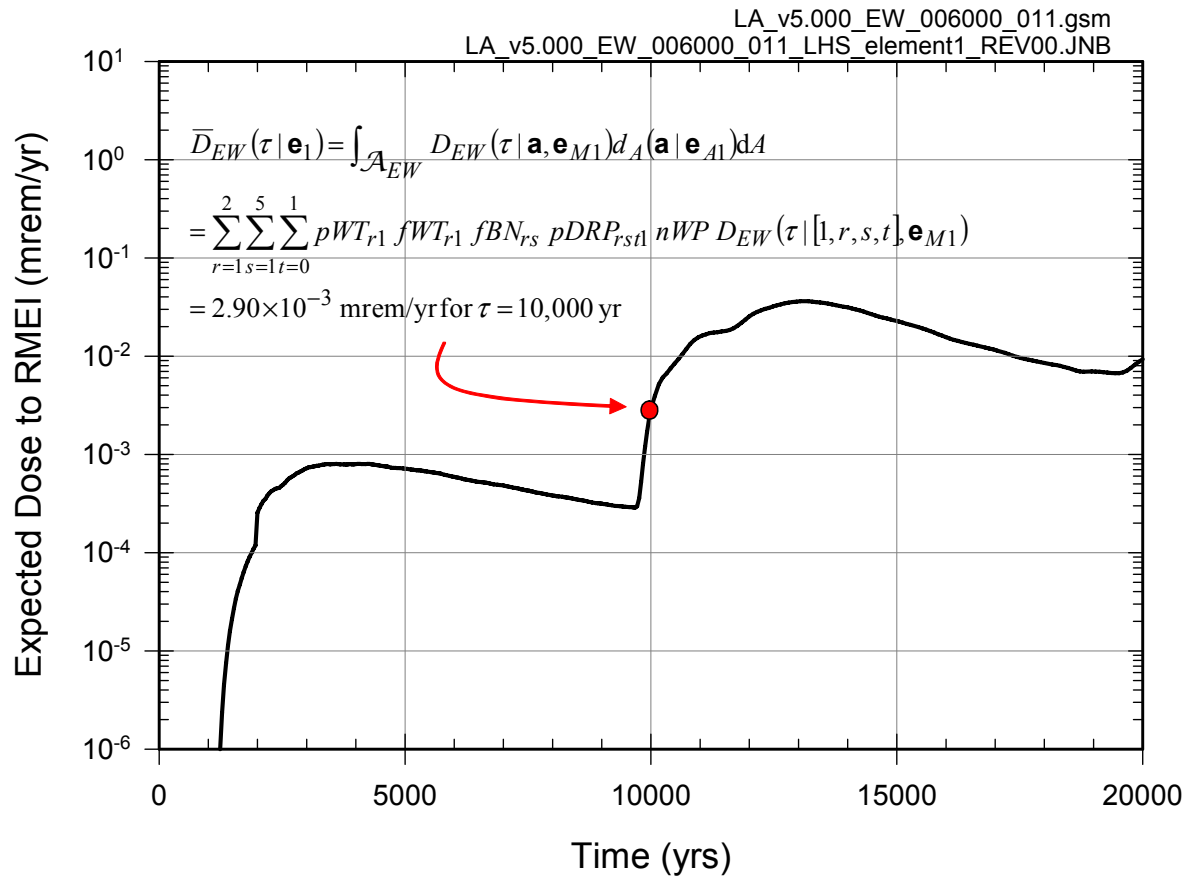
Source: Ouput DTNs: MO0709TSPAPLOT.000 [DIRS 183010]; MO0709TSPASENS.000 [DIRS 182982].

Figure J6.2-2. Summary of results obtained with LHS of size $nLHS = 300$ showing epistemic uncertainty in doses $D_{EW}(\tau|[1, r, 3, t], \mathbf{e}_M)$ for $0 \leq \tau \leq 20,000$ yr: (a) CSNF WP in bin 3 under non-dripping conditions (i.e., $D_{EW}(\tau|[1, 1, 3, 0], \mathbf{e}_{Mi})$, $i = 1, 2, \dots, nLHS = 300$), (b) CSNF WP in bin 3 under dripping conditions (i.e., $D_{EW}(\tau|[1, 1, 3, 1], \mathbf{e}_{Mi})$, $i = 1, 2, \dots, nLHS = 300$), (c) CDSP WP in bin 3 under non-dripping conditions (i.e., $D_{EW}(\tau|[1, 2, 3, 0], \mathbf{e}_{Mi})$, $i = 1, 2, \dots, nLHS = 300$), and (d) CDSP WP in bin 3 under dripping conditions (i.e., $D_{EW}(\tau|[1, 2, 3, 1], \mathbf{e}_{Mi})$, $i = 1, 2, \dots, nLHS = 300$).



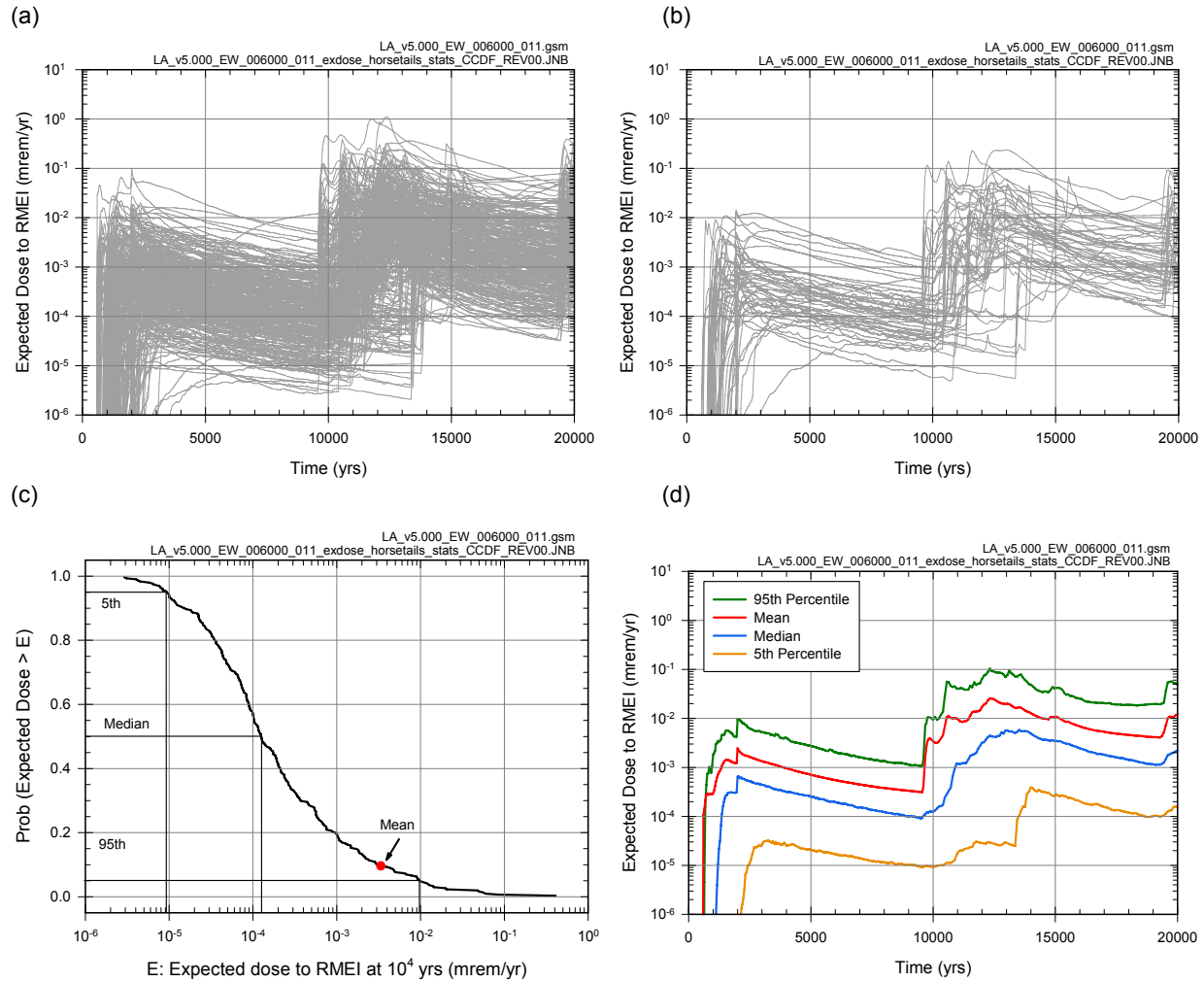
Source: Ouput DTNs: MO0709TSPAPLOT.000 [DIRS 183010]; and MO0709TSPAREGS.000 [DIRS 182976].

Figure J6.2-3. Box plots (Description: Box extends from 0.25 to 0.75 quantile; left and right bar and whisker extend to 0.1 and 0.9 quantile, respectively; x's represent values outside 0.1 to 0.9 quantile range; median and mean are indicated by light and dark vertical lines, respectively) summarizing results obtained with LHS of size $n_{LHS} = 300$ showing epistemic uncertainty in doses $D_{EW}(\tau|[1, r, s, t], \mathbf{e}_{Mi})$ for selected values of $\tau, r = 1, 2, s = 1, 2, 3, 4, 5, t = 0, 1$, and $i = 1, 2, \dots, n_{LHS} = 300$: (a, c, e) CSNF WPs at $\tau = 10,000, 15,000$ and $20,000$ yr, and (b, d, f) CDSP WPs at $\tau = 2000, 5000$ and $10,000$ yr.



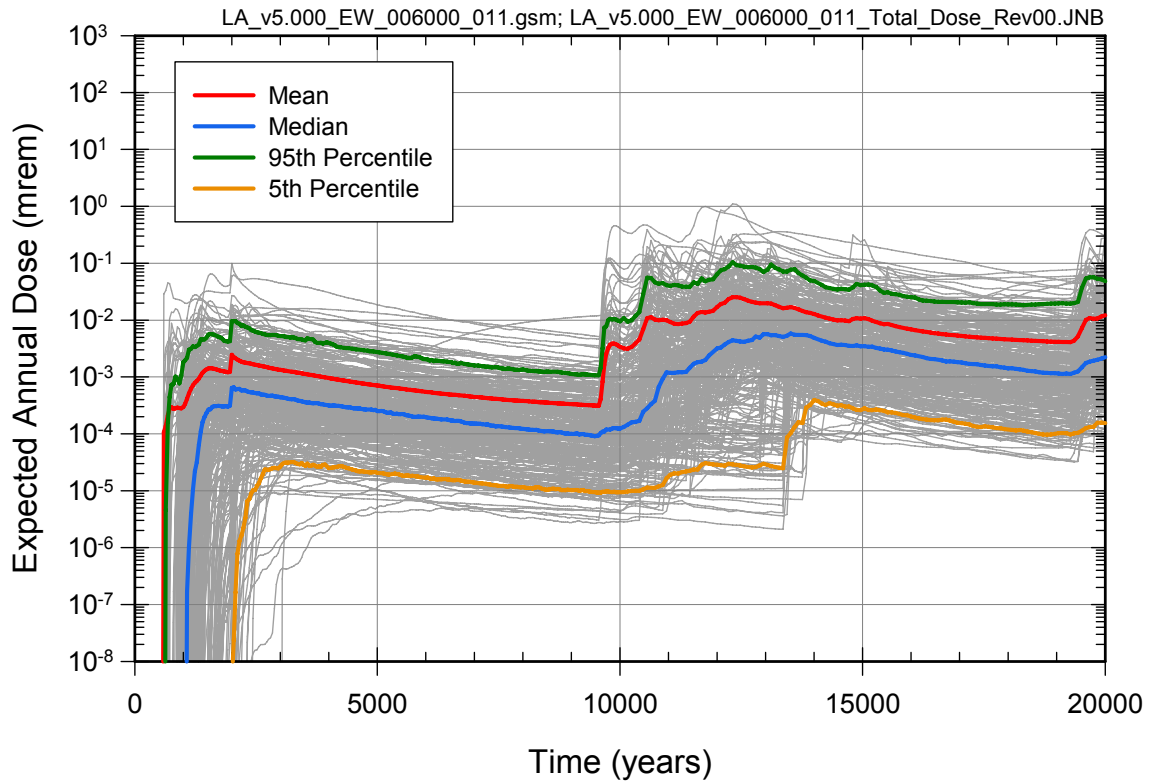
Source: Ouput DTNs: MO0709TSPAPLOT.000 [DIRS 183010]; and MO0709TSPAREGS.000 [DIRS 182976].

Figure J6.2-4. Estimate of $\bar{D}_{EW}(\tau|\mathbf{e}_1)$ for LHS element $\mathbf{e}_1 = [\mathbf{e}_{A1}, \mathbf{e}_{M1}]$ and $0 \leq \tau \leq 20,000$ yr with integration-based procedure indicated in Equation J6.2-2.



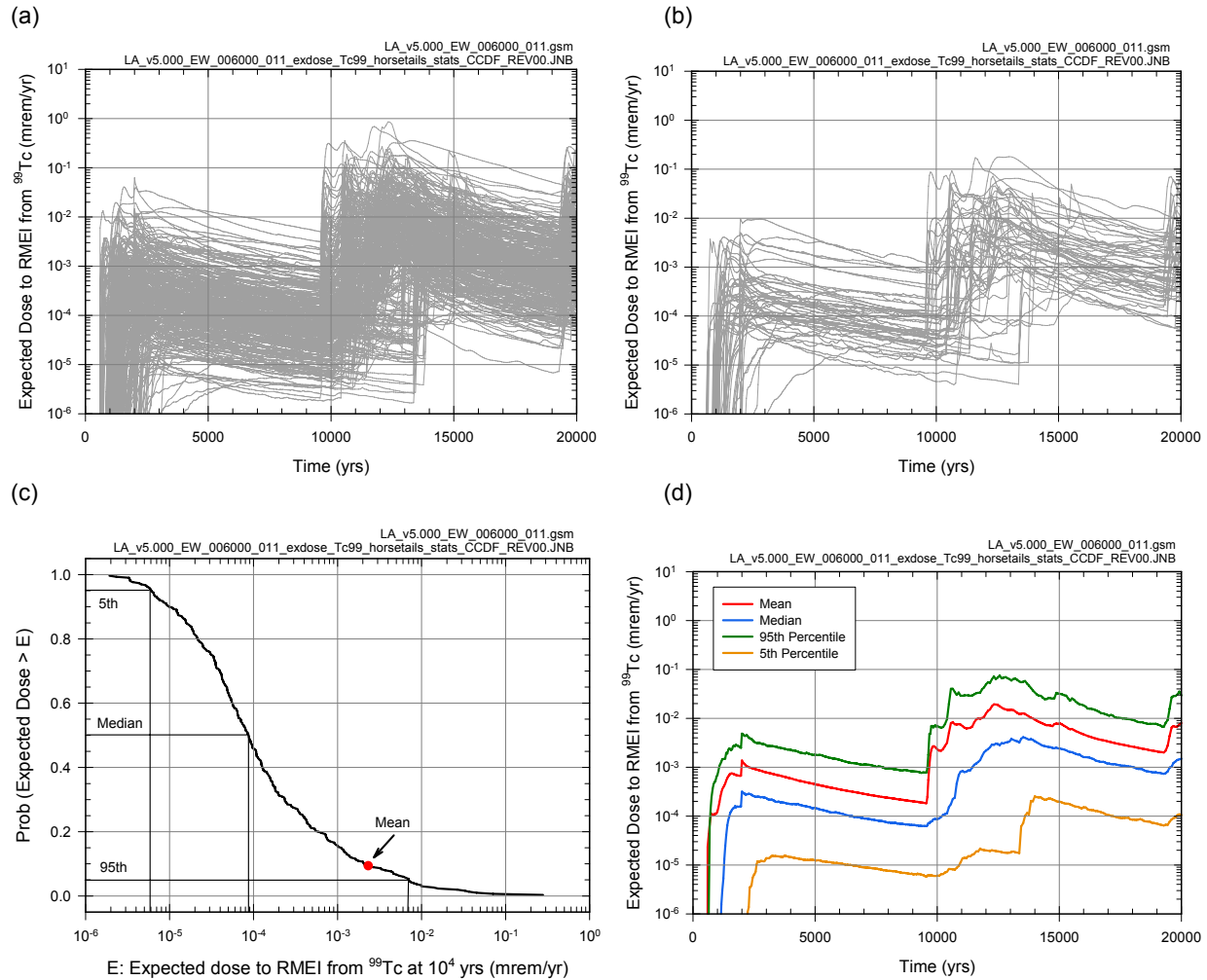
Source: Ouput DTNs: MO0709TSPAPLOT.000 [DIRS 183010]; and MO0709TSPAREGS.000 [DIRS 182976].

Figure J6.2-5. Estimate obtained with LHS of size $nLHS = 300$ showing epistemic uncertainty in expected dose $\bar{D}_{EW}(\tau|\mathbf{e})$ to RMEI for $0 \leq \tau \leq 20,000$ yr that at results when only early WP failure is considered: (a) expected dose $\bar{D}_{EW}(\tau|\mathbf{e}_i)$, $i = 1, 2, \dots, nLHS = 300$, (b) expected dose $\bar{D}_{EW}(\tau|\mathbf{e}_i)$, $i = 1, 2, \dots, 50$, (c) exceedance probabilities $p_E[D < \bar{D}_{EW}(\tau|\mathbf{e})]$ and quantiles $Q_q[\bar{D}_{EW}(\tau|\mathbf{e})]$, $q = 0.05, 0.5$ and 0.95 , for $\tau = 10^4$ yr, and (d) expected (mean) dose $\bar{\bar{D}}_{EW}(\tau)$ and quantiles $Q_q[\bar{\bar{D}}_{EW}(\tau|\mathbf{e})]$, $q = 0.05, 0.5, 0.95$.



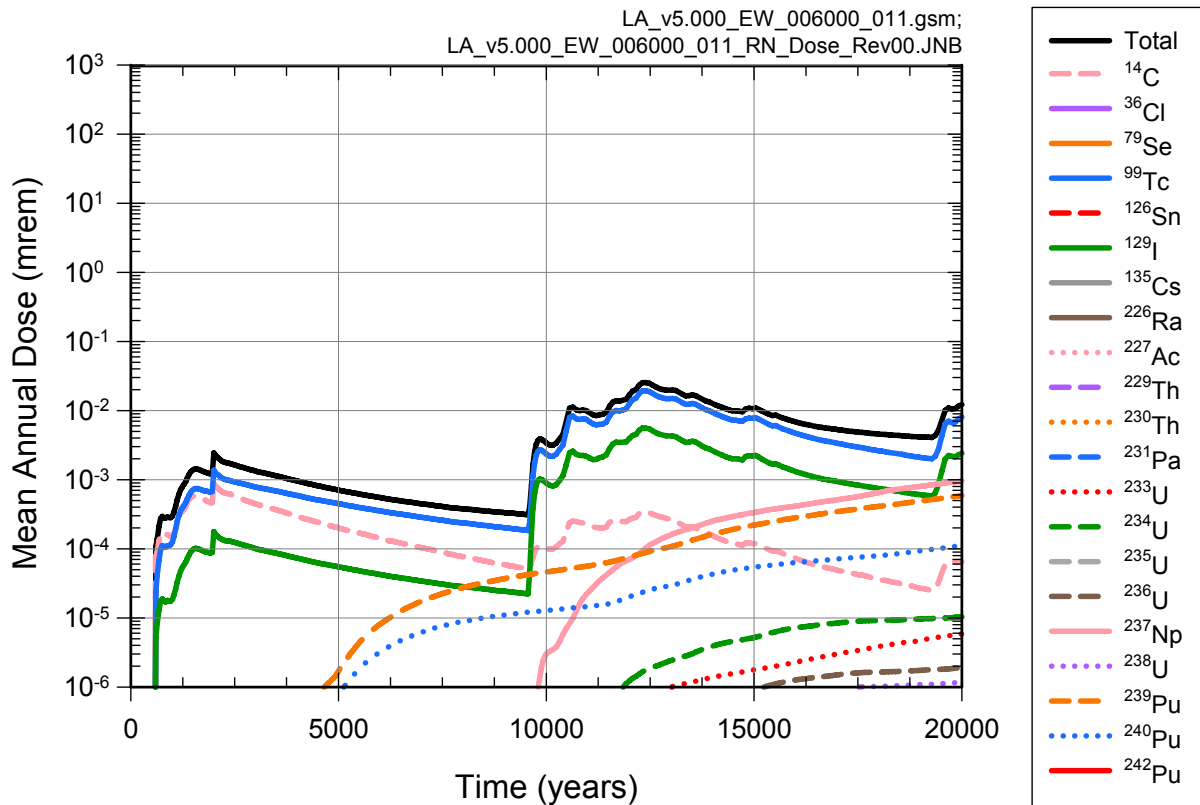
Source: Ouput DTNs: MO0709TSPAPLOT.000 [DIRS 183010]; and MO0709TSPAREGS.000 [DIRS 182976].

Figure J6.2-6. Summary of results obtained with LHS of size $n_{LHS} = 300$ showing epistemic uncertainty in expected dose $\bar{D}_{EW}(\tau|e)$ to RMEI for $0 \leq \tau \leq 20,000$ yr that results when only early WP failure is considered.



Source: Ouput DTNs: MO0709TSPAPLOT.000 [DIRS 183010]; and MO0709TSPAREGS.000 [DIRS 182976].

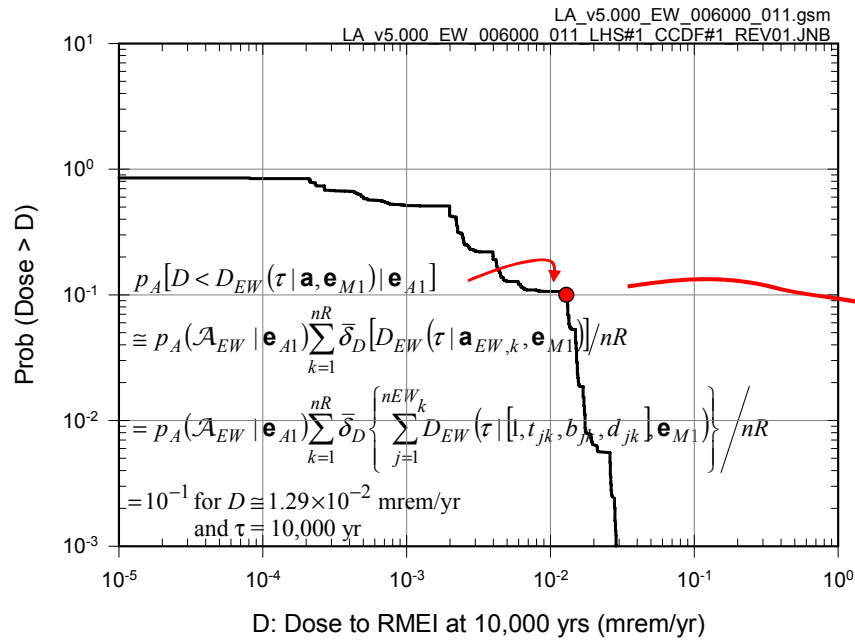
Figure J6.2-7. Estimate obtained with LHS of size $nLHS = 300$ showing epistemic uncertainty in expected dose $\bar{D}_{EW,r}(\tau|\mathbf{e})$ to RMEI for $0 \leq \tau \leq 20,000$ yr with r corresponding to ⁹⁹Tc that results when only early WP failure is considered: (a) expected dose $\bar{D}_{EW,r}(\tau|\mathbf{e}_i)$, $i = 1, 2, \dots, nLHS = 300$, (b) expected dose $\bar{D}_{EW,r}(\tau|\mathbf{e}_i)$, $i = 1, 2, \dots, 50$, (c) exceedance probabilities $p_{E|D < \bar{D}_{EW}(\tau|\mathbf{e})}$ and quantiles $Q_q[\bar{D}_{EW,r}(\tau|\mathbf{e})]$, $q = 0.05, 0.5$ and 0.95 , for $\tau = 10^4$ yr, and (d) expected (mean) dose $\bar{\bar{D}}_{EW,r}(\tau)$ and quantiles $Q_q[\bar{D}_{EW,r}(\tau|\mathbf{e})]$, $q = 0.05, 0.5, 0.95$.



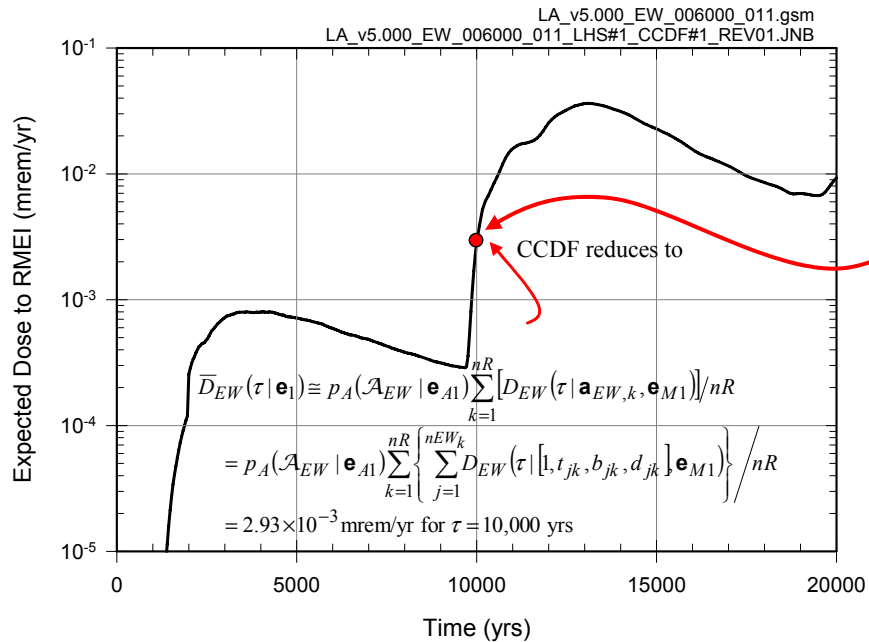
Source: Ouput DTNs: MO0709TSPAPLOT.000 [DIRS 183010]; and MO0709TSPAREGS.000 [DIRS 182976].

Figure J6.2-8. Estimates obtained with LHS of size $n_{LHS} = 300$ of expected (mean) dose $\bar{D}_{EW,r}(\tau)$ to RMEI for $0 \leq \tau \leq 20,000$ yr for individual radioactive species that result when only early WP failure is considered.

(a)

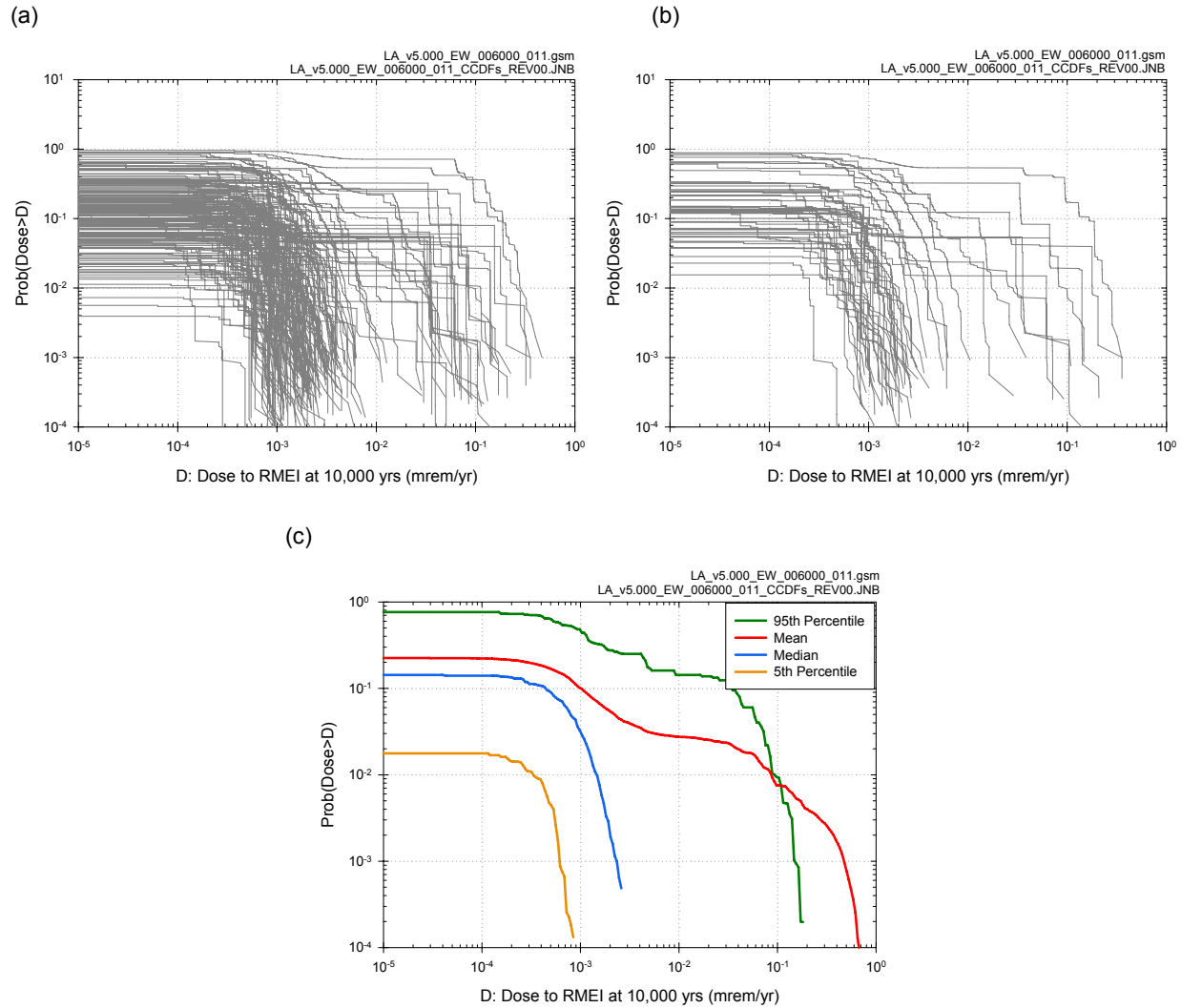


(b)



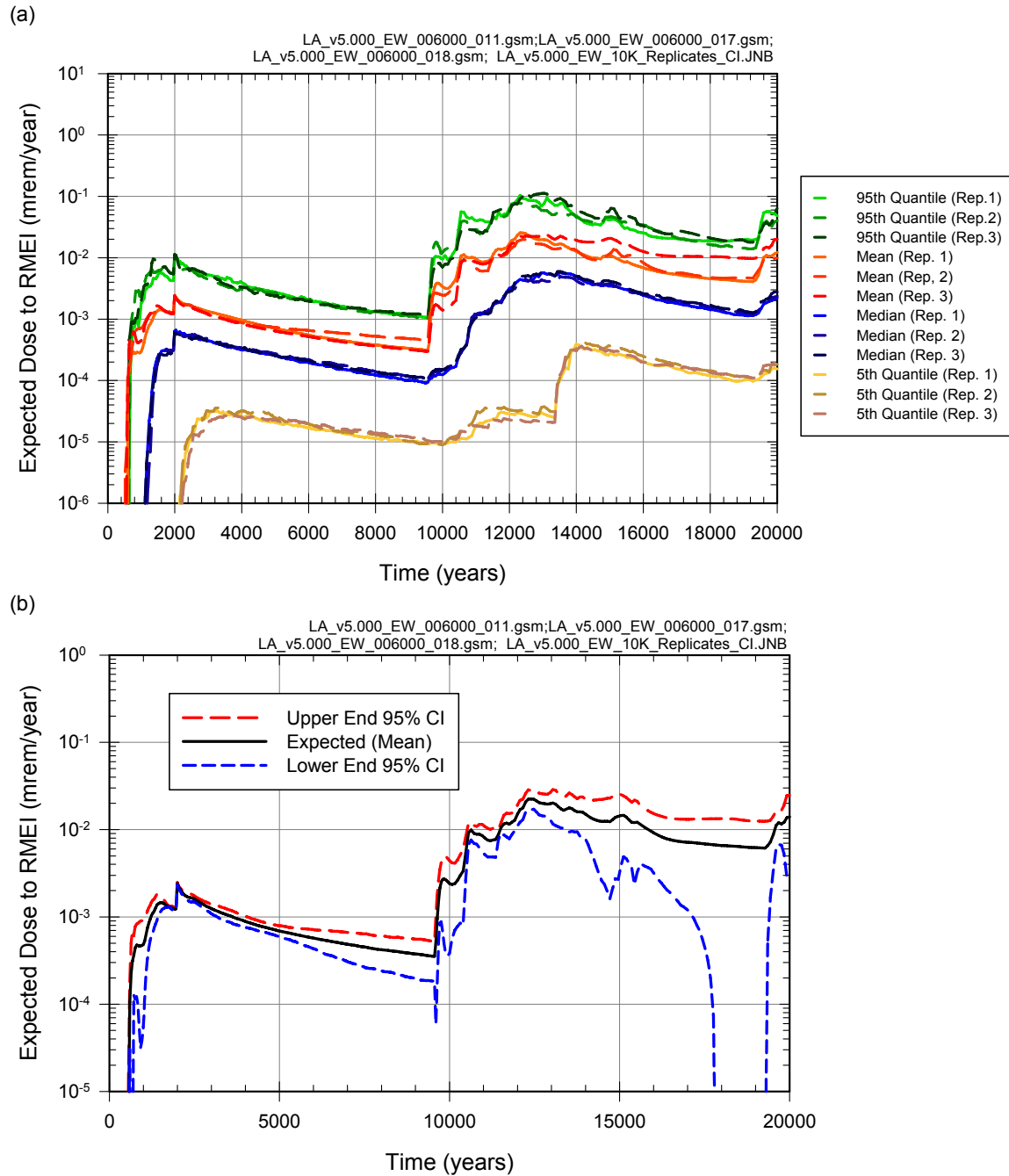
Source: Ouput DTNs: MO0709TSPAPLOT.000 [DIRS 183010]; and MO0709TSPAREGS.000 [DIRS 182976].

Figure J6.2-9. Results associated with $D_{EW}(\tau | \mathbf{a}_{EW}, \mathbf{e}_{M1})$ for LHS element $\mathbf{e}_1 = [\mathbf{e}_{A1}, \mathbf{e}_{M1}]$ obtained with sampling-based (Monte Carlo) procedures: (a) CCDF for $D_{EW}(10^4 \text{ yr} | \mathbf{a}_{EW}, \mathbf{e}_{M1})$ with exceedance probabilities $p_A[D < D_{EW}(10^4 \text{ yr} | \mathbf{a}, \mathbf{e}_{M1}) | \mathbf{e}_{A1}]$ defined in Equation (J6.2-12), and (b) expected dose $\bar{D}_{EW}(10^4 \text{ yr} | \mathbf{e}_1)$ associated with $D_{EW}(10^4 \text{ yr} | \mathbf{a}_{EW}, \mathbf{e}_{M1})$ as defined in Equation (J6.2-10).



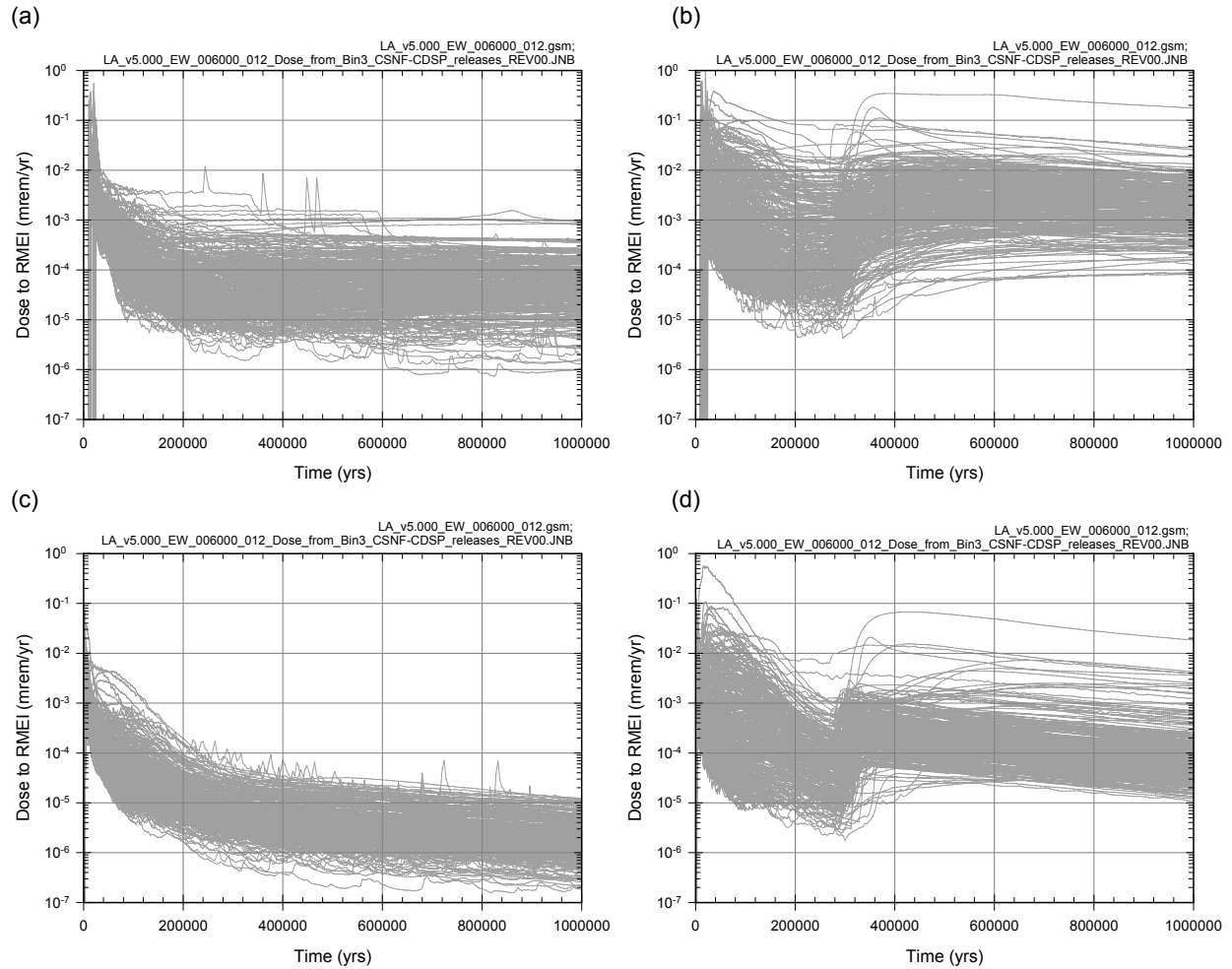
Source: Ouput DTNs: MO0709TSPAPLOT.000 [DIRS 183010]; and MO0709TSPAREGS.000 [DIRS 182976].

Figure J6.2-10. Results associated with $D_{EW}(10^4 \text{ yr} | \mathbf{a}_{EW}, \mathbf{e}_M)$ obtained with sampling-based (Monte Carlo) procedures for an LHS of size $n_{LHS} = 300$: (a) CCDFs for $D_{EW}(10^4 \text{ yr} | \mathbf{a}_{EW}, \mathbf{e}_M)$ with exceedance probabilities $p_A[D < D_{EW}(10^4 \text{ yr} | \mathbf{a}_{EW}, \mathbf{e}_M) | \mathbf{e}_{Ai}]$ defined in Equation J6.2-12 for $i = 1, 2, \dots, n_{LHS} = 300$, (b) CCDFs for $D_{EW}(10^4 \text{ yr} | \mathbf{a}_{EW}, \mathbf{e}_M)$ with exceedance probabilities $p_A[D < D_{EW}(10^4 \text{ yr} | \mathbf{a}_{EW}, \mathbf{e}_M) | \mathbf{e}_{Ai}]$ defined in Equation J6.2-13 for $i = 1, 2, \dots, 50$, and (c) expected (mean) CCDF and quantile curves, $q = 0.05, 0.5, 0.95$, for CCDFs in (a).



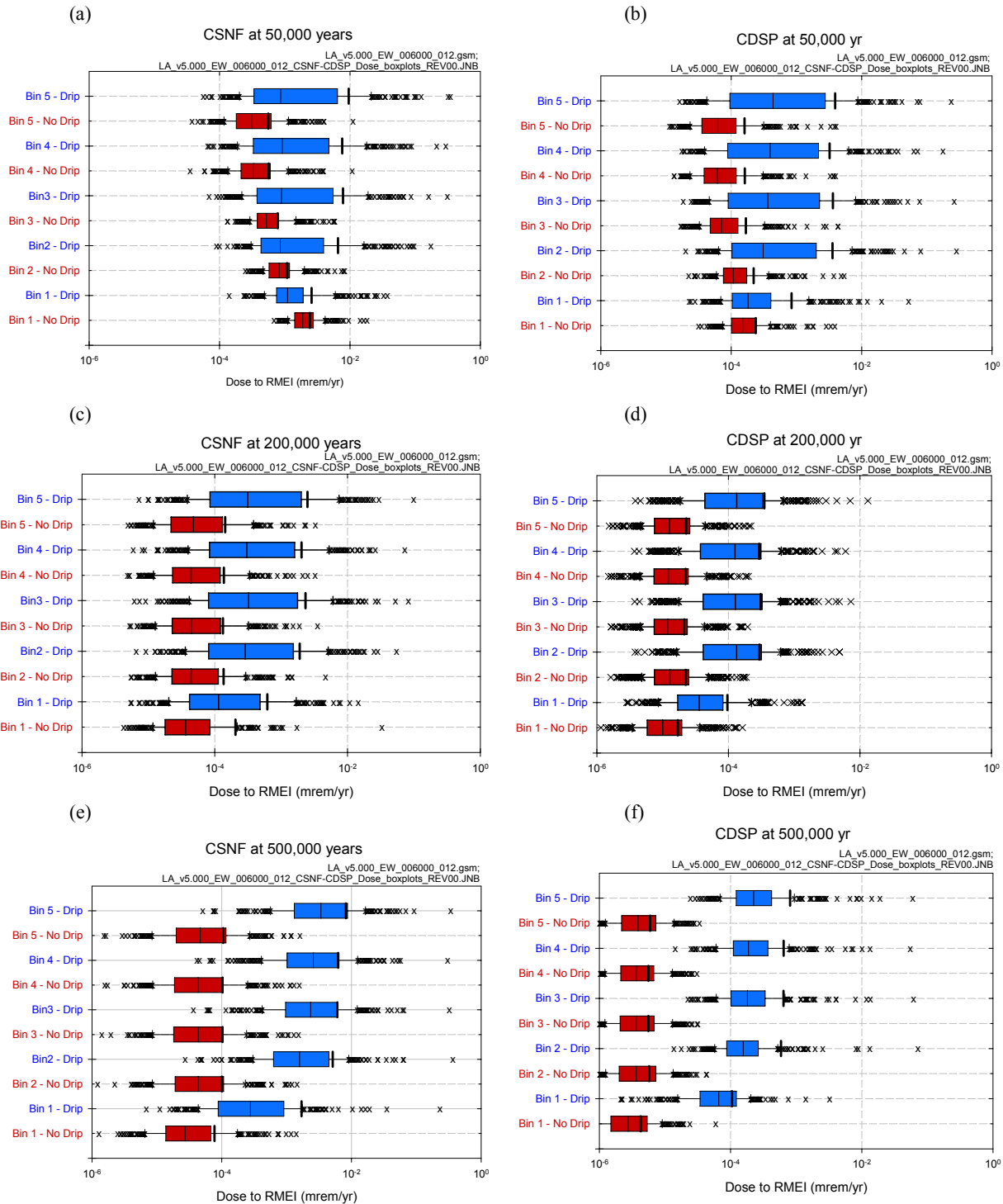
Source: Ouput DTNs: MO0709TSPAPLOT.000 [DIRS 183010]; MO0709TSPAREGS.000 [DIRS 182976]; and MO0709TSPASTAB.000 [DIRS 182983].

Figure J6.2-11. Assessment with replicated sampling of numerical error associated with use of an LHS of size $n_{LHS} = 300$ to determine epistemic uncertainty in expected dose $\bar{D}_{EW}(\tau|\mathbf{e})$ to RMEI for $0 \leq \tau \leq 20,000$ yr that results when only early WP failure is considered: (a) Replicated estimates of expected (mean) dose $\bar{D}_{EW}(\tau)$ and quantiles $Q_q[\bar{D}_{EW}(\tau|\mathbf{e})]$, $q = 0.05, 0.5, 0.95$, and (b) confidence intervals for estimates of expected (mean) dose $\bar{D}_{EW}(\tau)$.



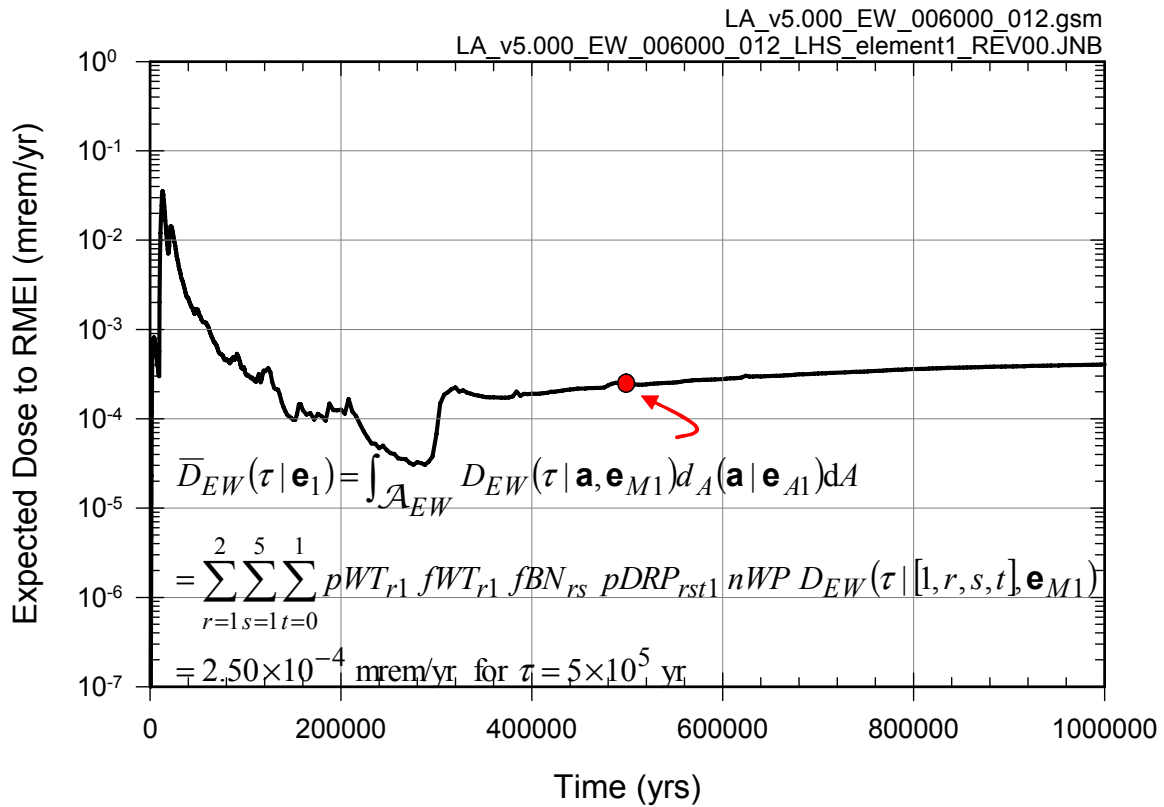
Source: Ouput DTNs: MO0709TSPAPLOT.000 [DIRS 183010]; and MO0709TSPAREGS.000 [DIRS 182976].

Figure J6.2-12. Summary of results obtained with LHS of size $nLHS = 300$ showing epistemic uncertainty in doses $D_{EW}(\tau|[1, r, s, t], \mathbf{e}_M)$ for $0 \leq \tau \leq 10^6$ yr: (a) CSNF WP in bin 3 under nondripping conditions (i.e., $D_{EW}(\tau|[1, 1, 3, 0], \mathbf{e}_{Mi})$, $i = 1, 2, \dots, nLHS = 300$), (b) CSNF WP in bin 3 under dripping conditions (i.e., $D_{EW}(\tau|[1, 1, 3, 1], \mathbf{e}_{Mi})$, $i = 1, 2, \dots, nLHS = 300$), (c) CDSP WP in bin 3 under nondripping conditions (i.e., $D_{EW}(\tau|[1, 2, 3, 0], \mathbf{e}_{Mi})$, $i = 1, 2, \dots, nLHS = 300$), and (d) CDSP WP in bin 3 under dripping conditions (i.e., $D_{EW}(\tau|[1, 2, 3, 1], \mathbf{e}_{Mi})$, $i = 1, 2, \dots, nLHS = 300$).



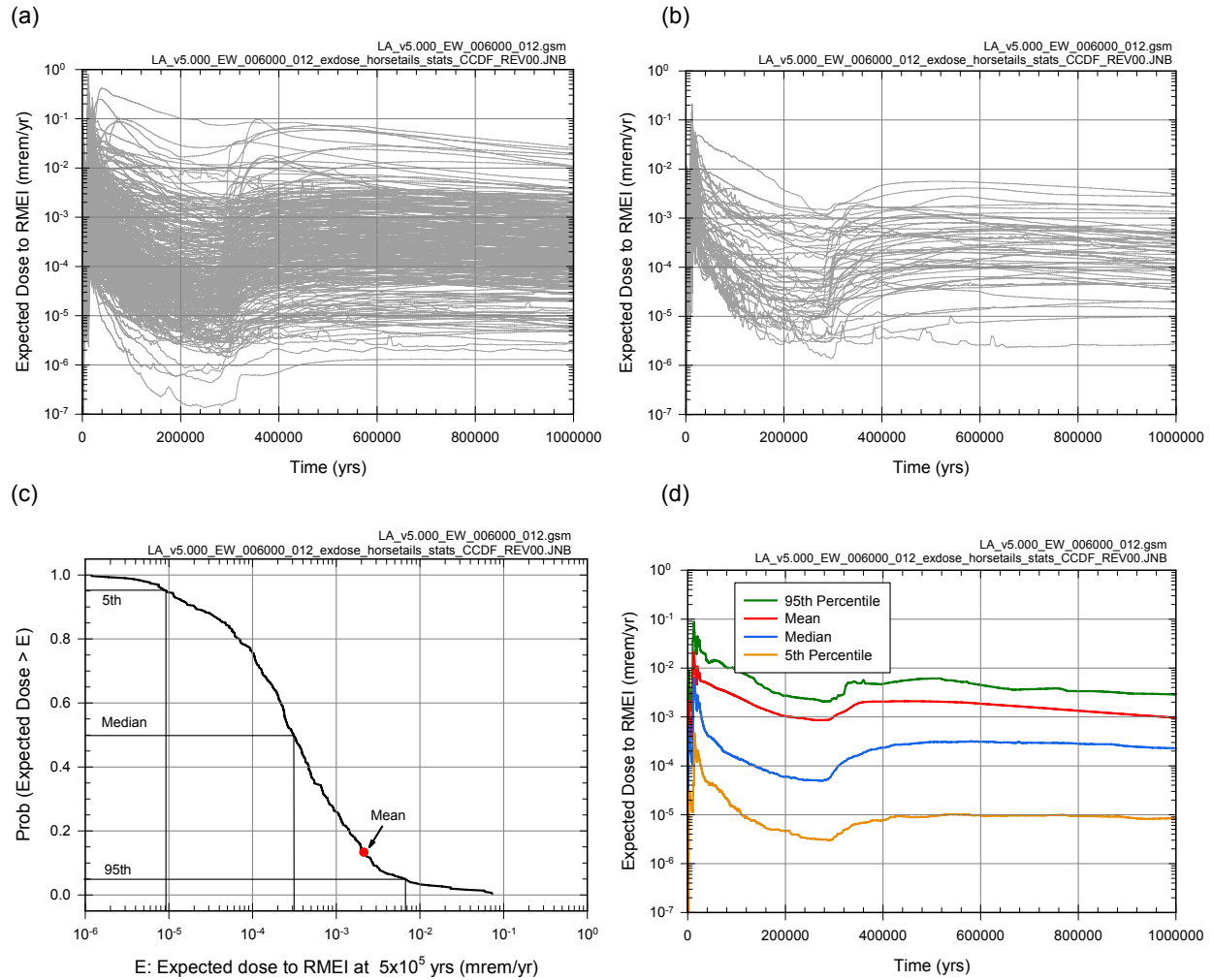
Source: Ouput DTNs: MO0709TSPAPLOT.000 [DIRS 183010]; and MO0709TSPAREGS.000 [DIRS 182976].

Figure J6.2-13. Box plots (see Figure J6.2-3 for description) summarizing results obtained with LHS of size $nLHS = 300$ showing epistemic uncertainty in doses $D_{EW}(\tau)[1, r, s, t], e_{Mi}$ for $\tau = 5 \times 10^4, 2 \times 10^5, 5 \times 10^5$ yr, $r = 1, 2, s = 1, 2, 3, 4, 5, t = 0, 1$, and $i = 1, 2, \dots, nLHS = 300$: (a, c, e) CSNF WPs for $\tau = 5 \times 10^4, 2 \times 10^5, 5 \times 10^5$ yr, and (b, d, f) CDSP WPs for $\tau = 5 \times 10^4, 2 \times 10^5, 5 \times 10^5$ yr.



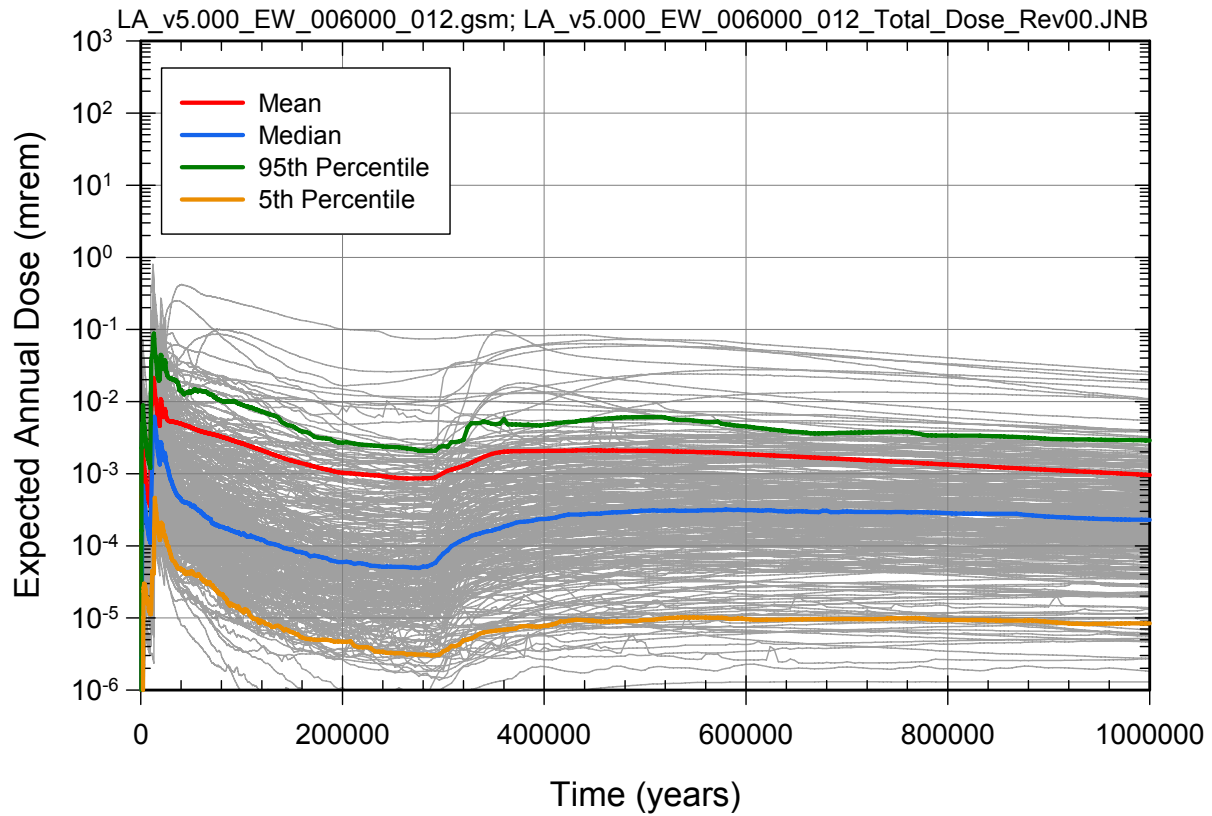
Source: Ouput DTNs: MO0709TSPAPLOT.000 [DIRS 183010]; and MO0709TSPAREGS.000 [DIRS 182976].

Figure J6.2-14. Estimate of $\bar{D}_{EW}(\tau | \mathbf{e}_1)$ for LHS element $\mathbf{e}_1 = [\mathbf{e}_{A1}, \mathbf{e}_{M1}]$ and $0 \leq \tau \leq 10^6$ yr with integration-based procedure indicated in Equation (J6.2-2).



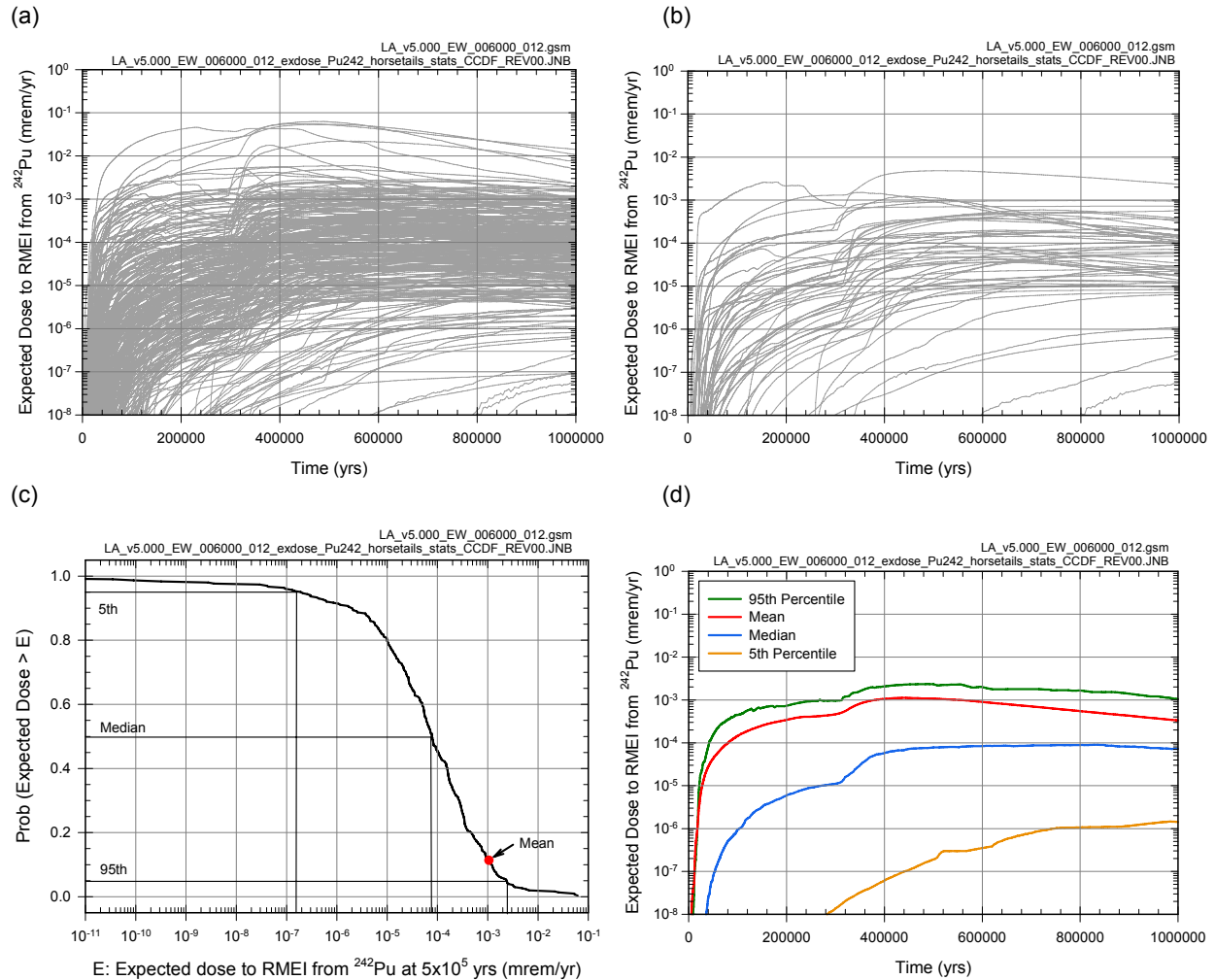
Source: Ouput DTNs: MO0709TSPAPLOT.000 [DIRS 183010]; and MO0709TSPAREGS.000 [DIRS 182976].

Figure J6.2-15. Estimate obtained with LHS of size $nLHS = 300$ showing epistemic uncertainty in expected dose $\bar{D}_{EW}(\tau|\mathbf{e})$ to RMEI for $0 \leq \tau \leq 10^6$ yr that at results when only early WP failure is considered: (a) expected dose $\bar{D}_{EW}(\tau|\mathbf{e}_i)$, $i = 1, 2, \dots, nLHS = 300$, (b) expected dose $\bar{D}_{EW}(\tau|\mathbf{e}_i)$, $i = 1, 2, \dots, 50$, (c) exceedance probabilities $p_E[D < \bar{D}_{EW}(\tau|\mathbf{e})]$ and quantiles $Q_q[\bar{D}_{EW}(\tau|\mathbf{e})]$, $q = 0.05, 0.5$ and 0.95 , for $\tau = 5 \times 10^5$ yr, and (d) expected (mean) dose $\bar{\bar{D}}_{EW}(\tau)$ and quantiles $Q_q[\bar{D}_{EW}(\tau|\mathbf{e})]$, $q = 0.05, 0.5, 0.95$.



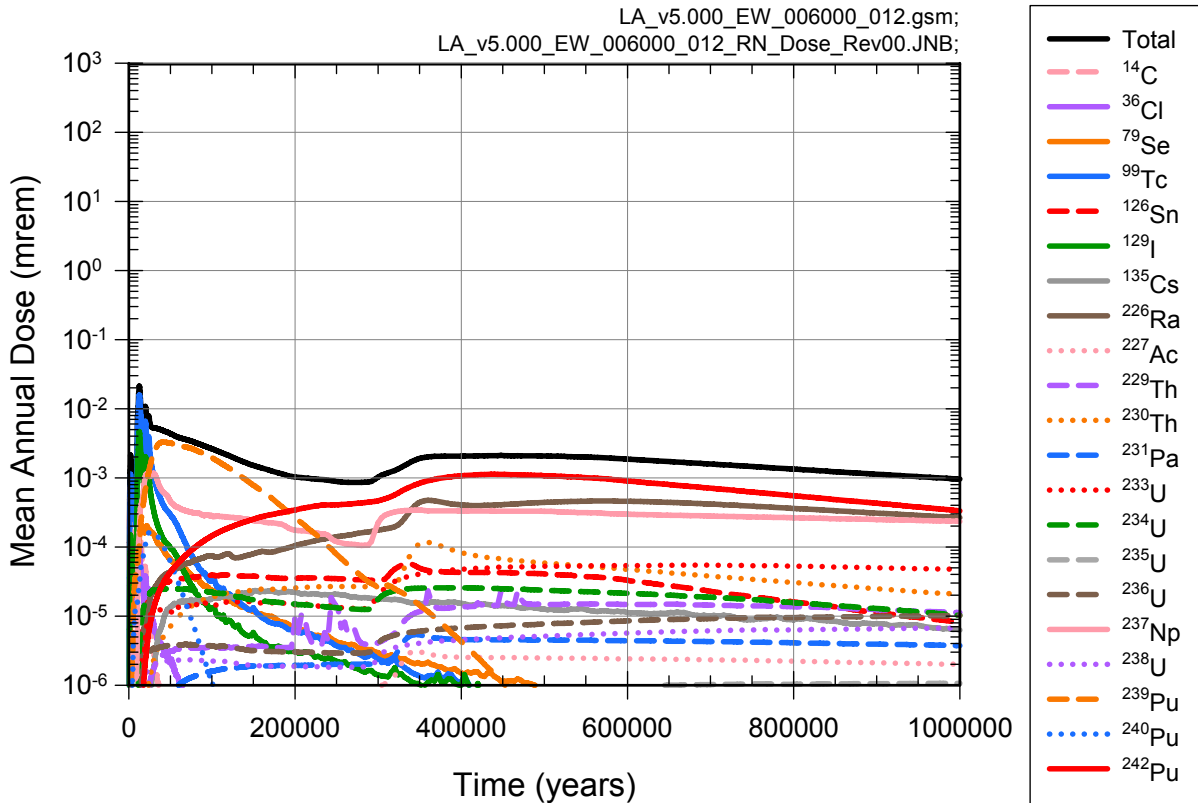
Source: Output DTNs: MO0709TSPAPLOT.000 [DIRS 183010]; and MO0709TSPAREGS.000 [DIRS 182976].

Figure J6.2-16. Summary of results obtained with LHS of size $nLHS = 300$ showing epistemic uncertainty in expected dose $\bar{D}_{EW}(\tau|\mathbf{e})$ to RMEI for $0 \leq \tau \leq 10^6$ yr that results when only early WP failure is considered.



Source: Ouput DTNs: MO0709TSPAPLOT.000 [DIRS 183010]; and MO0709TSPAREGS.000 [DIRS 182976].

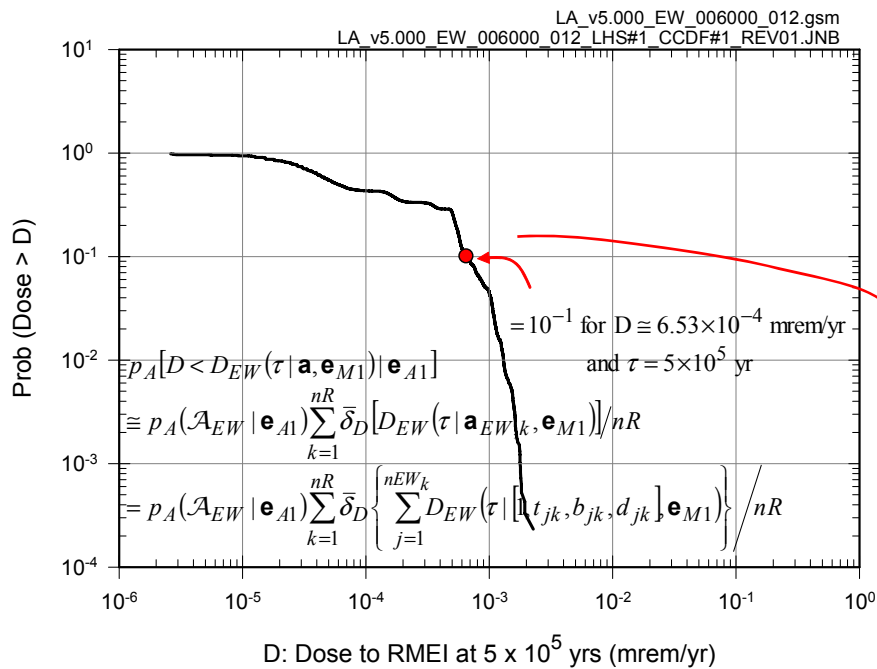
Figure J6.2-17. Estimate obtained with LHS of size $nLHS = 300$ showing epistemic uncertainty in expected dose $\bar{D}_{EW,r}(\tau|\mathbf{e})$ to RMEI for $0 \leq \tau \leq 10^6$ yr with r corresponding to ^{242}Pu that results when only early DS failure is considered: (a) expected dose $\bar{D}_{EW,r}(\tau|\mathbf{e}_i)$, $i = 1, 2, \dots, nLHS = 300$, (b) expected dose $\bar{D}_{EW,r}(\tau|\mathbf{e}_i)$, $i = 1, 2, \dots, 50$, (c) exceedance probabilities $p_E[D < \bar{D}_{EW,r}(\tau|\mathbf{e})]$ and quantiles $Q_q[\bar{D}_{EW,r}(\tau|\mathbf{e})]$, $q = 0.05, 0.5$ and 0.95 , for $\tau = 5 \times 10^5$ yr, and (d) expected (mean) dose $\bar{\bar{D}}_{EW,r}(\tau)$ and quantiles $Q_q[\bar{\bar{D}}_{EW,r}(\tau|\mathbf{e})]$, $q = 0.05, 0.5, 0.95$.



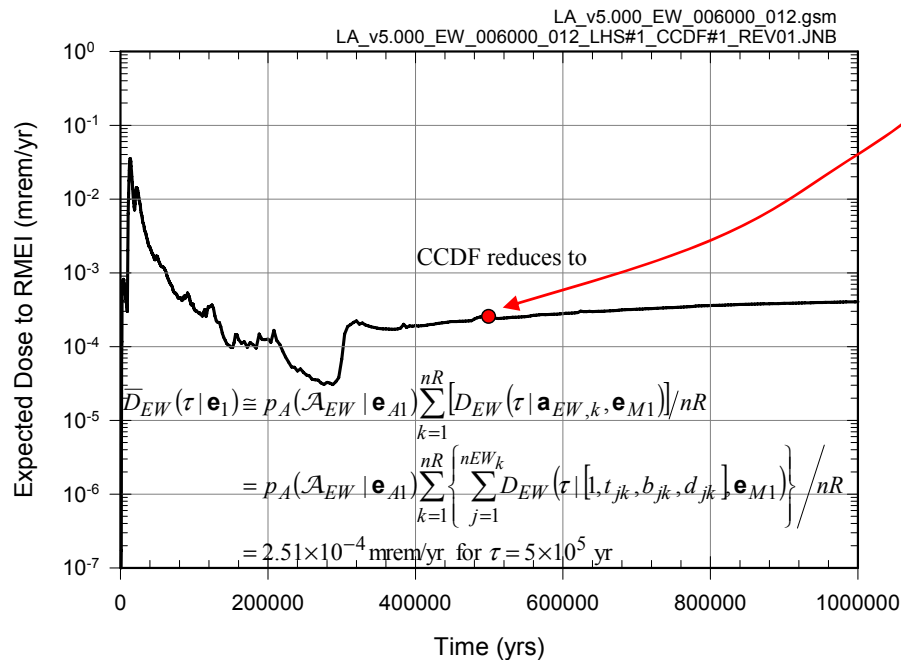
Source: Ouput DTNs: MO0709TSPAPLOT.000 [DIRS 183010]; and MO0709TSPAREGS.000 [DIRS 182976].

Figure J6.2-18. Estimates obtained with LHS of size $nLHS = 300$ of expected (mean) dose $\bar{D}_{EW,r}(\tau)$ to RMEI for $0 \leq \tau \leq 10^6$ yr for individual radioactive species that result when only early WP failure is considered.

(a)

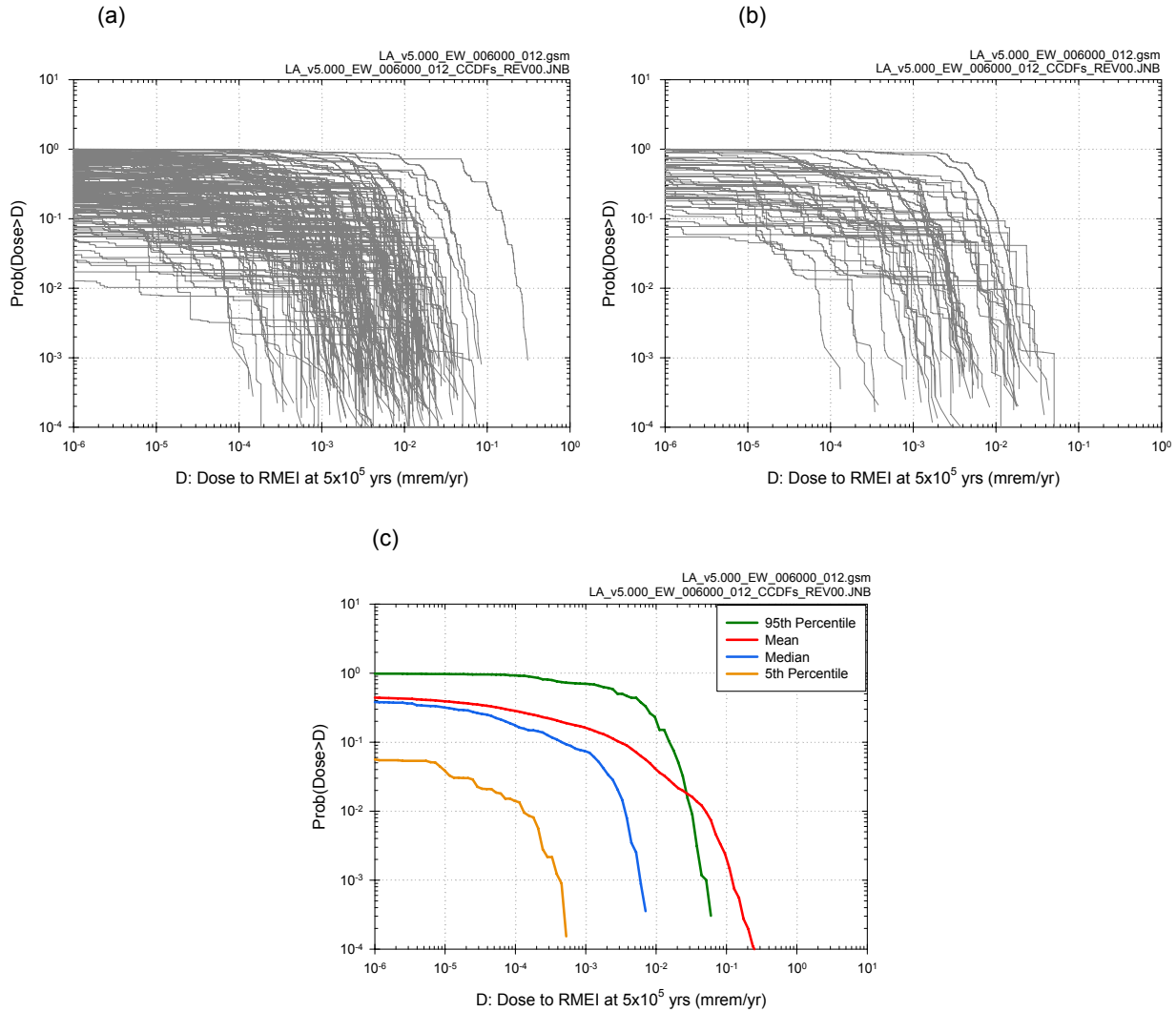


(b)



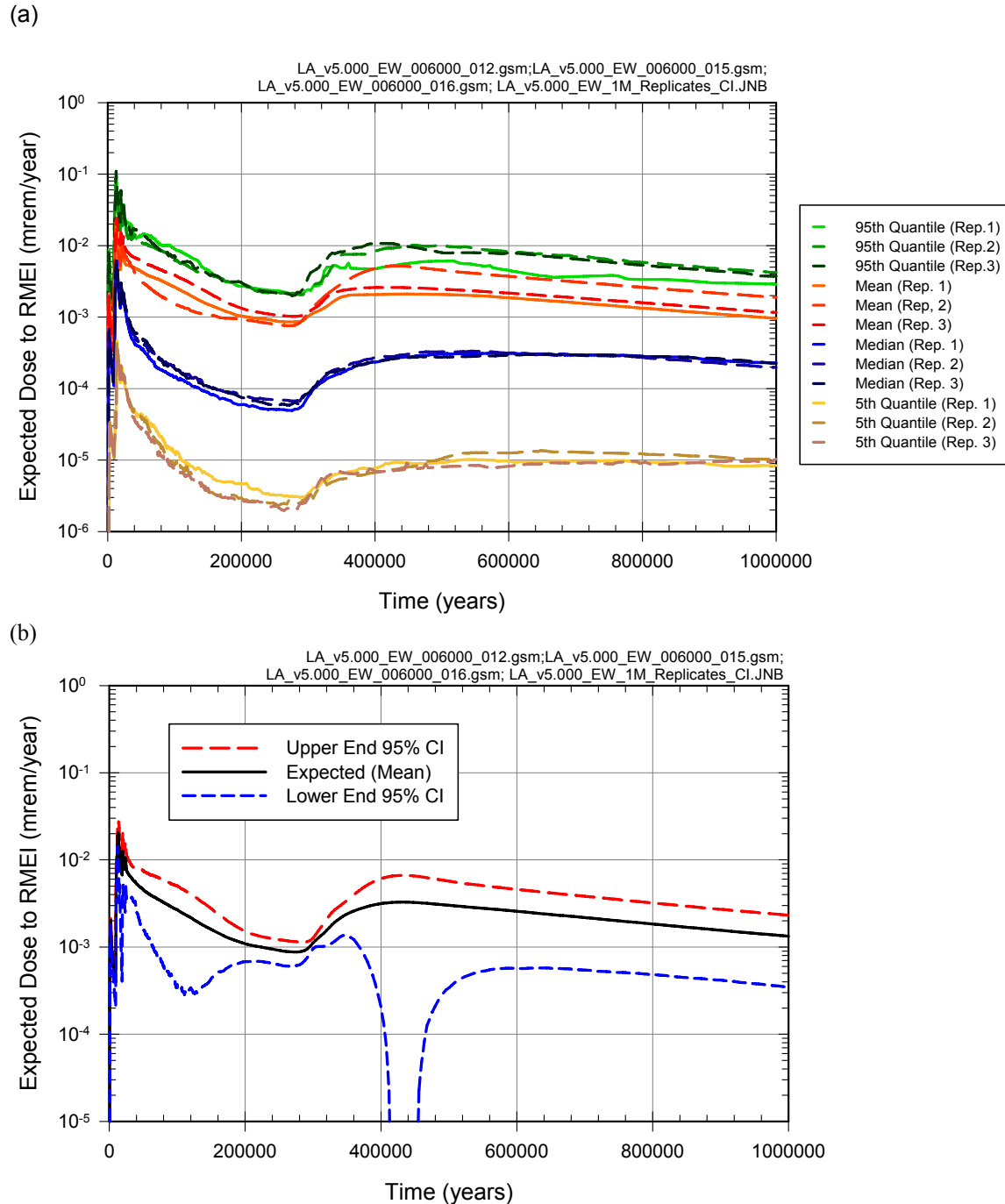
Source: Ouput DTNs: MO0709TSPAPLOT.000 [DIRS 183010]; and MO0709TSPAREGS.000 [DIRS 182976].

Figure J6.2-19. Results associated with $D_{EW}(\tau | \mathbf{a}_{EW}, \mathbf{e}_{M1})$ for LHS element $\mathbf{e}_1 = [\mathbf{e}_{A1}, \mathbf{e}_{M1}]$ obtained with sampling-based (Monte Carlo) procedures: (a) CCDF for $D_{EW}(5 \times 10^5 \text{ yr} | \mathbf{a}_{EW}, \mathbf{e}_{M1})$ with exceedance probabilities $p_A[D < D_{EW}(5 \times 10^5 \text{ yr} | \mathbf{a}, \mathbf{e}_{M1}) | \mathbf{e}_{A1}]$ defined in Equation (J6.2-12), and (b) expected dose $\bar{D}_{EW}(5 \times 10^5 \text{ yr} | \mathbf{e}_1)$ associated with $D_{EW}(5 \times 10^5 \text{ yr} | \mathbf{a}_{EW}, \mathbf{e}_{M1})$ as defined in Equation (J6.2-10).



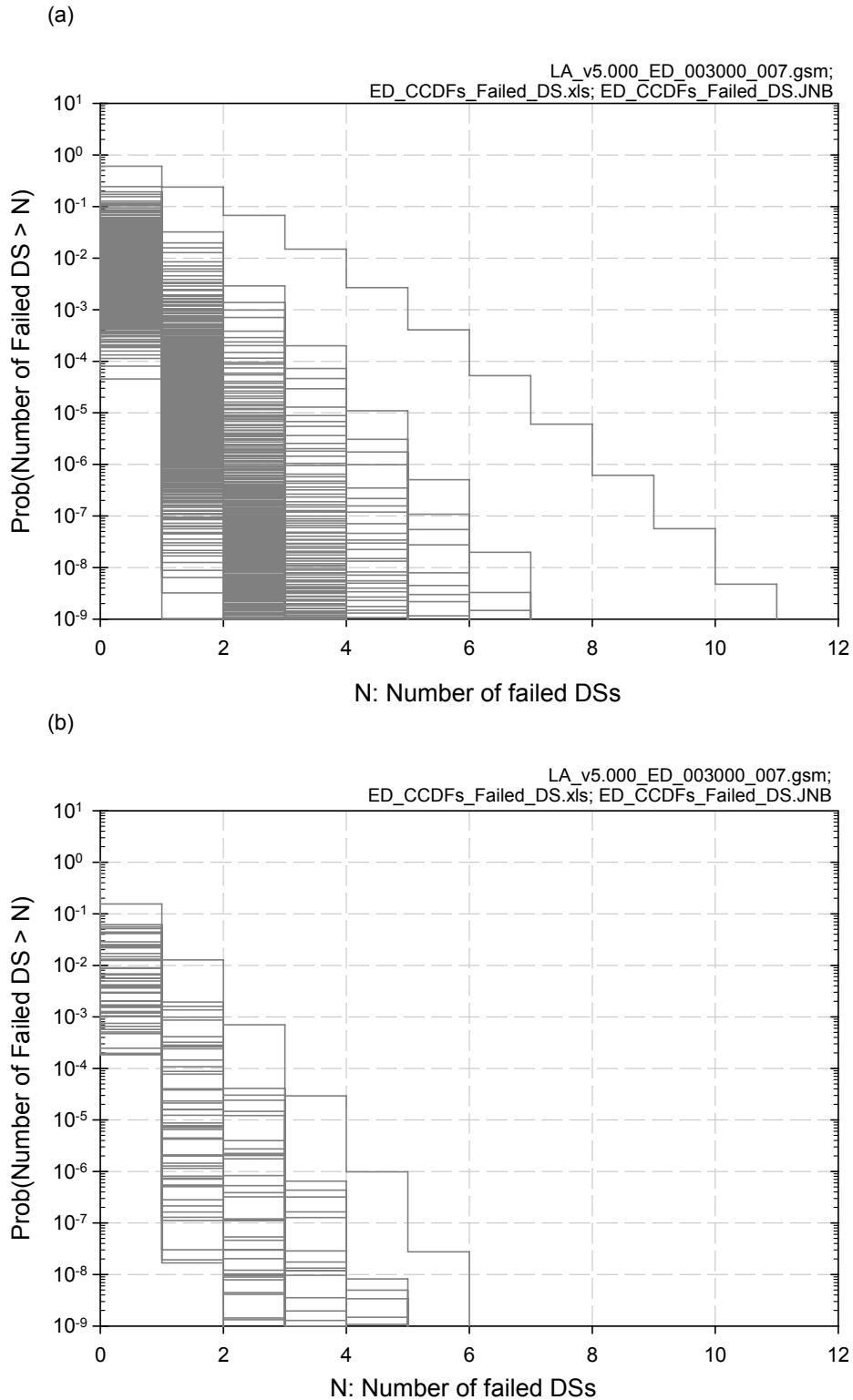
Source: Ouput DTNs: MO0709TSPAPLOT.000 [DIRS 183010]; and MO0709TSPAREGS.000 [DIRS 182976].

Figure J6.2-20. Results associated with $D_{EW}(5 \times 10^5 \text{ yr} | \mathbf{a}_{EW}, \mathbf{e}_M)$ obtained with sampling-based (Monte Carlo) procedures for an LHS of size $n_{LHS} = 300$: (a) CCDFs for $D_{EW}(5 \times 10^5 \text{ yr} | \mathbf{a}_{EW}, \mathbf{e}_{Mi})$ with exceedance probabilities $p_A[D < D_{EW}(5 \times 10^5 \text{ yr} | \mathbf{a}, \mathbf{e}_{Mi}) | \mathbf{e}_{Ai}]$ defined in Equation J66.2-12 for $i = 1, 2, \dots, n_{LHS} = 300$, (b) CCDFs for $D_{EW}(10^4 \text{ yr} | \mathbf{a}_{EW}, \mathbf{e}_{Mi})$ with exceedance probabilities $p_A[D < D_{EW}(5 \times 10^5 \text{ yr} | \mathbf{a}, \mathbf{e}_{Mi}) | \mathbf{e}_{Ai}]$ defined in Equation J6.2-20 for $i = 1, 2, \dots, 50$, and (c) expected (mean) CCDF and quantile curves, $q = 0.05, 0.5, 0.95$, for CCDFs in (a).



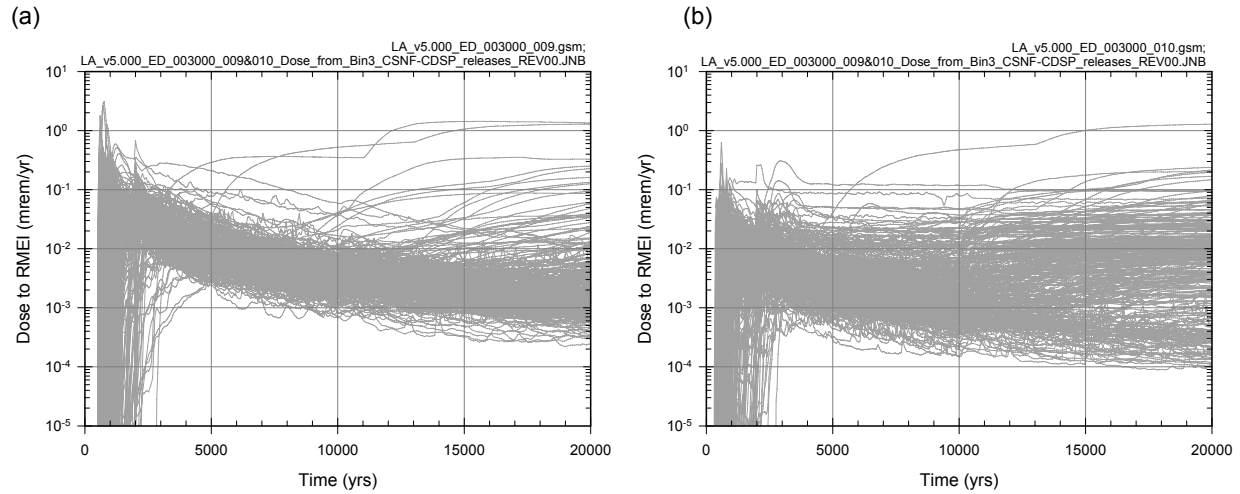
Source: Ouput DTNs: MO0709TSPAPLOT.000 [DIRS 183010]; MO0709TSPASTAB.000 [DIRS 182983]; and MO0709TSPAREGS.000 [DIRS 182976].

Figure J6.2-21. Assessment with replicated sampling of numerical error associated with use of an LHS of size $n_{LHS} = 300$ to determine epistemic uncertainty in expected dose $\bar{D}_{EW}(\tau|\mathbf{e})$ to RMEI for $0 \leq \tau \leq 10^6$ yr that results when only early WP failure is considered: (a) Replicated estimates of expected (mean) dose $\bar{\bar{D}}_{EW}(\tau)$ and quantiles $Q_q[\bar{D}_{EW}(\tau|\mathbf{e})]$, $q = 0.05, 0.5, 0.95$, and (b) confidence intervals for estimates of expected (mean) dose $\bar{\bar{D}}_{EW}(\tau)$.



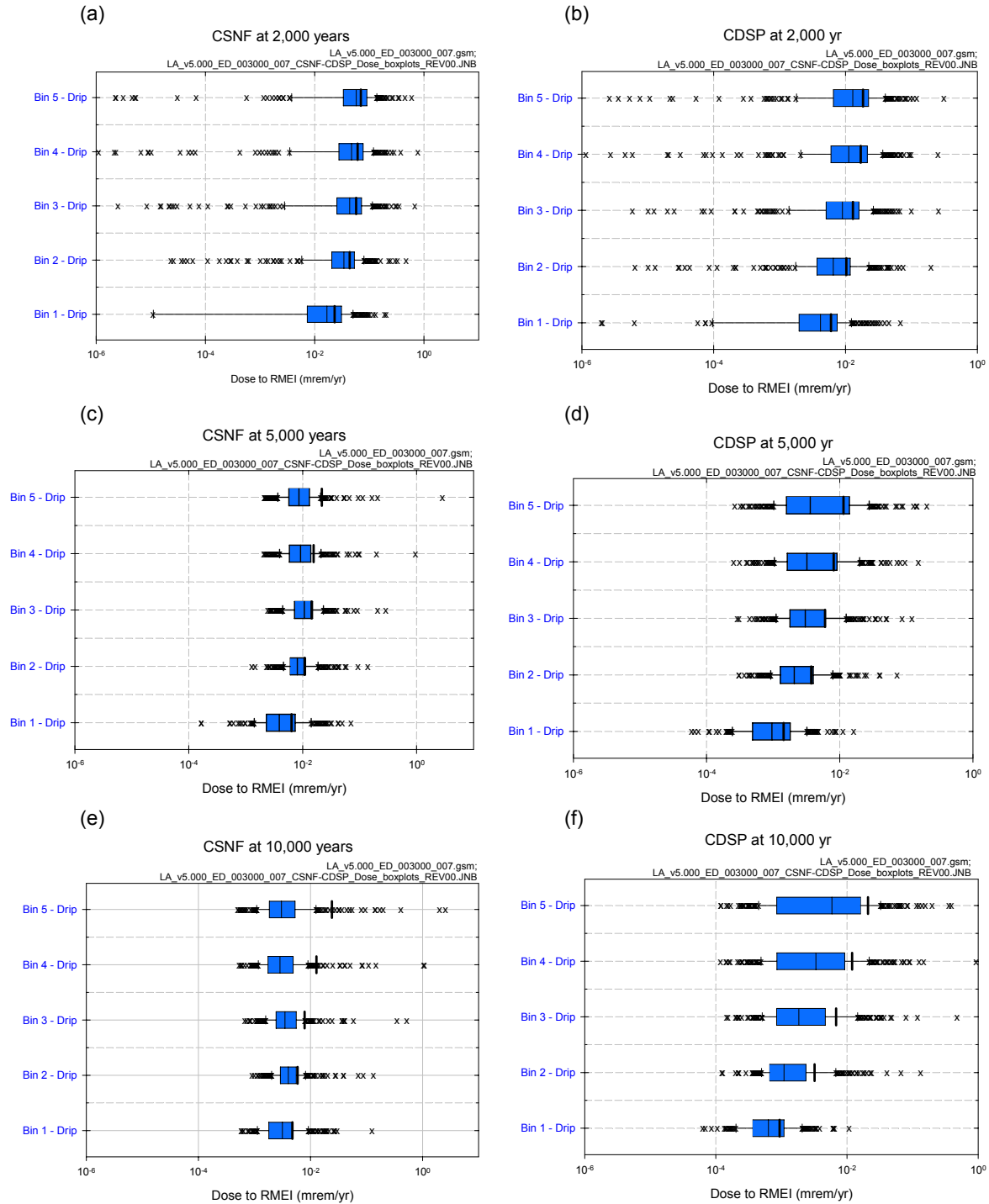
Source: Ouput DTNs: MO0709TSPAPLOT.000 [DIRS 183010]; and MO0709TSPAREGS.000 [DIRS 182976].

Figure J6.3-1. Complementary cumulative distribution functions (CCDFs) for number n_{ED} of DSs with early failure associated with individual elements of LHS of size $n_{LHS} = 300$ in Equation J4.9-1: (a) CCDFs for all 300 LHS elements, and (b) CCDFs for first 50 LHS elements.



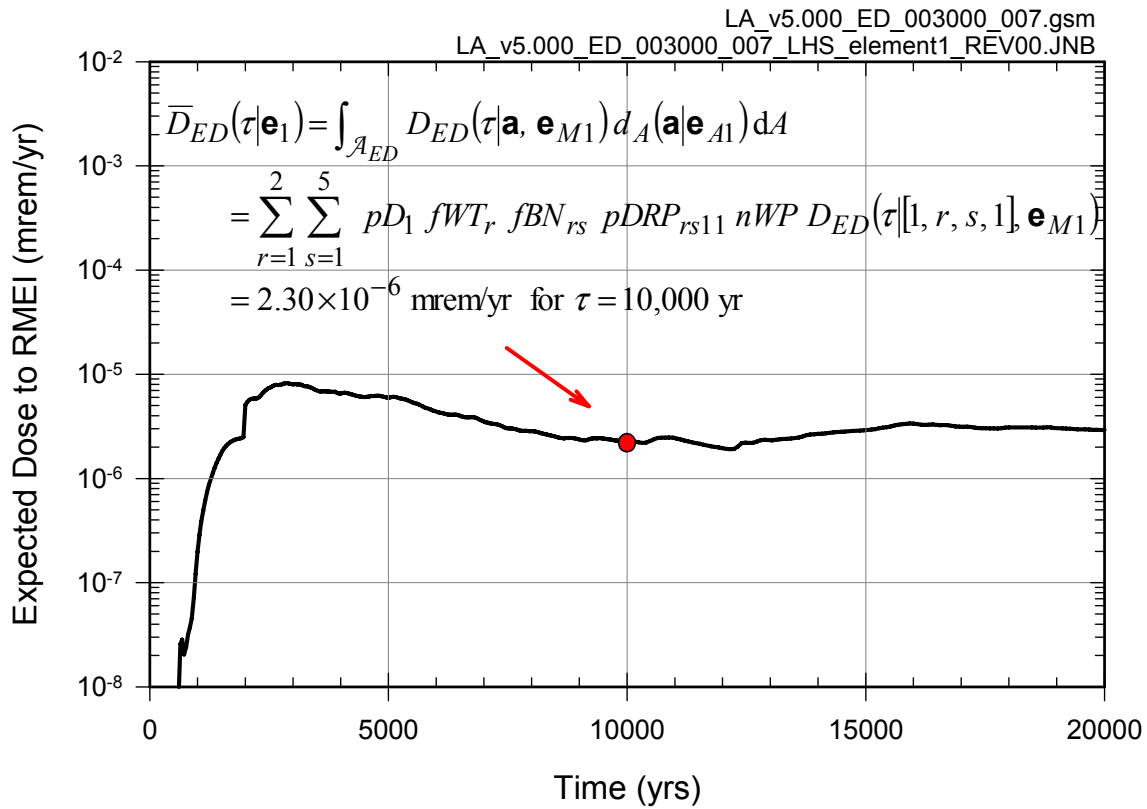
Source: Output DTNs: MO0709TSPAPLOT.000 [DIRS 183010]; and MO0709TSPASENS.000 [DIRS 182982].

Figure J6.3-2. Summary of results obtained with LHS of size $nLHS = 300$ showing epistemic uncertainty in doses $D_{ED}(\tau|[1, r, s, 1], \mathbf{e}_M)$ for $0 \leq \tau \leq 20,000$ yr: (a) CSNF WP in bin 3 under dripping conditions (i.e., $D_{ED}(\tau|[1, 1, 3, 1], \mathbf{e}_{Mi})$, $i = 1, 2, \dots, nLHS = 300$), and (b) CDSP WP in bin 3 under dripping conditions (i.e., $D_{ED}(\tau|[1, 2, 3, 1], \mathbf{e}_{Mi})$, $i = 1, 2, \dots, nLHS = 300$).



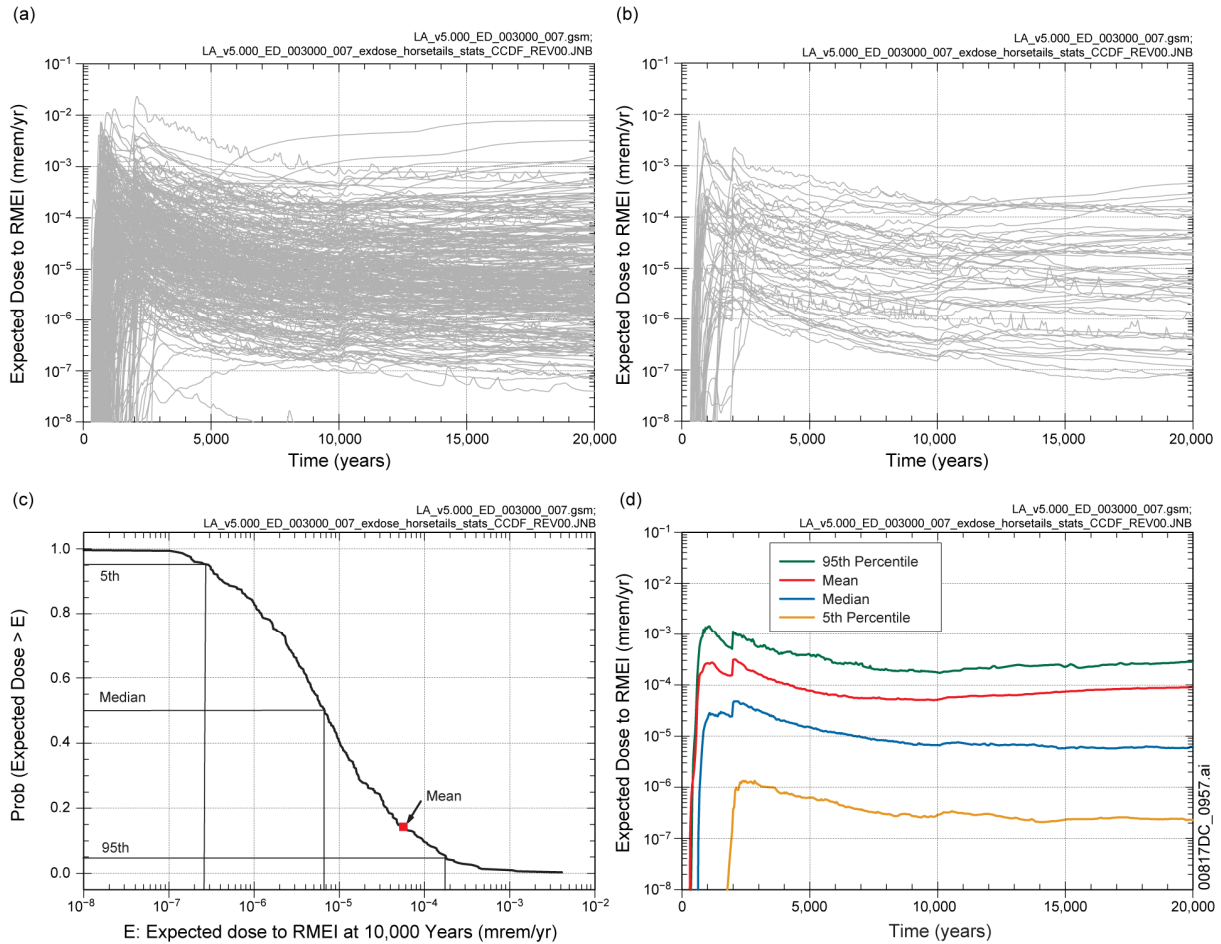
Source: Ouput DTNs: MO0709TSPAPLOT.000 [DIRS 183010]; and MO0709TSPAREGS.000 [DIRS 182976].

Figure J6.3-3. Box plots (see Figure J6.2-3 for description) summarizing results obtained with LHS of size $nLHS = 300$ showing epistemic uncertainty in doses $D_{ED}(\tau[1, r, s, 1], \mathbf{e}_M)$ for $\tau = 2000, 5000, 10,000$ yr, $r = 1, 2, s = 1, 2, 3, 4, 5, t = 1$, and $i = 1, 2, \dots, nLHS = 300$: (a, c, e) CSNF WPs at $\tau = 2000, 5000$ and $10,000$ yrs, and (b, d, f) CDSP WPs at $\tau = 2000, 5000$ and $10,000$ yrs.



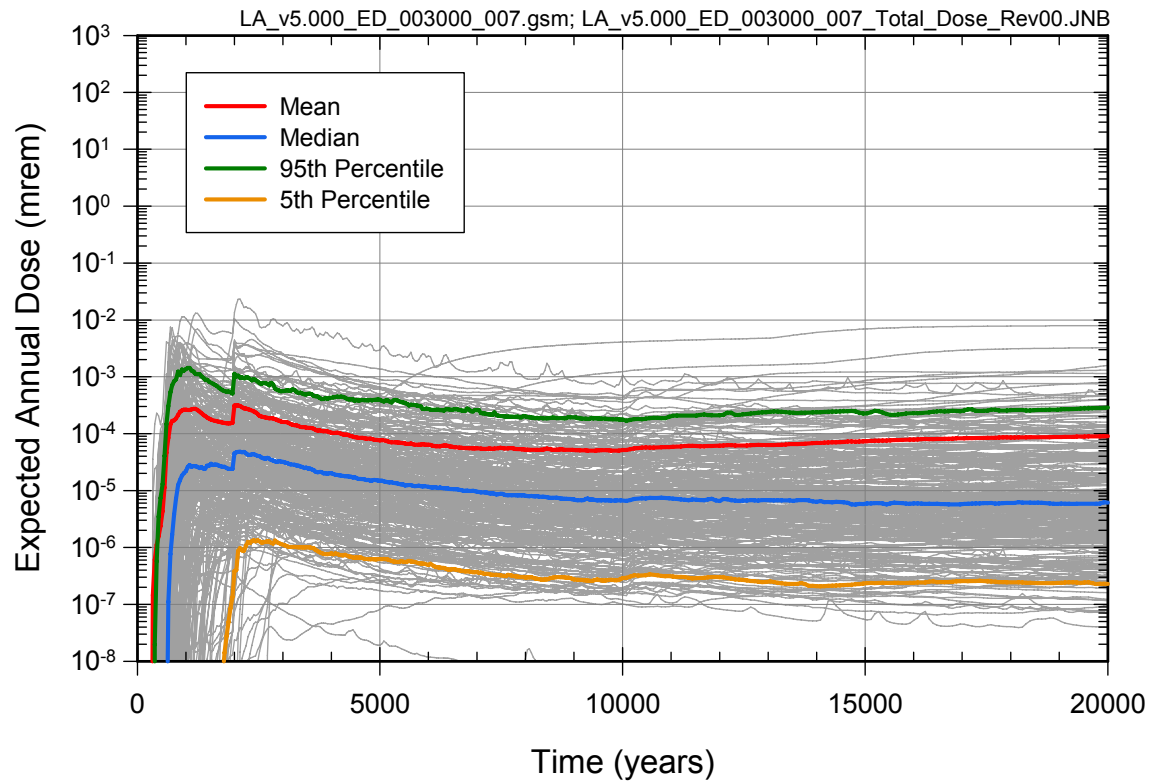
Source: Ouput DTNs: MO0709TSPAPLOT.000 [DIRS 183010]; and MO0709TSPAREGS.000 [DIRS 182976].

Figure J6.3-4. Estimate of $\bar{D}_{ED}(\tau|\mathbf{e}_1)$ for LHS element $\mathbf{e}_1 = [\mathbf{e}_{A1}, \mathbf{e}_{M1}]$ and $0 \leq \tau \leq 20,000$ yr with integration-based procedure indicated in Equation (J6.3-2).



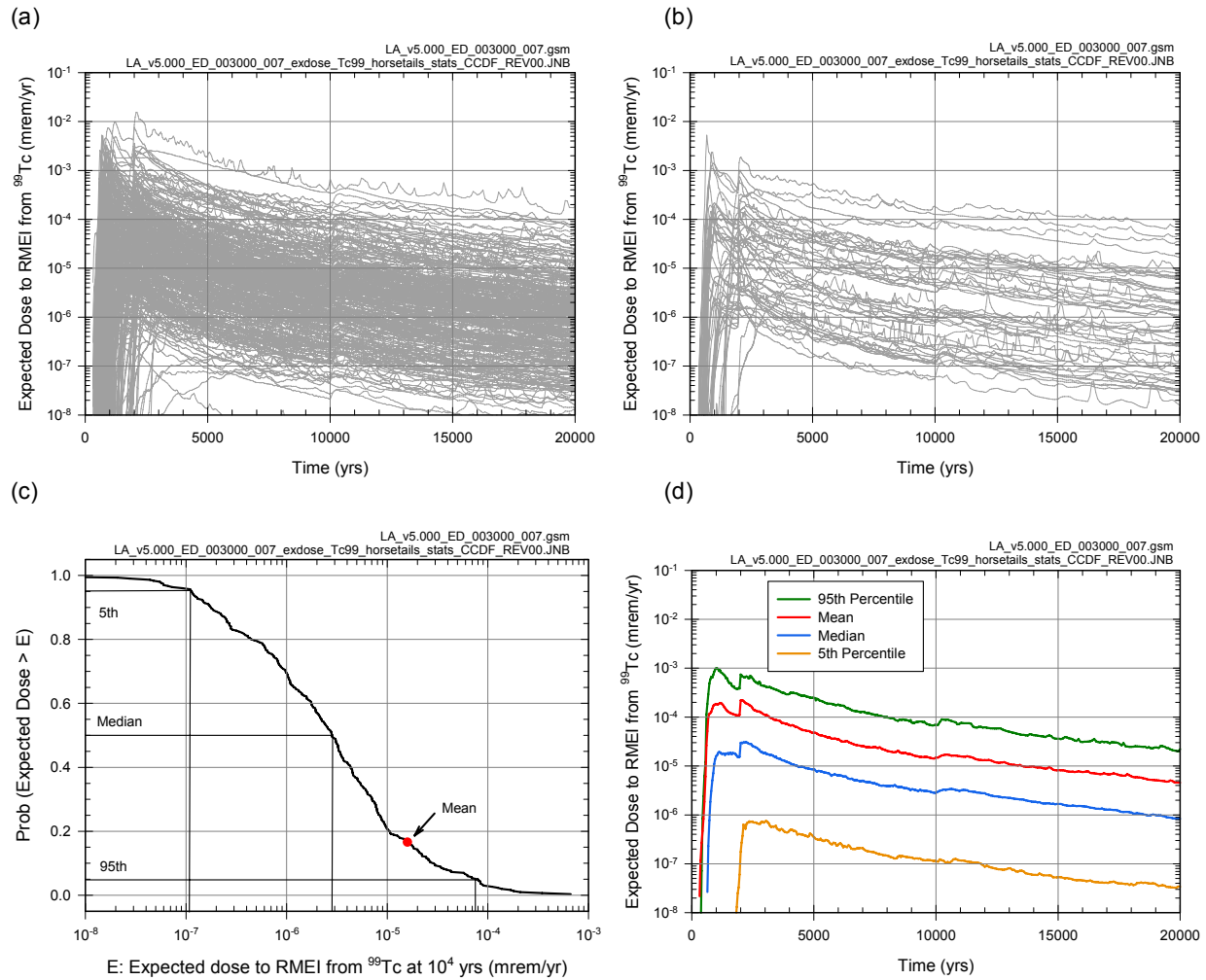
Source: Ouput DTNs: MO0709TSPAPLOT.000 [DIRS 183010]; and MO0709TSPAREGS.000 [DIRS 182976].

Figure J6.3-5. Estimate obtained with LHS of size $nLHS = 300$ showing epistemic uncertainty in expected dose $\bar{D}_{ED}(\tau|\mathbf{e})$ to RMEI for $0 \leq \tau \leq 20,000$ yr that results when only early DS failure is considered: (a) expected dose $\bar{D}_{ED}(\tau|\mathbf{e}_i)$, $i = 1, 2, \dots, nLHS = 300$, (b) expected dose $\bar{D}_{ED}(\tau|\mathbf{e}_i)$, $i = 1, 2, \dots, 50$, (c) exceedance probabilities $p_E[D < \bar{D}_{ED}(\tau|\mathbf{e})]$ and quantiles $Q_q[\bar{D}_{ED}(\tau|\mathbf{e})]$, $q = 0.05, 0.5$ and 0.95 , for $\tau = 10^4$ yr, and (d) expected (mean) dose $\bar{\bar{D}}_{ED}(\tau)$ and quantiles $Q_q[\bar{\bar{D}}_{ED}(\tau|\mathbf{e})]$, $q = 0.05, 0.5, 0.95$.



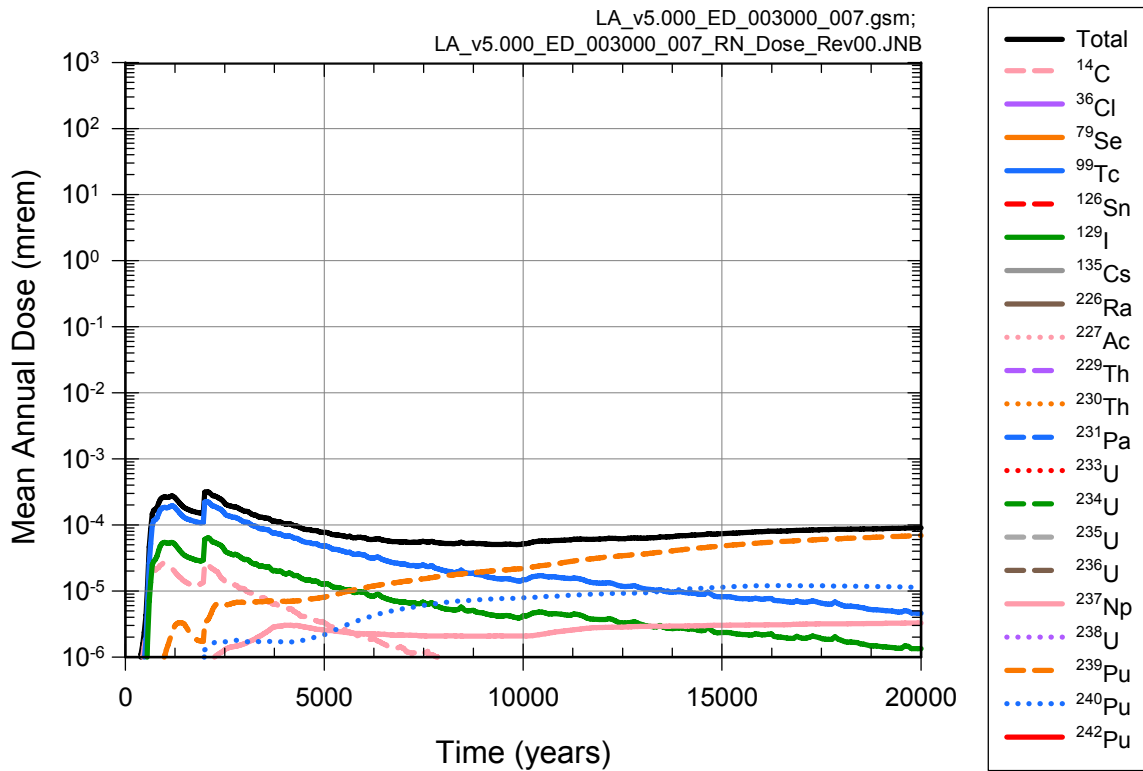
Source: Output DTNs: MO0709TSPAPLOT.000 [DIRS 183010]; and MO0709TSPAREGS.000 [DIRS 182976].

Figure J6.3-6. Summary of results obtained with LHS of size $nLHS = 300$ showing epistemic uncertainty in expected dose $\bar{D}_{ED}(\tau|\mathbf{e})$ to RMEI for $0 \leq \tau \leq 20,000$ yr that results when only early DS failure is considered.



Source: Output DTNs: MO0709TSPAPLOT.000 [DIRS 183010]; and MO0709TSPAREGS.000 [DIRS 182976].

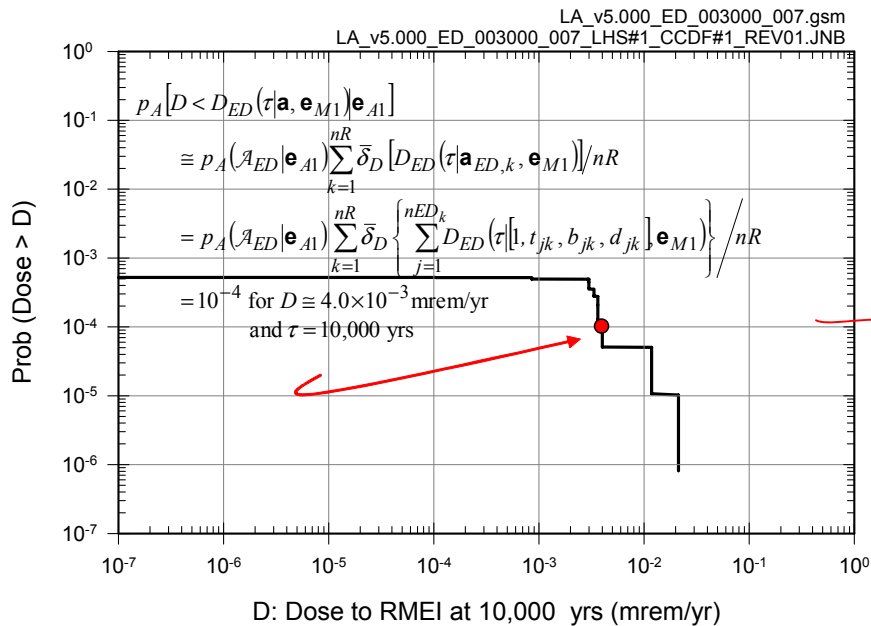
Figure J6.3-7. Estimate obtained with LHS of size $nLHS = 300$ showing epistemic uncertainty in expected dose $\bar{D}_{ED,r}(\tau|\mathbf{e})$ to RMEI for $0 \leq \tau \leq 20,000$ yr with r corresponding to ⁹⁹Tc that results when only early DS failure is considered: (a) expected dose $\bar{D}_{ED,r}(\tau|\mathbf{e}_i)$, $i = 1, 2, \dots, nLHS = 300$, (b) expected dose $\bar{D}_{ED,r}(\tau|\mathbf{e}_i)$, $i = 1, 2, \dots, 50$, (c) exceedance probabilities $p_E[D < \bar{D}_{ED,r}(\tau|\mathbf{e})]$ and quantiles $Q_q[\bar{D}_{ED,r}(\tau|\mathbf{e})]$, $q = 0.05, 0.5$ and 0.95 , for $\tau = 10^4$ yr, and (d) expected (mean) dose $\bar{D}_{ED,r}(\tau)$ and quantiles $Q_q[\bar{D}_{ED,r}(\tau|\mathbf{e})]$, $q = 0.05, 0.5, 0.95$.



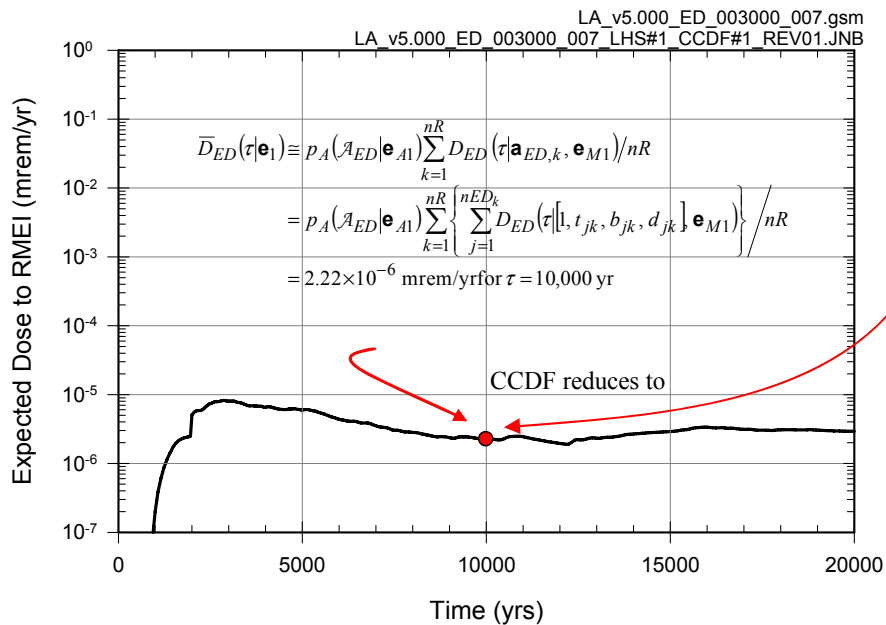
Source: Ouput DTNs: MO0709TSPAPLOT.000 [DIRS 183010]; and MO0709TSPAREGS.000 [DIRS 182976].

Figure J6.3-8. Estimates obtained with LHS of size $n_{LHS} = 300$ of expected (mean) dose $\bar{D}_{ED,r}(\tau)$ to RMEI for $0 \leq \tau \leq 20,000$ yr for individual radioactive species that result when only early DS failure is considered.

(a)

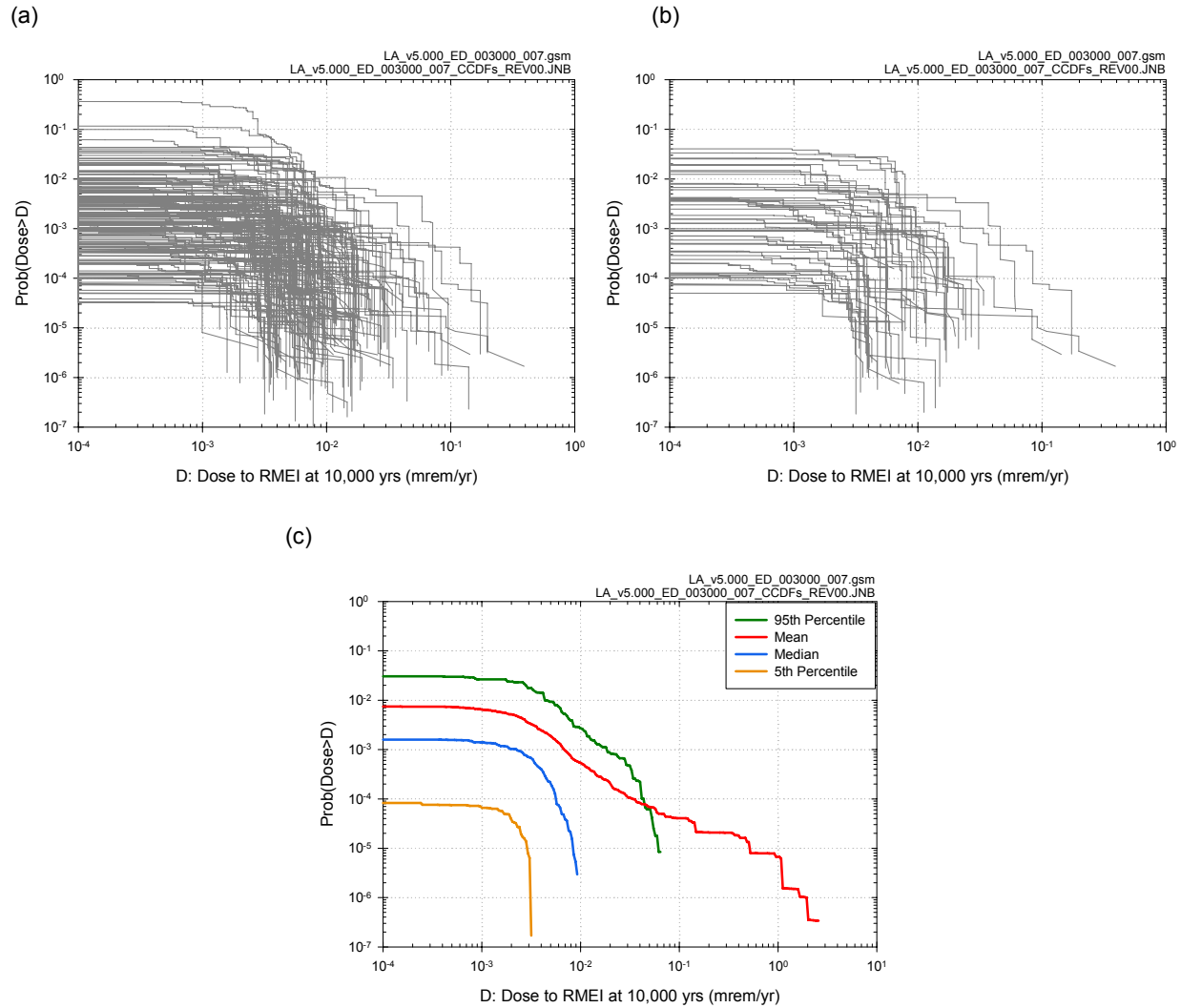


(b)



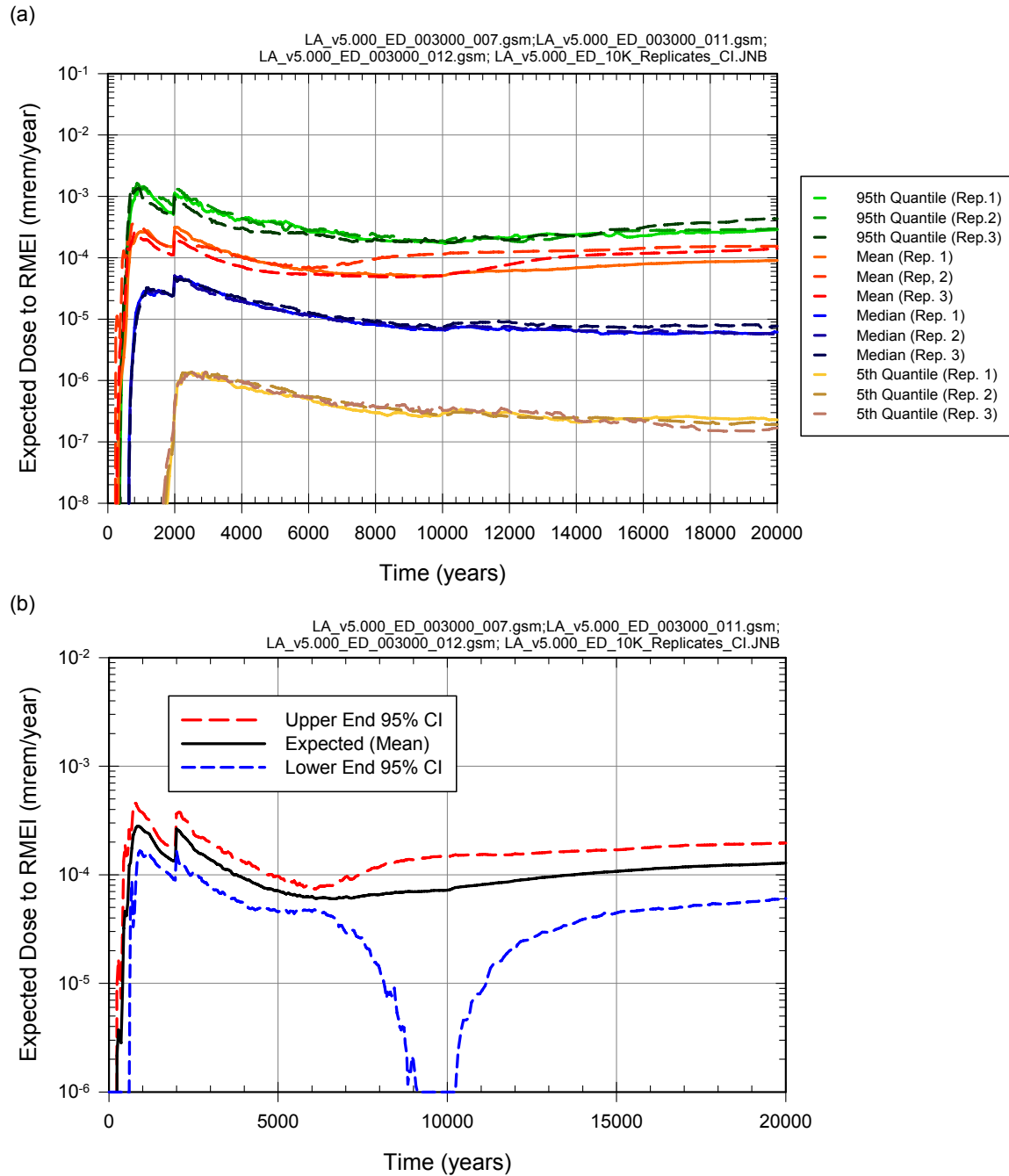
Source: Ouput DTNs: MO0709TSPAPLOT.000 [DIRS 183010]; and MO0709TSPAREGS.000 [DIRS 182976].

Figure J6.3-9. Results associated with $D_{ED}(\tau|\mathbf{a}_{ED}, \mathbf{e}_{M1})$ for LHS element $\mathbf{e}_1 = [\mathbf{e}_{A1}, \mathbf{e}_{M1}]$ obtained with sampling-based (Monte Carlo) procedures: (a) CCDF for $D_{ED}(10^4 \text{ yr}|\mathbf{a}_{ED}, \mathbf{e}_{M1})$ with exceedance probabilities $p_A[D < D_{ED}(10^4 \text{ yr}|\mathbf{a}, \mathbf{e}_{M1})|\mathbf{e}_{A1}]$ defined similarly to $p_A[D < D_{EW}(\tau|\mathbf{a}, \mathbf{e}_{M1})|\mathbf{e}_{A1}]$ in Equation (J6.2-12), and (b) expected dose $\bar{D}_{ED}(10^4 \text{ yr}|\mathbf{e}_1)$ associated with $D_{ED}(10^4 \text{ yr}|\mathbf{a}_{ED}, \mathbf{e}_{M1})$ defined similarly to $\bar{D}_{EW}(\tau|\mathbf{e}_1)$ in Equation (J6.2-10).



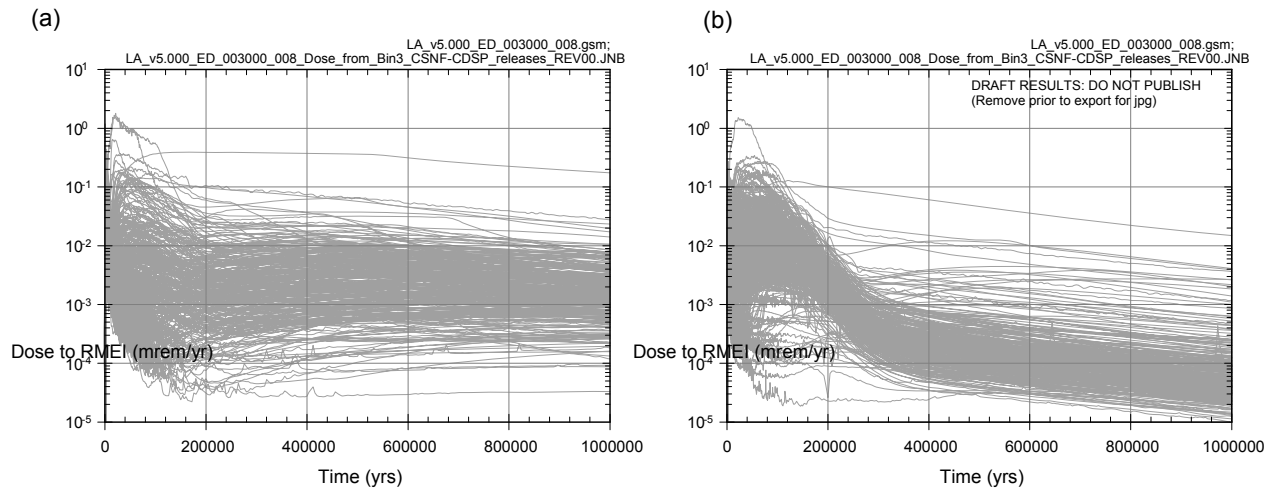
Source: Ouput DTNs: MO0709TSPAPLOT.000 [DIRS 183010]; and MO0709TSPAREGS.000 [DIRS 182976].

Figure J6.3-10. Results associated with $D_{ED}(10^4 \text{ yr} | \mathbf{a}_{ED}, \mathbf{e}_M)$ obtained with sampling-based (Monte Carlo) procedures for an LHS of size $n_{LHS} = 300$: (a) CCDFs for $D_{ED}(10^4 \text{ yr} | \mathbf{a}_{ED}, \mathbf{e}_{Mi})$ with exceedance probabilities $p_A[D < D_{ED}(10^4 \text{ yr} | \mathbf{a}, \mathbf{e}_{Mi}) | \mathbf{e}_{Ai}]$ defined similarly to $p_A[D < D_{EW}(\tau | \mathbf{a}, \mathbf{e}_{M1}) | \mathbf{e}_{A1}]$ in Equation (J6.2-12) for $i = 1, 2, \dots, n_{LHS} = 300$, (b) CCDFs for $D_{ED}(10^4 \text{ yr} | \mathbf{a}_{ED}, \mathbf{e}_{Mi})$ with exceedance probabilities $p_A[D < D_{ED}(10^4 \text{ yr} | \mathbf{a}, \mathbf{e}_{Mi}) | \mathbf{e}_{Ai}]$ defined similarly to $p_A[D < D_{EW}(\tau | \mathbf{a}, \mathbf{e}_{M1}) | \mathbf{e}_{A1}]$ in Equation (J6.2-12) for $i = 1, 2, \dots, 50$, and (c) expected (mean) CCDF and quantile curves, $q = 0.05, 0.5, 0.95$, for CCDFs in (a).



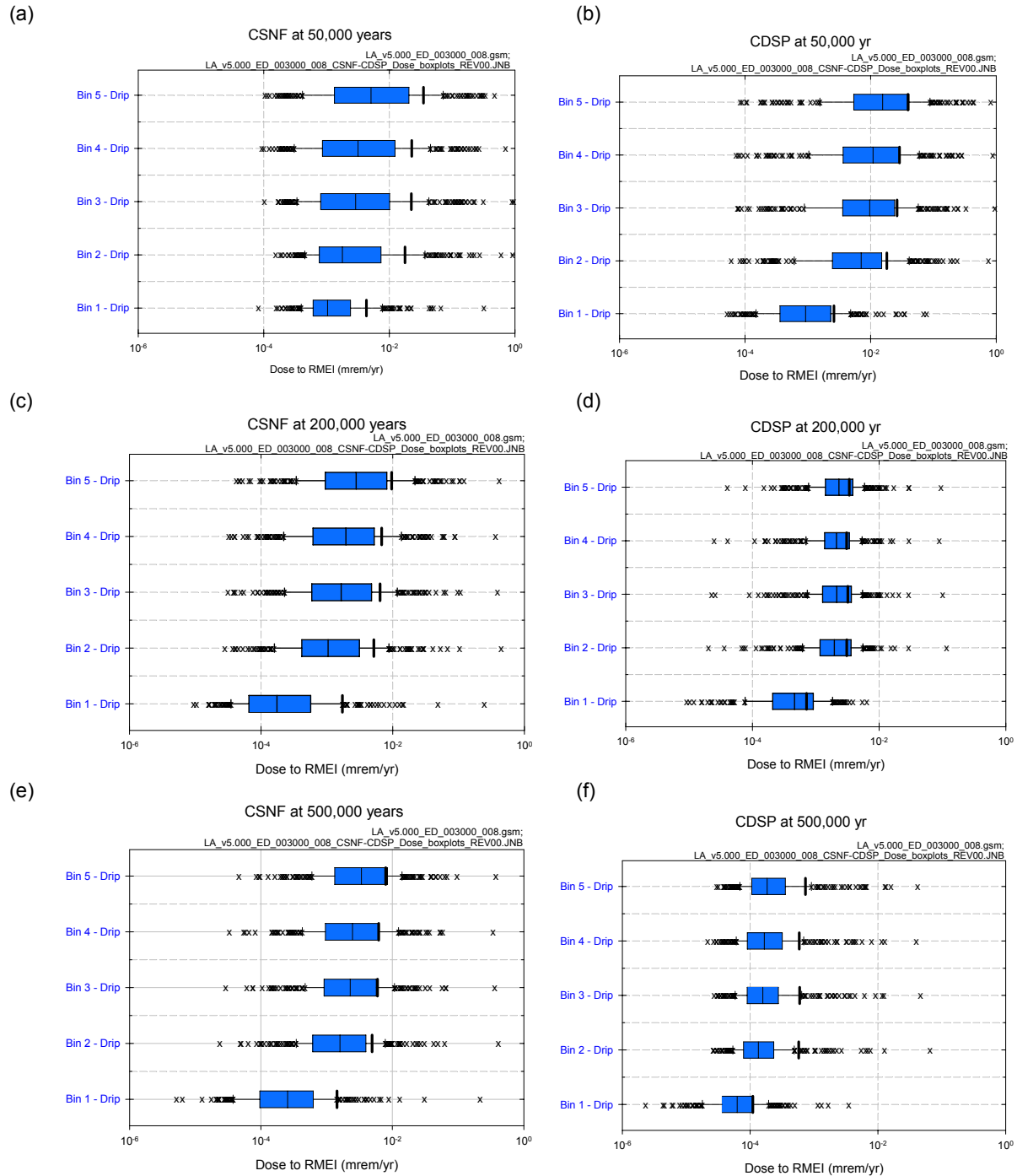
Source: Ouput DTNs: MO0709TSPAPLOT.000 [DIRS 183010]; MO0709TSPAREGS.000 [DIRS 182976]; and MO0709TSPASTAB.000 [DIRS 182983].

Figure J6.3-11. Assessment with replicated sampling of numerical error associated with use of an LHS of size $n_{LHS} = 300$ to determine epistemic uncertainty in expected dose $\bar{D}_{ED}(\tau|\mathbf{e})$ to RMEI for $0 \leq \tau \leq 20,000$ yr that results when only early DS failure is considered: (a) Replicated estimates of expected (mean) dose $\bar{D}_{ED}(\tau)$ and quantiles $Q_q[\bar{D}_{ED}(\tau|\mathbf{e})]$, $q = 0.05, 0.5, 0.95$, and (b) confidence intervals for estimates of expected (mean) dose $\bar{D}_{ED}(\tau)$.



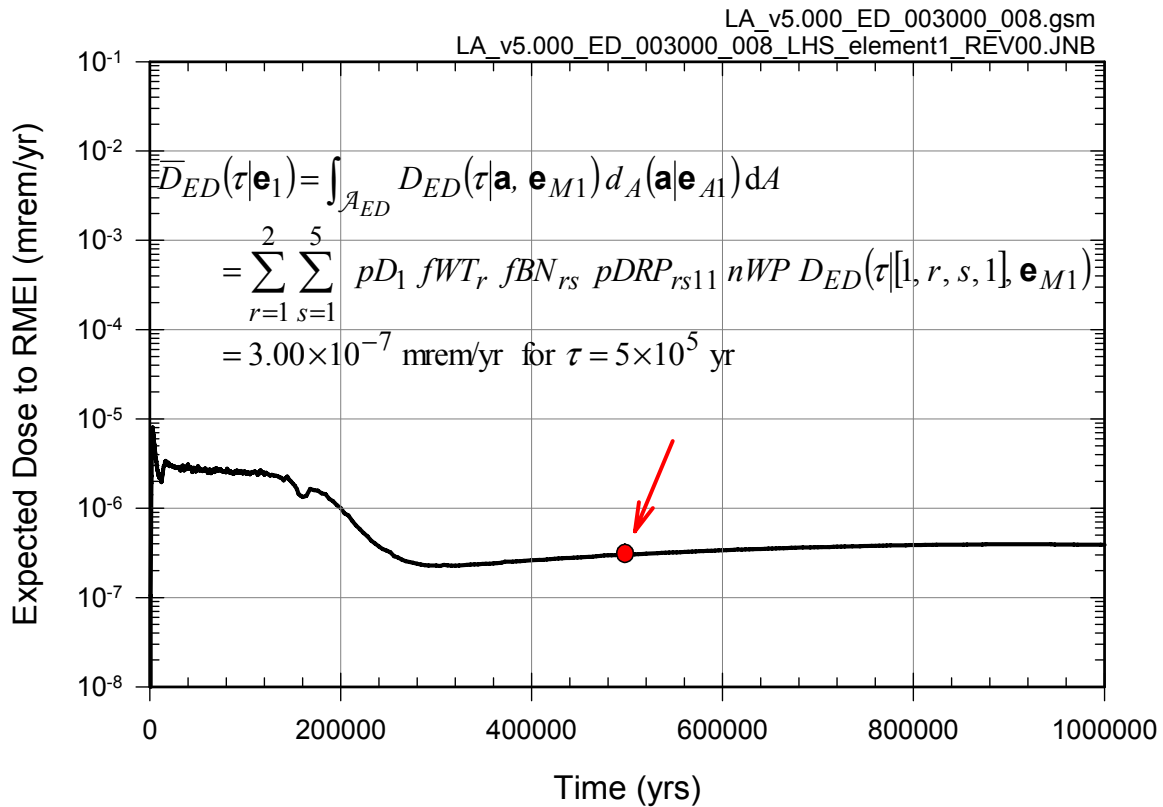
Source: Ouput DTNs: MO0709TSPAPLOT.000 [DIRS 183010]; and MO0709TSPAREGS.000 [DIRS 182976].

Figure J6.3-12. Summary of results obtained with LHS of size $nLHS = 300$ showing epistemic uncertainty in doses $D_{ED}(\tau|[1, r, s, 1], \mathbf{e}_M)$ for $0 \leq \tau \leq 10^6$ yr: (a) CSNF WP in bin 3 under dripping conditions (i.e., $D_{ED}(\tau|[1, 1, 3, 1], \mathbf{e}_{Mi}), i = 1, 2, \dots, nLHS = 300$) and (b) CDSP WP in bin 3 under dripping conditions (i.e., $D_{ED}(\tau|[1, 2, 3, 1], \mathbf{e}_{Mi}), i = 1, 2, \dots, nLHS = 300$).



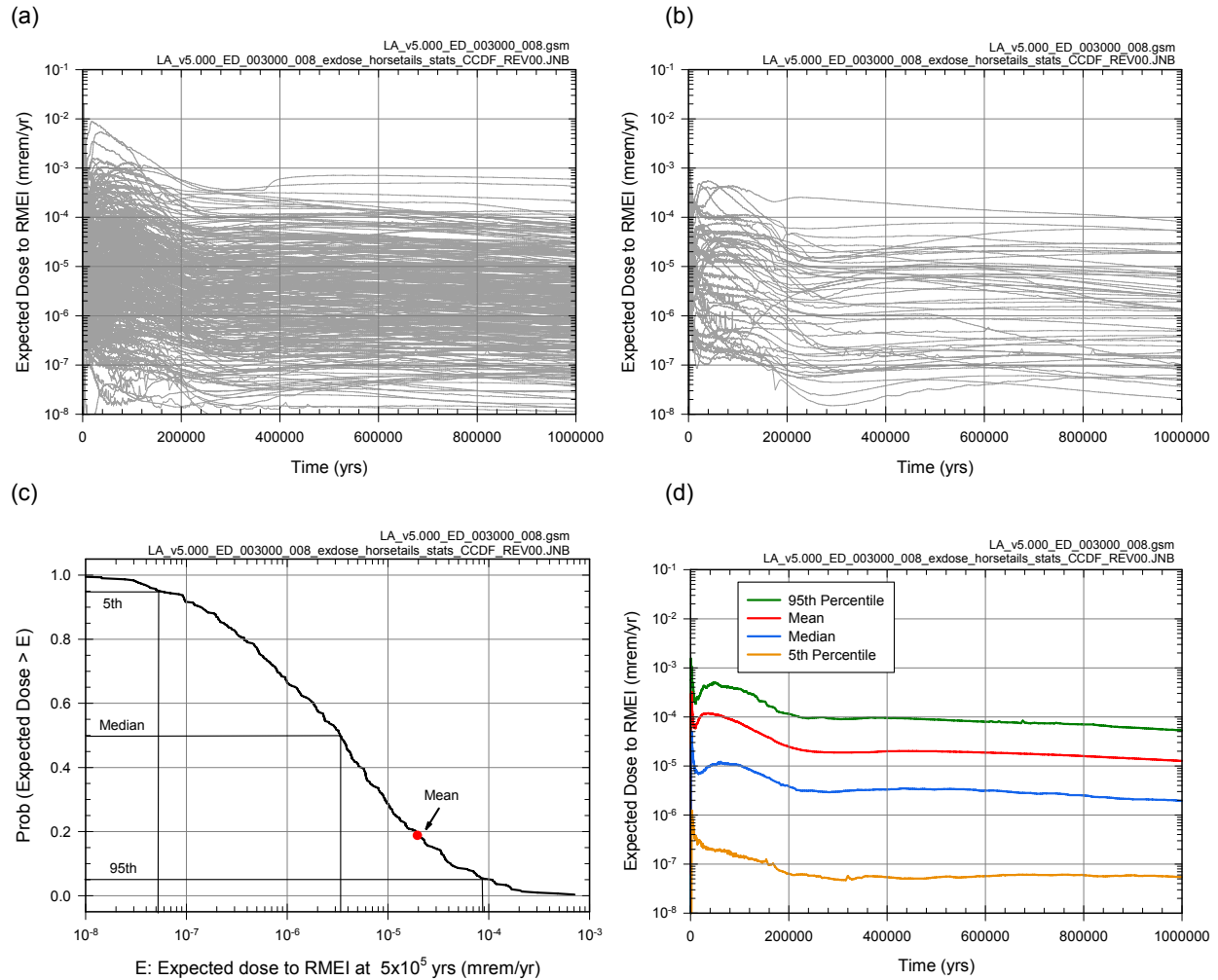
Source: Ouput DTNs: MO0709TSPAPLOT.000 [DIRS 183010]; and MO0709TSPAREGS.000 [DIRS 182976].

Figure J6.3-13. Box plots (see Figure J6.2-3 for description) summarizing results obtained with LHS of size $nLHS = 300$ showing epistemic uncertainty in doses $D_{ED}(\tau[1, r, s, 1], \mathbf{e}_{MI})$ for $\tau = 5 \times 10^4, 2 \times 10^5, 5 \times 10^5$ yr, $r = 1, 2, s = 1, 2, 3, 4, 5, t = 1$, and $i = 1, 2, \dots, nLHS = 300$: (a, c, e) CSNF WPs at $5 \times 10^4, 2 \times 10^5, 5 \times 10^5$ yr, and (b, d, f) CDSP WPs at $5 \times 10^4, 2 \times 10^5, 5 \times 10^5$ yr.



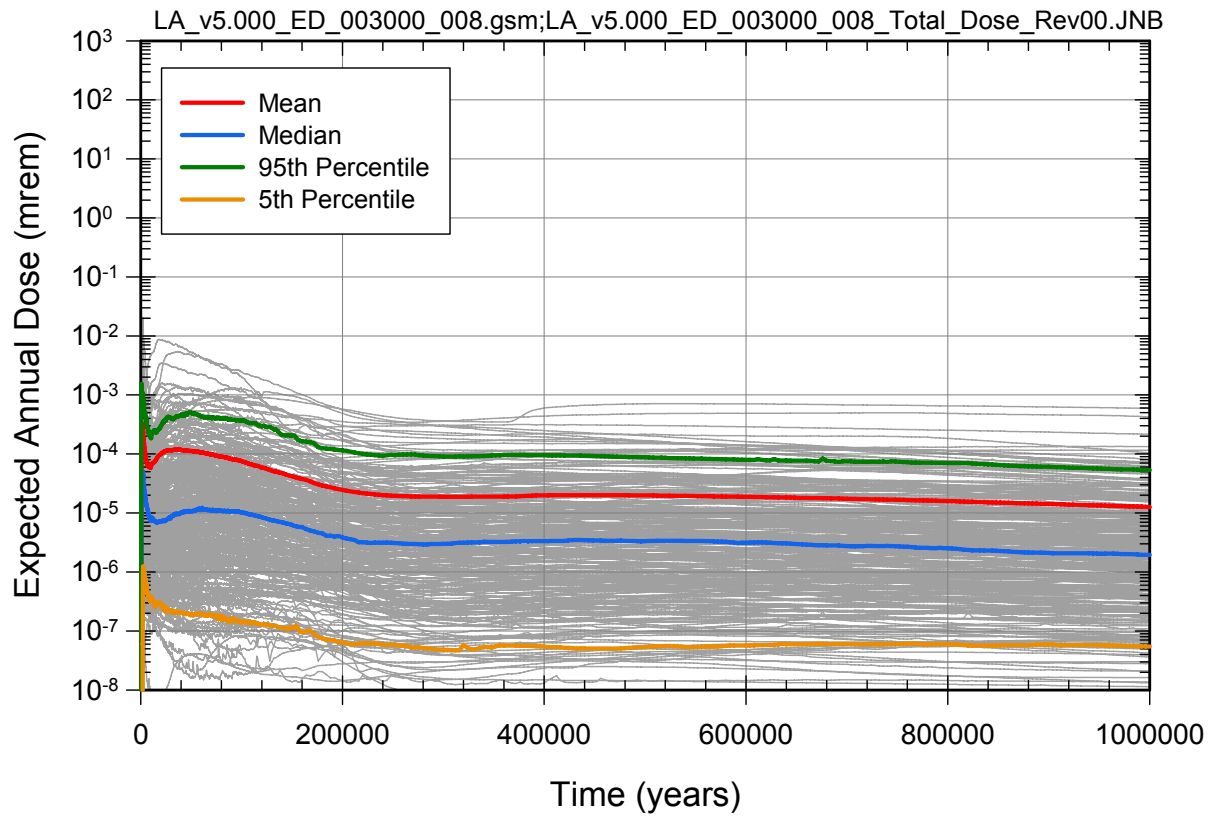
Source: Ouput DTNs: MO0709TSPAPLOT.000 [DIRS 183010]; and MO0709TSPAREGS.000 [DIRS 182976].

Figure J6.3-14. Estimate of $\bar{D}_{ED}(\tau|\mathbf{e}_1)$ for LHS element $\mathbf{e}_1 = [\mathbf{e}_{A1}, \mathbf{e}_{M1}]$ and $0 \leq \tau \leq 10^6$ yr with integration-based procedure indicated in Equation J6.2-2.



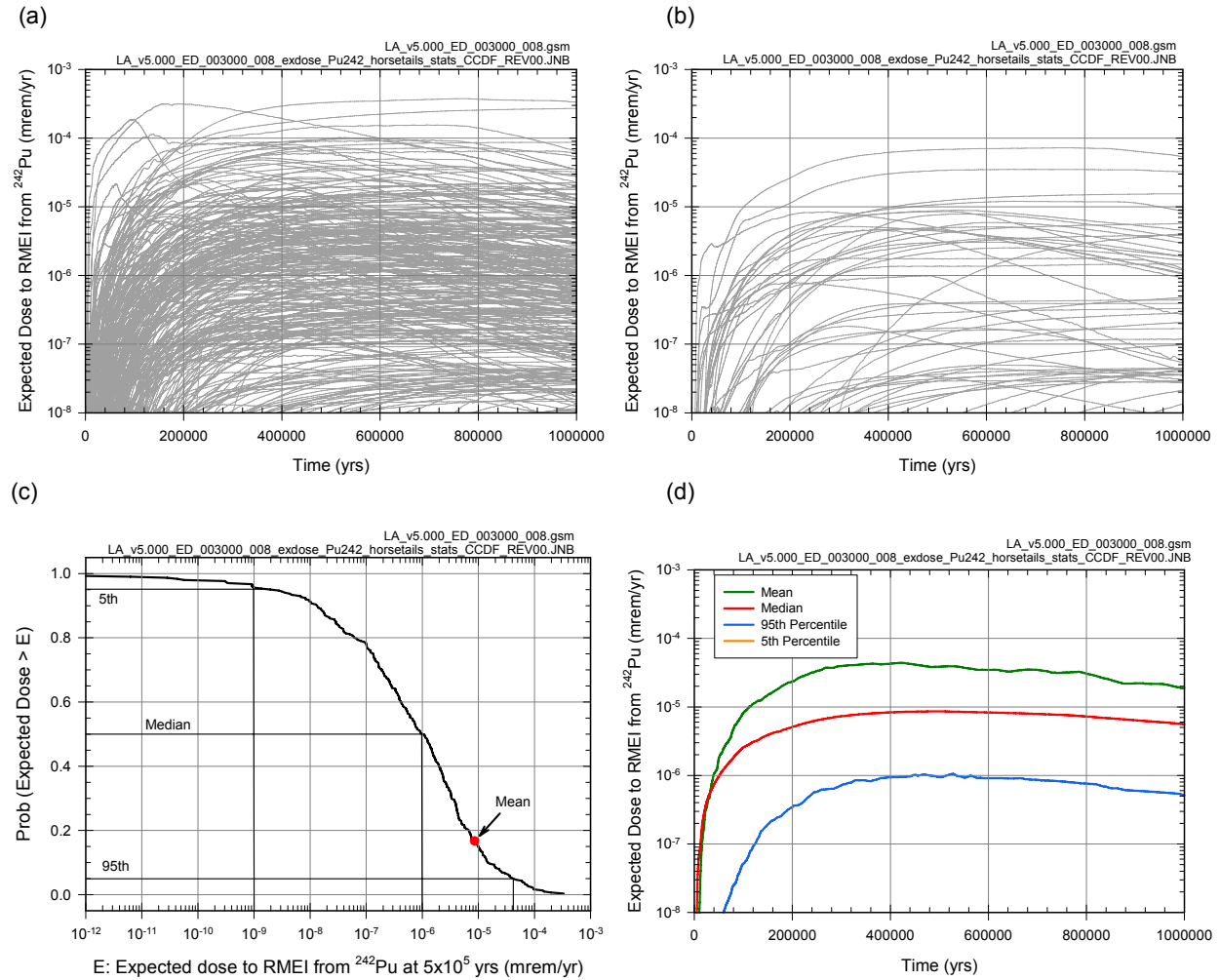
Source: Ouput DTNs: MO0709TSPAPLOT.000 [DIRS 183010]; and MO0709TSPAREGS.000 [DIRS 182976].

Figure J6.3-15. Estimate obtained with LHS of size $nLHS = 300$ showing epistemic uncertainty in expected dose $\bar{D}_{ED}(\tau|\mathbf{e})$ to RMEI for $0 \leq \tau \leq 10^6$ yr that results when only early DS failure is considered: (a) expected dose $\bar{D}_{ED}(\tau|\mathbf{e}_i)$, $i = 1, 2, \dots, nLHS = 300$, (b) expected dose $\bar{D}_{ED}(\tau|\mathbf{e}_i)$, $i = 1, 2, \dots, 50$, (c) exceedance probabilities $p_E[D < \bar{D}_{ED}(\tau|\mathbf{e})]$ and quantiles $Q_q[\bar{D}_{ED}(\tau|\mathbf{e})]$, $q = 0.05, 0.5$ and 0.95 , for $\tau = 5 \times 10^5$ yr, and (d) expected (mean) dose $\bar{\bar{D}}_{ED}(\tau)$ and quantiles $Q_q[\bar{\bar{D}}_{ED}(\tau|\mathbf{e})]$, $q = 0.05, 0.5, 0.95$.



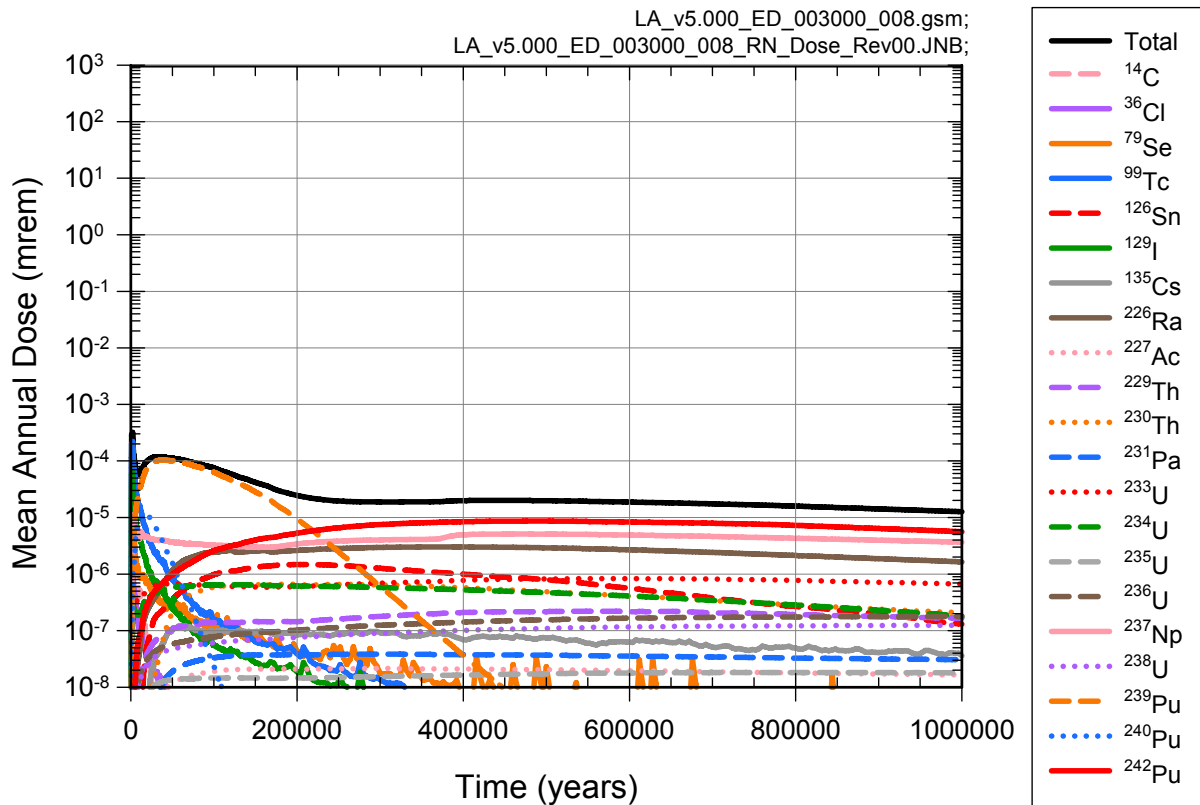
Source: Output DTNs: MO0709TSPAPLOT.000 [DIRS 183010]; and MO0709TSPAREGS.000 [DIRS 182976].

Figure J6.3-16. Summary of results obtained with LHS of size $nLHS = 300$ showing epistemic uncertainty in expected dose $\bar{D}_{ED}(\tau|\mathbf{a})$ to RMEI for $0 \leq \tau \leq 10^6$ yr that results when only early DS failure is considered.



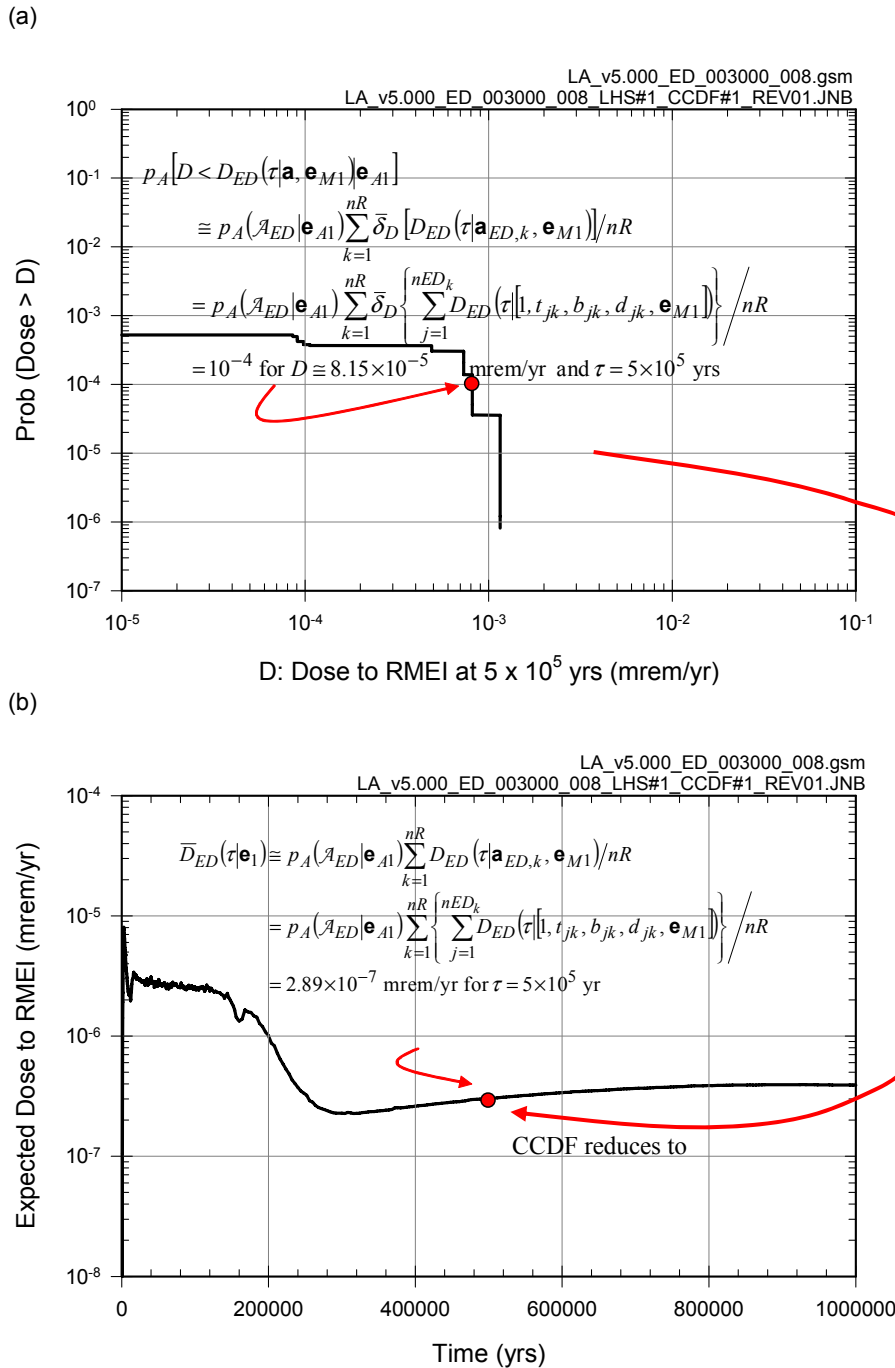
Source: Output DTNs: MO0709TSPAPLOT.000 [DIRS 183010]; and MO0709TSPAREGS.000 [DIRS 182976].

Figure J6.3-17. Estimate obtained with LHS of size $nLHS = 300$ showing epistemic uncertainty in expected dose $\bar{D}_{ED,r}(\tau|\mathbf{e})$ to RMEI for $0 \leq \tau \leq 10^6$ yr with r corresponding to ^{242}Pu that results when only early DS failure is considered: (a) expected dose $\bar{D}_{ED,r}(\tau|\mathbf{e}_i)$, $i = 1, 2, \dots, nLHS = 300$, (b) expected dose $\bar{D}_{ED,r}(\tau|\mathbf{e}_i)$, $i = 1, 2, \dots, 50$, (c) exceedance probabilities $p_E[D < \bar{D}_{ED,r}(\tau|\mathbf{e})]$ and quantiles $Q_q[\bar{D}_{ED,r}(\tau|\mathbf{e})]$, $q = 0.05, 0.5$ and 0.95 , for $\tau = 5 \times 10^5$ yr, and (d) expected (mean) dose $\bar{D}_{ED,r}(\tau)$ and quantiles $Q_q[\bar{D}_{ED,r}(\tau|\mathbf{e})]$, $q = 0.05, 0.5, 0.95$.



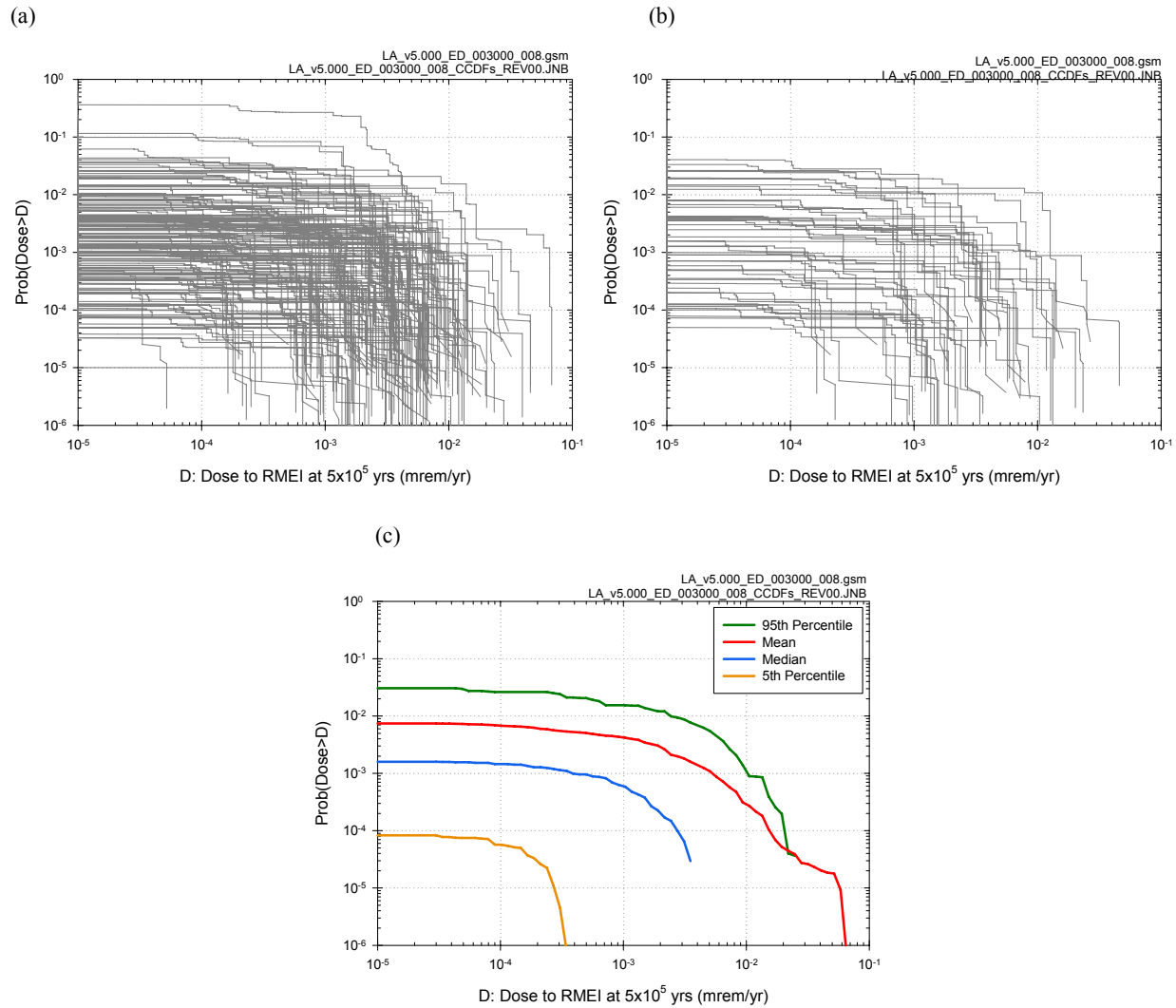
Source: Ouput DTNs: MO0709TSPAPLOT.000 [DIRS 183010]; and MO0709TSPAREGS.000 [DIRS 182976].

Figure J6.3-18. Estimates obtained with LHS of size $n_{LHS} = 300$ of expected (mean) dose $\bar{D}_{ED,r}(\tau)$ to RMEI for $0 \leq \tau \leq 10^6$ yr for individual radioactive species that result when only early DS failure is considered.



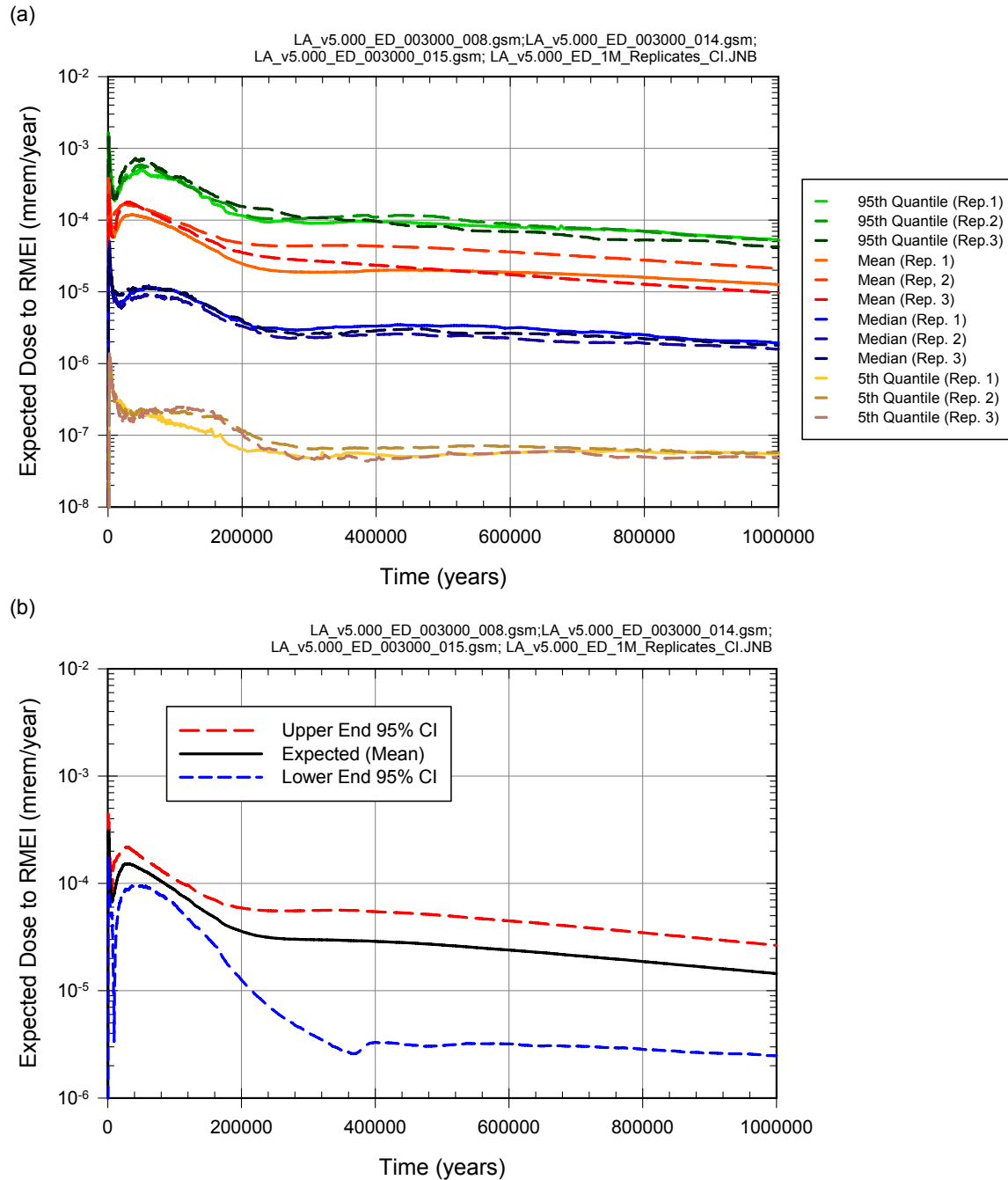
Source: Ouput DTNs: MO0709TSPAPLOT.000 [DIRS 183010]; and MO0709TSPAREGS.000 [DIRS 182976].

Figure J6.3-19. Results associated with $D_{ED}(\tau|\mathbf{a}_{ED}, \mathbf{e}_{M1})$ for LHS element $\mathbf{e}_1 = [\mathbf{e}_{A1}, \mathbf{e}_{M1}]$ obtained with sampling-based (Monte Carlo) procedures: (a) CCDF for $D_{ED}(5 \times 10^5 \text{ yr}|\mathbf{a}_{ED}, \mathbf{e}_{M1})$ with exceedance probabilities $p_A[D < D_{ED}(5 \times 10^5 \text{ yr}|\mathbf{a}_{ED}, \mathbf{e}_{M1})|\mathbf{e}_{A1}]$ defined similarly to $p_A[D < D_{EW}(\tau|\mathbf{a}, \mathbf{e}_{M1})|\mathbf{e}_{A1}]$ in Equation (J6.2-12), and (b) expected dose $\bar{D}_{ED}(5 \times 10^5 \text{ yr}|\mathbf{e}_1)$ associated with $D_{ED}(5 \times 10^5 \text{ yr}|\mathbf{a}_{ED}, \mathbf{e}_1)$ defined similarly to $\bar{D}_{EW}(\tau|\mathbf{e}_1)$ in Equation (J6.2-10).



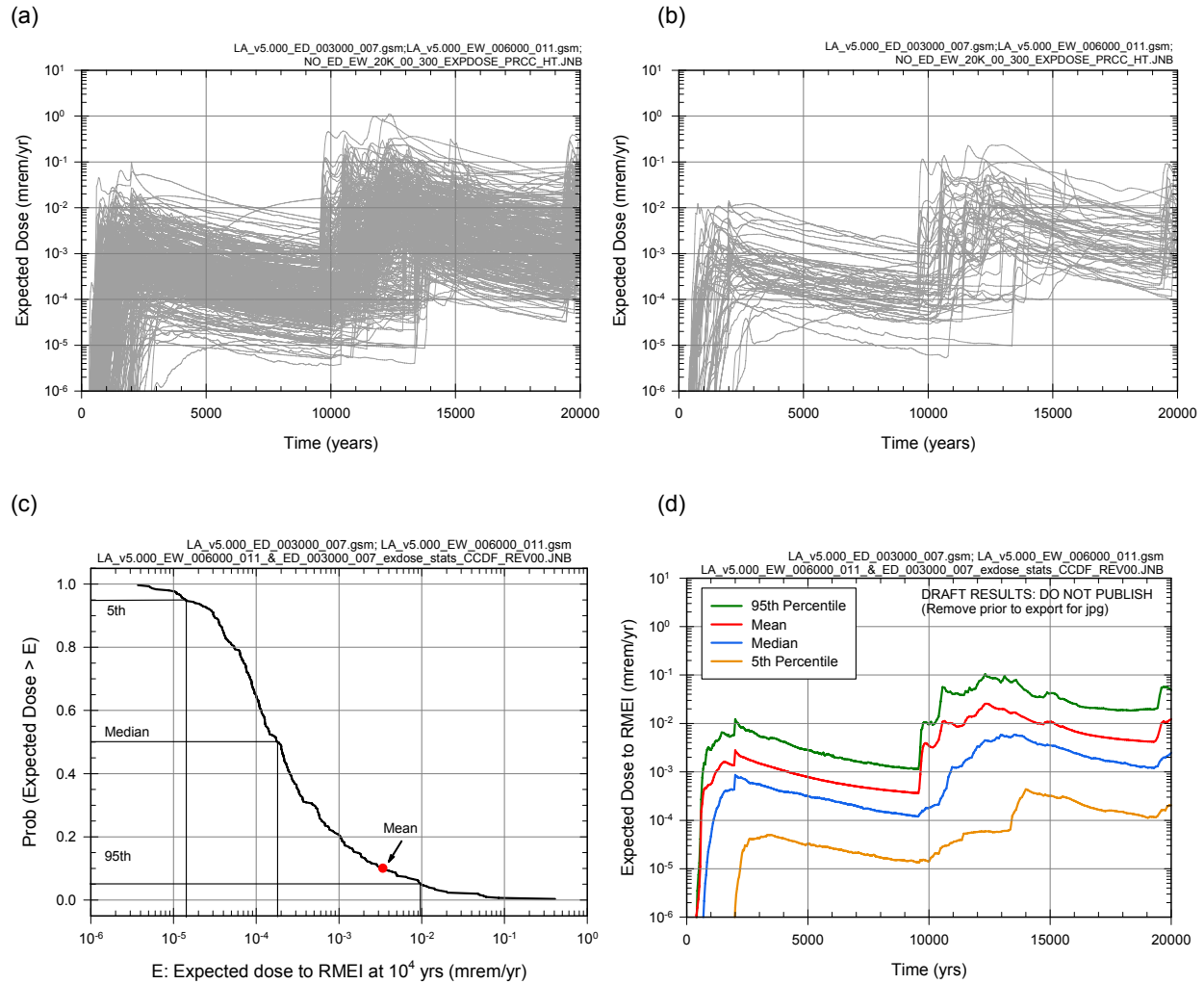
Source: Ouput DTNs: MO0709TSPAPLOT.000 [DIRS 183010]; and MO0709TSPAREGS.000 [DIRS 182976].

Figure J6.3-20. Results associated with $D_{ED}(5 \times 10^5 \text{ yr} | \mathbf{a}_{ED}, \mathbf{e}_M)$ obtained with sampling-based (Monte Carlo) procedures for an LHS of size $n_{LHS} = 300$: (a) CCDFs for $D_{ED}(5 \times 10^5 \text{ yr} | \mathbf{a}_{ED}, \mathbf{e}_{Mi})$ with exceedance probabilities $p_A[D < D_{ED}(5 \times 10^5 \text{ yr} | \mathbf{a}_{ED}, \mathbf{e}_{Mi}) | \mathbf{e}_{Ai}]$ defined similarly to $p_A[D < D_{EW}(\tau | \mathbf{a}, \mathbf{e}_{M1}) | \mathbf{e}_{A1}]$ in Equation (J6.2-12) for $i = 1, 2, \dots, n_{LHS} = 300$, (b) CCDFs for $D_{ED}(10^4 \text{ yr} | \mathbf{a}_{ED}, \mathbf{e}_{Mi})$ with exceedance probabilities $p_A[D < D_{ED}(5 \times 10^5 \text{ yr} | \mathbf{a}_{ED}, \mathbf{e}_{Mi}) | \mathbf{e}_{Ai}]$ defined similarly to $p_A[D < D_{EW}(\tau | \mathbf{a}, \mathbf{e}_{M1}) | \mathbf{e}_{A1}]$ in Equation (J6.2-12) for $i = 1, 2, \dots, 50$, and (c) expected (mean) CCDF and quantile curves, $q = 0.05, 0.5, 0.95$, for CCDFs in (a).



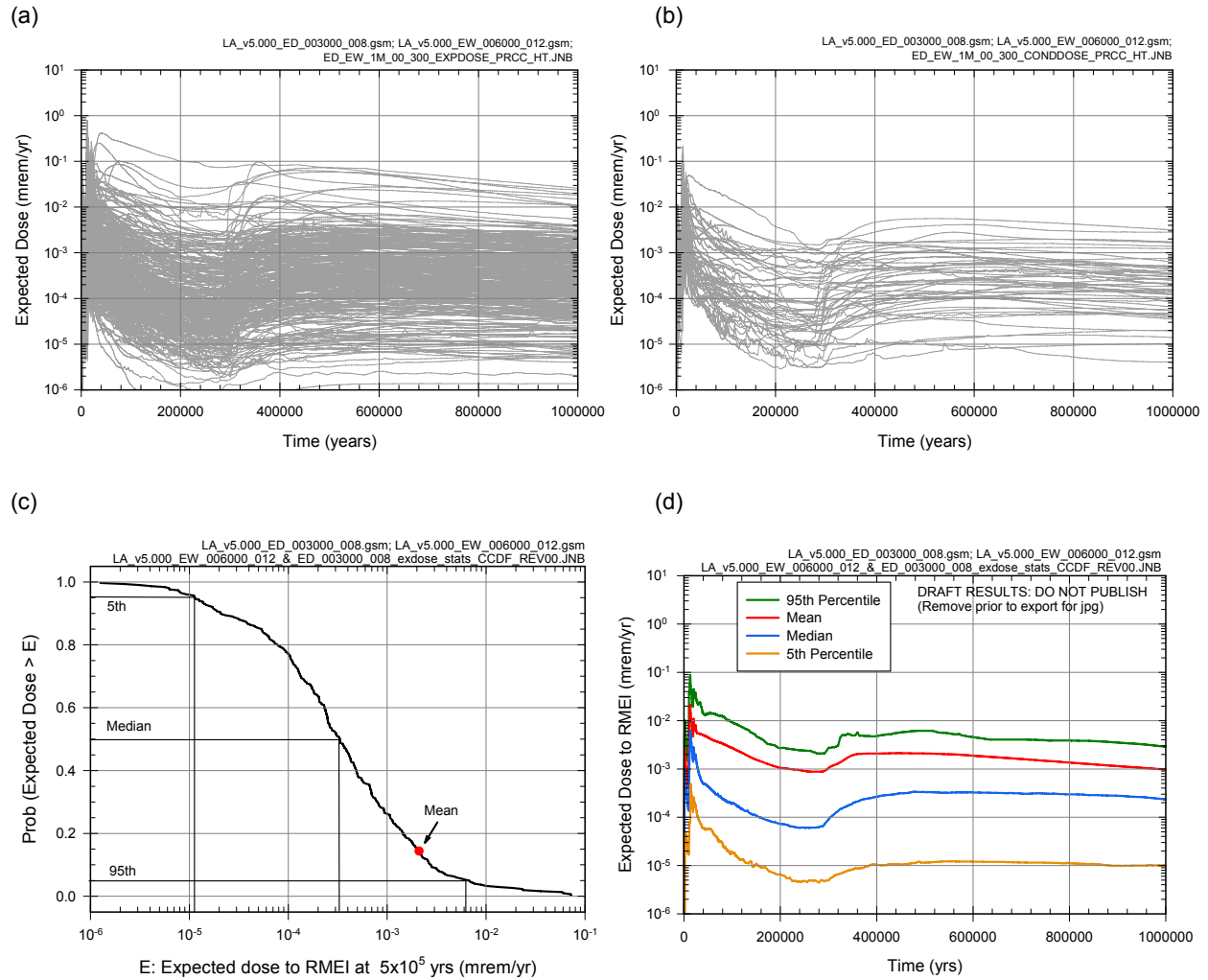
Source: Ouput DTNs: MO0709TSPAPLOT.000 [DIRS 183010]; MO0709TSPAREGS.000 [DIRS 182976]; and MO0709TSPASTAB.000 [DIRS 182983].

Figure J6.3-21. Assessment with replicated sampling of numerical error associated with use of an LHS of size $n_{LHS} = 300$ to determine epistemic uncertainty in expected dose $\bar{D}_{ED}(\tau|\mathbf{e})$ to RMEI for $0 \leq \tau \leq 10^6$ yr that results when only early DS failure is considered: (a) Replicated estimates of expected (mean) dose $\bar{D}_{ED}(\tau)$ and quantiles $Q_q[\bar{D}_{ED}(\tau|\mathbf{e})]$, $q = 0.05, 0.5, 0.95$, and (b) confidence intervals for estimates of expected (mean) dose $\bar{D}_{ED}(\tau)$.



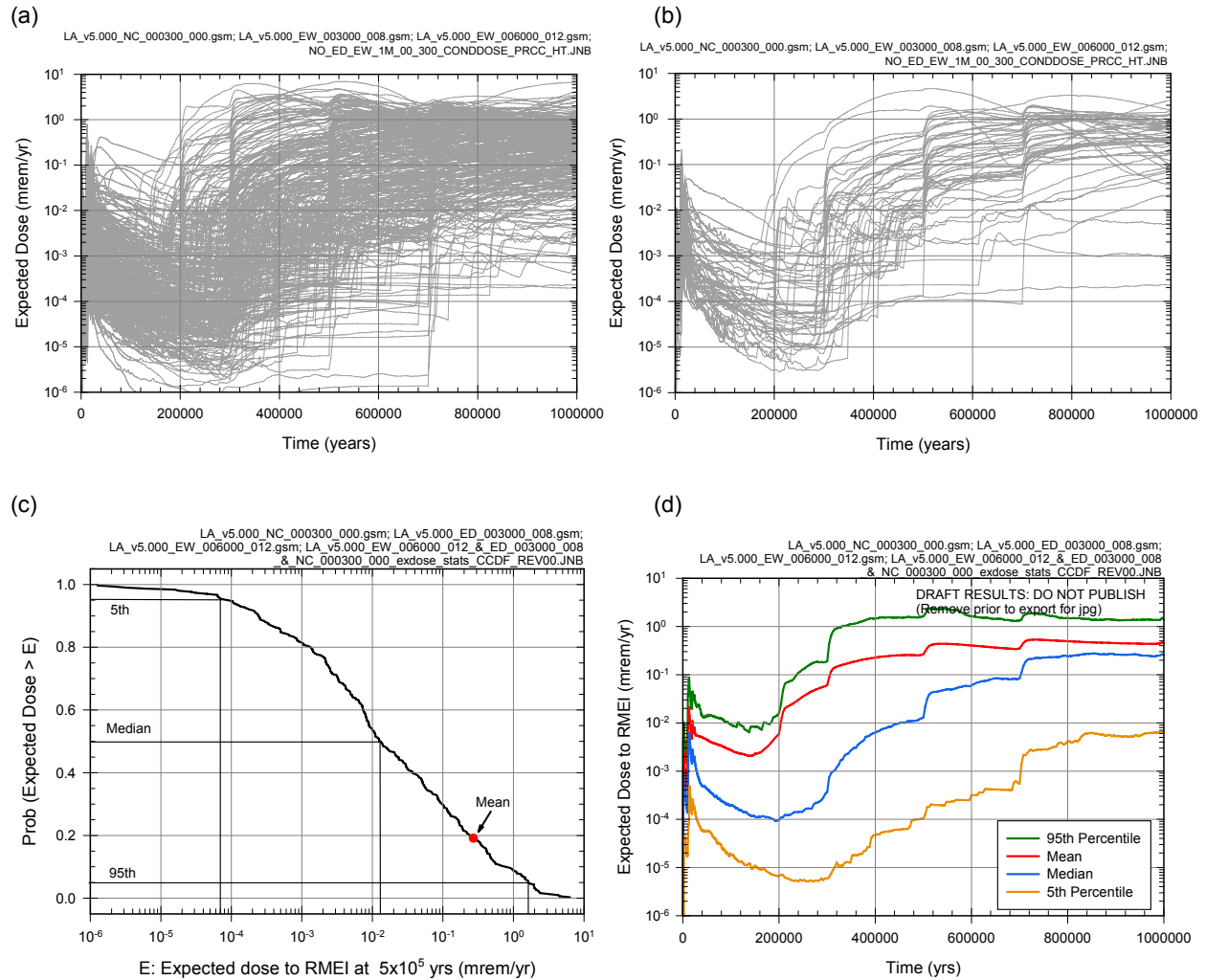
Source: Ouput DTNs: MO0709TSPAPLOT.000 [DIRS 183010]; and MO0709TSPAREGS.000 [DIRS 182976].

Figure J6.4-1. Estimate obtained with LHS of size $nLHS = 300$ showing epistemic uncertainty in expected dose $\bar{D}_E(\tau|\mathbf{e})$ to RMEI for $0 \leq \tau \leq 20,000$ yr that results when only early WP and early DS failures are considered: (a) expected dose $\bar{D}_E(\tau|\mathbf{e}_i)$, $i = 1, 2, \dots, nLHS = 300$, (b) expected dose $\bar{D}_E(\tau|\mathbf{e}_i)$, $i = 1, 2, \dots, 50$, (c) exceedance probabilities $p_E[D < \bar{D}_E(\tau|\mathbf{e})]$ and quantiles $Q_q[\bar{D}_E(\tau|\mathbf{e})]$, $q = 0.05, 0.5$ and 0.95 , for $\tau = 10^4$ yr, and (d) expected (mean) dose $\bar{\bar{D}}_E(\tau)$ and quantiles $Q_q[\bar{\bar{D}}_E(\tau|\mathbf{e})]$, $q = 0.05, 0.5, 0.95$.



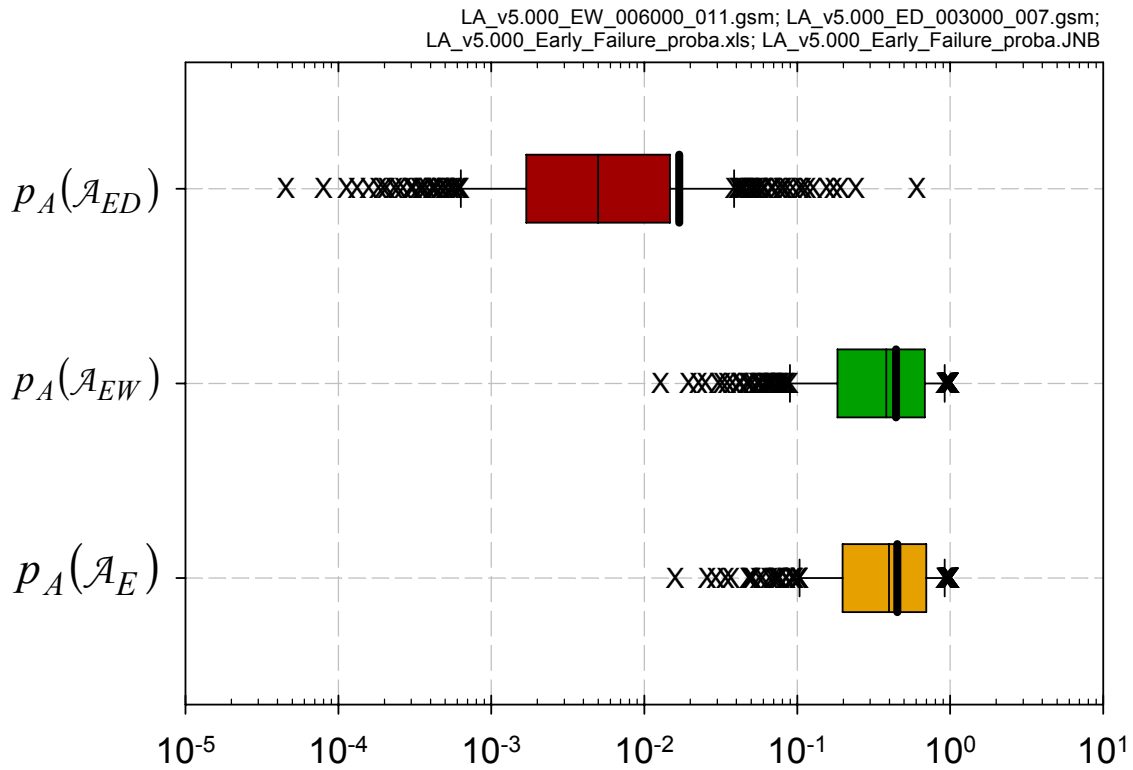
Source: Ouput DTNs: MO0709TSPAPLOT.000 [DIRS 183010]; and MO0709TSPAREGS.000 [DIRS 182976].

Figure J6.4-2. Estimate obtained with LHS of size $nLHS = 300$ showing epistemic uncertainty in expected dose $\bar{D}_E(\tau|\mathbf{e})$ to RMEI for $0 \leq \tau \leq 1,000,000$ yr that results when only early WP and early DS failures are considered: (a) expected dose $\bar{D}_E(\tau|\mathbf{e}_i)$, $i = 1, 2, \dots, nLHS = 300$, (b) expected dose $\bar{D}_E(\tau|\mathbf{e}_i)$, $i = 1, 2, \dots, 50$, (c) exceedance probabilities $p_E[D < \bar{D}_E(\tau|\mathbf{e})]$ and quantiles $Q_q[\bar{D}_E(\tau|\mathbf{e})]$, $q = 0.05, 0.5$ and 0.95 , for $\tau = 500,000$ yr, and (d) expected (mean) dose $\bar{\bar{D}}_E(\tau)$ and quantiles $Q_q[\bar{\bar{D}}_E(\tau|\mathbf{e})]$, $q = 0.05, 0.5, 0.95$.



Source: Ouput DTNs: MO0709TSPAPLOT.000 [DIRS 183010]; and MO0709TSPAREGS.000 [DIRS 182976].

Figure J6.4-3. Estimate obtained with LHS of size $n_{LHS} = 300$ showing epistemic uncertainty in expected dose $\bar{D}_{NE}(\tau|\mathbf{e})$ to RMEI for $0 \leq \tau \leq 1,000,000$ yr that results when only nominal process failures and early WP and early DS failures are considered: (a) expected dose $\bar{D}_{NE}(\tau|\mathbf{e}_i)$, $i = 1, 2, \dots, n_{LHS} = 300$, (b) expected dose $\bar{D}_{NE}(\tau|\mathbf{e}_i)$, $i = 1, 2, \dots, 50$, (c) exceedance probabilities $p_{E|D} < \bar{D}_{NE}(\tau|\mathbf{e})$ and quantiles $Q_q[\bar{D}_{NE}(\tau|\mathbf{e})]$, $q = 0.05, 0.5$ and 0.95 , for $\tau = 500,000$ yr, and (d) expected (mean) dose $\bar{D}_{NE}(\tau)$ and quantiles $Q_q[\bar{D}_{NE}(\tau|\mathbf{e})]$, $q = 0.05, 0.5, 0.95$.



Probability Early Failure : $p_A(\mathcal{A}_{ED})$, $p_A(\mathcal{A}_{EW})$ and $p_A(\mathcal{A}_E)$

Source: Ouput DTNs: MO0709TSPAPLOT.000 [DIRS 183010]; and MO0709TSPAREGS.000 [DIRS 182976].

Figure J6.5-1. Box plots (see Figure J6.2-3 for description) summarizing probabilities $p_A(\mathcal{A}_{ED}|\mathbf{e}_{Ai})$, $p_A(\mathcal{A}_{EW}|\mathbf{e}_{Ai})$ and $p_A(\mathcal{A}_E|\mathbf{e}_{Ai})$ for scenario classes \mathcal{A}_{ED} , \mathcal{A}_{EW} and \mathcal{A}_E obtained with LHS of size $nLHS = 300$.